Co-processing Pharmaceutical Ingredients to Engineer Novel Multifunctional Excipients

Sharad Mangal

B. Pharm, M. Pharm

A thesis submitted for the degree of Doctor of Philosophy in 2015 at Monash University, Drug Delivery, Disposition and Dynamics, Monash Institute of Pharmaceutical Sciences, 381, Royal Parade, Parkville, VIC 3052, Australia

Dedicated to my Parents

Shri Suresh Kumar Mangal and Mrs. Nirmala Mangal

Copyright notice

Table of Content

Abstract

The simplicity and cost-effectiveness of direct compression makes it a preferred method of commercial tablet manufacturing. Excipients play a central role in determining the success of direct compression. Currently available directly compressible excipients are typically effective at relatively high proportion of >50% (w/w). For high-dose APIs, incorporation of such high excipient load is inappropriate, as this may necessitate the formation of large tablets, which may be difficult to ingest. Thus, high-dose APIs (especially for poorly flowable and difficult to compact) are often considered unsuitable for tablet manufacturing by direct compression.

In interactive mixtures, small guest particles (typically <10 μm) adhere to larger host particles. We hypothesized that small binder particles could express a binder action as well as a flow additive action, if they could form a suitable interactive mixture with large APIs. However, many such small particles are highly cohesive, which limits their de-agglomeration, dispersion and consequently the ability to form a homogeneous interactive mixture. Thus, the aim of this thesis was to understand the impact of the cohesion of small binder particles on their interactive mixing behaviour and consequently extension of their potential excipient performance i.e., binder and flow additive actions.

A model pharmaceutical binder, polyvinylpyrrolidone (PVP) was co-sprayed with L-leucine to engineer small low-cohesion binder particles. In these composite particles, L-leucine enriched at the surfaces and manipulated the surface physico-chemical properties (such as morphology, surface energy and its crystalline character), which allowed control over cohesion.

Low cohesion small binder particles de-agglomerated efficiently and formed a more homogeneous interactive mixture with paracetamol (active pharmaceutical ingredient, API) compared with high cohesion binder particles. The homogeneous interactive mixing allowed

small binder particles to express enhanced binder and flow additive actions. The flow additive action improved while inherent binder activity reduced with reducing cohesion. This decline in binder activity was attributed to the reduction in the compactability (or bonding ability) of binder particles. However, manipulation of mechanical properties (increasing plastic deformability) allowed improvement of the binder activity of such low cohesion binder particles.

High performance excipients are necessary to facilitate direct compression of high-dose APIs. Our study showed that binder and flow additive action are mutually exclusive excipient properties and the knowledge of interactive mixing allowed creation of composite excipients with elements of both flow additive and binder action. Manipulation of the surface physico-chemical and mechanical properties via smart particle engineering enabled small binder particles to express an optimum flow additive and binder performances. Thus, this knowledge could enable rational engineering and development of high-performance direct compression excipients, which would enable direct compression of poorly compactable and poorly flowable high-dose APIs.

General declaration

In accordance with Monash University Doctorate Regulation 17.2 Doctor of Philosophy regulations the following declarations are made:

This thesis contains no material which has been accepted for the award of any other degree or diploma at any university or equivalent institution and that, to the best of my knowledge and belief, this thesis contains no material previously published or written by another person, except where due reference is made in the text of the thesis.

Thesis including published works

This thesis includes two original papers published in peer-reviewed journals and three unpublished papers. The core theme of the thesis is "Co-processing Pharmaceutical Ingredients to Engineer Novel Multifunctional Excipients". The ideas, development and writing up of all the papers in the thesis were the principal responsibility of myself, the candidate, working within the Drug Delivery, Disposition and Dynamics, Monash University under the supervision of Dr. Ian Larson and A/Prof. David AV Morton.

The inclusion of co-authors reflects the fact that the work came from active collaboration between researchers and acknowledges input into team-based research.

The structure of this thesis is as followed, introduction (including hypotheses and objectives), literature review, experimental chapters (chapters 3-7 as mentioned below) followed by conclusion and future directions.

In the case of chapters 3-7, my contribution to the work involved the following:

Thesis chapter	**Publication title**	**Publication status***	**Nature and extent of candidate's contribution**
3	The role of physico-chemical and bulk characteristics of co-spray dried L-leucine and polyvinylpyrrolidone on glidant and binder properties in interactive mixtures	Published	65%

4	Relationship between surface concentration of L-leucine and bulk powder properties in spray dried formulations	Published	55%
5	Applying surface energy derived cohesive-adhesive balance model in predicting the mixing, flow and compaction behaviour of interactive mixtures	Reviewer's comments received	65%
6	Relationship between the cohesion of guest particles on the flow behaviour of interactive mixtures	Accepted for publication	55%
7	Effect of the deformability of guest particles on the tensile strength of tablets from interactive mixtures	Accepted for publication	65%

I have renumbered sections of submitted or published papers in order to generate a consistent presentation within the thesis.

Signed:  **……**

Date: **11.03.2016**

Acknowledgements

Firstly, I would like to express my sincere gratitude to my advisors Dr. Ian Larson and A/Prof. David AV Morton and Dr. Felix Meiser for their continuous support, patience, motivation and immense knowledge.

Ian, you are a great person, a great mentor and a great motivator. You constantly encouraged me, which allowed me to overcome hurdles and keep faith in myself. Your knowledge, approach and insight, always helped me stay focussed, when I diverted from a real research perspective. In all regards, you supported me through this PhD like no other and your contribution to my development as a researcher is invaluable.

David, your persona as a researcher and an innovator starts at a point, where my words start failing to describe it. Your creativity has motivated me to ask new questions and of course answer the existing ones. You always gave me a sense of thinking beyond the obvious, which helped me pave the path to develop as a researcher. In many ways, I learned to stay happy and positive in all situations, which is a very important trait of a successful researcher.

Felix, unfortunately, I had you, as my supervisor for just first two years but your contribution to my PhD project is immense. You always asked provocative questions, which helped me solidify my project. I am grateful to have had you as a supervisor, co-author and a warm helping friend in difficult times.

I have no doubt that you are the best supervisors in this world, one can ever have.

Besides my advisors, I would like to thank my PhD panel committee members, Prof. Karen Hapgood and Prof. Peter Stewart for their insightful comments and encouragement, but also for the hard question, which helped me to widen and at the same time focus my research from various perspectives.

My sincere thanks also goes to extremely talented and brilliant colleagues Dr. Shyamal Das, Ruth Howell, Ken, Tomas, Gemma, Sally, Jamal, Purav, Kerry, Geoff, Igor and Lilies (Lily Qu and Lily Fitriani). Thanks you all for kindly accepting me as your team member and providing an opportunity to join you, and giving me access to the laboratory and research facilities. Without your precious support, it would not be possible to conduct this research. Also, thanks for making our office and labs such a fun place to work.

Igor, you deserve a special thanks for sharing your knowledge, expertise and insight on solid-state characterization. Geoff your help with IGC and all the stimulating discussions is also highly appreciated. I am sure; you guys will become one of the famous researchers in the world one day.

Mummy and Papa, your faith in me always kept me going. Your prayers have always kept me up, helped me and motivated me, as if you were always beside me telling, "Go achieve it". In no words, I can describe, how lucky I am, to have parents like you. I hope every child has parents like you. Sincere thanks to my sisters (Rakhi and Neetu) and brother (Sumit), who have always supported me in multiple ways.

I would like to thank my wife and naughty little son (Naksh) for giving me such a wonderful and joyous time at home. It would have never been this easy to go through this giant, stressful task of completing a PhD, without your support. Your smiles always eased the pressure off me and gave me a thousand reasons to stay motivated and work hard. No words would describe how thankful I am to god for having such a wonderful family.

Last but not the least, I would like to thank almighty god "Lord Ganesha" for all the blessings.

Publications and Communications

Peer reviewed journal papers

1. **Mangal S**, Lakio S, Gengenbach T, Morton DAV, Larson I. Effect of the deformability of guest particles on the tensile strength of tablets from interactive mixtures. Int J Pharm. Accepted for publication.
2. **Mangal S**, Meiser F, Morton DA, Larson I. Improving the functional performance of composite excipients through particle engineering and optimized interactive mixing. Special issue of Eur J Pharm Biopharm. Dedicated to 7th Granulation Conference; Reviewer's comments received.
3. **Mangal S**, Gengenbach T, Millington-Smith D, Armstrong B, Morton DAV, Larson I. Relationship between the cohesion of guest particles and the flow performance of interactive mixtures. Eur J Pharm Biopharm. Accepted for publication. doi: 10.1016/j.ejpb.2016.03.012.
4. **Mangal S**, Meiser F, Morton DA, Larson I. Particle engineering of excipients for direct compression: Understanding the role of material properties. Curr Pharm Des. 2015;21(40):5877-89.
5. **Mangal S**, Meiser F, Tan G, Gengenbach T, Denman J, Rowles MR, Larson I, Morton DA. Relationship between surface concentration of L-leucine and bulk powder properties in spray dried formulations. Eur J Pharm Biopharm. 2015; 94: 160–169.
6. **Mangal S**, Meiser F, Lakio S, Morton DA, Larson I. The role of physico-chemical and bulk characteristics of co-spray dried L-leucine and polyvinylpyrrolidone on glidant and binder properties in interactive mixtures. Int J Pharm. 2015; 479(2): 338-48.

Peer reviewed book chapter

1. **Mangal S**, Meiser F, Morton DA, Larson I. Particle engineering of polymers into multifunctional interactive excipients. In: Thakur VK, Thakur MK, Eds., Handbook of Polymers for Pharmaceutical Technologies, Scrivener Publishing LLC,2015;1–32.

Conference papers and/or presentations

1. **Mangal S**, Meiser F, Morton DA, Larson I. Engineering of Novel core-shell micro-excipient foe efficient tablet manufacturing: Employing the concept of interactive mixing. AAPS Annual Meeting and Exposition, San Diego, USA, 2–6 November, 2014. Abstract no. W4369. Poster Presentation.
2. **Mangal S**, Meiser F, Lakio S, Morton DA, Larson I. A multi-functional micro-excipient for tablet manufacturing: Applying the concept of interactive mixing. 5th FIP Pharmaceutical Sciences World Congress (PSWC), Melbourne, Australia 13-16 April, 2014. Abstract no. 327. Poster Presentation.
3. **Mangal S**, Lee L, Whittle S, Meiser F, Morton DA, Larson I. Co-processing pharmaceutical ingredients to engineer a novel multifunctional binder" 6th International Granulation Conference, Sheffield, UK, 26–28 June 2013. Abstract no. 75. Podium Presentation.
4. **Mangal S**, Meiser F, Morton DA, Larson I. Intelligent design of multifunctional micro-excipient: A new class of excipients. 8th Annual Postgraduate Research Symposium. Melbourne, Monash University, Australia, 13 November 2013. Podium Presentation.
5. **Mangal S**, Meiser F, Morton DA, Larson I. Co-processing pharmaceutical ingredients to engineer novel multifunctional excipients. 7th Annual Postgraduate Research Symposium. Melbourne, Monash University, Australia, 26 September, 2012. Podium Presentation.

Scholarships and awards

1. Postgraduate Publication Award, Monash Institute of Graduate Research (MIGR), Monash University, 2015.
2. Excipient Graduate Student Award, International Pharmaceutical Excipients Council (IPEC), 2014.
3. Monash Graduate Scholarship (MGS) and Monash International Postgraduate Research Scholarship (MIPRS), Monash Institute of Graduate Research (MIGR), Monash University, 2013.
4. Postgraduate Research Scholarship, Faculty of Pharmacy and Pharmaceutical Sciences, Monash University, 2012.

List of abbreviations

API	Active pharmaceutical ingredient
AFM	Atomic force microscopy
ANOVA	Analysis of variance
AUC	Area under curve
BFE	Basic flowability energy
CBD	Conditioned bulk density
D_{10}	Particle diameter at 10% undersize
D_{50}	Particle diameter at 50% undersize
D_{90}	Particle diameter at 90% undersize
DPI	Dry powder inhaler
DSC	Differential scanning calorimetry
EF	Elasticity Factor
ffc	Flow function co-efficient
γ_S^+	Acidic component of surface energy
γ_S^-	Basic component of surface energy
γ_s^P	Polar surface energy
γ^D	Dispersive surface energy

IGC	Inverse gas chromatography
Leu	L-leucine
Para	Paracetamol
PVP	Polyvinylpyrrolidone
P-XRD	Powder X ray Diffraction
SEM	Scanning electron microscopy
Tg	Glass transition temperature
ToF-SIMS	Time-of-flight secondary ion mass spectrometry
UV	Ultraviolet
W_{co}	Work of cohesion
W_{ad}	Work of adhesion
XPS	X-ray photoelectron spectroscopy

Chapter 1

Introduction

1 Introduction

Tablets are the most commonly used means of administering active pharmaceutical ingredients (APIs) to humans [1]. The cost-effectiveness, long shelf life (compared to liquid formulations), good compliance and ease of administration, storage and transportation, are some of the prime reasons for their consistent popularity [1].

In general, tablets are expected to be sufficiently strong (to withstand stresses), carry a constant API dose and exhibit a predictable and reproducible dissolution behaviour [2]. Typically, excipients such as diluents, binders, glidants, disintegrants and lubricants allow creation of tablets with these necessary properties [3].

Tablet manufacturing involves three key steps filling of powder into the die, compaction and ejection. Powder filling (into the die) determines the weight variation and uniformity of API dose [4, 5], while compaction determines the robustness and mechanical integrity of tablets [6, 7].

Powder properties such as flow and compactability determines its ability to fill into the die and to create mechanically stable tablets, respectively [5, 6]. Thus, characterization and optimization of powder flow and compactability are an integral part of tablet manufacturing.

1.1 Powder flow and compactability

In general, powder flow can be defined as the relative movement of particles against adjacent particles and/or surfaces [8]. Larger particles experience stronger gravitation forces relative to inter-particle forces, hence they tend to move freely and exhibit excellent flow behaviour [9]. In contrast, small particles (<10 μm) experience stronger inter-particle forces relative to gravitational forces and hence tend to agglomerate and exhibit poor flow [10, 11]. Particle

properties such as size, morphology and surface energy determine the magnitude of inter-particle forces and hence powder flow [12-20].

Compactibility is defined as the ability of powders to compact into the tablets of specific tensile strength [21]. Tensile strength represents the force required to fracture a tablet across its diameter and is believed to represent the robustness and mechanical integrity of tablets [22]. The fracture of tablets involves the separation of particles. Thus, the force required to facture a tablet depends on the number and strength of inter-particle bonds established between particles during compaction. The combined strength of these bonds also depends on particle properties such as size, morphology, surface energy, deformability, mechanism of deformation and surface energy [23-31].

1.2 Impact of excipients

In general, APIs lack the flow and/or compactability required for tablet manufacturing [2, 32-38]. Therefore, excipients are incorporated to correct these deficiencies. Processing *via* wet and dry granulation (agglomeration of individual particles into granules) transforms a powder blend (of APIs and excipients) into a relatively non-segregating, high compactability and readily flowable formulation [39, 40]. In granules, particles of API and excipients exist as agglomerates, thus granulation can largely mask the undesirable properties of individual components. Therefore, such formulations are relatively insensitive/independent of excipient performance (binder also referred as filler-binders) and often result in robust tablet formulations [40-42].

The drive of pharmaceutical companies to improve output and reduce costs has motivated the use of direct compression as a preferred way of tablet manufacturing [43]. Direct compression involves compaction of powder straight into tablets without a preceding resource-intensive granulation step. In such powder formulations, particle structure remains unaltered

and hence properties of individual components (both API and excipients) strongly affect the flow, compactability, and content uniformity. In such cases, the flow and compactability of poorly compactable and poorly flowable APIs can only be optimized by excipients [44-46].

1.3 Improving flow

As discussed earlier, poor flow is typically a result of strong inter-particle interactions [12]. Thus, improving flow requires decreasing these inter-particle forces. Increasing surface roughness by coating with nanoparticles such as silicon dioxide [13, 15, 47, 48] and increasing particle hydrophobicity by coating with lubricants such as magnesium stearate [49-51] are two of the commonly used and most effective strategies to improve the flow of cohesive powders. The excipients used for improving flow are typically referred to as "flow additives" and "glidants".

In general, flow additives are small particles that improve flow by adhering to larger cohesive particles [52-54]. These small particles act as spacer between larger particles (Figure 1.1), and thus increase inter-particle separation leading to improved flow [13]. Powder mixtures in which small particles (guest particles) (< 10 μm) adhere to relatively large particles (host particles) are referred as interactive mixture [55-57]. Thus, the flow additives predominantly work on the principle of interactive mixing [15].

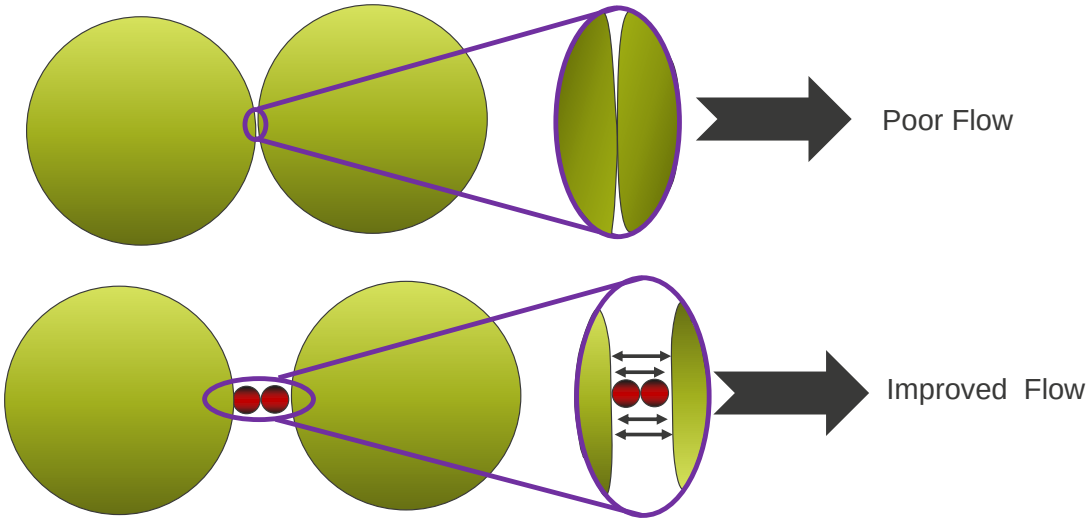

Figure 1.1 – Flow improvement mechanisms proposed for silicon dioxide

For efficient interactive mixing, the adhesion force between the small and large particles (work of adhesion, W_{ad}) must be stronger than the cohesion forces between the small particles (work of cohesion, W_{co}) (Figure 1.2) [58, 59]. Studies have suggested that the cohesive nature of small silicon dioxide and magnesium stearate limits their ability to disperse over large particles under low to medium shear mixing, which compromises their flow additive action to a considerable extent flow [9, 15, 47, 54]. Thus, low-cohesion small particles are desirable to achieve efficient interactive mixing and consequently efficient flow additive action.

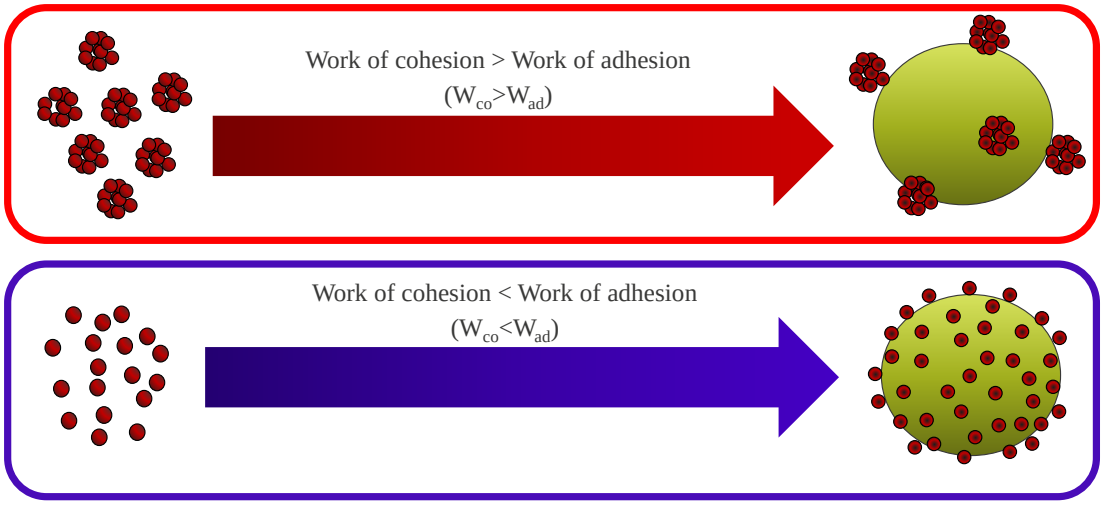

Figure 1.2 – The effect of the relative magnitude of cohesion and adhesion on the interactive mixing behaviour of small particles

Since, surface properties have a strong effect on the magnitude of inter-particle forces [60], engineering surface properties has evolved as one of the main techniques to control the cohesion of small particles. This includes, for example, dry coating and spray drying with excipients, such as magnesium stearate, phospholipids and L-leucine [14, 19, 61-63]. These techniques have been effectively explored in the area of dry powder inhalers, where particles of 1-5 µm aerodynamic diameter, with low cohesion and good dispersibility are desirable for their efficient delivery to lung [64, 65]. The surface engineering using these methods have been proposed to reduce cohesion by reducing surface energy as well as area of contact or inter-particle interactions [14, 16, 61]. For instance, co-spraying with L-leucine has been demonstrate to lead to formation of wrinkled and corrugated particles [16, 66, 67]. It was proposed that the interfacially active L-leucine alters the surface physico-chemical properties, which eventually determine the resultant bulk performance of spray-dried formulations. However, systematic studies investigating such relationships are lacking.

1.4 Improving compactability

Materials with poor compactability form mechanically weak tablets due to weak inter-particle bonding, which tend to laminate or break during production or handling [6, 7]. Thus, particle-particle net bonding strength must be increased to improve the compactability of such materials. Commonly, binders such as polyvinylpyrrolidone, microcrystalline cellulose and starch are used to improve material compactability [68-70]. The importance of binders is well recognised and hence there has been many efforts to improve their performance. Improved direct compression filler-binders were mainly created by physical manipulation and combination of existing excipients [1, 32, 71-74].

1.5 High-dose APIs

One of the common limitations of currently available direct compression excipients (filler-binders) is that they are typically required in a large proportion to achieve desirable formulation properties i.e., compactability and flow [37, 71, 75-77]. However, this may necessitate creating large tablets for formulating high-dose APIs as tablets. Recent research suggests that roughly one-third of the population find tablet swallowing difficult [78], thus swallowing large tablets may be particularly challenging which may reduce patient compliance and adherence. Furthermore, high excipient proportions may also raise concerns about content uniformity and high sensitivity of formulations to excipient related variations [37, 79-84]. Therefore, direct compression is considered unsuitable for high-dose APIs despite the simplicity and cost-effectiveness of this method compared with wet and dry granulation processes [77, 85].

1.6 Innovations in direct compression of high-dose APIs

Many attempts have been made to facilitate the direct compression of high-dose APIs. For example, coating with magnesium stearate at very low proportions was shown to improve the

flow of these APIs but it compromises compactability [86]. Similarly, coating of APIs with small cohesive particles at low proportions was shown to improve the compactability but compromise flow [87]. Wet coating of poorly compactable materials with highly bonding materials was also shown to improve compactability at very low excipient proportions, but the effect of such coating on powder flow was not investigated [75, 80].

Small binders are more effective at improving compactability than their larger counterparts at low proportion [68, 69, 88-90]. However, such small binders exhibit poor flow (as evident by their low bulk density, tapped density and angle of repose (Table 1.1)), which may be detrimental to direct compression. In addition, the differences between the size of APIs and excipient may cause segregation and thus variations in content uniformity, (unless specific physical interactions hold particles together for example in interactive mixtures [91]).

Table 1.1 – Particle size and flow specifications of common commercially available fine-grade excipients.

Excipient	Grade	Particle Size	Flow description	Ref.
Hydroxypropyl Cellulose	Fine grind	D_{10} = 16.6 ±5.1 µm D_{50} = 98.8 ±1.3 µm D_{90} = 341.8 ±31.7 µm	BD = 0.3 g/cm^3, TD = 0.4 g/cm^3, CI = 19.9	[92]
	Fine grind	<149.0 µm (>80 %)	NA	[93]
	Super fine powder (SPF)	D_{10} = 8.0 µm D_{50} = 20.0 µm D_{90} = 50.0 µm	AOR = 50˚, BD = 0.24 g/cm^3, TD = 0.41 g/cm^3	[93]
Low-substituted Hydroxypropyl cellulose	LH-11	D_{50} = 50.0 µm >150.0 µm (NMT 2 %)	AOR = 49˚, BD = 0.3 g/cm^3, TD = 0.6 g/cm^3	[94]
	LH-21	D_{50} = 40.0 µm	AOR = 45, BD = 0.4 g/cm^3,	[94]

		>75.0 µm (NMT 10 %)	TD = 0.6 g/cm^3	
	LH-31	D_{50} = 25.0 µm >40.0 µm (NMT 50 %)	AOR = 49, BD = 0.3 g/cm^3, TD = 0.6 g/cm^3	[94]
Microcrystalline cellulose	Avicel PH 102	D_{10} = 35.2 ±0.4 µm D_{50} = 109.2 ±0.8 µm D_{90} = 195.5 ±1.1 µm	AOR = 36˚, BD = 0.3 g/cm^3, TD = 0.4 g/cm^3, CI = 20.0	[92]
Ethyl cellulose	7 FP (fine particles)	Mean = 7.0-12.0 µm; Max = 100.0 µm	NA	[93]
	10 FP (fine particles)	Mean = 3.0-8.0 µm; Max = 140 µm	NA	[93]
	100 FP (fine particles)	Mean = 30.0-60.0 µm; Max = 150.0 µm	NA	[93]
Copovidone	Kolidone VA-64 fine	<50.0 µm (>90%)	BD = 0.1-0.2 g/cm^3	

BD = Bulk density,
TD = Tapped density
CI = Carr's Index
AOR = Angle of repose
Max. = Maximum
NMT = Not more than

1.7 Challenges in direct compression of high-dose APIs

As described earlier, improving flow requires minimizing inter-particle bonding, while improving compactability requires the opposite i.e., maximizing inter-particle bonding. Thus, flow and compactability might be seen as two fundamentally competing properties [95].

Attempts to facilitate direct compression of high-dose APIs have mainly focussed on improving one formulation attribute (i.e., compactability or flow), while its effect on the other formulation attribute was either ignored or was shown to be negatively affected. Therefore, further efforts are required to investigate approaches that can be effectively employed to optimize the flow as well as compactability of difficult APIs.

1.8 Hypotheses

We proposed that if binder particles are small enough (<10 μm) so as to form a suitable interactive mixture, it may not only express a binder (due to its higher effective surface area and better coverage [68, 70, 89]) but also a flow additive action (by acting as spacers and effectively increasing separation between large cohesive particles [15, 96]). However, cohesive nature of such small particles [10, 11] could impede their de-agglomeration and dispersion resulting in inhomogeneous interactive mixing [97]. Such inhomogeneous mixing was proposed to compromise their excipient performance i.e., flow additive and binder actions. Thus, it was considered important to control the cohesion of small binder particles for achieving optimum excipient performance.

Consequently, the following hypotheses were established:

- A low cohesion small (<10 μm) binder particles can form a relatively homogeneous interactive mixture with API compared with high cohesion small binder particles.
- At low proportions, these low cohesion binder particles will act as binders resulting in high tablet tensile strength.
- At low proportions, these low cohesion binder particles will also act as flow additives resulting in good blend flow.

1.9 Objectives

The specific objectives of this body of work are as follows;

1. To understand the effect of cohesion of small binder particles on their interactive mixing behaviour, binder and flow additive actions.
2. To investigate the relationship between the extent of surface manipulation *via* L-leucine and the change in surface physico-chemical properties and cohesion of small binder particles.
3. To investigate the relationship between interactive mixing behaviour with binder and flow additive action of small binder particles.
4. To investigate the relationship between the cohesion and flow additive action of small binder particles.
5. To investigate the effect of mechanical properties of low cohesion small particles on their binder activity.

These specific objectives 1 to 5 are addressed in chapter 3 to 7, respectively. As a thesis by publication, chapters 3-7 are presented in their original forms as published or submitted for publication.

1.10 References

[1] Mirani AG, Patankar SP, Borole VS, Pawar AS, Kadam VJ. Direct compression high functionality excipient using coprocessing technique: a brief review. Curr Drug Deliv 2011; 8(4): 426-35.

[2] Armstrong NA. Selection of excipients for direct compression tablet formulations. Pharm Tech Eur 1997: 24-30.

[3] Bolhuis GK, Armstrong NA. Excipients for direct compaction—an update. Pharm Dev Technol 2006; 11(1): 111-124.

[4] Staniforth JN. Powder flow. In: Aulton ME, Ed., Pharmaceutics: The science of dosage form design. 2nd ed., Edinbergh, UK: Churchill Livingstone, 2002; pp. 197–210.

[5] Sun CC. Setting the bar for powder flow properties in successful high speed tableting. Powder Technol 2010; 201(1): 106-108.

[6] Nyström C, Alderborn G, Duberg M, Karehill P-G. Bonding surface area and bonding mechanism-two important factors for the understanding of powder comparability. Drug Dev Ind Pharm 1993; 19(17-18): 2143-2196.

[7] Sun CC. Decoding powder tabletability: Roles of particle adhesion and plasticity. J Adhes Sci Technol 2011; 25(4-5): 483-499.

[8] Peleg M. Flowability of food powders and methods for its evaluation — A review. J Food Process Eng 1977; 1(4): 303-328.

[9] Mullarney MP, Beach LE, Davé RN, Langdon BA, Polizzi M, Blackwood DO. Applying dry powder coatings to pharmaceutical powders using a Comil for improving powder flow and bulk density. Powder Technol 2011; 212(3): 397-402.

[10] Castellanos A. The relationship between attractive interparticle forces and bulk behaviour in dry and uncharged fine powders. Adv Phys 2005; 54(4): 263-376.

[11] Jallo LJ, Chen Y, Bowen J, Etzler F, Dave R. Prediction of inter-particle adhesion force from surface energy and surface roughness. J Adhes Sci Technol 2011; 25(4-5): 367-384.

[12] Schulze D. Powders and bulk solids: Behavior, characterization, storage and flow In. Springer: Berlin–Heidelberg–NewYork–Tokyo, 2008.

[13] Chen Y, Yang J, Dave RN, Pfeffer R. Fluidization of coated group C powders. AIChE J 2008; 54(1): 104-121.

[14] Han X, Jallo L, To D, Ghoroi C, Dave R. Passivation of high-surface-energy sites of milled ibuprofen crystals via dry coating for reduced cohesion and improved flowability. J Pharm Sci 2013; 102(7): 2282-96.

[15] Yang J, Sliva A, Banerjee A, Dave RN, Pfeffer R. Dry particle coating for improving the flowability of cohesive powders. Powder Technol 2005; 158(1–3): 21-33.

[16] Chew NYK, Tang P, Chan HK, Raper JA. How much particle surface corrugation is sufficient to improve aerosol performance of powders? Pharm Res 2005; 22(1): 148-152.

[17] Lahde A, Raula J, Kauppinen EI. Simultaneous synthesis and coating of salbutamol sulphate nanoparticles with L-leucine in the gas phase. Int J Pharm 2008; 358(1-2): 256-62.

[18] Feng AL, Boraey MA, Gwin MA, Finlay PR, Kuehl PJ, Vehring R. Mechanistic models facilitate efficient development of leucine containing microparticles for pulmonary drug delivery. Int J Pharm 2011; 409(1–2): 156-163.

[19] Chew NY, Shekunov BY, Tong HH, Chow AH, Savage C, Wu J, Chan HK. Effect of amino acids on the dispersion of disodium cromoglycate powders. J Pharm Sci 2005; 94(10): 2289-300.

[20] Podczeck F. Particle-Particle adhesion in pharmaceutical powders handling. In. Imperial College Press: London, 1998.
[21] Leuenberger H. The compressibility and compactibility of powder systems. Int J Pharm 1982; 12(1): 41-55.
[22] Fell JT, Newton JM. Determination of tablet strength by the diametral-compression test. J Pharm Sci 1970; 59(5): 688-691.
[23] Fichtner F, Mahlin D, Welch K, Gaisford S, Alderborn G. Effect of surface energy on powder compactibility. Pharm Res 2008; 25(12): 2750-2759.
[24] Patel S, Kaushal AM, Bansal AK. Compression physics in the formulation development of tablets. Crit Rev Ther Drug 2006; 23(1): 1-66.
[25] Eriksson M, Alderborn G. The effect of particle fragmentation and deformation on the interparticulate bond formation process during powder compaction. Pharm Res 1995; 12(7): 1031-9.
[26] Alderborn G, Nystrom C. Studies on direct compression of tablets. IV. The effect of particle size on the mechanical strength of tablets. Acta Pharm Suec 1982; 19(5): 381-390.
[27] Alderborn G, Börjesson E, Glazer M, Nyström C. Studies on direct compression of tablets. XIX. The effect of particle size and shape on the mechanical strength of sodium bicarbonate tablets. Acta Pharm Suec 1988; 25(1): 31-40.
[28] van Veen B, van der Voort Maarschalk K, Bolhuis GK, Zuurman K, Frijlink HW. Tensile strength of tablets containing two materials with a different compaction behaviour. Int J Pharm 2000; 203(1–2): 71-79.
[29] Van der Voort Maarschalk K, Zuurman K, Van Steenbergen MJ, Hennink WE, Vromans H, Bolhuis GK, Lerk CF. Effect of compaction temperature on consolidation of amorphous copolymers with different glass transition temperatures. Pharm Res 1997; 14(4): 415-9.
[30] Van der Voort Maarschalk K, Vromans H, Bolhuis GK, Lerk CF. Influence of plasticizers on tableting properties of polymers. Drug Dev Ind Pharm 1998; 24(3): 261-8.
[31] El Gindy NA, Samaha MW. Tensile strength of some pharmaceutical compacts and their relation to surface free energy. Int J Pharm 1982; 13(1): 35-46.
[32] Rojas J, Buckner I, Kumar V. Co-proccessed excipients with enhanced direct compression functionality for improved tableting performance. Drug Dev Ind Pharm 2012; 38(10): 1159-1170.
[33] Cao X, Morganti M, Hancock BC, Masterson VM. Correlating particle hardness with powder compaction performance. J Pharm Sci 2010; 99(10): 4307-4316.
[34] Femi-Oyewo MN, Spring MS. Studies on paracetamol crystals produced by growth in aqueous solutions. Int J Pharm 1994; 112(1): 17-28.
[35] Sun C, Grant DJW. Influence of crystal structure on the tableting properties of sulfamerazine polymorphs. Pharm Res 2001; 18(3): 274-280.
[36] Garekani HA, Ford JL, Rubinstein MH, Rajabi-Siahboomi AR. Formation and compression characteristics of prismatic polyhedral and thin plate-like crystals of paracetamol. Int J Pharm 1999; 187(1): 77-89.
[37] Lakshman JP, Kowalski J, Vasanthavada M, Tong WQ, Joshi YM, Serajuddin ATM. Application of melt granulation technology to enhance tabletting properties of poorly compactible high-dose drugs. J Pharm Sci 2011; 100(4): 1553-1565.
[38] Modi SR, Khomane KS, Bansal AK. Impact of differential surface molecular environment on the interparticulate bonding strength of celecoxib crystal habits. Int J Pharm 2014; 460(1–2): 189-195.

[39] Iveson SM, Litster JD, Hapgood K, Ennis BJ. Nucleation, growth and breakage phenomena in agitated wet granulation processes: a review. Powder Technol 2001; 117(1–2): 3-39.
[40] Litster J, Ennis B. The science and engineering of granulation processes. In, ed. MA, USA: Kluwer Academic Publishers 2004; pp. 1-9.
[41] Ennis BJ, Parikh DM, Liu L. Theory of granulation: An engineering perspective. In, Handbook of pharmaceutical granulation technology. 3rd ed., NY, USA: Informa Healthcare, 2010; pp. 6-58.
[42] Kumar A, Gernaey KV, Beer TD, Nopens I. Model-based analysis of high shear wet granulation from batch to continuous processes in pharmaceutical production – A critical review. Eur J Pharm Biopharm 2013; 85(3, Part B): 814-832.
[43] McCormick D. Evolutions in direct compression. Pharm Tech 2005; 5(4): 52–62
[44] Thoorens G, Krier F, Leclercq B, Carlin B, Evrard B. Microcrystalline cellulose, a direct compression binder in a quality by design environment—A review. Int J Pharm 2014; 473(1-2): 64–72.
[45] Kása P, Bajdik J, Zsigmond Z, Pintye-Hódi K. Study of the compaction behaviour and compressibility of binary mixtures of some pharmaceutical excipients during direct compression. Chem Eng Process 2009; 48(4): 859-863.
[46] Carlin BAC. Direct compression and the role of filler-binders. In: Augsburger LL, Hoag SW, Eds., Pharmaceutical dosage forms: tablets. 3rd ed. Vol. 2, NY, USA: Informa Healthcare, 2008; pp. 173–216.
[47] Han X, Ghoroi C, Dave R. Dry coating of micronized API powders for improved dissolution of directly compacted tablets with high drug loading. Int J Pharm 2013; 442(1–2): 74-85.
[48] Han X, Ghoroi C, To D, Chen Y, Dave R. Simultaneous micronization and surface modification for improvement of flow and dissolution of drug particles. Int J Pharm 2011; 415(1-2): 185-95.
[49] Qu L, Zhou Q, Denman JA, Stewart PJ, Hapgood KP, Morton DAV. Influence of coating material on the flowability and dissolution of dry-coated fine ibuprofen powders. Eur J Pharm Sci 2015; 78: 264-272.
[50] Zhou Q, Denman JA, Gengenbach T, Das S, Qu L, Zhang H, Larson I, Stewart PJ, Morton DAV. Characterization of the surface properties of a model pharmaceutical fine powder modified with a pharmaceutical lubricant to improve flow via a mechanical dry coating approach. J Pharm Sci 2011; 100(8): 3421-3430.
[51] Zhou QT, Armstrong B, Larson I, Stewart PJ, Morton DAV. Understanding the influence of powder flowability, fluidization and de-agglomeration characteristics on the aerosolization of pharmaceutical model powders. Eur J Pharm Sci 2010; 40(5): 412-421.
[52] Jonat S, Albers P, Gray A, Schmidt PC. Investigation of the glidant properties of compacted colloidal silicon dioxide by angle of repose and X-ray photoelectron spectroscopy. Eur J Pharm Biopharm 2006; 63(3): 356-359.
[53] Jonat S, Hasenzahl S, Gray A, Schmidt PC. Mechanism of glidants: Investigation of the effect of different colloidal silicon dioxide types on powder flow by atomic force and scanning electron microscopy. J Pharm Sci 2004; 93(10): 2635-2644.
[54] Zhou Q, Qu L, Gengenbach T, Denman JA, Larson I, Stewart PJ, Morton DAV. Investigation of the extent of surface coating via mechanofusion with varying additive levels and the influences on bulk powder flow properties. Int J Pharm 2011; 413(1–2): 36-43.
[55] Zatloukal Z. Interactive powder mixtures. Ceska Slov Farm 2004; 53(4): 165-71.

[56] Wai Yip C, Hersey JA. Segregation in ordered powder mixtures. Powder Technol 1977; 16(1): 149-150.
[57] Mao C, Thalladi VR, Kim DK, Ma SH, Edgren D, Karaborni S. Harnessing ordered mixing to enable direct-compression process for low-dose tablet manufacturing at production scale. Powder Technol 2013; 239(0): 290-299.
[58] Begat P, Morton DV, Staniforth J, Price R. The cohesive-adhesive balances in dry powder inhaler formulations I: direct quantification by atomic force microscopy. Pharm Res 2004; 21(9): 1591-1597.
[59] Begat P, Morton DAV, Staniforth J, Price R. The cohesive-adhesive balances in dry powder inhaler formulations II: influence on fine particle delivery characteristics. Pharm Res 2004; 21(10): 1826-1833.
[60] Orband JLR, Geldart D. Direct measurement of powder cohesion using a torsional device. Powder Technol 1997; 92(1): 25-33.
[61] Zhou QT, Qu L, Larson I, Stewart PJ, Morton DAV. Improving aerosolization of drug powders by reducing powder intrinsic cohesion via a mechanical dry coating approach. Int J Pharm 2010; 394(1–2): 50-59.
[62] Staniforth JN, Harris H, Morton DAV, Bannister R, inventor, assignee Pharmaceutical compositions for inhalation containing magnesium stearate. 2002.
[63] Vehring R. Pharmaceutical particle engineering via spray drying. Pharm Res 2008; 25(5): 999-1022.
[64] Ganderton D, Morton DAV, Lucas P, inventor, assignee Improvements in or relating to powders. 2000.
[65] Morton DAV, Green M, Staniforth JN, Begat P, Price R, Young PM. The study of force control aditives in creating high-performance dry powder inhaler formulations. In, Respiratory Drug Delivery VIII: Arizona, USA, 2002.
[66] Lechuga-Ballesteros D, Kuo MC, inventor, assignee Dry powder compositions having improved dispersivity. 2001.
[67] Vehring R. Pharmaceutical particle engineering via spray drying. Pharmaceutical Research, 2008; 25(5): 999-1022.
[68] Mattsson S, Nyström C. Evaluation of strength-enhancing factors of a ductile binder in direct compression of sodium bicarbonate and calcium carbonate powders. Eur J Pharm Biopharm 2000; 10(1): 53-66.
[69] Mattsson SF, Nystrom C. Evaluation of critical binder properties affecting the compactibility of binary mixtures. Drug Dev Ind Pharm 2001; 27(3): 181-194.
[70] Kolter K, Flick D. Structure and dry binding activity of different polymers, including Kollidon VA 64. Drug Dev Ind Pharm 2000; 26(11): 1159-1165.
[71] Saha S, Shahiwala AF. Multifunctional coprocessed excipients for improved tabletting performance. Expert Opin Drug Deliv 2009; 6(2): 197-208.
[72] Nachaegari SK, Bansal AK. Coprocessed excipients for solid dosage forms. Pharm Tech 2004; 50(1): 52-64.
[73] Gohel MC, Jogani PD. Exploration of melt granulation technique for the development of coprocessed directly compressible adjuvant containing lactose and microcrystalline cellulose. Pharm Dev Technol 2003; 8(2): 175-185.
[74] Jivraj M, Martini LG, Thomson CM. An overview of the different excipients useful for the direct compression of tablets. Pharm Sci Tech Today 2000; 3(2): 58-63.
[75] Shi L, Sun CC. Transforming powder mechanical properties by core/shell structure: Compressible sand. J Pharm Sci 2010; 99(11): 4458-4462.
[76] Akande OF, Rubinstein MH, Ford JL. Examination of the compaction properties of a 1:1 acetaminophen:microcrystalline cellulose mixture using precompression and main compression. J Pharm Sci 1997; 86(8): 900-907.

[77] Armstrong NA. Tablet manufacture by direct compression. In: Swarbrick J, Ed., Encyclopedia of pharmaceutical technology. 3rd ed, NY, USA: Informa Healthcare, 2007; pp. 3673-3683.
[78] Llorca P-M. Discussion of prevalence and management of discomfort when swallowing pills: orodispersible tablets expand treatment options in patients with depression. Therapeutic Delivery 2011; 2(5): 611-622.
[79] Moreton C. Functionality and performance of excipients in a quality-by-design world part 2: Excipient variability, QbD and robust formulations. Am Pharm Rev 2009; 12: 40-45.
[80] Shi L, Sun C. Overcoming poor tabletability of pharmaceutical crystals by surface modification. Pharm Res 2011; 28(12): 3248-3255.
[81] Robertson MI. Regulatory issues with excipients. Int J Pharm 1999; 187(2): 273-276.
[82] Zheng JY, Robert LT. Development of low-dose solid oral tablets using direct compression In: Zheng JY, Ed., Formulation and analytical development for low-dose oral drug products. NJ, USA: John Wiley & Sons, 2009; pp. 159-204.
[83] Kumar V, inventor, Pharmalogix Inc., assignee Direct compression metformin hydrochloride tablets. US6117451 A. Sep 12, 2000.
[84] Friedman R. Pharmaceutical quality systems: US perspective. In, Pharmaceutical quality system (ICH Q10) conference: Brussels, Belgium., 2011.
[85] Brian AC. Direct compression and the role of filler-binders, Volume 2: Rational Design and Formulation. In, Pharmaceutical Dosage Forms: Tablets. Informa Healthcare, 2008; pp. 173-216.
[86] Qu L, Zhou Q, Gengenbach T, Denman JA, Stewart PJ, Hapgood KP, Gamlen M, Morton DAV. Investigation of the potential for direct compaction of a fine ibuprofen powder dry-coated with magnesium stearate. Drug Dev Ind Pharm 2014: 1-13.
[87] More PK, Khomane KS, Bansal AK. Flow and compaction behaviour of ultrafine coated ibuprofen. Int J Pharm 2013; 441(1-2): 527-34.
[88] Olsson H, Mattsson S, Nyström C. Evaluation of the effect of addition of polyethylene glycols of differing molecular weights on the mechanical strength of sodium chloride and sodium bicarbonate tablets. Int J Pharm 1998; 171(1): 31-44.
[89] Skinner GW, Harcum WW, Barnum PE, Guo J-H. The evaluation of fine-particle hydroxypropylcellulose as a roller compaction binder in pharmaceutical applications. Drug Dev Ind Pharm 1999; 25(10): 1121-1128.
[90] Alvarez-Lorenzo C, Gómez-Amoza JL, Martínez-Pacheco R, Souto C, Concheiro A. Evaluation of low-substituted hydroxypropylcelluloses (L-HPCs) as filler-binders for direct compression. Int J Pharm 2000; 197(1–2): 107-116.
[91] Hersey JA. Ordered mixing: A new concept in powder mixing practice. Powder Technol 1975; 11(1): 41-44.
[92] Katharina. M. Picker-Freyer., Thomas. Dürig. Physical mechanical and tablet formation properties of hydroxypropylcellulose: In pure Form and in mixtures. AAPS PharmSciTech 2007; 8(4).
[93] Kabir MA, Reo JP. Hydroxypropylcellulose. In: Rowe RC, Sheskey PJ, Quinn ME, Eds., Handbook of pharmaceutical excipients. 6th ed., Washington D.C., USA: Pharmaceutical Press, 2009; pp. 317-322.
[94] Hapgood KP, Obara S. Hydroxypropylcellulose, Low-substituted. In: Rowe RC, Sheskey PJ, Quinn ME, Eds., Handbook of pharmaceutical excipients. 6th ed., Washington D.C., USA: American Pharmacists Association, 2009; pp. 322-324.
[95] Li Q, Rudolph V, Weigl B, Earl A. Interparticle van der Waals force in powder flowability and compactibility. Int J Pharm 2004; 280(1–2): 77-93.

[96] Xie HY. The role of interparticle forces in the fluidization of fine particles. Powder Technol 1997; 94(2): 99-108.

[97] de Villiers MM, Lötter AP, van der Watt JG. Influence of surfactants and interactive mixing on the cohesiveproperties of a poorly wettable solid. Powder Technol 1993; 75(2): 159-165.

Chapter 2
Literature Review

***Parts of this chapter have been published as:**

Review

Mangal S, Meiser F, Morton DAV, Larson I, Particle engineering of excipients for direct compression: Understanding the role of material properties. Cur Pharm Des. 2015;21(40):5877-89.

Book chapter

Mangal S, Meiser F, Morton DA, Larson I. Particle engineering of polymers into multifunctional interactive excipients. In: Thakur VK, Thakur MK, Eds., Handbook of Polymers for Pharmaceutical Technologies, Scrivener Publishing LLC, 2015;1–32.

2 Declaration for Thesis Chapter 2

Declaration by candidate

In the case of Chapter 2, the nature and extent of my contribution to the work was the following:

Nature of contribution	**Extent of contribution (%)**
Writing the manuscript	75%

The following co-authors contributed to the work. If co-authors are students at Monash University, the extent of their contribution in percentage terms must be stated:

Name	**Nature of contribution**	**Extent of contribution (%) for student co-authors only**
Felix Meiser	Revision	5%
David AV Morton	Revision	10%
Ian Larson	Revision	10%

The undersigned hereby certify that the above declaration correctly reflects the nature and extent of the candidate's and co-authors' contributions to this work*.

Candidate's Signature	[redacted]	**Date 23.11.2015**
Main Supervisor's Signature	[redacted]	**Date 24/11/15**

*Note: Where the responsible author is not the candidate's main supervisor, the main supervisor should consult with the responsible author to agree on the respective contributions of the authors.

2.1 Abstract

Tablets represent the preferred and most commonly dispensed pharmaceutical dosage form for administering active pharmaceutical ingredients (APIs). Minimizing the cost and improving manufacturing output efficiency has motivated companies to use direct compression as a preferred method of tablet manufacturing. Excipients dictate the success of direct compression, notably by optimizing powder flow and compactability, thus there has been a surge in creating excipients specifically designed to meet these. Greater understanding of the tablet manufacturing process and particle engineering has allowed development of improved direct compression excipients. Despite this, significant practical disadvantages of direct compression remain relative to granulation, and this is partly due to the limitations of direct compression excipients. For instance, in formulating high-dose APIs, a high level of excipients is required and so tablets are likely to be much bigger. Creating improved excipients to enable direct compression of high-dose APIs requires knowledge of the relationship between fundamental material properties and excipient functionalities. In this chapter, we review the current understanding of the relationship between fundamental material properties and excipient functionalities for direct compression.

Keywords: Tableting, Excipients, Inter-particle interaction, Flow, Compactability, Direct compression

2.2 Tablets

Tablet manufacturing involves two main steps viz., filling of powder into the die followed by compression. Appropriate powder flow is necessary to achieve rapid and reproducible die filling, poor flow can potentially obstruct this process leading to unacceptably large dose variations [1]. The second important step in tablet manufacturing is compression of powders into the tablets of an optimum tensile strength [2]. The tensile strength relates to the mechanical integrity of the tablets [3], which determines their ability to withstand post compression operations such as coating, packaging, storage, transport and patient handling etc. Optimal tensile strength must also allow tablets to exhibit desirable API dissolution/release behaviour [4-6].

The majority of APIs, for example paracetamol, metformin, ibuprofen and ascorbic acid, lack the flow and/or compactability suitable for direct compression tablet manufacturing [7-14]. Thus, excipients are incorporated to improve compactability and flow [15-17]. The excipients used to improve flow and compactability are generally described as glidants (or flow additives) and binders (or filler-binders), respectively [15-17]. Tablet formulations may also contain other excipients such as lubricants to prevent material sticking to the die thus facilitating ejection [18] and disintegrants to enhance tablet disintegration [19].

The uniform mixing of excipient(s) with the API(s) is necessary to ensure optimum excipient performance as well as content uniformity. Therefore, the API/excipients blend should also achieve excellent content uniformity in addition to adequate flow and compactability [20, 21].

2.3 Tablet manufacturing methods

Wet granulation, dry granulation and direct compression are the most commonly used methods of tablet manufacturing. In both wet and dry granulation methods, API and excipient powders are agglomerated into larger secondary aggregates referred to as granules. Granulation should significantly improve both the flow and compactability of the formulation [22-25]. In addition, API and excipients are physically bound together in granules, so segregation tendency is negligible which ensures content homogeneity [22-25].

In the wet method, granulation is promoted by the addition of a liquid (with and without binder) followed by heat drying (see Figure 2.1); while in dry granulation, the API/excipient blend is compressed in a roller compacter into ribbon-like structures, which are then milled into granules (see Figure 2.1) [26]. In both processes, the granules are compacted into tablets. Dry granulation is preferred over wet granulation for heat and water/moisture sensitive APIs as neither additional heat nor water is needed [27, 28]. However, both wet and dry granulation methods require a number of unit prior to tablet manufacturing, which may significantly add to the cost, time and complexity of tablet manufacturing.

Direct compression involves blending of API and excipients followed by compression without any prior granulation (see Figure 2.1). The number of unit operations involved in direct compression is less than granulation-based methods. Therefore, direct compression is a relatively simple and cost-effective method, and is thus preferred [29]. In addition, direct compression does not utilise heat and moisture and thus is considered suitable for heat and water labile APIs [2].

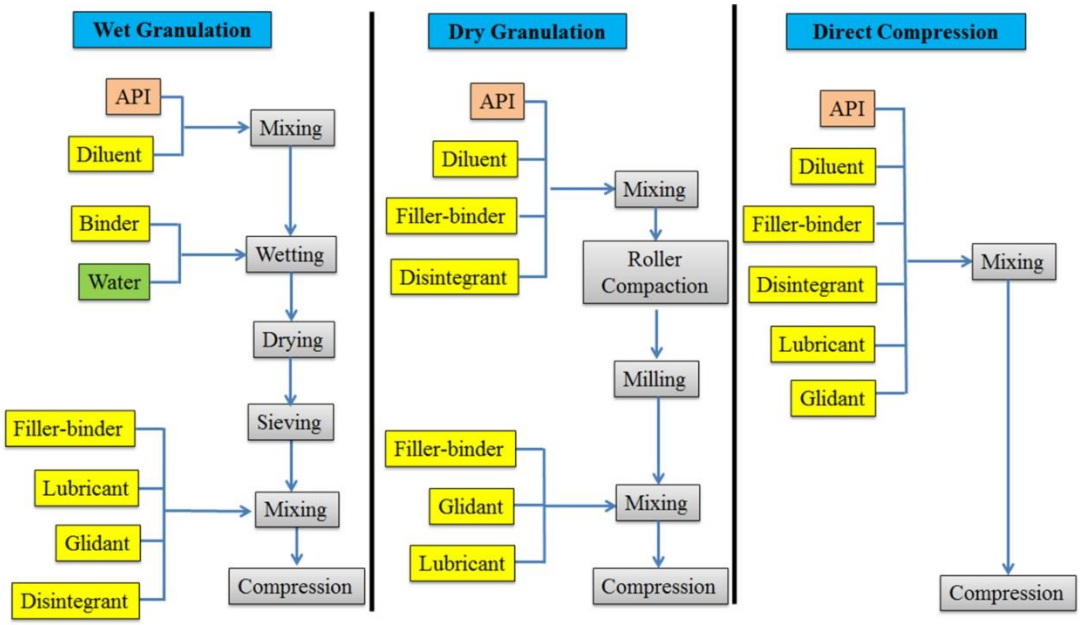

Figure 2.1 – The typical steps involved in wet granulation, dry granulation and direct compression tablet manufacturing [2]. Adapted and modified from Armstrong, 2005

2.4 The role of excipients

In wet and dry granulations, the properties of the API/excipient blends are partly altered by granulation. So, not only the excipients but also the blend processing (to form granules) significantly contribute towards achieving optimum formulation performance [23-25]. Conversely, the properties of the starting materials are unaltered in direct compression and thus have a profound impact on the behaviour (i.e., flow and compactability) of the resultant formulation. Additionally, the API and excipient particles are not bound together (as in granules) in direct compression blends, thus there is greater risk of segregation during handling and tableting [2, 30, 31]. Therefore, the properties of the starting materials (both APIs and excipients) greatly affect the content uniformity, flow and compactability of direct compression formulations [32, 33]. For poorly flowable and difficult to compact APIs, formulation performance i.e., flow and compactability mainly depends on excipients. Therefore, the excipients used in direct compression should enhance formulation performance to ensure

efficient tablet manufacturing [15, 34-37]. This has motivated scientists to create/engineer improved excipients for direct compression.

2.5 Excipients for direct compression

The common objective of excipient engineering is to achieve improved flow, compactability (flow and compactability are discussed in section 2.7) and dilution potential to make them suitable for direct compression [15, 32]. Dilution potential relates to the amount of excipient required to achieve optimum compactability [38-40]. Two models have been put forward to understand the relationship between the amount of excipient (typically a binder or a filler-binder) incorporated and the corresponding increase in tensile strength (see Figure 2.2) [41]. The first model suggests that the excipients are required to fill inter-particle voids in the tablets to give optimum tensile strength [41]. However, it is very difficult to form tablets without voids except in the case of very plastic materials [42]. Additionally, there is no guarantee that the excipient particles would specifically fill the voids in the tablets of API [41]. The second model suggests that there needs to be a monolayer of excipient particles around each API particle to give optimum tensile strength. However, this hypothesis assumes that the excipient added to a mixture will coat the API particles, while the excipient particles are actually randomly distributed in the mixtures unless specific inter-particle interactions facilitates adhesion of excipient to the API particles. Thus, both models have limitations and neither have been shown to accurately predict the amount of excipient needed for achieving maximum tensile strength [41, 43]. Therefore, the dilution potential of excipients is determined more traditionally by experimentally determining the improvement in compactability of poorly compactible APIs (e.g. paracetamol or ascorbic acid) achieved as a function of excipient proportions [38-40].

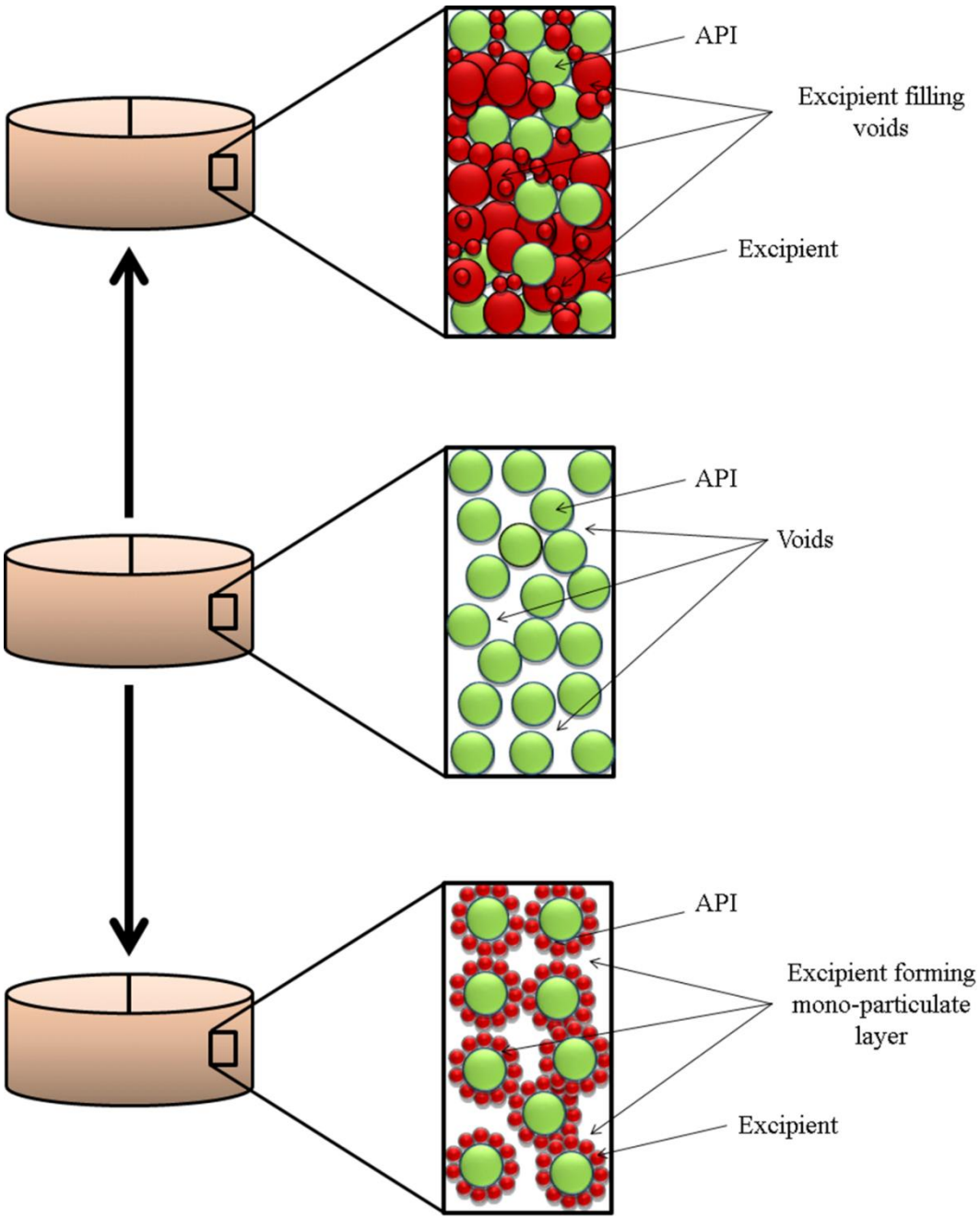

Figure 2.2 – Representation of models of the relationship between the amount of excipient and the corresponding increase in tensile strength

2.6 Engineering improved excipients

Improved excipients can be created either by synthesizing new excipients or by improving existing excipients [44]. The development of new chemical excipients requires extensive toxicology tests [45-47]. This is a costly preposition and so, in the last three decades, only a

few such new chemical excipients have been introduced in the market [48]. However, the excipients created by physical manipulation of existing generally regarded as safe (GRAS) excipients are also considered safe provided such physical manipulation does not give rise to any chemical change [49]. Thus, such physically modified excipients do not require expensive and lengthy safety and toxicity studies [45-47].

Physical manipulation involves the modification of existing excipients at particle and sub-particle levels (see Figure *2.3*). Modification of particle properties such as shape, size and size distribution, morphology and porosity is considered as particle-level manipulation [50]. The physical combination of two or more excipients *via* co-processing is considered as sub-particle level manipulation. Such manipulations are considered to affect excipient functionalities such as flowability, compactability and dilution potential [51, 52]. A number of excellent reviews have compiled the ways of creating directly compressible excipients and the improvement in performance achieved [7, 17, 50, 53-55]. However, the motive of this chapter is to review studies investigating how fundamental material properties contribute to excipient functionalities such as flow and compactability and the limitations of directly compressible excipients in high-dose APIs. In addition, we have also reviewed research efforts improve the tabletability of high-dose APIs.

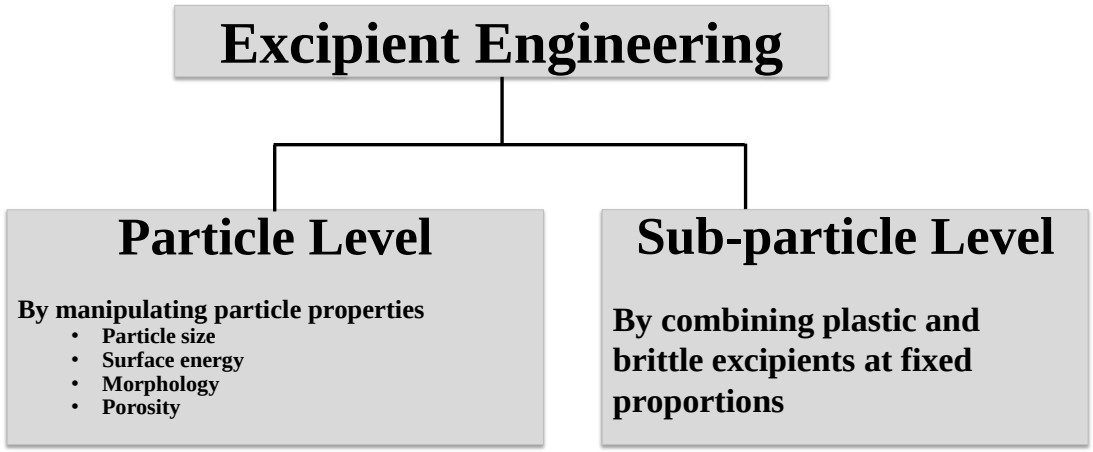

Figure 2.3 – Particle and sub-particle level pathways of excipient engineering

2.7 Fundamental material properties, compactability and flow

The term compactability describes the ability of a powder to form tablets i.e., the ability of a powder to compress into tablets of specified tensile strength [56, 57]. Powder compactability has been proposed to depend on the magnitude of inter-particle forces which hold the particles together in tablets [57, 58]. Other commonly used terminologies to describe the ability of a powder to form tablets are compressibility, and tabletability. Compressibility is the effect of compaction pressure on tablet porosity, and tabletability is the relationship between compaction pressure and tensile strength [56, 57].

In general, powder flow can be defined as the movement of particles relative to adjacent particles and/or surfaces [59]. For larger particles, gravity is generally greater than the inter-particle forces, hence they normally flow easily [60-62]. However, many smaller particles experience stronger inter-particle forces compared to gravity, thus such particles are cohesive and exhibit poor flow [62-64]. Therefore, like compactability, powder flow also depends on the magnitude of inter-particle forces [65, 66].

The magnitude of inter-particle forces is a result of the type of inter-particle bonds and the contact area over which these bonds are active (see

Figure *2.4*). Thus, both flow and compactability also depend on the type and the area of inter-particle interactions [57, 66-68]. Fundamental material properties such as physico-chemical and mechanical properties such as particle size, morphology and surface energy have been proposed to affect the type and area of inter-particle forces [69].

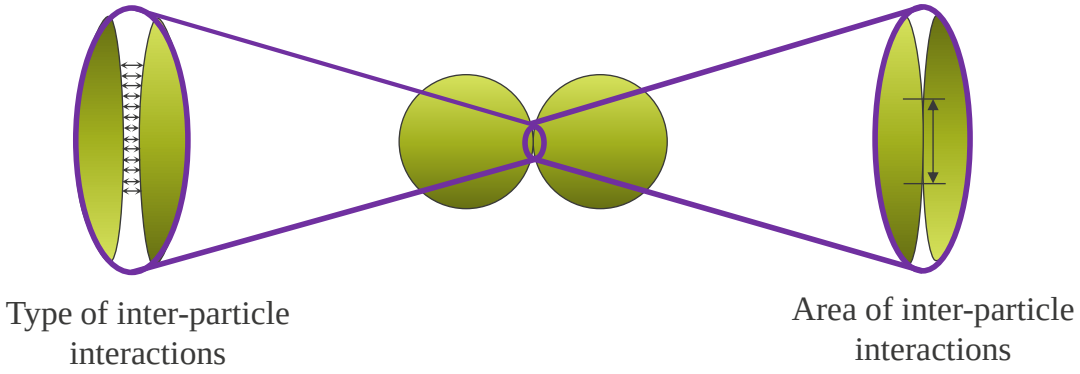

Figure 2.4 – Strength and area of inter-particle interactions

2.8 Types of inter-particle interactions

The most common types of forces that exist at particle-particle interfaces include solid bridging, capillary forces, mechanical interlocking (hooking and twisting of particles) and/or inter-molecular forces [58, 70, 71]. Additionally, surface energy has also been proposed to affect inter-particle bond strength [72, 73], which is also discussed here.

2.8.1 Solid bridging

Solid bridging represents the fusion of particles leading to the formation of a continuous solid bridge between particles [67]. It may be a result of partial melting, self-diffusion of atoms and/or recrystallization of solid material at particle-particle contact points [74-77]. Solid bridges are the strongest inter-particle bonds [67]. Thus, tablets in which particles bond *via* solid bridging also exhibit an retarded disintegration time [78]. Solid bridging is more important in the context of compactability than flow [74, 79]. Laboratory studies have shown that sodium chloride tends to form solid bridges at compression pressures of 100, 200 and 250 MPa [80]. It has also been proposed that plastic but not brittle materials tend to bond *via* solid bridging because brittle materials tend to fragment under compression which does not allow large stresses at inter-particulate contact points to be created [80]. Additionally, amorphous

materials are more likely to bond *via* solid bridges and the presence of moisture in a tablet increases the likelihood of solid bridges developing [78, 81]. Solid bridging typically increases with increasing particle size and compaction pressure [80].

2.8.2 Capillary forces

At higher relative humidities, water vapour in inter-particle spaces can condense on particle interfaces leading to the formation of liquid bridges. Such bridges affect inter-particle interactions and are referred to as capillary forces. They are also very strong attractive inter-particles forces [82, 83]. Capillary forces can affect both the flow as well as compactability to a considerable extent [84-87]. In general, an increase in capillary forces improves material compactability but deteriorates flow [83]. However, capillary forces mainly affect inter-particle interactions at environmental humidity exceeding 65% RH [88, 89].

2.8.3 Mechanical interlocking

Particles with extremely rough surfaces may also interact mechanically *via* interlocking due to hooking and/or twisting of particles together. This can increase inter-particle attraction forces [78]. The materials which bond predominantly by this mechanism can have low compact strength and lengthy disintegration times [78]. Furthermore, mechanical interlocking may also compromise powder flow, if surfaces are extremely rough [90].

2.8.4 Long-range forces

Forces such as electrostatic forces, van der Waals forces and hydrogen bonds are examples of long-range forces. These forces are active when the distance between the particles is between 1-10 nm [80, 91].

2.8.4.1 Electrostatic forces

Particles may build charge at their surfaces, when rubbed against surfaces [92]. When two charged particles approach one another, they either attract or repel each other depending on their charge. These forces are referred to as electrostatic forces. Electrostatic forces are relatively weak (compared to van der Walls forces [83]) and are believed to contribute insignificantly to the tensile strength of tablets [67, 93], as surface charge can neutralize/diffuse relatively quickly over time and with exposure to normal humidity [94].

2.8.4.2 Van der Walls forces

Van der Waals forces arise due to electrical dipoles in atoms thus represent ubiquitous inter-particle forces. These forces are considered as the principle forces governing particle-particle interactions [83, 95]. Therefore, emphasis is place on understanding the role of these forces on material flow and compactability [65, 91, 96] [97, 98]. It is generally agreed that strong van der Waals force are associated with improved compactability but poor flow and *vice-versa* [67, 97-99]. Numerous theoretical models have been developed to quantify the strength of van der Waals forces [58, 72, 73, 93, 100].

2.8.4.3 Hydrogen bonding

Some pharmaceutical materials such as microcrystalline cellulose and sucrose bond *via* hydrogen bonding under compression. Hydrogen bonds are also considered as relatively strong inter-particle bonds [34, 67]. However, the effect of these bonding forces on flow behaviour is not understood.

2.8.5 Surface energy

Inter-particulate forces are also a function of the surface energy of particles [72, 73]. Surface energy depends on a number of factors such as chemical nature, crystal polymorph etc. [97, 101-103]. Pharmaceutical powders exhibit surface energy heterogeneity i.e., there is a distribution of surface energies depending upon sample variability [101, 104, 105]. Pharmaceutical crystals consist of organic molecules and generally each face, edge and defect of a crystal has different proportions of chemical functional groups that are present at the surfaces of a single particle, which may give rise to surface energy heterogeneity [105, 106]. The surface energy ultimately affects inter-particle interactions, which affects material properties such as compactability [67] and powder flow [103].

Previous studies have investigated the relationship between compactability and surface free energy [97, 98, 107]. A linear relationship was found between surface free energy (literature values) and the tensile strength of pharmaceutical materials such as aspirin, griseofulvin, indomethacin, magnesium stearate, potassium chloride, sodium chloride and phenacetin [107]. A reduction in surface energy of lactose *via* surface coating with polysorbate 80 has also been shown to result in a reduction in compactability. However, at higher compaction forces, the effect of surface energy on compactability decreased [97]. This was attributed to the formation of solid bridges as the strength of these bridges is independent of surface energy [97].

The flow improvement achieved by surface coating with glidant particles has been shown to be associated with reduced surface energy [68]. This was attributed to the preferential adhesion of small particles to high-energy sites on cohesive particles reducing the net surface free energy [108-111]. Micronization has been reported to increase the surface energy of

particles, which was proposed to have detrimental effect on their flow [103]. However, there is little published direct evidence of a relationship between surface energy and powder flow.

2.9 Inter-particle bonding area

Inter-particle bonding area is the effective surface area over which the inter-particle forces act [67]. Particles can deform under the influence of inter-particle as well as external forces, thus the true area of inter-particles contact is difficult to accurately estimate [112]. The effect of contact area on compactability and flow is traditionally assessed by investigating particle properties such as physico-mechanical behaviour (elastic/plastic and brittle deformation), size and surface morphology [67].

2.9.1 Physico-mechanical behaviour

Particles tend to compress *via* either plastic/elastic deformation or brittle fracture (see Figure 2.5) or by a combination of these mechanisms [36]. Table 2.1 lists some pharmaceutical materials with characteristic brittle or plastic compression behaviours. Compression of brittle materials results in a substantial reduction in particle size due to particle fracture. This creates greater area for inter-particle bonding. Elastic materials tend to undergo reversible deformation, while plastic materials deform permanently with the creation of larger areas for inter-particle

bonding [67]. Therefore, materials with greater plasticity offer larger areas for inter-particle bonding and hence exhibit higher compactability compared to more elastic materials [113].

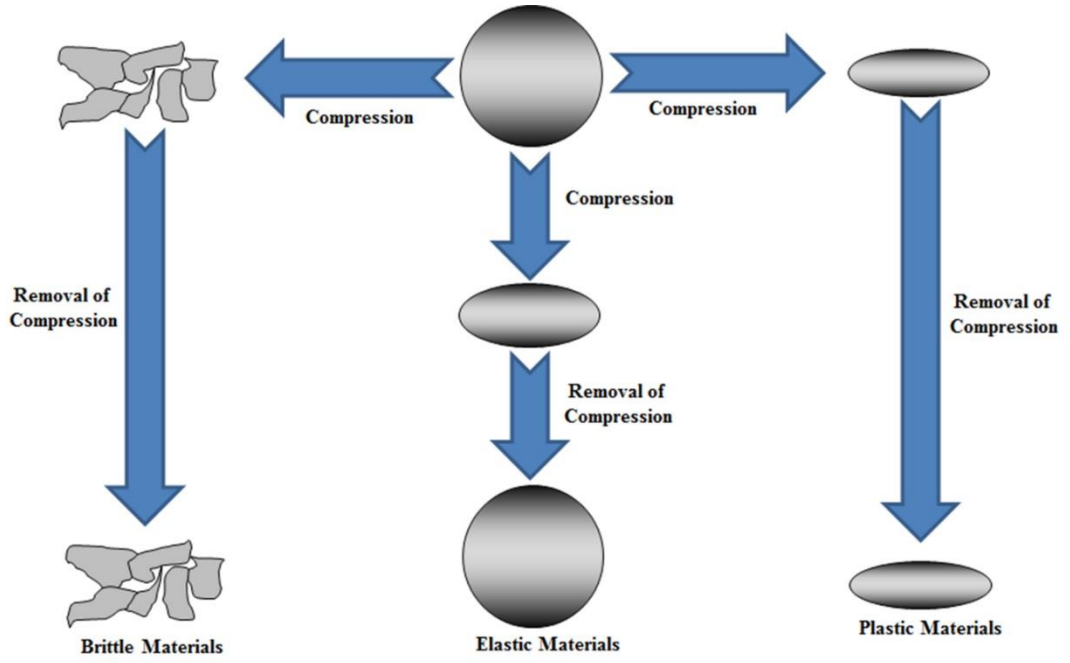

Figure 2.5 – Compression behaviour of plastic, elastic and brittle materials

Plastic materials are also generally believed to exhibit better compactability than brittle materials [15, 32, 38, 39, 57]. For example, plastic microcrystalline cellulose (MCC) exhibits higher compactability than brittle dicalcium phosphate (DCP) [38]. During compaction, brittle particles fracture to cause an increased total surface area available for bonding. However, if the fragments do not deform plastically after fracture (i.e., they only deform elastically), a strong tablet may not be formed. Thus, plastic deformation is considered vital to achieve optimal tensile strength [57].

Table 2.1 – Physico-mechanical behaviour of some pharmaceutical materials

Physico-mechanical behaviour	Name of excipients

Plastic	Polyvinylpyrrolidone (PVP) [114], Polyethylene glycol (PEG) [114], Sodium bicarbonate [43], Sodium chloride [115], Vinylpyrrolidone-vinyl acetate copolymers (Kollidon VA 64) [116], MCC [42], Inulin [117, 118], Isomalt [119, 120], Sorbitol [121], Chitin [121]
Brittle	DCP [122, 123], Xylitol [124], Fumed colloidal silicon dioxide [125], Sucrose [126], Mannitol [127], α-lactose monohydrate [121, 128]

The compactability of plastic materials reduces substantially due to surface lubrication with materials such as magnesium stearate [129-133]. It was proposed that the lubricants are low bonding materials and form a film around the materials which interferes with the inter-particle bonding of such materials and hence compromises their compactability [102, 129, 132]. This phenomenon is termed as "lubricant sensitivity". In contrast, brittle excipients exhibit limited sensitivity to surface lubrication as they fragment and therefore create new lubricant-free surfaces which can participate in inter-particle bonding [50, 130]. In fact, lubricated powders may surprisingly exhibit higher compactability due to lubricant related efficient packing behaviour of powders during compaction [134].

In addition, plastic materials deform in a time dependent manner and are typically referred to as viscous or viscoelastic material [135]. A change in the compression speed significantly affects the deformation of such materials [136, 137]. At higher compression speeds, the time available for plastic materials to deform is shorter [136-138]. This leads to higher elastic recovery which reduces the area of inter-particle bonding and consequently the compactability [136-138]. For example, the pressure at which MCC deforms plastically

increases with the speed of compression because of a reduction in the amount of plastic deformation caused by the time-dependent nature of plastic flow [136]. This is termed "strain-rate sensitivity". This can be determined by measuring the relative difference between yield pressure values at a high and low compression speed [136]. Unlike plastic materials, fragmenting material are less sensitive to the variations in compression speed [136-138].

For materials to deform plastically, it is important that the applied pressure exceeds their yield pressure (the pressure above which plastic materials tend to deform plastically and below which they are predominantly elastic) [136-138]. For crystals, these mechanical properties are determined by their structures. Dislocation and the presence of multiple slip planes, especially those involving flat slip planes, determine how easily a crystal undergoes plastic deformation [57, 139]. However, for amorphous materials, the difference between their glass transition temperature (Tg), and the experimental temperature determines their mechanical behaviour [140]. When their Tg is above the experimental temperature, amorphous materials are in the glassy state and exhibit greater resistance to deformation. However, materials change from a glassy to a more plastic structure and the resistance against deformation decreases dramatically when the Tg is close to the experimental temperature [141]. In consequence, the deformability and hence the compactability of such plastic materials strongly depend on their Tg [140].

Physico-mechanical properties such as particle deformation (plastic/elastic) may also influence flow. It has been proposed that the particles can also deform plastically at particle-particle contact points under the influence of inter-particle forces [112]. This can increase the area of inter-particle contacts and consequently affect flow. The magnitude of deformation at the contact point depends on the particle size, as smaller particles exhibit greater resistance to

deformation compared to larger particles [65, 142]. Thus, both consolidation force and inter-particle forces can significantly influence flow.

2.9.2 Particle size

A number of studies have investigated the relationship between particle size and compactability. The compactability of plastic materials increases as particle size is reduced [115, 143-145]. This was attributed to the larger surface area of smaller particles, which offer larger areas for inter-particle interaction compared with larger particles. Conversely, the compactability of brittle materials is typically independent of their particle size. This was attributed to the tendency of these materials to fracture during compaction, which negates the influence of such differences in initial particle size [143, 146]. As discussed earlier, every material exhibits a characteristic mechanical behaviour, however, changes in particle size may also lead to changes in mechanical behaviour of materials, for example, from plastic to rigid or brittle to plastic [123, 147-149]. Particle size also affects the flow and smaller particles typically exhibit poor flow [62-64].

The binder efficiency of plastically deformable materials improves with a reduced particle size, indicating a relationship between surface area and binder activity [43, 114, 150]. Hence, attempts have been made to improve binder activity of excipients by reducing their particle size. This has resulted in the production of several excipients in fine and extra-fine grades. Such excipients are indeed shown to exhibit improved binder activity compared to their larger counterparts [150, 151]. However, the reduction in particle size also decreases the flow [152-154]. This is especially important in direct compression, where excipients critically affect the flow performance of the formulations. In addition, blending large API and smaller excipients may potentially result in segregation during operations (unless true interactive blending is achieved) [32].

2.9.3 Surface morphology

Particle shape and surface roughness have also been argued to affect compactability. Particles with irregular shape and higher surface roughness are proposed to favour plastic deformation because of the higher degree of surface asperities and crystal defects, and thus exhibit greater compactability [145, 155, 156]. In contrast, the compactability of brittle materials is less affected by particle shape and surface texture [143, 155, 156]. For example, plastically deforming materials such as microcrystalline cellulose and sodium chloride experienced reduced bonding strengths as their surface roughness decreased. However, the bonding strengths of brittle materials such as lactose and calcium phosphate were insensitive to particle roughness since the area of contact was maximized after fracture [155].

The surface morphology of particles can also affect flow by affecting the area with which particles are in contact with each other. Rough particles have reduced surface area available for inter-particle interactions compared to smooth particles, thus they can exhibit lower cohesion and better flow [65]. Except for the case of excessively rough surfaces which may inhibit flow due to mechanical interlocking of particle [90]. It has been proposed that a glidant (silicon dioxide) may improve the flow of cohesive particles by adhering to them and reducing the contact area [66]. The contact area in such blends is also shown to be proportional to the diameter of glidant particles, where smaller glidants were shown to exhibit better flow improvements [63, 66]. In this context, when the surface coverage is very low the flow improvements are negligible [63]. However, as the surface coverage is increased, substantial flow improvement can be achieved [63, 64, 68, 157-160]. A minimum surface coverage of 40 % has been proposed for efficient flow improvement [161]. Some studies have suggested that inter-particle forces may be minimized by altering the surface morphology and creating rough/corrugated particles [104, 162-164].

2.10 Relationship between compactability and flow

Clearly, both contact area and strength of inter-particle interactions are critical factors affecting compactability and flow. Reducing the contact area and strength of inter-particle interactions improves flow but compromises compactability. In contrast, increasing the contact area and strength of inter-particle interactions improves compactability but compromises flow. For example, compactability may be increased by reducing particle size or by reducing the elasticity, while improving flowability requires the opposite changes.

Flow and compactability can therefore be seen as two competing objectives (see Figure 2.6). Thus, there appears to be a fundamental contradiction in creating direct compression excipients with improved flow and compactability. Therefore, functionality can only be improved to a certain extent *via* particle-level manipulation of existing excipients [53]. For example, the flow of Avicel® PH-200 is improved by increasing particle size but its compactability is lower compared to Avicel® PH-101 [165].

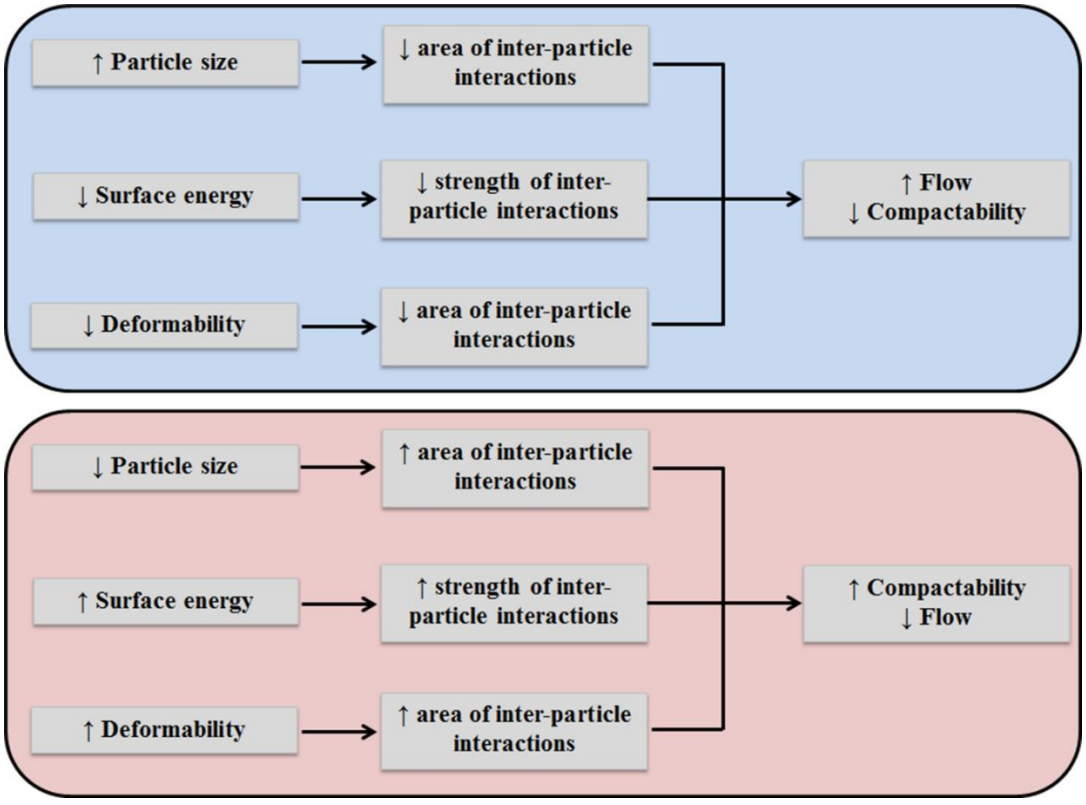

Figure 2.6 – Relationship between flow and compactability

2.11 Co-processed excipients

As discussed earlier, improved excipients can also be created by co-processing two or more excipients at sub-particle level to synergistically combine their functionalities and mask the undesirable properties of individual excipients [44]. These co-processed excipients were created with the aim to address this contradiction and achieve a balance of both good flow and compactability [50, 53, 166, 167]. In such excipients, plastic materials are incorporated to impart excellent binder activity, while brittle materials are incorporated to allow fracture of excipient particles under compression to create larger contact area for inter-particle interaction. This allows the initial particle size to be kept large to assist flow without affecting the area available for binding action under compression [50, 168]. In addition, plastic materials could impart excellent binder activity, while brittle materials could minimize the sensitivity of excipient to speed of compression and surface lubrication [32, 169-172]. Thus, the combination of plastic and brittle materials could maximize compactability and flow whilst minimizing the effect of lubrication and compression speed on intrinsic excipient compactability [20, 32].

These co-processed excipients are generally found to be superior to the physical mixture of their constituting excipients in the same proportions [124, 173-181]. In theory, a balance of brittle and plastic properties should be complementary but in practice the inferior bonding of the brittle materials (which are generally incorporated in larger proportions to plastic materials (see Table 2.2)) reduces the binder efficiency [15]. For instance, cellactose could not produce tablets of minimum acceptable tensile strength (1.7 MPa [6]) with as low as 37.5 % w/w of paracetamol [178]. Ludipress exhibit lower dilution potential than Avicel PH® 101 [174].

To overcome the poor binding caused by relative high proportions of brittle materials, an excipient with high proportions of plastic material (MCC- 98 %) and low proportions of brittle material (colloidal silicon dioxide- 2 %) has also been tested in direct compression [33, 125, 182]. This excipient (SMCC) demonstrated lower sensitivity to lubricant and speed of compression but caused no change in tensile strength compared to physical mixtures of MCC and colloidal silicon dioxide [171]. In addition, the tensile strength of tablets consisting of SMCC (Prosolv®) and ascorbic acid dropped below 1.7 MPa with 50 % w/w ascorbic acid [125]. It has been argued that MCC is currently the optimum binder [15, 32, 39, 183, 184], and this is attributed to its ability to deform plastically and to bond *via* hydrogen bonds [185, 186]. However, SMCC has also been argued to exhibit superior binder properties compared to MCC for some APIs and nutritional products. Others have reported Kollidon® VA 64 as the most effective binder due to its low Tg, which results in high plasticity [116].

Table 2.2 – Compositions of some commercial directly compressible co-processed excipients

Excipient	**Composition**		**References**
	Brittle Material	**Plastic Material**	
Ludipress	93% α-lactose monohydrate	3.5% PVP + 3.5 % Cross-linked PVP	[169, 174]
Cellactose	75 % α-lactose monohydrate	25 % Cellulose powder	[168, 187]
MicoceLac	75 % α-lactose monohydrate	25 % MCC	[168, 177]
Starlac	85 % α-lactose monohydrate	15 % Maize starch	[50, 188]

2.12 High-dose APIs

Current directly compressible excipients generally exhibit relatively low binder efficiency/dilution potential. Thus, they are ineffective at improving the compactability of APIs at high API proportions [189-192]. These excipients are only effective at improving compactability when incorporated in large proportions (usually > 40%) [189-192]. The use of excipients in such large proportions may lead to limitations, such as unacceptably large tablets, content uniformity issues and a greater risk of excipient related quality variations [12, 48, 193-197]. For example, MCC, despite its excellent binder action, could not be effectively used for creation of acceptable tablets containing paracetamol by direct compression [198]. At low proportions, the tablets were fragile and prone to capping tablets. Coherent tablets were only achieved at higher proportions of MCC making the size of tablets impractically large [198]. Thus, the direct compression process almost invariably applies to formulations containing potent/low to medium dose APIs [2, 17]. However, high-dose APIs with inherently poor compactability, for example paracetamol, metformin, ascorbic acid and aspirin, are difficult to be directly compressed into intact tablets with sufficient tensile strength [8, 9, 12, 107, 198]. Consequently, formulation scientists are often forced to struggle with challenges created by poor API mechanical properties, a leading cause of delay in development and manufacturing of tablet products [199].

Attempts have been made to modify API properties to improve their suitability for tablet manufacturing, for example, *via* crystal engineering to enhance their compaction properties [10, 139, 200-203]. However, engineering crystal API properties is considered less practical industrially as the new crystal form needs safety/toxicity assessment for regulatory approval which may significantly delay commercialization [193]. In addition, each API has a limited number of crystal forms which may or may not have satisfactory compactability [204].

Recently, the surface coating of poorly compactible materials with highly bonding polymers such as hydroxypropyl cellulose and PVP was shown to profoundly improve compactability. It was proposed that the surface coating allows replacement of weak inter-particle bonds between poorly compressible materials with stronger polymer-polymer interactions [189, 193]. However, the effect of such a coating on flow performance was not evaluated. Dry coating the surface of ibuprofen with silicon dioxide has also been shown to not only improve flow but also compactability. It was shown that the blends containing as much as 70 % API resulted in satisfactorily tablets [205]. However, colloidal silica is not a good tableting lubricant. Dry coating ibuprofen with magnesium stearate has also been shown to improve flow but reduce compactability. However, this strategy showed that blends containing up to 80 % API could be successfully tableted [206]. It was also shown that the interactive mixing of ultrafine ibuprofen particles improved the compactability of large ibuprofen particles, however, the flow performance deteriorated [207]. The interactive mixing of low cohesion, small excipient particles (< 5 μm) has been shown to improve the flow and compactability of a surface lubricated (magnesium stearate coated) pharmaceutical excipient at as low as 10 % w/w [208]. It was also proposed that co-spraying an excipient with L-leucine achieved both flow and compactability benefits [208]. These recent innovations may in time and with further research, understanding and optimisation, provide new opportunities to create new and improved strategies for direct compression.

2.13 Conclusion

Flow and compactability are two essential formulation attributes for efficient tablet manufacturing. Consequently, the excipients for direct compression are engineered to impart better flow and compactability. The magnitude of inter-particle interactions forces determines the flow and compactability. These forces need to be minimized for improved

flow performance; however, materials with low inter-particle interaction may exhibit poor compactability. Thus, the inter-particle forces should be optimally balanced to satisfy the need of particulate flow and compactability.

The success of direct compression tablet manufacturing lies in understanding the limitations of APIs and effectively overcoming these limitations by combination with suitable optimized excipients. Understanding the relationships between fundamental material properties and inter-particle interactions has resulted in the development of a number of improved excipients for direct compression. These efforts mainly involved physical manipulation of existing excipients. Typically, these excipients exhibit superior flow and compactability and are thus more suitable for direct compression. However, the majority of existing directly compressible excipients exhibit low dilution potential, which significantly limits their application especially in the case of poorly compactible and poorly flowable high-dose APIs. Thus, more efforts are required to create excipients suited to serve the needs of such APIs. In addition, it is equally important to achieve an optimum balance between functional improvement and cost. Continued successful development, optimisation and implementation of efficient excipients for high-dose API may significantly reduce the associated cost, time and complexity of tablet manufacturing.

2.14 References

[1] Sun CC. Setting the bar for powder flow properties in successful high speed tableting. Powder Technol 2010; 201(1): 106-108.

[2] Armstrong NA. Tablet manufacture by direct compression. In: Swarbrick J, Ed., Encyclopedia of pharmaceutical technology. 3rd ed, NY, USA: Informa Healthcare, 2007; pp. 3673-3683.

[3] Fell JT, Newton JM. Determination of tablet strength by the diametral-compression test. J Pharm Sci 1970; 59(5): 688-691.

[4] Kitazawa S, Johno I, Ito Y, Teramura S, Okado J. Effects of hardness on the disintegration time and the dissolution rate of uncoated caffeine tablets. J Pharm Pharmacol 1975; 27(10): 765-70.

[5] Kachrimanis K, Nikolakakis I, Malamataris S. Tensile strength and disintegration of tableted silicified microcrystalline cellulose: influences of interparticle bonding. J Pharm Sci 2003; 92(7): 1489-501.

[6] Pitt KG, Heasley MG. Determination of the tensile strength of elongated tablets. Powder Technol 2013; 238: 169-175.

[7] Rojas J, Buckner I, Kumar V. Co-proccessed excipients with enhanced direct compression functionality for improved tableting performance. Drug Dev Ind Pharm 2012; 38(10): 1159-1170.

[8] Cao X, Morganti M, Hancock BC, Masterson VM. Correlating particle hardness with powder compaction performance. J Pharm Sci 2010; 99(10): 4307-4316.

[9] Femi-Oyewo MN, Spring MS. Studies on paracetamol crystals produced by growth in aqueous solutions. Int J Pharm 1994; 112(1): 17-28.

[10] Sun C, Grant DJW. Influence of crystal structure on the tableting properties of sulfamerazine polymorphs. Pharm Res 2001; 18(3): 274-280.

[11] Garekani HA, Ford JL, Rubinstein MH, Rajabi-Siahboomi AR. Formation and compression characteristics of prismatic polyhedral and thin plate-like crystals of paracetamol. Int J Pharm 1999; 187(1): 77-89.

[12] Lakshman JP, Kowalski J, Vasanthavada M, Tong WQ, Joshi YM, Serajuddin ATM. Application of melt granulation technology to enhance tabletting properties of poorly compactible high-dose drugs. J Pharm Sci 2011; 100(4): 1553-1565.

[13] Armstrong NA. Selection of excipients for direct compression tablet formulations. Pharm Tech Eur 1997: 24-30.

[14] Modi SR, Khomane KS, Bansal AK. Impact of differential surface molecular environment on the interparticulate bonding strength of celecoxib crystal habits. Int J Pharm 2014; 460(1–2): 189-195.

[15] Carlin BAC. Direct compression and the role of filler-binders. In: Augsburger LL, Hoag SW, Eds., Pharmaceutical dosage forms: tablets. 3rd ed. Vol. 2, NY, USA: Informa Healthcare, 2008; pp. 173–216.

[16] Pifferi G, Santoro P, Pedrani M. Quality and functionality of excipients. Farmaco 1999; 54(1–2): 1-14.

[17] Jivraj M, Martini LG, Thomson CM. An overview of the different excipients useful for the direct compression of tablets. Pharm Sci Tech Today 2000; 3(2): 58-63.

[18] Peck GE, Baley GJ, McCurdy VE, Banker GS. Tablet formulation and design. In: Lieberman HA, Lachman L, Schwartz JB, Eds., Pharmaceutical dosage forms: Tablets. 2nd ed., NY, USA: Marcel Dekker, 1989; pp. 108–110.

[19] Late SG, Yu YY, Banga AK. Effects of disintegration-promoting agent, lubricants and moisture treatment on optimized fast disintegrating tablets. Int J Pharm 2009; 365(1-2): 4-11.
[20] Bolhuis GK, Armstrong NA. Excipients for direct compaction—an update. Pharm Dev Technol 2006; 11(1): 111-124.
[21] Guerin E, Tchoreloff P, Leclerc B, Tanguy D, Deleuil M, Couarraze G. Rheological characterization of pharmaceutical powders using tap testing, shear cell and mercury porosimeter. Int J Pharm 1999; 189(1): 91-103.
[22] Huang W, Shi Y, Wang C, Yu K, Sun F, Li Y. Using spray-dried lactose monohydrate in wet granulation method for a low-dose oral formulation of a paliperidone derivative. Powder Technol 2013; 246(0): 379-394.
[23] Ennis BJ, Parikh DM, Liu L. Theory of granulation: An engineering perspective. In, Handbook of pharmaceutical granulation technology. 3rd ed., NY, USA: Informa Healthcare, 2010; pp. 6-58.
[24] Kumar A, Gernaey KV, Beer TD, Nopens I. Model-based analysis of high shear wet granulation from batch to continuous processes in pharmaceutical production – A critical review. Eur J Pharm Biopharm 2013; 85(3, Part B): 814-832.
[25] Litster J, Ennis B. The science and engineering of granulation processes. In, ed. MA, USA: Kluwer Academic Publishers 2004; pp. 1-9.
[26] Meeus L. Direct compression versus granulation. Pharm Tech Eur 2011; 23 (3): 21-22.
[27] Bindhumadhavan G, Seville JPK, Adams MJ, Greenwood RW, Fitzpatrick S. Roll compaction of a pharmaceutical excipient: Experimental validation of rolling theory for granular solids. Chem Eng Sci 2005; 60(14): 3891-3897.
[28] Kleinebudde P. Roll compaction/dry granulation: pharmaceutical applications. Eur J Pharm Biopharm 2004; 58(2): 317-326.
[29] McCormick D. Evolutions in direct compression. Pharm Tech 2005; 5(4): 52–62
[30] Venables HJ, Wells JI. Powder mixing. Drug Dev Ind Pharm 2001; 27(7): 599-612.
[31] Swaminathan V, Kildsig DO. Polydisperse powder mixtures: effect of particle size and shape on mixture stability. Drug Dev Ind Pharm 2002; 28(1): 41-8.
[32] Bolhuis GK, Waard H. Compaction properties of directly compressible materials In: Alderborn G, Nystrom C, Eds., Pharmaceutical powder compaction technology. NY, USA: Marcel Dekker, 1996; pp. 419-500.
[33] Hentzschel CM, Sakmann A, Leopold CS. Comparison of traditional and novel tableting excipients: physical and compaction properties. Pharm Dev Technol 2012; 17(6): 649-53.
[34] Thoorens G, Krier F, Leclercq B, Carlin B, Evrard B. Microcrystalline cellulose, a direct compression binder in a quality by design environment—A review. Int J Pharm 2014; 473(1-2): 64–72.
[35] Kása P, Bajdik J, Zsigmond Z, Pintye-Hódi K. Study of the compaction behaviour and compressibility of binary mixtures of some pharmaceutical excipients during direct compression. Chem Eng Process 2009; 48(4): 859-863.
[36] Patel S, Kaushal AM, Bansal AK. Compression physics in the formulation development of tablets. Crit Rev Ther Drug 2006; 23(1): 1-66.
[37] Tho I, Bauer-Brandl A. Quality by design (QbD) approaches for the compression step of tableting. Expert Opin Drug Deliv 2011; 8(12): 1631-1644.
[38] Wells JI, Langridge JR. Dicalcium phosphate dihydrate–microcrystalline cellulose systems in direct compression tabletting. Int J Pharm Techol Prod Manf 1981; 2(2): 1-8.

[39] Habib Y, Augsburger L, Reier G, Wheatley T, Shangraw R. Dilution potential: a new perspective. Pharm Dev Technol 1996; 1(2): 205-12.
[40] Minchom CM, Armstrong NA. A proposed technique for expressing the capacity of directly compressible tablet diluents. J Pharm Pharmacol 1989; 39: 69.
[41] Olsson H, Mattsson S, Nyström C. Evaluation of the effect of addition of polyethylene glycols of differing molecular weights on the mechanical strength of sodium chloride and sodium bicarbonate tablets. Int J Pharm 1998; 171(1): 31-44.
[42] Sun CC. True density of microcrystalline cellulose. J Pharm Sci 2005; 94(10): 2132-4.
[43] Mattsson S, Nyström C. Evaluation of strength-enhancing factors of a ductile binder in direct compression of sodium bicarbonate and calcium carbonate powders. Eur J Pharm Biopharm 2000; 10(1): 53-66.
[44] Reimerdes D. The near future of tablet excipients. Manuf Chemist 1993; 64: 14-15.
[45] US food and drug administration, centre for drug evaluation and research, guidance for industry; Nonclinical studies for the safety evaluation of pharmaceutical excipients. 2005.
[46] Moreton RC. Tablet excipients to the Year 2001: A look into the crystal ball. Drug Dev Ind Pharm 1996; 22(1): 11-23.
[47] Pico RG, Sullivan TM. Regulation of pharmaceutical excipients. In: Katdare A, Chaubal M, Eds., Excipient development for pharmaceutical, biotechnology, and drug delivery systems. NY, USA: Informa Healthcare, 2006; pp. 37-50.
[48] Moreton C. Functionality and performance of excipients in a quality-by-design world part 2: Excipient variability, QbD and robust formulations. Am Pharm Rev 2009; 12: 40-45.
[49] Tobyn MJ, McCarthy GP, Staniforth JN, Edge S. Physicochemical comparison between microcrystalline cellulose and silicified microcrystalline cellulose. Int J Pharm 1998; 169(2): 183-194.
[50] Saha S, Shahiwala AF. Multifunctional coprocessed excipients for improved tabletting performance. Expert Opin Drug Deliv 2009; 6(2): 197-208.
[51] Ticehurst MD, Marziano I. Integration of active pharmaceutical ingredient solid form selection and particle engineering into drug product design. J Pharm Pharmacol 2015; 67(6): 782-802.
[52] Leane M, Pitt K, Reynolds G. A proposal for a drug product Manufacturing Classification System (MCS) for oral solid dosage forms. Pharm Dev Technol 2015; 20(1): 12-21.
[53] Nachaegari SK, Bansal AK. Coprocessed excipients for solid dosage forms. Pharm Tech 2004; 50(1): 52-64.
[54] Mirani AG, Patankar SP, Borole VS, Pawar AS, Kadam VJ. Direct compression high functionality excipient using coprocessing technique: a brief review. Curr Drug Deliv 2011; 8(4): 426-35.
[55] Gohel MC, Jogani PD. Exploration of melt granulation technique for the development of coprocessed directly compressible adjuvant containing lactose and microcrystalline cellulose. Pharm Dev Technol 2003; 8(2): 175-185.
[56] Leuenberger H. The compressibility and compactibility of powder systems. Int J Pharm 1982; 12(1): 41-55.
[57] Sun CC. Decoding powder tabletability: Roles of particle adhesion and plasticity. J Adhes Sci Technol 2011; 25(4-5): 483-499.
[58] Rumpf H. The strength of granules and agglomeration. In: Knepper WA, Ed., Agglomeration. NY, USA: John Wiley and Sons, 1962; pp. 379-418.

[59] Peleg M. Flowability of food powders and methods for its evaluation — A review. J Food Process Eng 1977; 1(4): 303-328.
[60] Stewart PJ. Particle interaction in pharmaceutical systems. Pharm Int 1986; 7: 146-149.
[61] Staniforth JN. Powder flow. In: Aulton ME, Ed., Pharmaceutics: The science of dosage form design. 2nd ed., Edinbergh, UK: Churchill Livingstone, 2002; pp. 197–210.
[62] Mullarney MP, Beach LE, Davé RN, Langdon BA, Polizzi M, Blackwood DO. Applying dry powder coatings to pharmaceutical powders using a Comil for improving powder flow and bulk density. Powder Technol 2011; 212(3): 397-402.
[63] Yang J, Sliva A, Banerjee A, Dave RN, Pfeffer R. Dry particle coating for improving the flowability of cohesive powders. Powder Technol 2005; 158(1–3): 21-33.
[64] Jallo LJ, Chen Y, Bowen J, Etzler F, Dave R. Prediction of inter-particle adhesion force from surface energy and surface roughness. J Adhes Sci Technol 2011; 25(4-5): 367-384.
[65] Castellanos A. The relationship between attractive interparticle forces and bulk behaviour in dry and uncharged fine powders. Adv Phys 2005; 54(4): 263-376.
[66] Chen Y, Yang J, Dave RN, Pfeffer R. Fluidization of coated group C powders. AIChE Journal 2008; 54(1): 104-121.
[67] Nyström C, Alderborn G, Duberg M, Karehill P-G. Bonding surface area and bonding mechanism-two important factors for the understanding of powder comparability. Drug Dev Ind Pharm 1993; 19(17-18): 2143-2196.
[68] Han X, Jallo L, To D, Ghoroi C, Dave R. Passivation of high-surface-energy sites of milled ibuprofen crystals via dry coating for reduced cohesion and improved flowability. J Pharm Sci 2013; 102(7): 2282-96.
[69] Podczeck F. Fundamentals of adhesion of particles to surfaces. In, Particle-Particle adhesion in pharmaceutical powder handling. London: Imperial College Press, 1998; pp. 1-80.
[70] Luangtana-Anan M, Fell JT. Bonding mechanisms in tabletting. Int J Pharm 1990; 60(3): 197-202.
[71] Sutton H. Flow properties of powders and the role of surface character. In: Parfitt G, Sing K, Eds., Characterization of powder surfaces. NY, USA: Academic Press, 1976; pp. 107-58.
[72] Johnson KL, Kendall K, Roberts AD. Surface energy and the contact of elastic solids. P Roy Soc Lond A Mat 1971; 324(1558): 301-313.
[73] Derjaguin BV, Muller VM, Toporov YP. Effect of contact deformations on the adhesion of particles. J Colloid Interf Sci 1975; 53(2): 314-326.
[74] Down GRB, McMullen JN. The effect of interparticulate friction and moisture on the crushing strength of sodium chloride compacts. Powder Technol 1985; 42(2): 169-174.
[75] Mitchell AG, Down GRB. Recrystallization after powder compaction. Int J Pharm 1984; 22(2-3): 337-344.
[76] Ahlneck C, Alderborn G. Moisture adsorption and tabletting. II. The effect on tensile strength and air permeability of the relative humidity during storage of tablets of 3 crystalline materials. Int J Pharm 1989; 56(2): 143-150.
[77] Pietsch WB. Adhesion and agglomeration of solids during storage, flow and handling—A survey. J Eng Ind 1969; 91(2): 435-448.
[78] Fuhrer C. Substance behaviour in direct compression. Labo-Pharma Probl Tech 1977; 269: 759-762.

[79] Das S, Larson I, Young P, Stewart P. Influence of storage relative humidity on the dispersion of salmeterol xinafoate powders for inhalation. J Pharm Sci 2009; 98(3): 1015-27.
[80] Adolfsson Å, Olsson H, Nyström C. Effect of particle size and compaction load on interparticulate bonding structure for some pharmaceutical materials studied by compaction and strength characterisation in butanol. Eur J Pharm Biopharm 1997; 44(3): 243-251.
[81] Sebhatu T, Ahlneck C, Alderborn G. The effect of moisture content on the compression and bond-formation properties of amorphous lactose particles. International Journal of Pharmaceutics 1997; 146(1): 101-114.
[82] Zimon AD. Fundamental concepts of particle adhesion. In, Adhesion of Dust and Powder. Springer US, 1982; pp. 1-30.
[83] Schulze D. Powders and bulk solids: Behavior, characterization, storage and flow In. Springer: Berlin–Heidelberg–NewYork–Tokyo, 2008.
[84] Chowhan ZT. Role of binders in moisture-induced hardness increase in compressed tablets and its effect on in vitro disintegration and dissolution. J Pharm Sci 1980; 69(1): 1-4.
[85] Nokhodchi A. An overview of the effect of moisture on compaction and compression. Pharmaceutical Technology 2005; 29(1): 46-66.
[86] Garr JSM, Rubinstein MH. The influence of moisture content on the consolidation and compaction properties of paracetamol. Int J Pharm 1992; 81(2-3): 187-192.
[87] Faqih AM, Mehrotra A, Hammond SV, Muzzio FJ. Effect of moisture and magnesium stearate concentration on flow properties of cohesive granular materials. Int J Pharm 2007; 336(2): 338-45.
[88] Zimon AD. Adhesion in a gas medium. Sources of adhesion. In, Adhesion of Dust and Powder. Springer US, 1982; pp. 93-144.
[89] Podczeck F, Newton JM, James MB. Influence of relative humidity of storage air on the adhesion and autoadhesion of micronized particles to particulate and compacted powder surfaces. J Colloid Interf Sci 1997; 187(2): 484-91.
[90] Sou T, Kaminskas LM, Nguyen T-H, Carlberg R, McIntosh MP, Morton DAV. The effect of amino acid excipients on morphology and solid-state properties of multi-component spray-dried formulations for pulmonary delivery of biomacromolecules. Eur J Pharm Biopharm 2013; 83(2): 234-243.
[91] Israelachvili JN. Van der Waals forces. In: Israelachvili JN, Ed., Intermolecular and surface forces 3rd ed., MA, USA: Academic Press, 2011; pp. 107-132.
[92] Staniforth JN, Rees JE. Electrostatic charge interactions in ordered powder mixes. J Pharm Pharmacol 1982; 34(2): 69-76.
[93] Karehill PG, Nyström C. Studies on direct compression of tablets XXI. Investigation of bonding mechanisms of some directly compressed materials by strength characterization in media with different dielectric constants (relative permittivity). Int J Pharm 1990; 61(3): 251-260.
[94] Olsson H, Adolfsson Å, Nyström C. Compaction and measurement of tablets in liquids with different dielectric constants for determination of bonding mechanisms—Evaluation of the concept. Int J Pharm 1996; 143(2): 233-245.
[95] Ibrahim T, Burk R, Etzler F, Neuman R. Direct adhesion measurements of pharmaceutical particles to gelatin capsule surfaces. J Adhes Sci Technol 2000; 14: 1225-1242.
[96] Visser J. Particle adhesion and removal: A review. Particul Sci Technol 1995; 13(3-4): 169-196.

[97] Fichtner F, Mahlin D, Welch K, Gaisford S, Alderborn G. Effect of surface energy on powder compactibility. Pharm Res 2008; 25(12): 2750-2759.
[98] Li Q, Rudolph V, Weigl B, Earl A. Interparticle van der Waals force in powder flowability and compactibility. Int J Pharm 2004; 280(1–2): 77-93.
[99] Chen Y, Yang J, Dave RN, Pfeffer R. Fluidization of coated group C powders. AIChE J 2008; 54(1): 104-121.
[100] Krupp H. Particle adhesion: Theory and experiments. Adv Colloid Interface Sci 1967; 1: 119-239.
[101] Ho R, Wilson DA, Heng JYY. Crystal habits and the variation in surface energy heterogeneity. Cryst Growth Des 2009; 9(11): 4907-4911.
[102] Zhou Q, Denman JA, Gengenbach T, Das S, Qu L, Zhang H, Larson I, Stewart PJ, Morton DAV. Characterization of the surface properties of a model pharmaceutical fine powder modified with a pharmaceutical lubricant to improve flow via a mechanical dry coating approach. J Pharm Sci 2011; 100(8): 3421-3430.
[103] Feeley JC, York P, Sumby BS, Dicks H. Determination of surface properties and flow characteristics of salbutamol sulphate, before and after micronisation. Int J Pharm 1998; 172(1–2): 89-96.
[104] Chow AHL, Tong HHY, Chattopadhyay P, Shekunov BY. Particle engineering for pulmonary drug delivery. Pharm Res 2007; 24(3): 411-437.
[105] Ho R, Naderi M, Heng JY, Williams D, Thielmann F, Bouza P, Keith A, Thiele G, Burnett D. Effect of milling on particle shape and surface energy heterogeneity of needle-shaped crystals. Pharm Res 2012; 29(10): 2806-2816.
[106] Buckton G, Gill H. The importance of surface energetics of powders for drug delivery and the establishment of inverse gas chromatography. Adv Drug Deliv Rev 2007; 59(14): 1474-1479.
[107] El Gindy NA, Samaha MW. Tensile strength of some pharmaceutical compacts and their relation to surface free energy. Int J Pharm 1982; 13(1): 35-46.
[108] Adi H, Larson I, Stewart PJ. Adhesion and redistribution of salmeterol xinafoate particles in sugar-based mixtures for inhalation. Int J Pharm 2007; 337(1-2): 229-38.
[109] Adi H, Larson I, Chiou H, Young P, Traini D, Stewart P. Agglomerate strength and dipersion of salmeterol xinafoate from powder mixtures for inhalation. Pharm Res 2006; 23(11): 2556-2565.
[110] Zeng XM, Pandhal KH, Martin GP. The influence of lactose carrier on the content homogeneity and dispersibility of beclomethasone dipropionate from dry powder aerosols. Int J Pharm 2000; 197(1–2): 41-52.
[111] Israelachvili JN. Van der Waals forces between particles and surfaces. In: Israelachvili JN, Ed., Intermolecular and surface forces 3rd ed., MA, USA: Academic Press, 2011; pp. 253-289.
[112] Restagno F, Crassous J, Cottin-Bizonne C, Charlaix E. Adhesion between weakly rough beads. Phys Rev E 2002; 65(4): 042301.
[113] Rubinstein MH, Jackson IM. Stress relaxation behaviour of compacts of sodium chloride and polyethylene. Int J Pharm 1987; 36(2–3): 99-104.
[114] Mattsson SF, Nystrom C. Evaluation of critical binder properties affecting the compactibility of binary mixtures. Drug Dev Ind Pharm 2001; 27(3): 181-194.
[115] Hersey JF, Bayraktar GF, Shotton E. The effect of particle size on the strength of sodium chloride tablets. J Pharm Pharmacol 1967; 19(24S-30S).
[116] Kolter K, Flick D. Structure and dry binding activity of different polymers, including Kollidon VA 64. Drug Dev Ind Pharm 2000; 26(11): 1159-1165.
[117] Bolhuis GK, Eissens AC, Adrichem TP, Wesselingh JA, Frijlink HW. Hollow filler-binders as excipients for direct compaction. Pharm Res 2003; 20(3): 515-8.

[118] Eissens AC, Bolhuis GK, Hinrichs WLJ, Frijlink HW. Inulin as filler-binder for tablets prepared by direct compaction. Eur J Pharm Sci 2002; 15(1): 31-38.
[119] Bolhuis GK, Engelhart JJP, Eissens AC. Compaction properties of isomalt. Eur J Pharm Biopharm 2009; 72(3): 621-625.
[120] Ndindayino F, Henrist D, Kiekens F, Van den Mooter G, Vervaet C, Remon JP. Direct compression properties of melt-extruded isomalt. Int J Pharm 2002; 235(1–2): 149-157.
[121] Rojas J, Ciro Y, Correa L. Functionality of chitin as a direct compression excipient: An acetaminophen comparative study. Carbohydr Polym 2014; 103(0): 134-139.
[122] Schmidt PC, Leitritz M. Compression force/time-profiles of microcrystalline cellulose, dicalcium phosphate dihydrate and their binary mixtures--a critical consideration of experimental parameters. Eur J Pharm Biopharm 1997; 44(3): 303-313.
[123] Roberts RJ, Rowe RC. Brittle/ductile behaviour in pharmaceutical materials used in tabletting. Int J Pharm 1987; 36: 205-209.
[124] Morris LE, Moore JC, Schwartz JB. Characterization and performance of a new direct compression excipient for chewable tablets: Xylitab®. Drug Dev Ind Pharm 1996; 22(9-10): 925-932.
[125] Muzikova J, Novakova P. A study of the properties of compacts from silicified microcrystalline celluloses. Drug Dev Ind Pharm 2007; 33(7): 775-81.
[126] Roberts RJ, Rowe RC. Brittle-ductile transitions in sucrose and the influence of lateral stresses during compaction. J Pharm Pharmacol 2000; 52(2): 147-50.
[127] Gharaibeh SF, Aburub A. Use of first derivative of displacement vs. force profiles to determine deformation behavior of compressed powders. AAPS PharmSciTech 2013; 14(1): 398-401.
[128] Alpar O, Hersey JA, Shotton E. The compression properties of lactose. J Pharm Pharmacol 1970; 22(S1): 1S-7S.
[129] Hussain MSH, York P, Timmins P, Humphrey P. Secondary ion mass spectrometry (SIMS) evaluation of magnesium stearate distribution and its effects on the physico-technical properties of sodium chloride tablets. Powder Technol 1990; 60(1): 39-45.
[130] De Boer AH, Bolhuis GK, Lerk CF. Bonding characteristics by scanning electron microscopy of powders mixed with magnesium stearate. Powder Technol 1978; 20(1): 75-82.
[131] Almaya A, Aburub A. Effect of particle size on compaction of materials with different deformation mechanisms with and without lubricants. AAPS PharmSciTech 2008; 9(2): 414-418.
[132] Bolhuis GK, Lerk CF, Zijlstra HT, De Boer AH. Film formation by magnesium stearate during mixing and its effect on tabletting. Pharm Weekbl 1975; 110(16): 317-325.
[133] Lerk CF, Bolhuis GK, Smedema SS. Interaction of lubricants and colloidal silica during mixing with excipients. I. Its effect on tabletting. Pharm Acta Helv 1977; 52(3): 33-9.
[134] Vromans H, Lerk CF. Densification properties and compactibility of mixtures of pharmaceutical excipients with and without magnesium stearate. Int J Pharm 1988; 46(3): 183-192.
[135] Rees JE, Rue PJ. Time-dependent deformation of some direct compression excipients. J Pharm Pharmacol 1978; 30(10): 601-7.
[136] Roberts RJ, Rowe RC. The effect of punch velocity on the compaction of a variety of materials. J Pharm Pharmacol 1985; 37(6): 377-384.
[137] Armstrong NA, Palfrey LP. The effect of machine speed on the consolidation of four directly compressible tablet diluents. J Pharm Pharmacol 1989; 41(3): 149-151.

[138] Cook GD, Summers MP. Effect of compression speed on the tensile strength of tablets of binary mixtures containing aspirin. J Pharm Pharmacol 1990; 42(7): 462-467.
[139] Joiris E, Martino P, Berneron C, Guyot-Hermann A-M, Guyot J-C. Compression behavior of orthorhombic paracetamol. Pharm Res 1998; 15(7): 1122-1130.
[140] Van der Voort Maarschalk K, Vromans H, Bolhuis GK, Lerk CF. Influence of plasticizers on tableting properties of polymers. Drug Dev Ind Pharm 1998; 24(3): 261-8.
[141] Salmen NL, Back EL. The influence of water on the glass transition temperature of cellulose. TAPPI 1977; 60(12): 137-140.
[142] Tomas J. Assessment of mechanical properties of cohesive particulate solids. Part 1: Particle contact constitutive model. Particul Sci Technol 2001; 19(2): 95-110.
[143] Alderborn G, Nystrom C. Studies on direct compression of tablets. IV. The effect of particle size on the mechanical strength of tablets. Acta Pharm Suec 1982; 19(5): 381-390.
[144] McKenna A, McCafferty DF. Effect of particle size on the compaction mechanism and tensile strength of tablets. J Pharm Pharmacol 1982; 34(6): 347-351.
[145] Alderborn G, Börjesson E, Glazer M, Nyström C. Studies on direct compression of tablets. XIX. The effect of particle size and shape on the mechanical strength of sodium bicarbonate tablets. Acta Pharm Suec 1988; 25(1): 31-40.
[146] Eriksson M, Alderborn G. The effect of particle fragmentation and deformation on the interparticulate bond formation process during powder compaction. Pharm Res 1995; 12(7): 1031-9.
[147] Gerad B, Klaas K, John L. New developments in spray-dried lactose. Pharm Tech 2004: 26-30.
[148] De Boer AH, Vromans H, Lerk CF, Bolhuis GK, Kussendrager KD, Bosch H. Studies on tableting properties of lactose. Part III. The consolidation behaviour of sieve fractions of crystalline alpha-lactose monohydrate. Pharm Weekbl Sci Journal 1986; 8(2): 145-50.
[149] Alderborn G, Nystrom C. Studies on direct compression of tablets XIV. The effect of powder fineness on the relation between tablet permeametry surface area and compaction pressure. Powder Technol 1985; 44(1): 37-42.
[150] Skinner GW, Harcum WW, Barnum PE, Guo J-H. The evaluation of fine-particle hydroxypropylcellulose as a roller compaction binder in pharmaceutical applications. Drug Dev Ind Pharm 1999; 25(10): 1121-1128.
[151] Alvarez-Lorenzo C, Gómez-Amoza JL, Martínez-Pacheco R, Souto C, Concheiro A. Evaluation of low-substituted hydroxypropylcelluloses (L-HPCs) as filler-binders for direct compression. Int J Pharm 2000; 197(1–2): 107-116.
[152] Picker-Freyer KM, Dürig T. Physical mechanical and tablet formation properties of hydroxypropylcellulose: In pure form and in mixtures. AAPS PharmSciTech 2007; 8(4).
[153] Kabir MA, Reo JP. Hydroxypropylcellulose. In: Rowe RC, Sheskey PJ, Quinn ME, Eds., Handbook of pharmaceutical excipients. 6th ed., Washington D.C., USA: Pharmaceutical Press, 2009; pp. 317-322.
[154] Hapgood KP, Obara S. Hydroxypropylcellulose, Low-substituted. In: Rowe RC, Sheskey PJ, Quinn ME, Eds., Handbook of pharmaceutical excipients. 6th ed., Washington D.C., USA: American Pharmacists Association, 2009; pp. 322-324.
[155] Narayan P, Hancock BC. The relationship between the particle properties, mechanical behavior, and surface roughness of some pharmaceutical excipient compacts. Mat Sci Eng A 2003; 355(1–2): 24-36.

[156] Wong LW, Pilpel N. The effect of particle shape on the mechanical properties of powders. Int J Pharm 1990; 59(2): 145-154.
[157] Meyer K, Zimmermann I. Effect of glidants in binary powder mixtures. Powder Technol 2004; 139(1): 40-54.
[158] Chen Y, Jallo L, Quintanilla MAS, Dave R. Characterization of particle and bulk level cohesion reduction of surface modified fine aluminum powders. Colloid Surface A 2010; 361(1–3): 66-80.
[159] Jallo LJ, Schoenitz M, Dreizin EL, Dave RN, Johnson CE. The effect of surface modification of aluminum powder on its flowability, combustion and reactivity. Powder Technol 2010; 204(1): 63-70.
[160] Ghoroi C, Han X, To D, Jallo L, Gurumurthy L, Davé RN. Dispersion of fine and ultrafine powders through surface modification and rapid expansion. Chem Eng Sci 2013; 85(0): 11-24.
[161] Chen Y, Quintanilla MA, Yang J, Valverde JM, Dave RN. Pull-off force of coated fine powders under small consolidation. Phys Rev E Stat Nonlin Soft Matter Phys 2009; 79(4 Pt 1): 1-14.
[162] Raula J, Eerikainen H, Kauppinen EI. Influence of the solvent composition on the aerosol synthesis of pharmaceutical polymer nanoparticles. Int J Pharm 2004; 284(1-2): 13-21.
[163] Raula J, Kuivanena A, Lähde A, Jiang H, Antopolsky M, Kansikas J, Kauppinena EI. Synthesis of L-leucine nanoparticles via physical vapor deposition at varying saturation conditions. J Aerosol Sci 2007; 38: 1172 – 1184.
[164] Raula J, Lahde A, Kauppinen EI. A novel gas phase method for the combined synthesis and coating of pharmaceutical particles. Pharm Res 2008; 25(1): 242-5.
[165] Lerk CE, Bolhuis GK. Comparative evaluation of excipients for direct compression, II. Pharmaceutisch Weekblad 1974; 109: 945-955.
[166] Chow K, Tong HH, Lum S, Chow AH. Engineering of pharmaceutical materials: an industrial perspective. J Pharm Sci 2008; 97(8): 2855-77.
[167] Gupta P, Nachaegari S, Bansal A. Improved excipient functionality by coprocessing. In: Katdare A, Chaubal MV, Eds., Excipient development for pharmaceutical, biotechnology, and drug delivery systems. 1st ed., NY, USA: Informa Healthcare, 2006; pp. 109-126.
[168] Web Page: Publisher SPI Pharma; Cited 2015 22 April. Available from: http://spipharma.com/documents/document/1155.
[169] Heinz R, Wolf H, Schuchmann H, End L, Kolter K. Formulation and development of tablets based on Ludipress and scale-up from laboratory to production scale. Drug Dev Ind Pharm 2000; 26(5): 513-521.
[170] Muzikova J, Zvolankova J. A study of the properties of tablets from coprocessed dry binders composed of alpha-lactose monohydrate and different types of cellulose. Ceska Slov Farm 2007; 56(6): 269-75.
[171] van Veen B, Bolhuis GK, Wu YS, Zuurman K, Frijlink HW. Compaction mechanism and tablet strength of unlubricated and lubricated (silicified) microcrystalline cellulose. Eur J Pharm Biopharm 2005; 59(1): 133-8.
[172] Li J, Carlin B, Ruszkay T, inventor, FMC Corporation assignee Co-processed microcrystalline cellulose and sugar alcohol as an excipient for tablet formulations. WO2008057267 A2. May 15, 2008.
[173] Flores LE, Arellano RL, Díaz Esquivel JJ. Study of load capacity of avicel PH-200 and cellactose, two direct compression excipients, using experimental design. Drug Dev Ind Pharm 2000; 26(4): 465-469.

[174] Baykara T, Duman G, Özşener KŞ, Ordu Ş, Özateş B. Comparing the compressibility of Ludipress with the other direct tableting agents by using acetaminophen as an active ingredient. Drug Dev Ind Pharm 1991; 17(17): 2359-2371.
[175] Lahdenpaa E, Antikainen O, Yliruusi J. Direct compression with silicified and non-silicified microcrystalline cellulose : study of some properties of powders and tablets. STP Pharma Sci 2001; 11(2): 129-35.
[176] Schmidt PC, Rubensdörfer CJW. Evaluation of Ludipress as a "multipurpose excipient" for direct compression: part II: interactive blending and tableting with micronized glibenclamide. Drug Dev Ind Pharm 1994; 20(18): 2927-2952.
[177] Michoel A, Rombaut P, Verhoye A. Comparative evaluation of co-processed lactose and microcrystalline cellulose with their physical mixtures in the formulation of folic acid tablets. Pharm Dev Technol 2002; 7(1): 79-87.
[178] Casalderrey M, Souto C, Concheiro A, Gómez-Amoza JL, Martínez-Pacheco R. A comparison of drug loading capacity of cellactose with two ad hoc processed lactose–cellulose direct compression excipients. Chem Pharm Bull 2004; 52(4): 398-401.
[179] Luukkonen P, Schæfer T, Hellén L, Juppo AM, Yliruusi J. Rheological characterization of microcrystalline cellulose and silicified microcrystalline cellulose wet masses using a mixer torque rheometer. Int J Pharm 1999; 188(2): 181-192.
[180] Freitag F, Runge J, Kleinebudde P. Coprocessing of powdered cellulose and magnesium carbonate: direct tableting versus tableting after roll compaction/dry granulation. Pharm Dev Technol 2005; 10(3): 353-62.
[181] Schmidt PC, Rubensdörfer CJW. Evaluation of Ludipress as a "multipurpose excipeent" for direct compression: Part I: Powder characteristics and tableting properties. Drug Dev Ind Pharm 1994; 20(18): 2899-2925.
[182] Rojas J, Kumar V. Effect of silicification on the tableting performance of cellulose II: a novel multifunctional excipient. Chem Pharm Bull 2012; 60(5): 603-11.
[183] Bolhuis GK, Lerk CF, Moes JR, Mulder CWA. Comparative evaluation of excipients for direct compression. Pharmaceutisch Weekblad 1979; 1(1): 1223-1233.
[184] Hiestand HEN, Smith DP. Indices of tableting performance. Powder Technol 1984; 38(2): 145-159.
[185] Reier GE, Shangraw RF. Microcrystalline cellulose in tableting. J Pharm Sci 1966; 55(5): 510-514.
[186] Shangraw RF. Compressed tablets by direct compression in pharmaceutical dosage forms. In: Leiberman HA, Lachman L, Schwatz JB, Eds., Tablets. 2nd ed. Vol. 1,, NY, USA: Marcel Dekker, 1990; pp. 195-246.
[187] Arida AI, Al-Tabakha MM. Cellactose® a co-processed excipient: A comparison study. Pharm Dev Technol 2008; 13(2): 165-175.
[188] Gohel MC, Jogani PD. A review of co-processed directly compressible excipients. J Pharm Pharmacol 2005; 8(1): 76-93.
[189] Shi L, Sun CC. Transforming powder mechanical properties by core/shell structure: Compressible sand. J Pharm Sci 2010; 99(11): 4458-4462.
[190] Blattner D, Kolb M, Leuenberger H. Percolation theory and compactibility of binary powder systems. Pharm Res 1990; 7(2): 113-117.
[191] Strydom SJ, Otto DP, Liebenberg W, Lvov YM, de Villiers MM. Preparation and characterization of directly compactible layer-by-layer nanocoated cellulose. Int J Pharm 2011; 404(1–2): 57-65.
[192] Akande OF, Rubinstein MH, Ford JL. Examination of the compaction properties of a 1:1 acetaminophen:microcrystalline cellulose mixture using precompression and main compression. J Pharm Sci 1997; 86(8): 900-907.

[193] Shi L, Sun C. Overcoming poor tabletability of pharmaceutical crystals by surface modification. Pharm Res 2011; 28(12): 3248-3255.
[194] Robertson MI. Regulatory issues with excipients. Int J Pharm 1999; 187(2): 273-276.
[195] Zheng JY, Robert LT. Development of low-dose solid oral tablets using direct compression In: Zheng JY, Ed., Formulation and analytical development for low-dose oral drug products. NJ, USA: John Wiley & Sons, 2009; pp. 159-204.
[196] Kumar V, inventor, Pharmalogix Inc., assignee Direct compression metformin hydrochloride tablets. US6117451 A. Sep 12, 2000.
[197] Friedman R. Pharmaceutical quality systems: US perspective. In, Pharmaceutical quality system (ICH Q10) conference: Brussels, Belgium., 2011.
[198] Hunter EA, Sherwood BE, Zeleznik JA, inventor, Edward Mendell Co., Inc., assignee Directly compressible high load acetaminophen formulations. US5733578 A. Mar 31, 1998.
[199] Leuenberger H, Lanz M. Pharmaceutical powder technology — from art to science: the challenge of the FDA's Process Analytical Technology initiative. Adv Powder Technol 2005; 16(1): 3-25.
[200] Sun CC, Hou H. Improving mechanical properties of caffeine and methyl gallate crystals by cocrystallization. Cryst Growth Des 2008; 8(5): 1575-1579.
[201] Karki S, Friščić T, Fábián L, Laity PR, Day GM, Jones W. Improving mechanical properties of crystalline solids by cocrystal formation: New compressible forms of paracetamol. Adv Mater 2009; 21(38-39): 3905-3909.
[202] Bernstein J. Molecular crystals: Pinching polymorphs. Nat Mater 2005; 4(6): 427-428.
[203] Sun C, Grant DJW. Improved tableting properties of p-hydroxybenzoic acid by water of crystallization: a molecular insight. Pharm Res 2004; 21(2): 382-386.
[204] Chattoraj S, Shi L, Sun CC. Profoundly improving flow properties of a cohesive cellulose powder by surface coating with nano-silica through comilling. J Pharm Sci 2011; 100(11): 4943-4952.
[205] Han X, Ghoroi C, Dave R. Dry coating of micronized API powders for improved dissolution of directly compacted tablets with high drug loading. Int J Pharm 2013; 442(1–2): 74-85.
[206] Qu L, Zhou Q, Gengenbach T, Denman JA, Stewart PJ, Hapgood KP, Gamlen M, Morton DAV. Investigation of the potential for direct compaction of a fine ibuprofen powder dry-coated with magnesium stearate. Drug Dev Ind Pharm 2014: 1-13.
[207] More PK, Khomane KS, Bansal AK. Flow and compaction behaviour of ultrafine coated ibuprofen. Int J Pharm 2013; 441(1-2): 527-34.
[208] Morton DAV, Orlando L, Zhou Q, Ho LC-H, inventor, Monash University, assignee Binder powders. US20140050795 A1. 2012.

Chapter-3

To understand the effect of cohesion of small binder particles on their interactive mixing behaviour, binder and flow additive actions

Sharad Mangal, Felix Meiser, Satu Lakio, David Morton*, Ian Larson*

Drug Delivery, Disposition and Dynamics, Monash Institute of Pharmaceutical Science, 381 Royal Parade, Parkville, VIC 3052, Australia

* Corresponding Authors

***Published as:**
Mangal S, Meiser F, Lakio S, Morton DA, Larson I. The role of physico-chemical and bulk characteristics of co-spray-dried L-leucine and polyvinylpyrrolidone on glidant and binder properties in interactive mixtures. Int J Pharm. 2015; 479(2): 338-48.

3 Declaration for Thesis Chapter 3

Declaration by candidate

In the case of Chapter 3, the nature and extent of my contribution to the work was the following:

Nature of contribution	**Extent of contribution (%)**
Study initiation, formation of hypothesis, laboratory work, data collection, analysis and interpretation and writing the manuscript	65%

The following co-authors contributed to the work. If co-authors are students at Monash University, the extent of their contribution in percentage terms must be stated:

Name	**Nature of contribution**	**Extent of contribution (%) for student co-authors only**
Felix Meiser	Supervision and manuscript revision	10%
Satu Lakio	Manuscript revision	5%
David AV Morton	Supervision and manuscript revision	10%
Ian Larson	Supervision and manuscript revision	10%

The undersigned hereby certify that the above declaration correctly reflects the nature and extent of the candidate's and co-authors' contributions to this work*.

Candidate's Signature	[redacted]	**Date 23.11.2015**
Main Supervisor's Signature	[redacted]	**Date 24/11/15**

*Note: Where the responsible author is not the candidate's main supervisor, the main supervisor should consult with the responsible author to agree on the respective contributions of the authors.

3.1 Commentary

This work was carried out as initial proof of concept to investigate if small binder particles can express a binder as well as a flow additive actions by forming interactive mixture. We hypothesized that small binder particles with low cohesion, de-agglomerate efficiently and so form a homogeneous interactive mixture, thus express an enhanced binder and flow additive actions. In this study, low cohesion binder particles were created by co-spraying a model pharmaceutical binder (PVP) with L-leucine, while PVP spray-dried without L-leucine was used as control high cohesion particles. To test our hypothesis, we investigated the effect of cohesion of small binder particles on their interactive mixing behaviour and the resultant binder and flow additive actions.

3.2 Abstract

In this study, polyvinylpyrrolidone (PVP) was spray-dried with L-leucine (PVP-Leu) to create a prototype multifunctional interactive excipient.

The physico-chemical and bulk properties such as particle size, surface composition, surface energy and bulk cohesion of PVP-Leu was measured and compared against pure spray-dried PVP (PVP-SD). The mixing behaviour of these excipients and their effect on flow and binding activity of paracetamol was assessed.

The mean particle sizes of PVP-Leu PVP-SD and PVP were 2.5, 2.1 and 21.9 μm, respectively. Surface composition characterization indicated that L-leucine achieved higher concentration on the surface compared to the bulk of the PVP-Leu particles. The surface energy of PVP-Leu was significantly lower compared to PVP-SD. In addition, PVP-Leu exhibited a significantly lower bulk cohesion compared with PVP-SD. The excipients were blended with paracetamol and qualitative characterization indicated that PVP-Leu blended more homogeneously with paracetamol compared to PVP-SD. Both PVP-Leu and PVP-SD then exhibited a significantly improved binder activity compared to PVP (commercial unmodified PVP). The flow of the paracetamol was markedly improved with PVP-Leu while PVP-SD and PVP had negligible effect on its flow.

This study reveals how physico-chemical and bulk properties of such prototype interactive excipients can play a key role in determining multi-factorial excipient performance.

Keywords: Polyvinylpyrrolidone, Lubricant, Interactive excipient, Co-processed excipients

3.3 Graphical Abstract

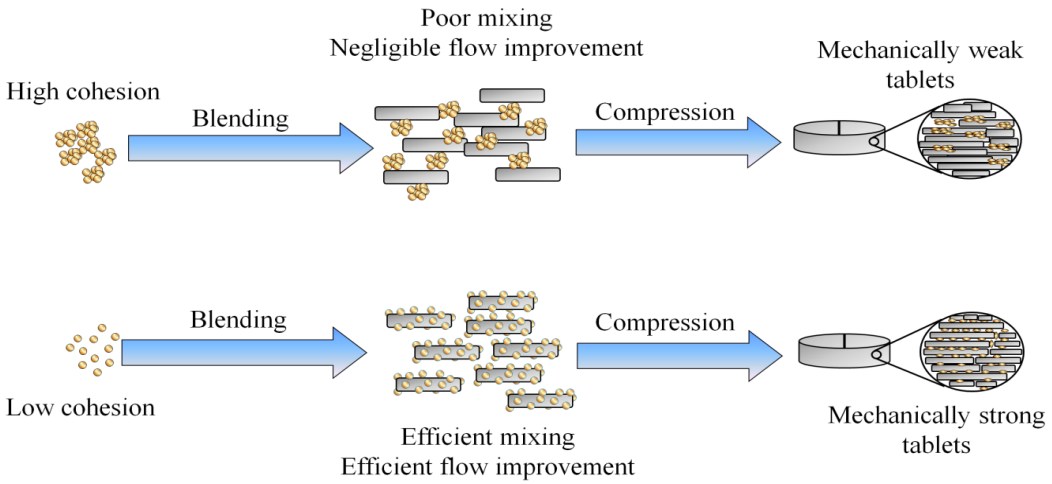

3.4 Introduction

Tablets are the most commonly used pharmaceutical preparation, despite the availability of many advanced pharmaceutical formulations [1]. For any active pharmaceutical ingredient (API) to be transformed into the tablets of satisfactory quality, the formulation must exhibit three essential attributes i.e., good flow, high compactability and excellent content uniformity [2]:

- good flow is necessary for the rapid and reproducible filling of powder into the die to minimize weight variation,
- high compactability is required to ensure that the tablets are sufficiently strong to withstand handling during manufacturing and transportation,
- excellent content uniformity is necessary for a consistent API dose.

The majority of APIs lack the requisite flow and compactability for tablet manufacturing [3]. Therefore, the flow and compactability of such APIs is typically improved by a granulation step (either wet or dry), which involves agglomeration of API and excipients into larger particulate structures i.e., granules. In such structures, the physico-mechanical inadequacies of both APIs and excipients are masked to an extent, facilitating efficient tablet manufacturing. In contrast, direct compression involves the mixing of API(s) with excipient(s) without a preliminary granulation, therefore the physico-mechanical properties of the individual components i.e., API(s) and excipient(s) have greater impact on the powder blend performance i.e., flow and compactability. Hence, the role of excipients is critical to ensure formation of robust tablets in direct compression [2, 4]. Therefore, there is a ubiquitous need for optimisation of excipients in the drive for more efficient tablet manufacturing using direct compression.

Improved and optimised excipients have mainly been generated *via* physical manipulation of existing excipient materials [5-8]. The main objective of excipient engineering is to improve both flow and compactability of the excipients. Particle size manipulation is one of the most commonly used approaches to optimize the flow and compactability of the excipients. However, typically flow and compactability are inherently competing characteristics, which makes it challenging to achieve an optimum balance of excipient flow and compactability at a given particle size [9]. Large particle size is usually associated with improved flow. However, a smaller particle size is associated with improved compactability due to an increase in the surface area [10-12]. Additionally, there is also the requirement to match particle size of the excipients and API to achieve good content uniformity, which typically requires particle size of APIs and excipients to be in the same order (except for ordered/interactive powder mixtures). The obligation to satisfy such competing objectives has made excipient design for direct compression a challenging task, and efforts to improve excipient functionality have resulted in a qualified success so far [13].

The concept of interactive mixing involves the adhesion of smaller particles to relatively larger particles facilitating their homogeneous distribution [14-18]. As particles become smaller, their interactive ability increases and particles below 10 μm are considered to be highly interactive in nature [19]. We propose that an excipient with the ability to form interactive mixture with the API(s) may exert an efficient binder action due to its higher effective surface area and better coverage [10-12]. Additionally, adhesion of an appropriate form of smaller particles to larger cohesive API could also reduce inter-particle cohesion between API particles therefore exerting a flow additive action, as typically observed with flow aids such as silica [20, 21]. So, in principle we propose that such an interactive excipient might not only improve binder action and facilitate flow but could also give robust content uniformity.

For interactive mixing to occur, the cohesion forces acting between the individual components, especially the smaller component must be overcome *via* energy applied through mixing. Small particles (<10 μm) are considered to be highly cohesive in nature as the inter-particle forces (cohesive forces arising from electrostatic, capillary or van der Waals interactions) significantly exceed external forces such as gravity resulting in agglomeration [22]. The ability of the mixing process to split agglomerates into individual particles decreases with increasing inter-particle cohesion forces, which makes de-agglomeration difficult [23]. This may compromise the ability of smaller excipient particles to form interactive mixtures with larger API particles, compromising their functional performance. Therefore, controlling inter-particle cohesion is considered to be a key aspect of creating such interactive excipients.

L-leucine has been reported to act as a lubricant in tablet formulation [24, 25]. In addition, it has also been previously employed to reduce cohesion and improve the dispersibility of spray-dried fine particles in dry powder inhaler research [26-28]. In this study, polyvinylpyrrolidone (PVP) was chosen as a polymeric binder and L-leucine was chosen as a lubricant to control inter-particle cohesion. PVP was spray-dried with L-leucine to generate micron-sized interactive excipient. The effect of L-leucine on the surface composition, surface energy and bulk cohesion was assessed. Paracetamol was selected as model poorly flowable and poorly compressible API [29, 30] to investigate the mixing behaviour of excipients and their impact on flow and tabletability.

3.5 Materials and methods

Paracetamol of analytical grade was procured from Sigma–Aldrich (St. Louis, MO, USA). PVP K-10 (average molecular weight ~ 10,000 Da), was purchased from Sigma–Aldrich (St. Louis, MO, USA). L-leucine was purchased from Ajinomoto Co. Inc. (Tokyo, Japan). The water used in the formulations was of Milli-Q grade (Millipore Corporation, MA, USA).

Magnesium stearate was procured from Mallinckrodt Pharmaceuticals (Mallinckrodt Pharmaceuticals, St. Louis, MO, USA). Hydrophobic fumed silica (Aerosil® R 972) was procured from Evonik Industries (Essen, Germany). Copolyvidone (Kollidone® VA 64) and Ludipress® LCE were kindly donated by BASF (Ludwigshafen, Germany). Silicified microcrystalline cellulose (Prosolv®, SMCC) was kindly donated by JRS Pharma (Rosenberg, Germany). Microcrystalline cellulose (Avicel®, PH-105) was kindly donated by FMC biopolymer (Philadelphia, PA, USA), Lactose monohydrate (Tablettose®70) was kindly donated by Meggle (Wasserburg, Germany) and hydroxypropylcellulose (HPC-SSL-SFP®) was received as kind donation from Nisso (New York, NY, USA). Presilanized glass columns and silanized glass wool for the measurement of surface energies were purchased from Surface Measurement Systems Ltd. (London, UK). Pre-silanized glass beads were purchased from Sigma–Aldrich GmBH (Steinheim, Germany).

3.5.1 Method of preparation

Briefly, PVP (K-10) and L-leucine were weighed accurately and dissolved in Milli-Q water with the aid of stirring. The resultant solution was spray-dried with a Buchi-190 Mini spray-dryer (Buchi Laboratory Equipment, Flawil, Switzerland). The operating conditions employed were: inlet temperature, 125 °C; spray flow rate, 800 L/h and pump setting, 10 mL/min. These conditions resulted in an outlet temperature of approximately 70 °C. The spray-dried particles were collected and stored in heat sealed aluminium bags for further evaluation and use. PVP alone spray-dried under similar conditions (PVP-SD) and PVP as received from the supplier (PVP) were used as comparators.

3.5.2 Particle size and size distribution

Particle size measurements were performed using a Malvern Mastersizer 2000 (Malvern Instruments Ltd., Malvern, UK) dry cell. An air pressure of 2.0 bar was used to disperse. The

feed rate was varied between 20 – 60% according to the ability of the powder to de-agglomerate. Measurements for each formulation were performed in triplicate. The in-built software provided values of D_{50} (volume median diameter), D_{10} (10% volume below this diameter) and D_{90} (90% volume below this diameter). An obscuration factor of 2 – 5 was targeted and the results were considered valid if the obscuration in this range was attained during the measurement.

3.5.3 Scanning electron microscopy (SEM): surface morphology

The shape and surface morphology of the excipients were visualised by SEM (Phenom™, FEI Company, Hillsboro, OR, USA). Double-sided adhesive carbon tape was placed on an aluminium stub and, after stripping off the upper side of the adhesive, a small amount of sample was scattered on the stub and dispersed by tapping lightly on the edge of the stub. The stubs were then coated with a fine gold film at an electrical potential of 2.0 kV at 25 mA for 3 min with a sputter coater (EMITECH K550X, Quorum Technologies, London, UK). The coated stubs were then loaded onto the SEM docking bay and images were captured at various magnifications.

3.5.4 Surface composition characterization

X-ray photoelectron spectroscopy (XPS) analysis was performed using an AXIS Ultra DLD spectrometer (Kratos Analytical Inc., Manchester, UK) with a mono-chromated Al K_α source at a power of 180 W (15kV × 12mA), a hemispherical analyser operating in the fixed analyser transmission mode and the standard aperture (analysis area: 0.3 mm × 0.7 mm). The total pressure in the main vacuum chamber during analysis was typically 10^{-8} mbar. Survey spectra were acquired at a pass energy of 160 eV. To obtain more detailed information about chemical structure, oxidation states etc., high resolution spectra were recorded from individual peaks at 20 eV pass energy (yielding a typical peak width for polymers of 1.0 eV). Samples were filled

into shallow wells of custom-built sample holders. One lot of each sample was prepared and 2 different locations were analysed on each sample at a nominal photoelectron emission angle of 0º with respect to the surface normal. Since the actual emission angle is ill-defined in the case of such micro-particles (ranging from 0º to 90º) the sampling depth may range from 0 nm to approximately 5 – 10 nm. Binding energies were referenced to the aliphatic hydrocarbon peak at 285.0 eV. Reference spectra of the pure PVP and L-leucine were recorded, normalised, and then used as model components to calculate curvefits for the spectra of the spray-dried formulations. The relative peak area of PVP and L-leucine for the co-sprayed PVP-Leu formulation, therefore directly represents relative surface atomic fractions (or mass fraction given the number of carbon (C) and nitrogen (N) atoms are same) of L-leucine and PVP.

3.5.5 Inverse gas chromatography (IGC)

Surface energies were determined with an inverse gas chromatography (iGC 2000, Surface Measurement Systems Ltd., London, UK) at infinite dilution. Due to the small particle size of the spray-dried powders, columns packed with spray-dried formulations exerted low porosities and over pressured. In order to alleviate over pressuring, formulations were blended with 80% (w/w) of 250 µm acid washed pre-silanized glass beads. Blends were packed into pre-silanized glass columns (300 mm × 3 mm internal diameter) by gentle tapping, until no cracks, hollows, or channels were visible in the powder bed. The columns were loosely stoppered with silanized glass wool at both ends to prevent sample movement. Packing of samples was performed in a relative humidity (RH) controlled environment with humidity <20% RH.

Before measurement, packed columns were pre-conditioned with a helium stream at 10 standard cubic centimetre per minute (sccm) for 2 h at 303 K and 0% RH. Dispersive (non-polar) energy measurements were achieved with the use of a series of n-alkanes (chromatography grade decane, nonane, octane, heptane and hexane), while the polar surface

energy measurements were achieved with the use of acidic and basic probes –chromatography grade chloroform and ethyl acetate, respectively. For all probes, a concentration of 0.03 p/p0 (where p is the partial pressure and p0 is the saturation vapour pressure) was used. Helium at a flow rate of 10 sccm was used to carry the probes through the stationary phase and the system was kept at 303 K at 0% RH. Dead volumes were based on the retention volume of methane gas at 0.03 p/p0, detection of probes was achieved with a flame ionization detector. Replicates of three were conducted for all samples. The values of acidic (γ^+) and basic (γ^-) and the molecular cross sectional area of the specific probes are presented in Table 3.1. Results were analysed with SMS-iGC analysis software v1.3.

Table 3.1 – Values of acidic and basic and the molecular cross sectional area of chloroform and ethyl acetate

Probe	**γ^+ (mJ/m^2)**	**γ^- (mJ/m^2)**	**Molecular cross sectional area (m^2)**
Chloroform	3.38	0	4.40×10^{-19}
Ethyl acetate	0	19.2	3.30×10^{-19}

The dispersive surface energy was calculated according to the theory described by Schultz [31] while the polar energy was calculated based on the theory proposed by Good-van Oss-Chaudhury [32] where the polar energy can be split into two components - an acidic component, γ^+, and a basic component, γ^-. The polar surface energy can be calculated by following equation [32, 33]:

$$\gamma_s^P = \sqrt{\gamma_S^+ \gamma_S^-} \qquad \text{Eq. (1.1)}$$

The total surface energy of the material is the additive effect of both the dispersive (γ^D) and polar (γ^P) components [34]. Upon determination of the dispersive and polar surface energies, the work of cohesion (w_{co}) for interactions was calculated using the following equation [35, 36]:

$$w_{co} = 2\sqrt{\gamma_1^D.\gamma_1^D} + 2\sqrt{\gamma_1^P.\gamma_1^P} \qquad \text{Eq. (1.2)}$$

where, γ_1^D and γ_1^P represent the dispersive and polar energies acting between particles of solid 1.

3.5.6 Bulk cohesion

Bulk cohesion of spray-dried excipients (PVP-Leu and PVP-SD) was measured with a FT4 shear cell (Freeman Technology Ltd., Worcestershire, UK). For the shear tests, the powders were loaded into a 1 mL shear cell module and conditioned. Then, the powder bed was pre-consolidated at a normal stress of 9 kPa using a vented piston. Shear tests were carried out at normal stresses of 3, 4, 5, 6 and 7 kPa. The shear stress at each normal stress was recorded and yield loci were derived as curves to represent the maximum shear stress the sample can support under a certain normal stress. The cohesion of each sample was calculated by extrapolating the yield loci to zero normal stress as given by following equation [19]:

$$\tau = C + \sigma \tan \eta \qquad \text{Eq. (1.3)}$$

where, τ is the shear stress, σ is the normal stress, η is the angle of friction, and C is the cohesion force.

3.5.7 Blending

A 50 g blend was prepared by mixing paracetamol with predetermined quantities of each excipient in a 250 ml glass jar using a Turbula mixer T2F (Willy A. Bachofen, Muttenz,

Switzerland) at 72 rpm for 5 min. The blends of paracetamol with PVP, PVP-SD and PVP-Leu were denoted as PVP/Para, PVP-SD/Para and PVP-Leu/Para, respectively.

3.5.8 Assessment of blending behaviour

The blending behaviour of excipients and paracetamol was qualitatively assessed by SEM (Phenom^{TM}, FEI Company, Hillsboro, OR, USA). In addition, the content of paracetamol was also quantified using assay method (USP29-NF24) to ensure that the blending of small (excipient) and large (paracetamol) powder components resulted in homogenous powder mixtures. Briefly, 120 mg of blend was dissolved in 10 mL of methanol and diluted with water to 500 mL. Five millilitre of this solution was diluted to 100 mL and the absorbance of this solution was recorded using UV spectrophotometry (UV-1800, Shimadzu Corporation, Kyoto, Japan) at 240 nm. The absorption spectrum of PVP-Leu and PVP was scanned in the range 190 – 400 nm to ensure that PVP and PVP-Leu did not interfere with the absorbance of paracetamol. The results suggested that the wavelength of PVP and PVP-Leu was sufficiently low to not affect the assay results (Appendix 3.1). The concentration of paracetamol in the solution was determined using a standard curve (R^2=0.9997, Appendix 3.2). Ten samples were measured to assess the quantity of paracetamol in each blend. The paracetamol content and the variability was expressed as mean and standard deviation.

3.5.9 Blend flow characterization

The effect of various excipients on flow of paracetamol was evaluated using: (i) conditioned bulk density (CBD), (ii) aeration and (iii) compressibility programs of the FT4 powder rheometer system (Freeman Technology Ltd., Worcestershire, UK).

3.5.9.1 Conditioned bulk density (CBD)

Powders with good flowability pack efficiently leading to a relatively high bulk density [37, 38]. The conditioned bulk density, CBD, was used to determine the powder flowability and packing. Since this test involves a conditioning cycle before each measurement, it was considered to be more reproducible and relatively reliable in comparison to traditional tests [19, 39]. The CBD of different blends was assessed using the method as described elsewhere [40]. Approximately 12 g powder samples (in case of Silica/Para blends approximately 15 g blends given its greater bulk density) were gently filled into a 25 cm^3 cylindrical vessel fitted with a 10 cm^3 extension vessel on top of it via a split assembly. The samples were conditioned using a conditioning blade (helix angle of −5 degrees, 23.5 mm in diameter and tip speed 100 mm/s) which created a uniform powder bed in a low stress packing state. The cylindrical vessel was then split with the help of splitting assembly, which allowed the excess powder to be removed leaving only the powder in 25 cm^3 cylindrical vessel. The weight of the powder was than recorded automatically and the conditioned bulk density was calculated by dividing the weight of the powder by the volume of the vessel.

3.5.9.2 Aeration

The aeration test is intended to measure the change in the flow properties of the powder under the influence of an air stream. The aeration test was performed in a 35 cm^3 cylindrical vessel mounted on a perforated base that acted as an air inlet port [41]. These tests were carried out at air flow rates of 0, 2.0, 4.0, 6.0, 8.0 and 10.0 mm/s. At each flow rate the energy required to move the rotating blade from the top of the vessel to bottom was calculated. The energy required to move the blade through the powder bed at maximum air flow rate i.e. 10 mm/s, was used to compare the effect of selected excipients on the flow behaviour of paracetamol blends. In all the test cycles, the tip speed of the conditioning blade was 100 mm/s.

3.5.9.3 Compressibility

The compressibility is another indicator of whether a powder is cohesive or free flowing [42]. The test shows the ability of a powder to be compressed (decrease the volume) under the influence of an increasing normal stress [43]. Compressibility gives an indication of the packing efficiency of the powders, and is considered to have bearing on the powder flow [19]. High compressibility is often associated with high cohesivity of the powders, in addition to other factors such as bulk density and packing structure [42]. The compressibility test is a measurement of changes in volume of a powder as a function of applied stress (range from 1 to 15 kPa) [40]. The change in volume i.e. the compressibility of different blends at 15 kPa, was used for comparison. For each test, all powder samples were tested in triplicate and average values were reported.

3.5.10 Tensile strength of tablets

Tablet strength relates to the ability of the tablets to withstand damage due to mechanical handling and transport (USP29-NF24). To minimize effect of humidity related variations on the tensile strength, all the blends were stored in controlled humidity (42.9% RH) environment until the constant weight was achieved. Blends were directly filled into the die by manually weighing 105 ±5 mg and the tablets were manufactured using a computer-controlled tablet press (Gamlen Tableting Ltd., Nottingham, UK). The tablets were compressed at 80, 120 and 154 MPa compression pressures using a flat punch and die 6 mm in diameter. The die and punch were lubricated with magnesium stearate prior to each compression to reduce the friction between die wall and tablet edges [44, 45]. The punch speed was 1 mm/s. The dimensions (diameter and thickness) of each tablet were measured. The breaking force of the tablets was measured using an Erweka hardness tester (TBH-30, Erweka, Heusenstamm, Germany). The tensile strength of the tablets was calculated using the following equation [46];

$$\sigma = \frac{2F}{\pi DH} \qquad \text{Eq. (1.4)}$$

where, σ is tensile strength, F is the breaking force, D is the tablet diameter, and H is the tablet thickness.

3.5.11 Statistical analysis

Results are expressed as Mean ±standard deviation (SD) and the statistical analysis was performed on tensile strength and surface energy data *via* one-way analysis of variance (ANOVA) with Tukey–Kramer multiple comparison post-hoc tests using SPSS™ software (SPSS Inc., IBM Corporation, New York, NY, USA). The asterisks over graphs denote the statistical differences of groups compared to PVP-Leu where *$p < 0.05$, **$p < 0.01$ and ***$p < 0.001$, respectively and ns denotes not significant ($p > 0.05$).

3.6 Results

3.6.1 Particle size and size distribution

The particle size and size distribution (span) of PVP, PVP-SD, PVP-Leu and paracetamol are represented in Table 3.2. The particle size analysis indicated that PVP exhibited a particle size D_{90} of 56 µm, whereas the spray-dried interactive excipients i.e., PVP-SD and PVP-Leu exhibited particle sizes D_{90} of 4.2 and 5.5 µm, respectively. It was also noted that the particle size of PVP-SD and PVP-Leu was approximately the same suggesting that addition of L-leucine does not substantially change the particle size. The particle size distribution plots of each of PVP, PVP-SD and PVP-Leu are represented in Figure 3.1. It was noted that the size distribution of PVP-Leu, PVP-SD and PVP was mono-modal in each case. The interquartile coefficient of skewness (IQCS) and span data reported that the particle size distribution of PVP, PVP-SD and PVP-Leu was narrow (Table 3.2). However, the particle size distribution of paracetamol was bimodal with greater IQCS and span values.

Table 3.2 – Particle size of PVP, PVP-SD, PVP-Leu and paracetamol. Data presented as Mean ±SD (n = 3).

Formulations	**Particle size (µm)**			**Span**	**IQCS**
	D_{10}	**D_{50}**	**D_{90}**		
PVP	8.2 ±0.1	26.6 ±0.2	56.7 ±0.6	1.8 ±0.0	0.2 ±0.0
PVP-SD	1.1 ±0.1	2.1 ±0.1	4.3 ±0.1	1.5 ±0.1	0.2 ±0.0
PVP-Leu	1.4 ±0.1	2.8 ±0.0	5.5 ±0.1	1.5 ±0.1	0.1 ±0.0

Paracetamol	3.7 ±0.1	21.4 ±0.3	151.5 ±5.0	6.8 ±0.1	0.5 ±0.0

IQCS = interquartile coefficient of skewness

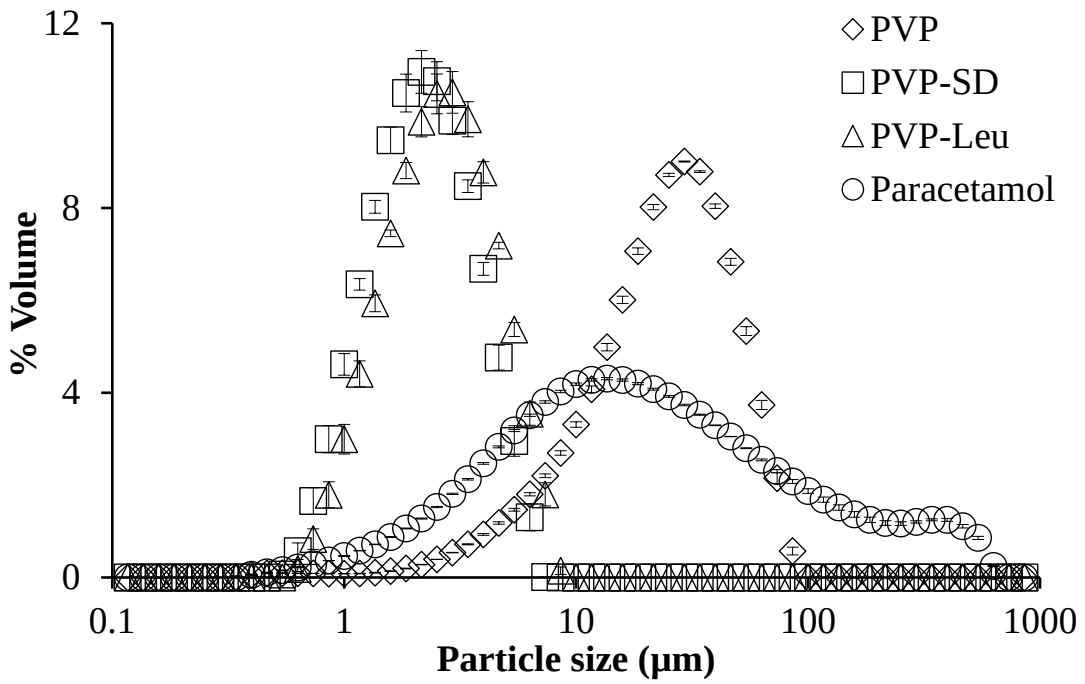

Figure 3.1 – Particle size distribution graphs of PVP, PVP-SD, PVP-Leu and paracetamol. Data presented as Mean ±SD (n = 3).

3.6.2 Scanning electron microscopy (SEM): Surface morphology

From SEM images, the PVP and PVP-SD particles were observed to be relatively smooth. In contrast, PVP-Leu particles were more corrugated (Figure 3.2). This morphological change in PVP-Leu particles may be attributed to the interfacial activity of L-leucine. It was proposed that co-spraying with L-leucine results in its enrichment at the droplet surface early in the drying phase and as the drying progresses L-leucine concentration reaches super-saturation and then crystallizes leading to the formation of shell [47]. This L-leucine enriched shell interferes with the evaporation of water vapour on further drying resulting in pressure build up followed

by eventual escape of water vapour affecting shell integrity and morphology [47]. In addition, PVP-SD appeared to be highly agglomerated, whereas, PVP-Leu appeared as more discrete individual particles suggesting that L-leucine could reduce the cohesive forces between fine PVP particles.

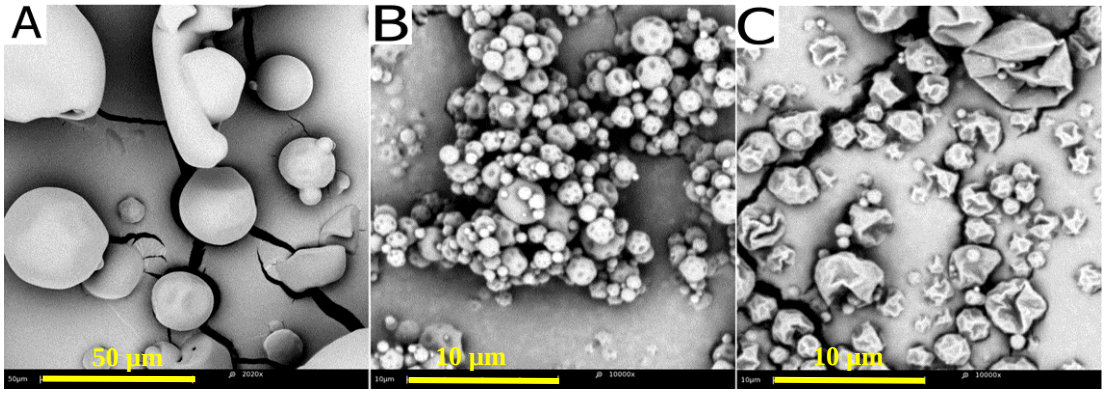

Figure 3.2 – Representative SEM images of PVP (A), PVP-SD (B) and PVP-Leu (C).

3.6.3 Surface composition characterization: XPS

The surface fractions PVP and L-leucine in spray-dried formulations were estimated based on the C 1s and N 1s high resolution spectra. L-leucine formed a significant proportion of surface of PVP-Leu formulation. On a (w/w) basis, L-leucine was approximately 81.7% of the surface material of PVP-Leu particles (Table 3.3) implying on the basis of their bulk composition, the formation of core-shell particulate structures. This suggests that L-leucine enriched the surface of the spray-dried formulations. The results presented here are consistent with the previous findings [48]. Both interfacial activity and low water solubility of L-leucine were considered to be the factors explaining the ability of L-leucine to enrich the surface of the spray-dried formulations [27, 49].

Table 3.3 – Surface PVP and L-leucine composition (% w/w) of spray-dried formulations.

Formulations	% (w/w) PVP and L-leucine surface concentrations			
	PVP (C 1s)	**L-leucine (C 1s)**	**PVP (N 1s)**	**L-leucine (N 1s)**
PVP-SD	100.0 ±0.0	0.0 ±0.0	100.0 ±0.0	0.0 ±0.0
PVP-Leu	18.3 ±1.8	81.7 ±1.8	19.7 ±1.9	80.3 ±1.9

Where 1s refers to the electron orbital

3.6.4 Inverse gas chromatography (IGC)

The surface energy (polar, dispersive and total) data of PVP-SD and PVP-Leu are presented in Figure 3.3. The addition of L-leucine resulted in a significant reduction in the polar surface energy, whereas it resulted in no change in the dispersive surface energy of the spray-dried formulations. The work of cohesion of PVP-SD (280.7 ±21.5 mJ/m^2) was significantly higher than that of PVP-Leu (116.9 ±5.5 mJ/m^2) indicating that L-leucine contributes to the energy of cohesive interaction. The SEM images also show a lower degree of agglomeration of the PVP-Leu particles compared to the PVP-SD particles indicating a reduction in cohesion upon co-spraying with L-leucine.

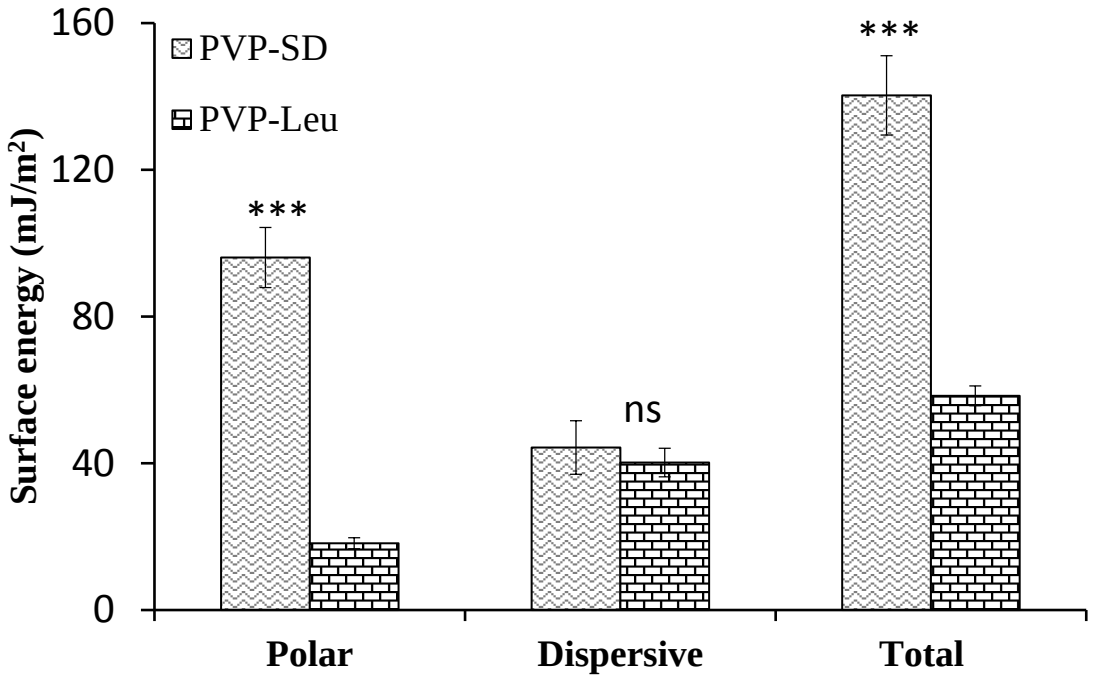

Figure 3.3 – Surface energy data of PVP-Leu and PVP-SD. Data presented as Mean ±SD (n = 3).

3.6.5 Bulk cohesion

The FT4 shear cell test was used to determine the cohesion and flow function co-efficient (ffc) of PVP-SD and PVP-Leu. The shear cell data indicated that PVP-SD demonstrated a relatively high cohesion and low ffc (Table 3.4). As per ffc classification, PVP-SD can be referred to as 'very cohesive' [19]. Co-spraying with L-leucine resulted in a marked reduction in cohesion and a significant increase in ffc. The results showed that L-leucine resulted in a marked reduction in surface energy and a substantial change in the surface morphology of the spray-dried particles from smooth to corrugated. Both of these factors are considered to be effective in controlling inter-particle cohesion [50-52]. However, it is not clear from such earlier works, by which mechanism L-leucine predominantly controls the bulk cohesion, and this requires further investigation.

Table 3.4 Shear cell data i.e. cohesion and flow function coefficient (ffc) of PVP-SD and PVP-Leu. Data presented as Mean ±SD (n = 3).

Formulations	Cohesion (kPa)	Flow function coefficient (ffc)
PVP-SD	3.8 ±0.4	1.3 ±0.1
PVP-Leu	0.7 ±0.0	5.8 ±0.1

3.6.6 Blending behaviour

The SEM images showed that PVP-Leu and PVP-SD appear as adhered in structured mixtures to the surface of paracetamol (Figure 3.4). This is consistent with their micron-scale particle size and likely to be driven mainly by van der Waals forces [17]. Furthermore, PVP-Leu appears as forming a more uniform mono-layer, whereas PVP-SD appears as more irregular clumps or agglomerates over the surface of API particles. This can be attributed to the higher inter-particle cohesion of PVP-SD relative to PVP-Leu, which would de-agglomerate less efficiently resulting in less homogeneous distribution over API particles.

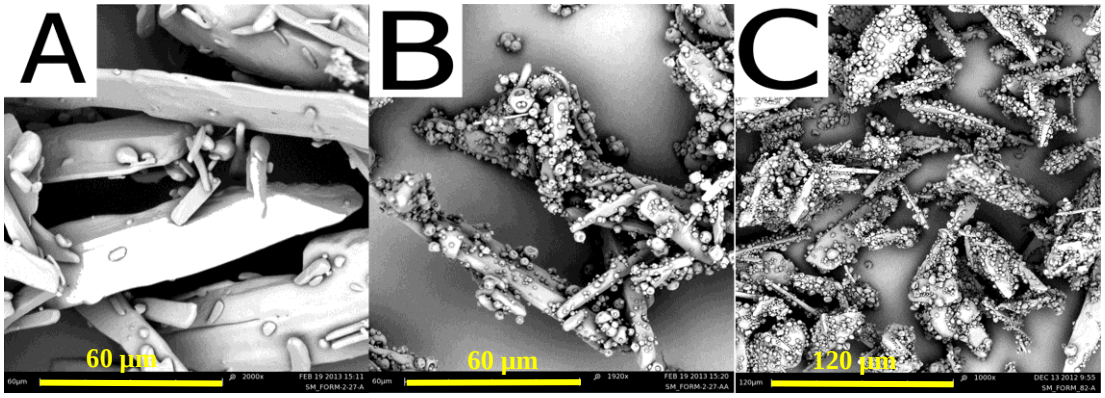

Figure 3.4 – Representative SEM images of PVP/Para (A), PVP-SD/Para (B) and PVP-Leu/Para (C).

The content of paracetamol was also quantitative assessed and results are presented in Table 3.5. The results showed that the paracetamol content in both PVP-SD and PVP-Leu blends was > 95% (Table 3.5). This indicated that interactive mixing is an efficient approach to achieving uniform mixing (if not homogeneous distribution).

Table 3.5 – Assay content of paracetamol in various API/excipient blends. Data presented as Mean ±SD (n = 10).

Excipient/API ratio	**% Paracetamol detected**		
	PVP/Para	**PVP-SD/Para**	**PVP-Leu/Para**
05/95	97.4 ±1.7	99.4 ±2.2	97.7 ±1.2
10/90	96.9 ±2.7	96.0 ±2.3	96.4 ±1.1
15/85	97.3 ±0.9	95.1 ±3.8	98.2 ±0.9
20/80	97.5 ±1.2	96.5 ±4.5	98.5 ±1.7

3.6.7 Blend Flow Characterization

3.6.7.1 Conditioned Bulk Density (CBD)

The CBD values of the powder blends are shown in Figure 3.5A. The CBD of paracetamol was low and incorporation of PVP-Leu led to the marked increase in the CBD of paracetamol, which might be due to improved flow of the PVP-Leu/Para blends [53-55]. This improved flow can be attributed to the ability of PVP-Leu to reduce the cohesion of paracetamol particles. Surprisingly, despite the ability of PVP-SD to adhere to paracetamol particles, little change in

bulk density of the blend was recorded for these blends. The conditioned bulk density data indicated that PVP-Leu/Para blends pack better than PVP-SD/Para, PVP/Para and PVP+Leu/Para (PVP+Leu/Para indicates the blend consisting of physical mix of PVP (13.5% (w/w)), L-leucine (1.5% (w/w)) and Paracetamol (85% (w/w))) blends.

The flow additive ability of PVP-Leu was also compared to the flow additive silica. The results indicated that silica (at as low as 0.0625% (w/w)) led to a much higher increase in CBD compared to PVP-Leu. As the silica/Para blend with 0.0625% silica had the highest CBD, this blend was used to grade the flow additive functionality of PVP-Leu in further testing.

3.6.7.2 Aeration

The aeration test was also used to characterize powder blend flow. The powder fluidization behaviour data are shown in Figure 3.5B. The results indicated that the energy required to rotate the blade was highest with paracetamol, and that the addition of PVP-Leu, PVP-SD and PVP resulted in a drop in the energy requirement. It was noted that paracetamol, PVP-SD/Para, PVP/Para and PVP+Leu/Para resulted in observed plug formation during the tests. At higher air velocities, lifting of the powder plug was observed consistent with the cohesive nature of these blends. No such plug formation was observed with PVP-Leu or silica blends and air flow through the powder bed resulted in good fluidization behaviour consistent with reduced cohesion.

Consequently, paracetamol, PVP/Para, PVP-SD/Para and PVP+Leu/Para blends were less sensitive to the fluidising air (more detailed data is provided in Appendix 3.3) due to the stronger inter-particle forces which compromised fluidization and dispersion of the powder [56].

3.6.7.3 Compressibility

The compressibility of paracetamol and different blends is shown in Figure 3.5C. Paracetamol showed the highest compressibility and incorporation of excipients caused a decrease in compressibility. However, the reduction in compressibility was greatest with the addition of PVP-Leu and silica suggesting better packing and thereby improved flow. This change in compressibility was found to be concentration dependent, where a drop in compressibility was noted up to 10% (w/w) PVP-Leu concentration after which no decrease in the compressibility was noted (more detailed data is provided in Appendix 3.4). It was also noted that blends containing silica had a higher compressibility than blends containing PVP-Leu suggesting that the flow improvement achieved using silica was greater compared to PVP-Leu.

It should be noted that the level of applied stress used in this test was much lower than that is typically used for determining compressibility in a tableting context, and thus is not representative of tableting behaviour. In powders with poor flowability, relatively large voids are formed due to the high inter-particle interaction forces, whereas free-flowing powders exhibit low inter-particle cohesion and therefore pack well. Thus, it would be expected that poorly flowing bulk solids be more compressible [19, 42, 43, 57].

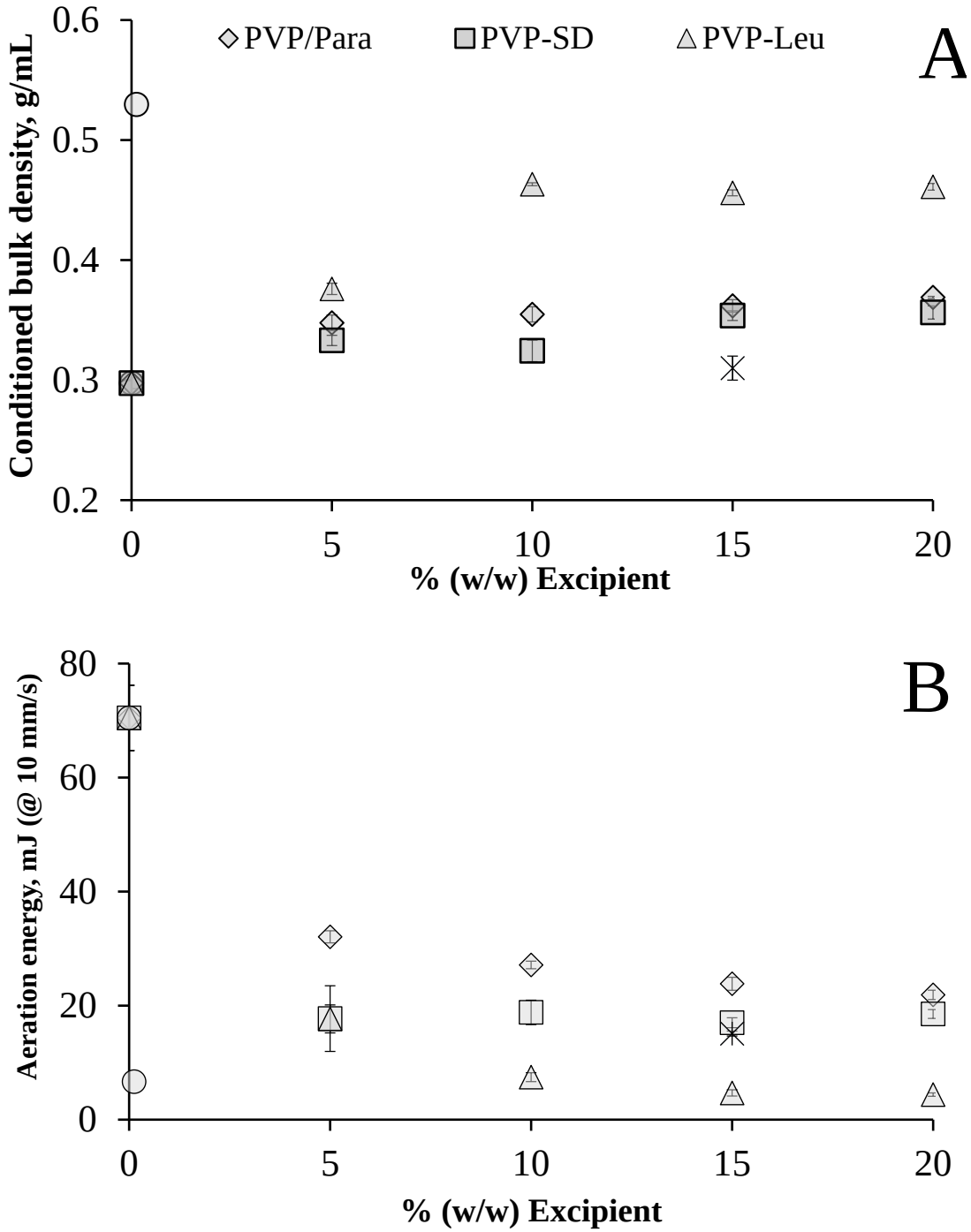
A
PVP/Para
PVP-SD
PVP-Leu
Conditioned bulk density, g/mL
0.6
0.5
0.4
0.3
0.2
0
5
10
15
20
% (w/w) Excipient
B
Aeration energy, mJ (@ 10 mm/s)
80
60
40
20
0
0
5
10
15
20
% (w/w) Excipient

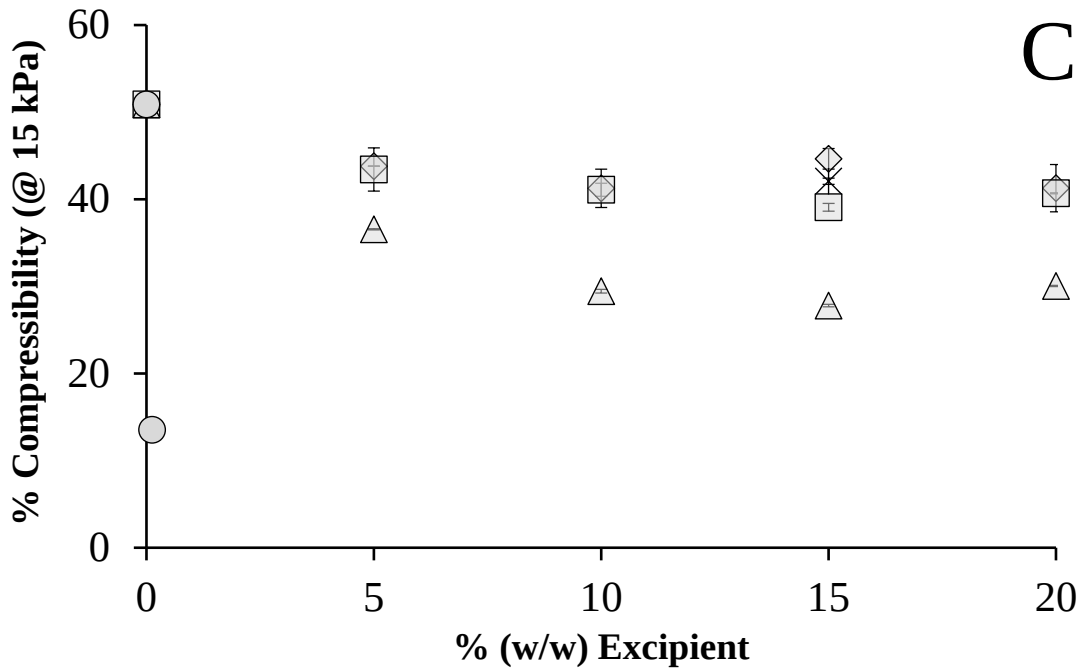

Figure 3.5 – The Conditioned Bulk Density (A), Aeration Energy (B) and Compressibility (C) data of PVP/Para, PVP-SD/Para and PVP-Leu/Para, PVP+Leu/Para and Silica/Para blends. Data presented as Mean ±SD (n = 3). Where, PVP+Leu/Para indicates the blend consisting of physical mix of PVP (13.5% (w/w)), L-leucine (1.5 % (w/w)) and paracetamol (85% (w/w)).

3.6.8 Tensile strength of tablets

Compression of pure paracetamol resulted in fragile and capped tablets indicating its physico-mechanical inability to form coherent tablets. Incorporation of PVP-Leu facilitated formation of coherent tablets with no capping or lamination. At lower amounts (5 and 10% (w/w)), PVP blends resulted in weak tablets as evident by frequent lamination of the tablets (Figure 3.6 A and B). However, PVP-Leu blends resulted in the formation of substantially stronger and more coherent tablets at as low as 5% (w/w) with tensile strength approaching >1.7 MPa, which is considered as reasonable for large scale manufacturing [58]. With higher PVP-Leu concentrations an increase in the tablet tensile strength was recorded which appeared to achieve a maximum at about 15% (w/w), and no further increase in tensile strength was recorded with

higher excipient concentrations. It was noted that PVP-Leu achieved higher tensile strength compared to PVP-SD at lower proportion (5%), consistent with the importance of the homogeneous dispersion of the interactive excipient on tablet performance. However, PVP-SD containing tablets achieved similar and then higher tensile strengths compared to PVP-Leu at higher proportions (Figure 3.6C and D) where the surface distribution was negated by quantity of additive.

Commercially available directly compressible binders were also used to compare the binder performance of PVP-Leu and PVP-SD at 15% (w/w) because at this proportion both PVP-Leu and PVP-SD appeared to result in optimum tensile strength. It was noted that majority of directly compressible excipients including silicified microcrystalline cellulose (SMCC, Prosolv®), lactose monohydrate (Tablettose-70®), Ludipress-LCE® and copolyvidone (Kollidone VA-64®) failed to create coherent tablets and, hence, do not appear in Figure 3.6C.

Only Hydroxypropyl cellulose (HPC-SSL-SFP®) and microcrystalline cellulose (Avicel PH-105®) blends could produce coherent tablets; however the tensile strength was significantly lower than blends containing PVP-Leu (Figure 3.6C).

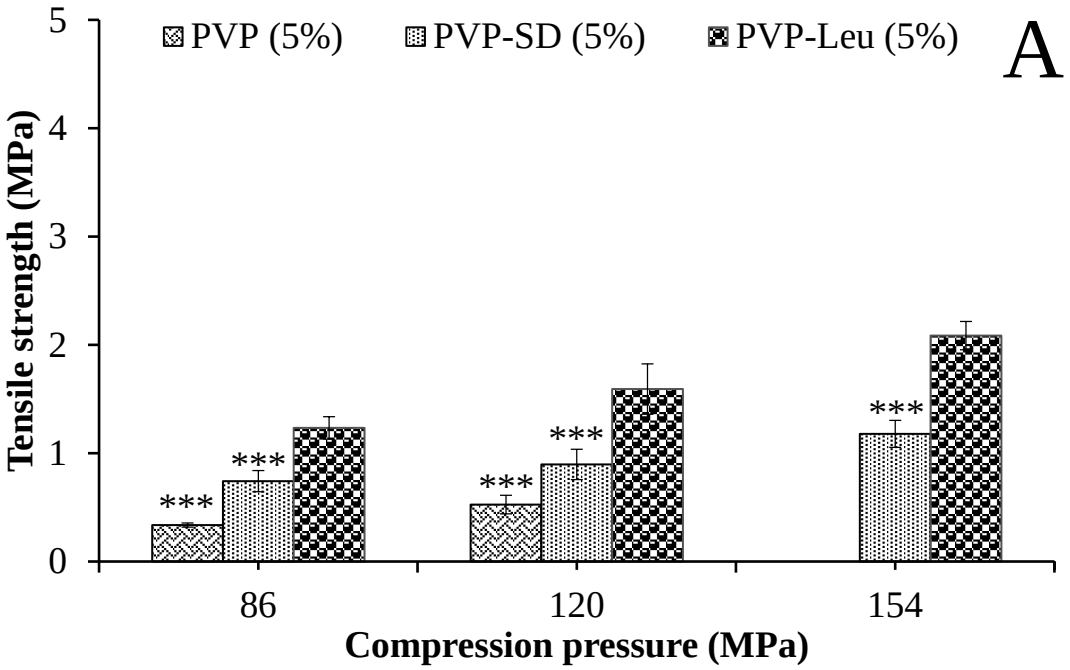
PVP (5%)
PVP-SD (5%)
PVP-Leu (5%)
A
Tensile strength (MPa)
0
1
2
3
4
5
***
***
***
***
***
86
120
154
Compression pressure (MPa)

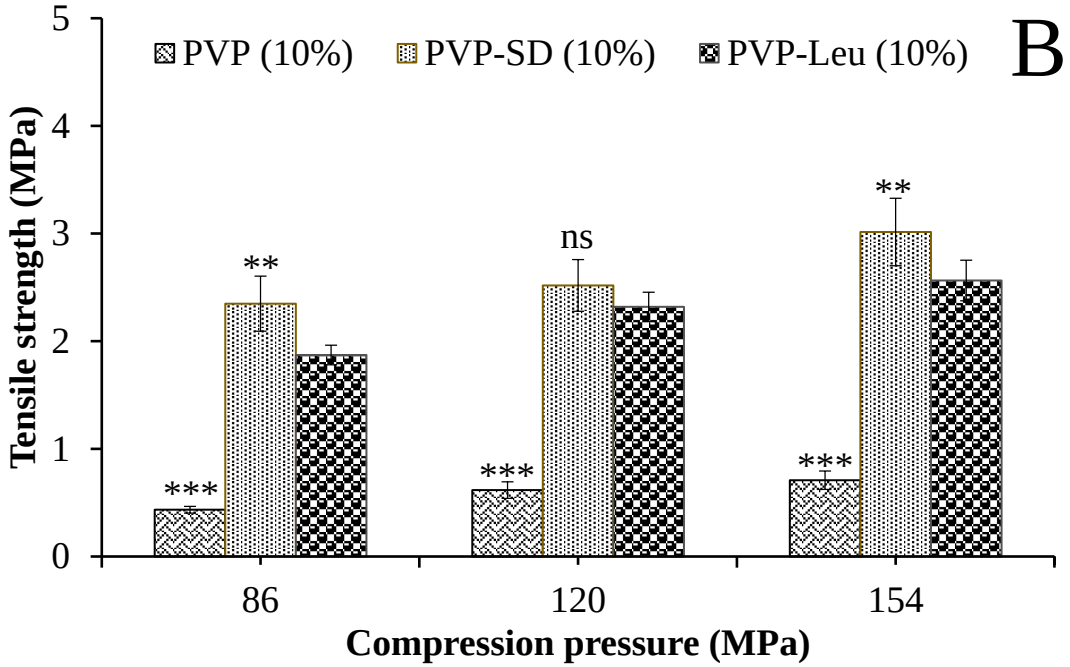
PVP (10%)
PVP-SD (10%)
PVP-Leu (10%)
B
Tensile strength (MPa)
0
1
2
3
4
5
***
**
***
ns
***
**
86
120
154
Compression pressure (MPa)

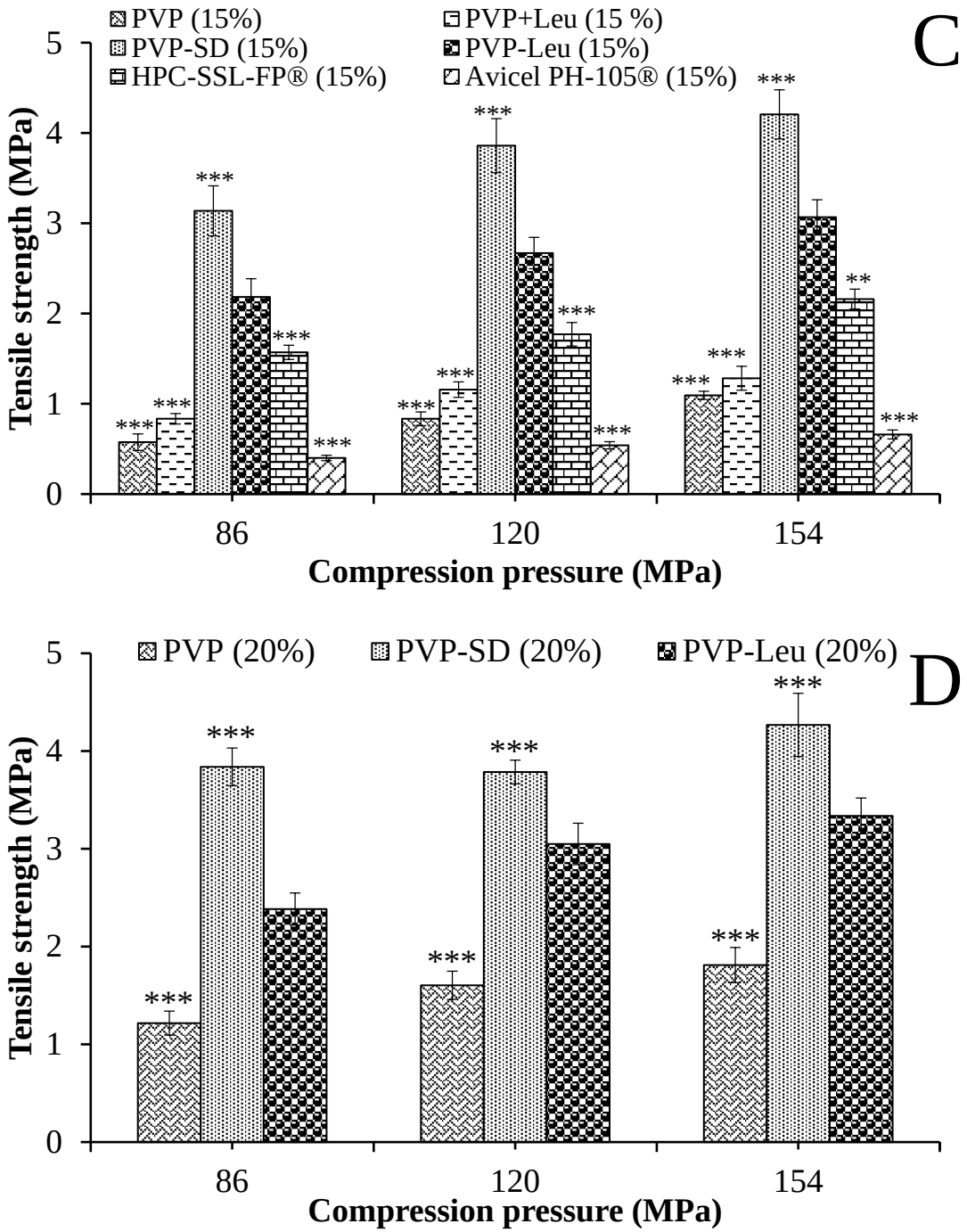

Figure 3.6 –Tensile strength of tablets prepared from different excipients. Data presented as Mean ±SD (n = 5). Compacts of formulation PVP 5% compressed at 154 MPa showed consistent lamination and the tensile strength of the tablets could not be measured, therefore the bar did not appear in graph A.

The lubricant activity of PVP-Leu was investigated by measuring the tablet ejection force. It was found that PVP-Leu does not facilitate ejection (data not shown).

3.7 Discussion

Although tableting is one of the most common processes in pharmaceutical manufacturing, we argue that a true fundamental and mechanistic understanding of tablet formation process is relatively limited. With US Food and Drug Administration's (US-FDA) Quality in the 21st century initiative, which includes the quality by design (QbD) and process analytical technologies (PAT), it is becoming increasingly important to understand the impact of formulation process as well as material variability on the performance and manufacturability of new drug products [59]. A number of drug product recalls identified excipient variability as a contributor to failure of the drug product [60] indicating a potential weakness in the full understanding and control over excipient manufacturing and functionality. Creating improved excipients is considered to be a key for minimizing the impact of excipient related product malfunction. Furthermore, excipients with multiple functionalities could reduce the number of excipients in the formulations, and with fewer and lesser excipients whose roles and functionalities are better understood, the variability to influence process and product consistency in product manufacturing should be reduced.

In this study, binding activity was chosen as the key excipient functionality to be improved because of the fact that a binder (typically referred to as a ‘filler-binder’) forms the largest proportion of a typical direct compression formulation and therefore is a major source of variability in directly compressible tablet formulations. It was reported that binders with smaller particle size exhibit better binder efficiency due to an increase in the surface area available for inter-particulate bonding, as the particles become smaller [10-12]. In our study, this size-binder efficiency relationship together with knowledge and understanding of

interactive mixing has been used to create an alternative strategy for improving tableting excipients. Surface manipulation *via* co-spraying is demonstrated as a potential new approach to overcome cohesion traditionally associated with reduced particle size and an effective strategy at controlling inter-particle excipient cohesion. However, the effect of such manipulation (surface and bulk properties) on interactive mixing, flow additive action and binder activity is not known. Therefore, we aimed at investigating the impact of L-leucine on the physico-chemical and bulk properties of the spray-dried interactive excipient and also to understand the effect of underlying changes on performance of such excipients.

It was noted that PVP-SD was extremely cohesive and did not appear to de-agglomerate and disperse homogeneously over drug particles upon mixing. Incorporation of L-leucine in the spray feed helped reducing cohesion. Reducing cohesion facilitated more homogeneous dispersion of interactive excipient particles over API particles. The XPS data indicated that L-leucine achieved higher surface concentrations as compared to the bulk of PVP-Leu particles. L-leucine also resulted in a marked reduction in surface energy and bulk cohesion.

The impact of interactive excipients on the flow of API blends was assessed and PVP-Leu resulted in a marked improvement. This is attributed to the ability of PVP-Leu particles to act as "spacers" between coarse particles effectively increasing contact separation distance and, therefore, decreasing van der Waals attractions between paracetamol particles reducing cohesion and improving flow [20, 21]. The observation that PVP-SD had no effect on the flow performance of the formulation confirmed that controlling surface properties and cohesion was a key to achieving such functionality.

The glidant performance of PVP-Leu was compared against the benchmark glidant silica and silica was found to exert a better glidant performance. This is likely due to the much

smaller particle size of silica compared to PVP-Leu as the contact area of interacting particle surfaces decreased with decreasing particle size [20, 61, 62]. We proposed that by manipulating the size and surface characteristics further, such as hydrophobicity and surface energy, glidant performance of such interactive excipients can be further optimized. Studies investigating the relationship between particle size, surface hydrophobicity, surface energy and excipient functionalities such as interactive mixing ability, glidant action and binder properties are underway. Additionally, the effect of API properties such as particle size, compression mechanism and surface energy on the performance of interactive excipients is also being investigated.

Both PVP-SD and PVP-Leu demonstrated an improved binder performance compared to PVP and other directly compressible excipients. This showed that interactive mixing is a highly promising alternative approach for enhanced functional performance of the excipients. While the binder performance of PVP-Leu was better at lower excipient proportions, PVP-SD resulted in stronger tablets compared to PVP-Leu at higher proportions. We propose that this might be due to the reduced surface energy noted in case of PVP-Leu as compared to PVP-SD [63]. However, further studies are required to understand the relationship between surface energy and binder activity of such interactive excipients.

The results presented here show that both physico-chemical and mechanical properties affect the functional performance of the interactive excipients. The surface modification using L-leucine allowed controlling bulk cohesion *via* its effect of surface energy and/or surface morphology. Reducing cohesion improved the mixing efficiency and flow additive ability of the interactive excipient. Although, the binder activity of the PVP-Leu was excellent compared to other existing binders but L-leucine also appeared to compromise the binder activity of PVP-Leu as compared to PVP-SD, which might be due to a reduced surface energy observed with

PVP-Leu. In theory, the change in surface energy may affect both the flow additive action and binder activity by affecting the van der Waals forces of interactions, where a reduction in surface energy could result in better flow additive action and reduce binder activity and vice versa [37, 64]. Studies investigating the relationship between surface concentration of L-leucine and surface energy as well as the relationship between surface energy and binder activity of the interactive excipients are underway. This could help understanding the key particle properties that controls excipient performance and would facilitate achieving optimum particle design for improved performance. In addition, investigating detailed tableting properties of such interactive excipient might give further insight into its comprehensive applications of such excipients in the creation of robust and innovative tablet formulations.

3.8 Conclusion

This paper presents the first demonstration of a multicomponent interactive binder-glidant excipient, coupled with detailed physico-chemical characterisation of these materials to illustrate the fundamental mechanisms behind its design and functionality. The paper provides an understanding of how we may design interactive excipients with controlled particle size, core and surface properties to allow all the basic requirements of a formulation: i.e. good flow, high compactability and excellent uniformity. In summary, the paper outlines the application of an interdisciplinary approach of interactive mixing to create multi-functional excipients for enhanced tablet formulations.

3.9 Acknowledgement

Sharad Mangal is thankful to Monash Institute of Graduate Research (MIGR) for providing Monash Graduate Scholarship (MGS) and Monash International Postgraduate Research Scholarship (MIPRS). Satu Lakio would like to acknowledge The Osk. Huttunen Foundation, The Finnish Cultural Foundation and The Emil Aaltonen Foundation for financial support.

3.10 References

[1] Andrews GP. Advances in solid dosage form manufacturing technology. Philosophical Transactions of The Royal Society A- Mathematical Physical and Engineering Sciences 2007; 365(1861): 2935-2949.

[2] Bolhuis GK, Armstrong NA. Excipients for direct compaction—an update. Pharm Dev Technol 2006; 11(1): 111-124.

[3] Rojas J, Buckner I, Kumar V. Co-proccessed excipients with enhanced direct compression functionality for improved tableting performance. Drug Dev Ind Pharm 2012; 38(10): 1159-1170.

[4] Bolhius GK, Waard Hd. Materials for direct compaction. In: Alderborn G, Nystrom C, eds., Pharmaceutical Powder Compaction Technology. Informa Healthcare: New York, 1996; pp. 419-500.

[5] Reimerdes D. The near future of tablet excipients. Manuf Chemist 1993; 64: 14-15.

[6] Saha S, Shahiwala AF. Multifunctional coprocessed excipients for improved tabletting performance. Expert Opin Drug Deliv 2009; 6(2): 197-208.

[7] Tobyn MJ, McCarthy GP, Staniforth JN, Edge S. Physicochemical comparison between microcrystalline cellulose and silicified microcrystalline cellulose. Int J Pharm 1998; 169(2): 183-194.

[8] Tian JL, Tian C, Ke X. Comparative evaluation of a co-processed self-lubricating excipient LubriTose SD as a direct compression vehicle. J Drug Del Sci Tech 2012; 22(6): 562-567.

[9] Peck GE, Anderson NR, Banker GS. Principles of improved tablet production system design. In: Liebermann HA, Lachman L, Schwartz JB, eds., Pharmaceutical Dosage Froms: Tablets. Lea & Febiger 1990; pp. 1-76.

[10] Skinner GW, Harcum WW, Barnum PE, Guo J-H. The evaluation of fine-particle hydroxypropylcellulose as a roller compaction binder in pharmaceutical applications. Drug Dev Ind Pharm 1999; 25(10): 1121-1128.

[11] Mattsson S, Nyström C. Evaluation of strength-enhancing factors of a ductile binder in direct compression of sodium bicarbonate and calcium carbonate powders. Eur J Pharm Biopharm 2000; 10(1): 53-66.

[12] Kolter K, Flick D. Structure and dry binding activity of different polymers, including Kollidon VA 64. Drug Dev Ind Pharm 2000; 26(11): 1159-1165.

[13] Nachaegari SK, Bansal AK. Coprocessed excipients for solid dosage forms. Pharm Tech 2004; 50(1): 52-64.

[14] Stephenson PL, Thiel WJ. The effect of humidity on the production of ordered mixtures. Powder Technol 1980; 25(1): 115-119.

[15] Crooks MJ, Ho R. Ordered mixing in direct compression of tablets. Powder Technol 1976; 14(1): 161-167.

[16] Staniforth JN, Rees JE. Electrostatic charge interactions in ordered powder mixes. J Pharm Pharmacol 1982; 34(2): 69-76.

[17] Staniforth JN. Ordered mixing or spontaneous granulation? Powder Technol 1985; 45(1): 73-77.

[18] Hersey JA. Ordered mixing: A new concept in powder mixing practice. Powder Technol 1975; 11(1): 41-44.

[19] Schulze D. Powders and bulk solids: Behavior, characterization, storage and flow In. Springer: Berlin–Heidelberg–NewYork–Tokyo, 2008.

[20] Yang J, Sliva A, Banerjee A, Dave RN, Pfeffer R. Dry particle coating for improving the flowability of cohesive powders. Powder Technol. 2005; 158(1–3): 21-33.

[21] Xie HY. The role of interparticle forces in the fluidization of fine particles. Powder Technol 1997; 94(2): 99-108.
[22] Jallo LJ, Chen Y, Bowen J, Etzler F, Dave R. Prediction of inter-particle adhesion force from surface energy and surface roughness. J Adhes Sci Technol 2011; 25(4-5): 367-384.
[23] de Villiers MM, Lötter AP, van der Watt JG. Influence of surfactants and interactive mixing on the cohesiveproperties of a poorly wettable solid. Powder Technol 1993; 75(2): 159-165.
[24] Rotthäuser B, Kraus G, Schmidt PC. Optimization of an effervescent tablet formulation using a central composite design optimization of an effervescent tablet formulation containing spray dried l-leucine and polyethylene glycol 6000 as lubricants using a central composite design. Int J Pharm 1998; 46(1): 85-94.
[25] Röscheisen G, Schmidt PC. Preparation and optimization of l-leucine as lubricant for effervescent tablet formulations. Pharm Acta Helv 1995; 70(2): 133-139.
[26] Yang JJ, Liu CY, Quan LH, Liao YH. Preparation and in vitro aerosol performance of spray-dried Shuang-Huang-Lian corrugated particles in carrier-based dry powder inhalers. AAPS pharmSciTech 2012; 13(3): 816-825.
[27] Sou T, Kaminskas LM, Nguyen T-H, Carlberg R, McIntosh MP, Morton DAV. The effect of amino acid excipients on morphology and solid-state properties of multi-component spray-dried formulations for pulmonary delivery of biomacromolecules. Eur J Pharm Biopharm 2013; 83(2): 234-243.
[28] Sou T, Orlando L, McIntosh MP, Kaminskas LM, Morton DAV. Investigating the interactions of amino acid components on a mannitol-based spray-dried powder formulation for pulmonary delivery: A design of experiment approach. Int J Pharm 2011; 421(2): 220-229.
[29] Minchom CM, Armstrong NA. A proposed technique for expressing the capacity of directly compressible tablet diluents. J Pharm Pharmacol 1989; 39: 69.
[30] Armstrong NA. Tablet manufacture by direct compression. In: Swarbrick J, Ed., Encyclopedia of pharmaceutical technology. 3rd ed, NY, USA: Informa Healthcare, 2007; pp. 3673-3683.
[31] Schultz J, Lavielle L, Martin C. The Role of the Interface in Carbon Fibre-Epoxy Composites. J. Adhesion 1987; 23(1): 45-60.
[32] van Oss CJ, Chaudhury MK, Good RJ. Monopolar surfaces. Adv Colloid Interface Sci 1987; 28(1): 35-64.
[33] Traini D, Young PM, Thielmann F, Acharya M. The influence of lactose pseudopolymorphic form on salbutamol sulfate-lactose interactions in DPI formulations. Drug Dev Ind Pharm 2008; 34(9): 992-1001.
[34] Fowkes FM. Attractive forces at interfaces. Ind Eng Chem Res 1964; 56(12): 40-52.
[35] van Oss CJ. Acid—base interfacial interactions in aqueous media. Colloids Surf A 1993; 78: 1-49.
[36] Van Oss CJ, Good RJ, Chaudhury MK. Additive and nonadditive surface tension components and the interpretation of contact angles. Langmuir 1988; 4(4): 884-891.
[37] Castellanos A. The relationship between attractive interparticle forces and bulk behaviour in dry and uncharged fine powders. Adv Phys 2005; 54(4): 263-376.
[38] Abdullah EC, Geldart D. The use of bulk density measurements as flowability indicators. Powder Technol 1999; 102(2): 151-165.
[39] Freeman R. Predicting flowability and characterizing powders. Pharm Dev Technol Eur 2004; 16(1): 41.

[40] Freeman R. Measuring the flow properties of consolidated, conditioned and aerated powders — A comparative study using a powder rheometer and a rotational shear cell. Powder Technol 2007; 174(1–2): 25-33.
[41] Freeman T, Price R. Dynamic powder characterization for DPI formulation. Drug Del Technol 2009; 9(5): 50–55.
[42] Fu X, Huck D, Makein L, Armstrong B, Willen U, Freeman T. Effect of particle shape and size on flow properties of lactose powders. Particuology 2012; 10(2): 203-208.
[43] Turki D, Fatah N. Behavior and fluidization of the cohesive powders: Agglomerates sizes approach. Braz J Chem Eng 2008; 25(4): 697-711.
[44] Gharaibeh SF, Aburub A. Use of first derivative of displacement vs. force profiles to determine deformation behavior of compressed powders. AAPS PharmSciTech 2013; 14(1): 398-401.
[45] Gupta A, Hamad M, Tawakkul M, Sayeed V, Khan M. Difference in the lubrication efficiency of bovine and vegetable-derived magnesium stearate during tabletting. AAPS PharmSciTech 2009; 10(2): 500-504.
[46] Fell JT, Newton JM. Determination of tablet strength by the diametral-compression test. J Pharm Sci 1970; 59(5): 688-691.
[47] Vehring R. Pharmaceutical particle engineering via spray drying. Pharm Res 2008; 25(5): 999-1022.
[48] Chew NYK, Shekunov BY, Tong HHY, Chow AHL, Savage C, Wu J, Chan HK. Effect of amino acids on the dispersion of disodium cromoglycate powders. J. Pharm. Sci. 2005; 94(10): 2289-2300.
[49] Feng AL, Boraey MA, Gwin MA, Finlay PR, Kuehl PJ, Vehring R. Mechanistic models facilitate efficient development of leucine containing microparticles for pulmonary drug delivery. Int J Pharm 2011; 409(1–2): 156-163.
[50] Derjaguin BV, Muller VM, Toporov YP. Effect of contact deformations on the adhesion of particles. J Colloid Interf Sci 1975; 53(2): 314-326.
[51] Johnson KL, Kendall K, Roberts AD. Surface energy and the contact of elastic solids. P Roy Soc Lond A Mat 1971; 324(1558): 301-313.
[52] Chew NYK, Tang P, Chan HK, Raper JA. How much particle surface corrugation is sufficient to improve aerosol performance of powders? Pharm Res 2005; 22(1): 148-152.
[53] Kato Y, Ohkuma M, Shimada Y, Sunada H. Evaluation of the flowability of surface-modified preparations by the measurement of the inter-particle adhesive force. J Drug Deliv Sci Technol 2005; 15(3): 217-221
[54] Staniforth JN. Powder flow. In: Aulton ME, Ed., Pharmaceutics: The science of dosage form design. 2nd ed., Edinbergh, UK: Churchill Livingstone, 2002; pp. 197–210.
[55] Harnby N, Hawkins AE, Vandame D. The use of bulk density determination as a means of typifying the flow characteristics of loosely compacted powders under conditions of variable relative humidity. Chem Eng Sci 1987; 42(4): 879-888.
[56] Han X, Jallo L, To D, Ghoroi C, Dave R. Passivation of high-surface-energy sites of milled ibuprofen crystals via dry coating for reduced cohesion and improved flowability. J Pharm Sci 2013; 102(7): 2282-96.
[57] Turki D, Fatah N. Description of consolidation forces on nanometric powders. Brazilian Journal of Chemical Engineering 2010; 27(4): 555-562.
[58] Pitt KG, Heasley MG. Determination of the tensile strength of elongated tablets. Powder Technol 2013; 238: 169-175.
[59] Yu LX. Pharmaceutical quality by design: product and process development, understanding, and control. Pharm Res 2008; 25(4): 781-791.

[60] Friedman R. Pharmaceutical quality systems: US perspective. In, Pharmaceutical quality system (ICH Q10) conference: Brussels, Belgium., 2011.
[61] Jonat S, Hasenzahl S, Gray A, Schmidt PC. Mechanism of glidants: Investigation of the effect of different colloidal silicon dioxide types on powder flow by atomic force and scanning electron microscopy. J Pharm Sci 2004; 93(10): 2635-2644.
[62] Meyer K, Zimmermann I. Effect of glidants in binary powder mixtures. Powder Technol 2004; 139(1): 40-54.
[63] Sun CC. Decoding powder tabletability: Roles of particle adhesion and plasticity. J Adhes Sci Technol 2011; 25(4-5): 483-499.
[64] Patel S, Kaushal AM, Bansal AK. Compression physics in the formulation development of tablets. Crit Rev Ther Drug 2006; 23(1): 1-66.

3.11 Appendix

3.11.1 Appendix 3.1 – UV Absorbance vs wavelength plots of stock solution used for the creating paracetamol standard curve and PVP-Leu solutions of differing concentrations.

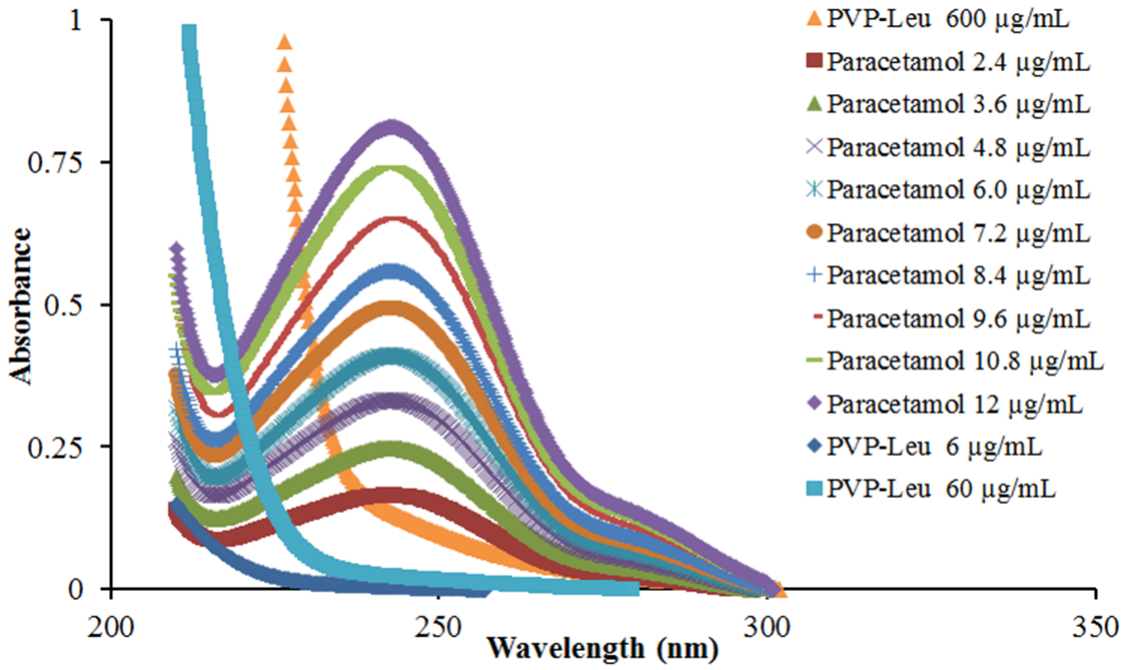

3.11.2 Appendix 3.2 – Standard curve of paracetamol. Absorbance as a function of concertation µg/mL.

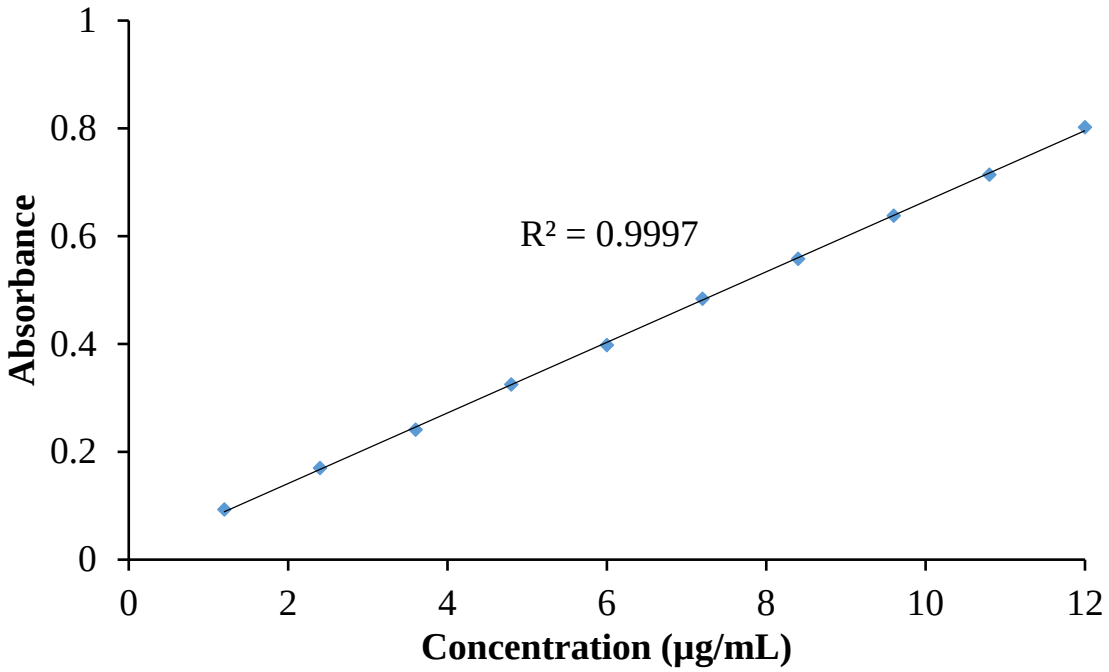

3.11.3 **Appendix 3.3 –** Aeration energy profiles of studies powder formulations as a function of air velocity. Data presented as Mean ±SD (n = 3).

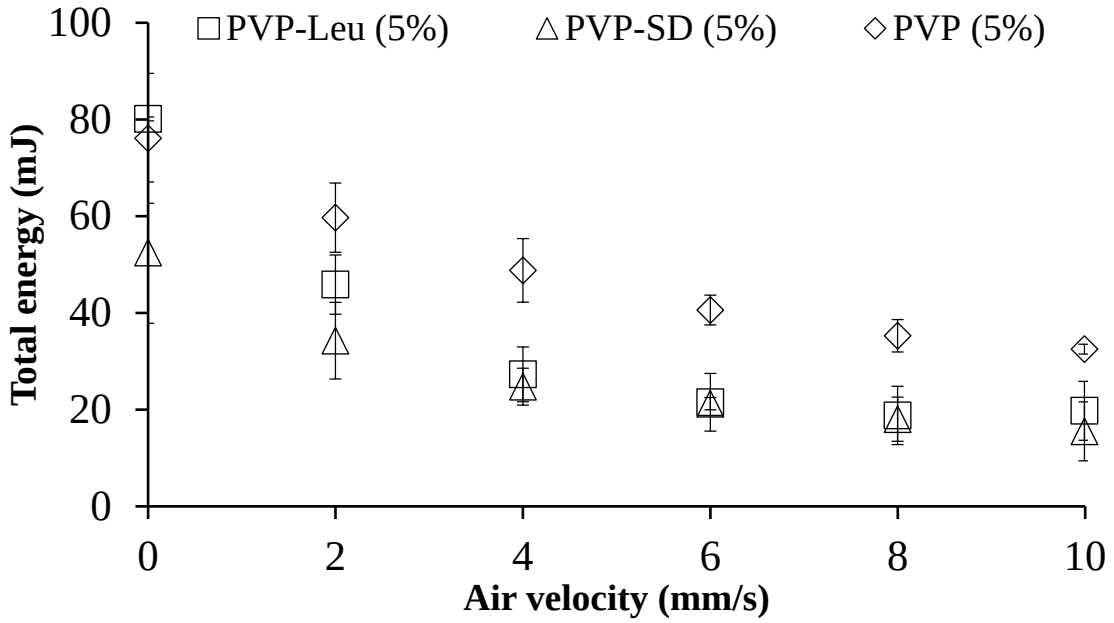

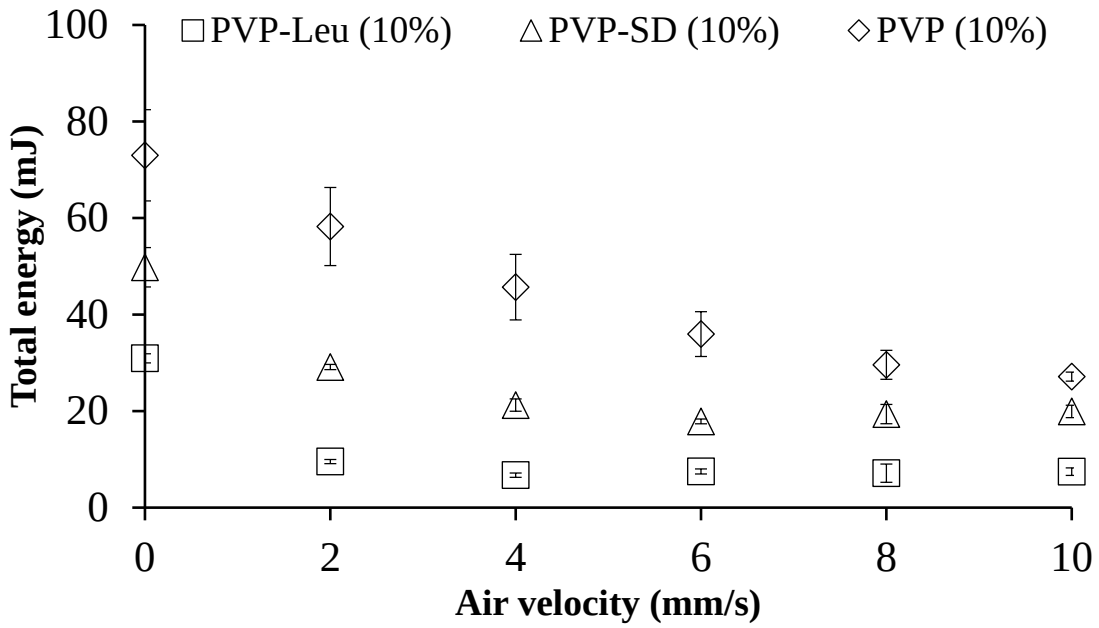

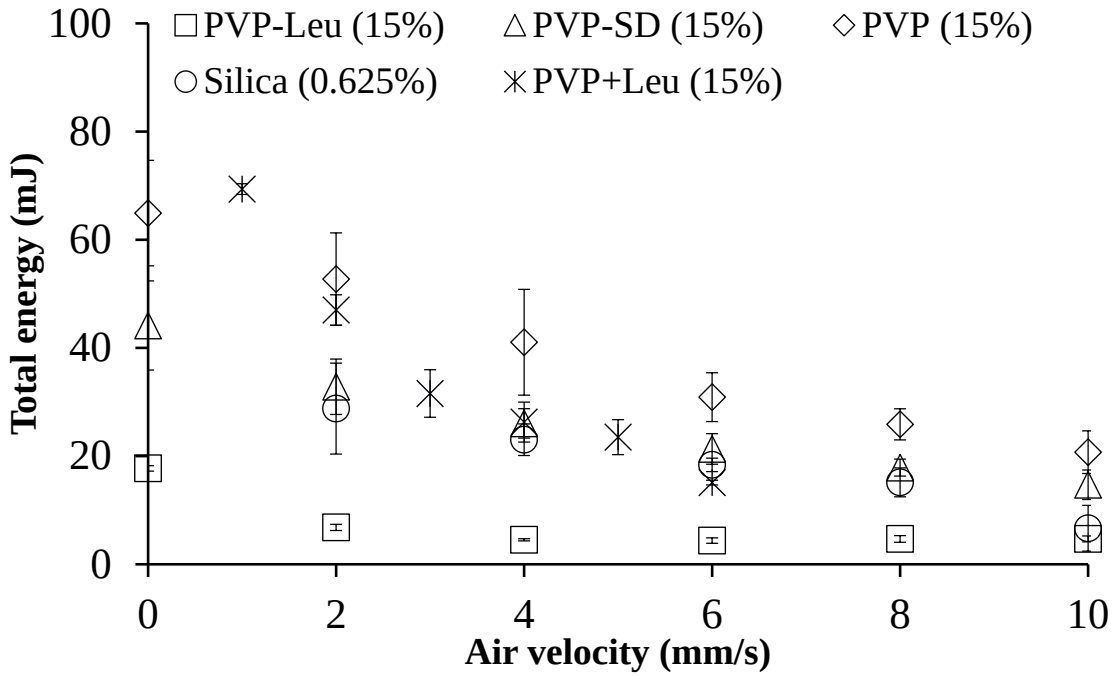
□PVP-Leu (15%)
△PVP-SD (15%)
◇PVP (15%)
○Silica (0.625%)
✳PVP+Leu (15%)
Total energy (mJ)
Air velocity (mm/s)
0
20
40
60
80
100
0
2
4
6
8
10

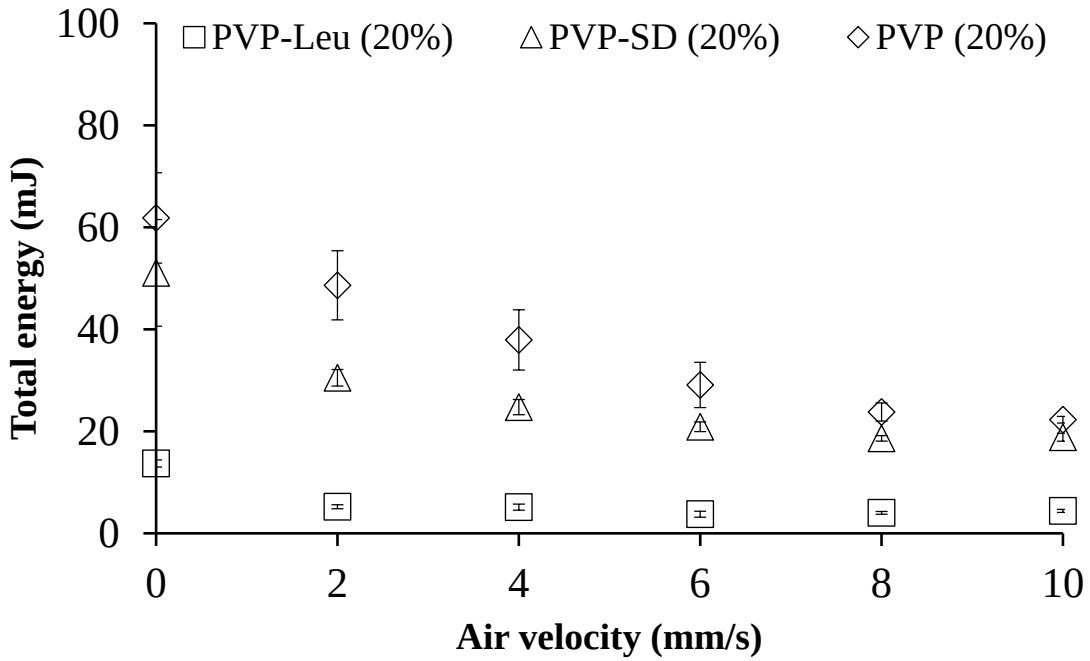
□PVP-Leu (20%)
△PVP-SD (20%)
◇PVP (20%)
Total energy (mJ)
Air velocity (mm/s)
0
20
40
60
80
100
0
2
4
6
8
10

3.11.4 **Appendix 3**.4 – Compressibility (%) profiles of studied powder formulations as a function of applied normal stress. Data presented as Mean ±SD (n = 3).

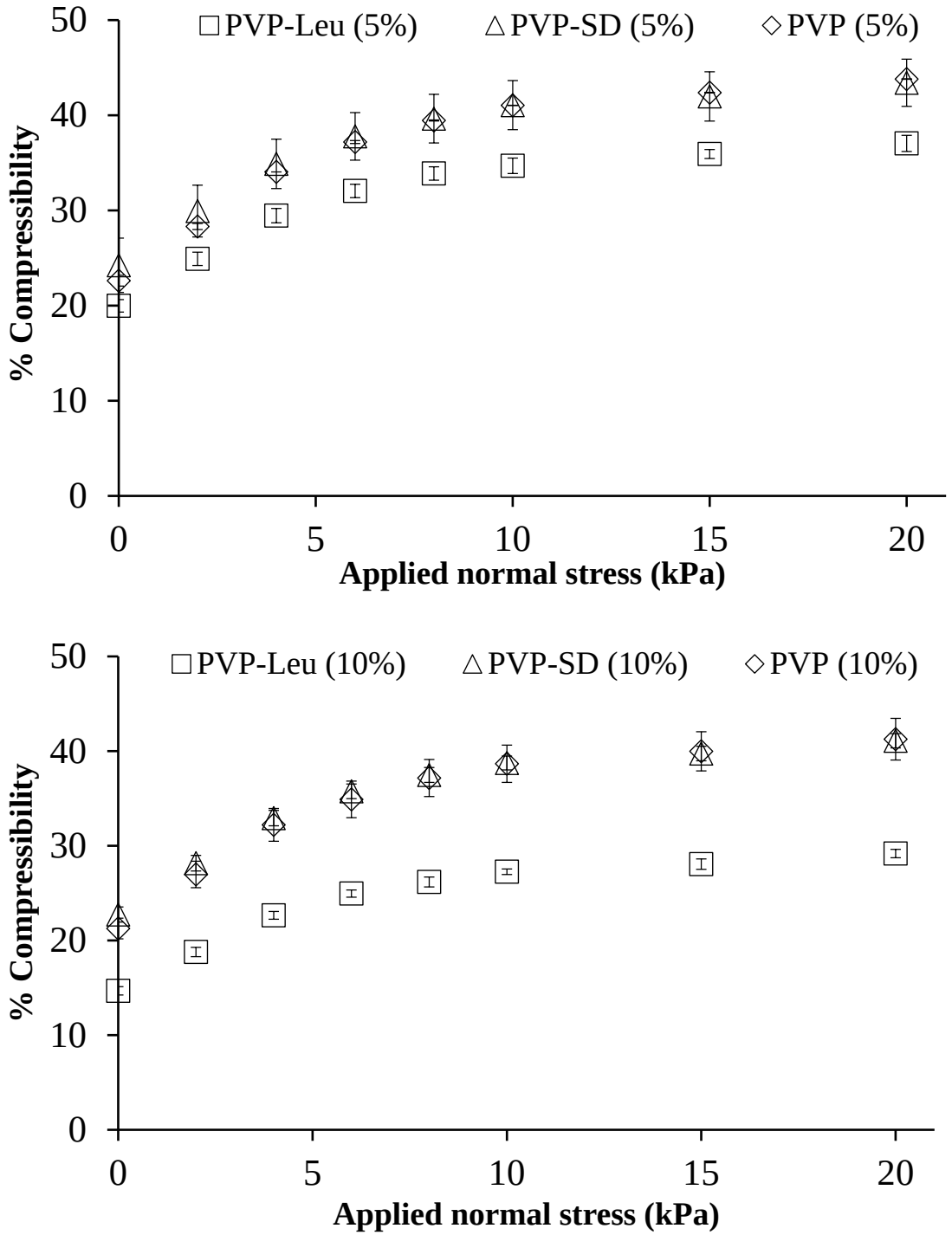

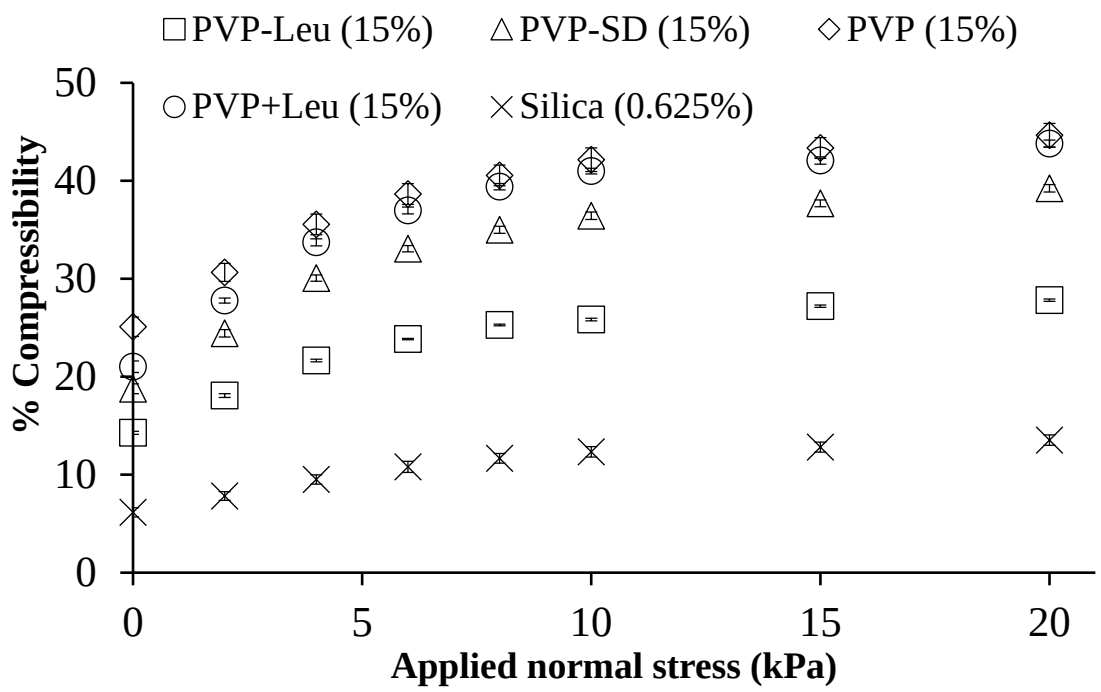
□PVP-Leu (15%)
△PVP-SD (15%)
◇PVP (15%)
○PVP+Leu (15%)
×Silica (0.625%)
% Compressibility
0
10
20
30
40
50
0
5
10
15
20
Applied normal stress (kPa)

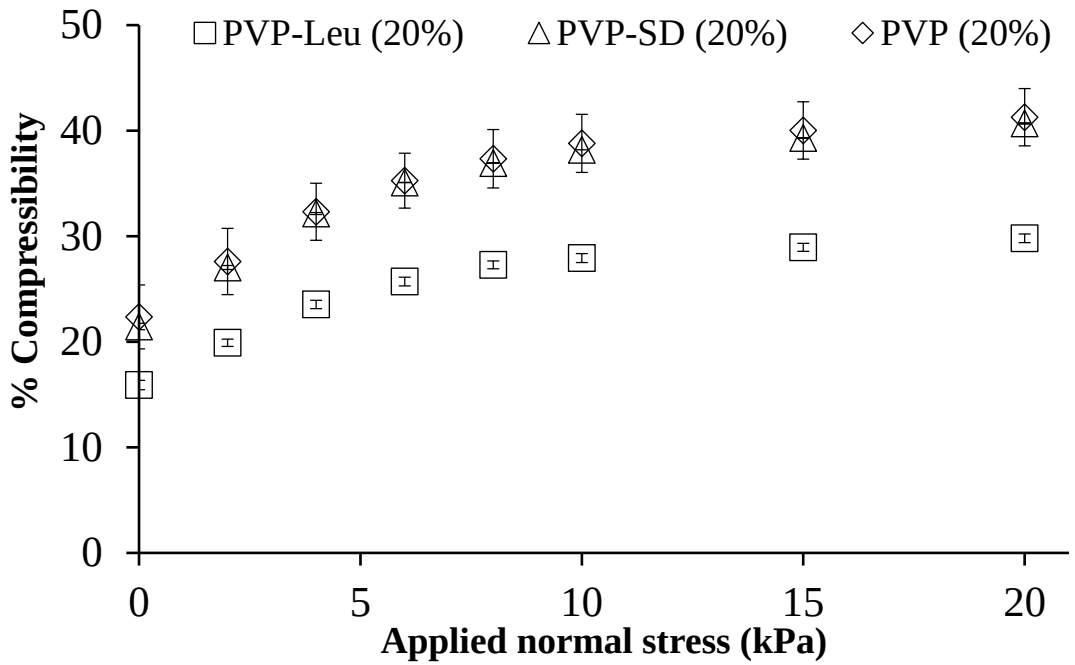
□PVP-Leu (20%)
△PVP-SD (20%)
◇PVP (20%)
% Compressibility
0
10
20
30
40
50
0
5
10
15
20
Applied normal stress (kPa)

Chapter 4

To investigate the relationship between the extent of surface manipulation *via* L-leucine and the change in surface physico-chemical properties and cohesion of small binder particles

Sharad Mangal[1], Felix Meiser[1], Geoffrey Tan[1], Thomas Gengenbach[2], John Denman[3], Matthew R Rowles[4], Ian Larson[1]*, David AV Morton[1]*

[1] Drug Delivery, Disposition and Dynamics, Monash University, 381 Royal Parade, Parkville, VIC-3052, Australia
[2] CSIRO Materials Science and Engineering, Bayview Avenue, Clayton, VIC-3168, Australia
[3] Ian Wark Research Institute, University of South Australia, Mawson Lakes, SA-5095, Australia
[4] Melbourne School of Engineering, The University of Melbourne, Victoria-3010, Australia
* Corresponding Authors

***Published as:**
Mangal S, Meiser F, Tan G, Gengenbach T, Denman J, Rowles MR, Larson I, Morton DA. Relationship between surface concentration of L-leucine and bulk powder properties in spray-dried formulations. Eur J Pharm Biopharm. 2015; 94: 160–169.

4 Declaration for Thesis Chapter 4

Declaration by candidate

In the case of Chapter 4, the nature and extent of my contribution to the work was the following:

Nature of contribution	**Extent of contribution (%)**
Study initiation, formation of hypothesis, laboratory work, data collection, analysis and interpretation and writing the manuscript	55%

The following co-authors contributed to the work. If co-authors are students at Monash University, the extent of their contribution in percentage terms must be stated:

Name	**Nature of contribution**	**Extent of contribution (%) for student co-authors only**
Felix Meiser	Supervision and manuscript revision	5%
Geoffrey Tan	IGC characterization and proofreading	5%
Thomas Gengenbach	XPS characterization and proofreading	5%
John Denman	ToF-SIMS characterization and proofreading	5%
Matthew R. Rowles	P-XRD characterization and proofreading	5%
David AV Morton	Supervision and manuscript revision	10%
Ian Larson	Supervision and manuscript revision	10%

The undersigned hereby certify that the above declaration correctly reflects the nature and extent of the candidate's and co-authors' contributions to this work*.

Candidate's Signature		**Date 23.11.2015**
Main Supervisor's Signature	[redacted]	**Date 24/11/15**

*Note: Where the responsible author is not the candidate's main supervisor, the main supervisor should consult with the responsible author to agree on the respective contributions of the authors.

4.1 Commentary

In the previous chapter, L-leucine was shown to reduce the surface energy, increase surface asperity and reduce the cohesion of small particles. These observations were speculated to be a result of saturation of L-leucine at the drying surface of the particles as they form. In this chapter, we address objective 2 "to investigate the relationship between the extent of surface manipulation *via* L-leucine and the change in surface physico-chemical properties and cohesion of small binder particles". We hypothesized that surface L-leucine concentration controls the powder physico-chemical properties, which dictates the magnitude of inter-particle interaction and hence the bulk performance i.e., cohesion of small particles.

This understanding was considered important for further optimisation and to gain a deeper insight into the effect of cohesion of small binder particles on their interactive mixing behaviour. This may also help rationalize the resultant changes in excipient's functional performance i.e., flow additive and binder actions as a function of the cohesion of small binder particles in later studies.

4.2 Abstract

The amino acid L-leucine has been demonstrated to act as a lubricant and improve the dispersibility of otherwise cohesive fine particles. It was hypothesized that optimum surface L-leucine concentration is necessary to achieve optimal surface and bulk powder properties.

Polyvinylpyrrolidone was spray-dried with different concentration of L-leucine and the change in surface composition of the formulations was determined using x-ray photoelectron spectroscopy (XPS) and time of flight- secondary ion mass spectrometry (ToF-SIMS). The formulations were also subjected to powder X-ray diffraction analysis in order to understand the relationship between surface concentration and solid-state properties of L-leucine. In addition, the morphology, surface energy and bulk cohesion of spray-dried formulations were assessed to understand the relation between surface L-leucine concentration and surface and bulk properties.

The surface concentration of L-leucine increased with higher feed concentrations and plateaued at about 10% L-leucine. Higher surface L-leucine concentration also resulted in the formation of larger L-leucine crystals and not much change in crystal size was noted above 10% L-leucine. A change in surface morphology from spherical to increasingly corrugated was also recorded. Specific collapsed/folded over particles were only seen in formulations with 10% or higher L-leucine feed concentration suggesting a change in particle surface formation process. In addition, bulk cohesion also reduced to a stable value with 10% L-leucine concentration.

Thus, the surface concentration of L-leucine governs particle formation and optimum surface L-leucine concentration results in optimum surface and bulk powder properties.

Keywords: L-leucine, Polyvinylpyrrolidone, Surface mapping, Inter-particle cohesion, Spray-drying

4.3 Graphical abstract

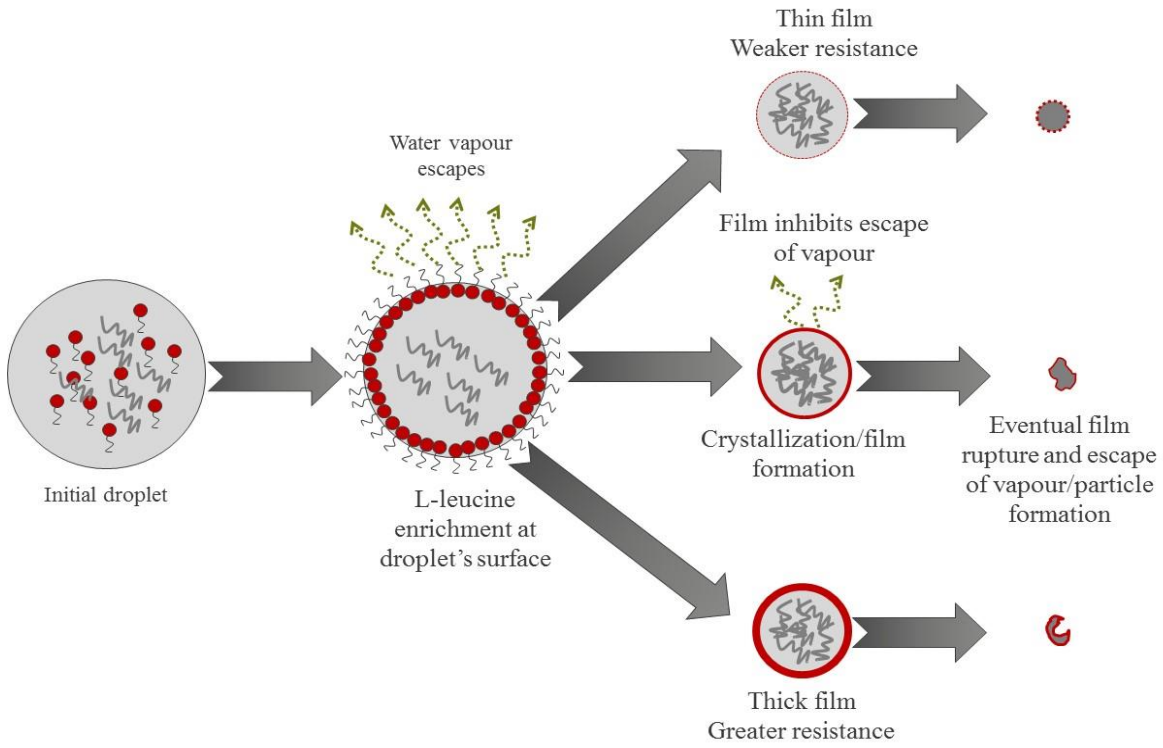

4.4 Introduction

Fine particles (typically <10 μm) are routinely found in a range of dry powder pharmaceutical operations and continue to attract significant research interest [1, 2]. Such fine powders have been explored in tablet formulations for their enhanced dissolution and tendency to form interactive mixtures particularly in the context of low-dose formulations to achieve content uniformity [2, 3]. However, the major challenge with the use of such fine particles is their highly cohesive nature and a tendency to agglomerate which can limit their extent of use and effectiveness in dry powder applications [4, 5]. In practice, particle cohesion needs to be controlled to limit agglomeration and also facilitate de-agglomeration.

Co-spraying materials with L-leucine has been shown to limit agglomeration and improve dispersion of fine particles mainly in the context of inhaled drug delivery [6, 7]. It has been proposed that the use of L-leucine will reduce cohesion and improve dispersibility by controlling the surface texture of spray-dried particles [8, 9]. L-leucine is believed to migrate to the surface of the droplets followed by formation of a shell early in the drying phase [10]. This L-leucine rich shell interferes with the diffusion of water vapour leading to formation of corrugated particles [11]. Corrugated particles experience significantly reduced contact area and consequently lower inter-particle cohesion [12, 13].

A recent study proposed that rather than surface corrugation, the solid-state properties of L-leucine play a leading role in determining its effectiveness in controlling cohesion [14]. It was proposed that L-leucine crystallizes early in the spray-drying owing to its low water solubility [11]. Crystals of L-leucine exhibit lower mobility in the receding/drying droplet and result in formation of an L-leucine enriched shell. It was also reported that the effectiveness of L-leucine increases as its crystallinity increases and the optimum effectiveness is typically achieved in the formulations with fully crystalline L-leucine [14]. However, L-leucine was

recently also argued to exist as a partially ordered molecular structure, which was proposed to be result of its lamellar self-assembly on the surface of the spray-dried particles [15].

Recently, our group illustrated that the enhanced powder properties achieved by co-spraying cohesive materials with L-leucine could be used to create a multi-functional interactive excipient for tablet formulations [16]. It was demonstrated that L-leucine achieves substantially higher concentrations on the surface than the bulk and results in significant reduction in surface energy of spray-dried formulations [16]. However, it is unknown how L-leucine affects the surface energy and particle formation of the spray-dried formulations. The influence of surface structure and concentration of L-leucine on physico-chemical and bulk powder properties is also relatively unexplored. In this study, we hypothesized that the surface concentration L-leucine dictates surface physico-chemical properties, which in turn determines the bulk properties. In addition, optimum surface physico-chemical and bulk powder properties are achieved at optimum surface L-leucine concentration. This insight could help understanding supporting a "quality by design" approach to optimize formulation performance.

For this study, polyvinylpyrrolidone (PVP) was spray-dried with different concentrations of L-leucine. The surface composition of spray-dried formulations was examined using state-of–the-art techniques: X-ray photoelectron spectroscopy (XPS) and time of flight- secondary ion mass spectrometry (ToF-SIMS). The solid-state property of L-leucine was determined using powder-X-ray diffraction (P-XRD), while the surface physico-chemical properties such as surface energy and morphology were determined using inverse gas chromatography (IGC) and scanning electron microscopy (SEM) respectively. Finally, the intrinsic bulk cohesion of the powders was determined using powder shear testing.

4.5 Materials and methods

PVP (average molecular weight ~ 10,000 Da), was purchased from Sigma–Aldrich (St. Louis, Missouri, USA). L-leucine was purchased from Ajinomoto Co. Inc. (Tokyo, Japan). Acid washed silanized glass beads (250 µm) were obtained from Sigma (Sigma–Aldrich, Steinheim, Germany).

4.5.1 Method of preparation

Aqueous solutions of PVP in combination with various proportions of L-leucine (as shown in Table 4.1) were spray-dried using the method as described previously [17]. Briefly, PVP and L-leucine were weighed accurately and dissolved in water with the aid of magnetic stirring. The resultant solutions were spray-dried using a Buchi-190 mini spray-dryer (Buchi Laboratory Equipment, Flawil, Switzerland) with a 0.5 mm two-fluid nozzle. The standard operating conditions employed during spray-drying were: inlet temperature, 125 ±5 °C; spray air flow rate, 800 L/h and liquid solution feed rate, 10 mL/min. These conditions resulted in an outlet temperature of 70 ±2 °C. The powders then obtained were collected immediately and stored in a sealed aluminium bag to prevent exposure to humidity.

Table 4.1 – Compositions of various spray-dried formulations

Formulation Codes	PVP (% w/v)	L-leucine (% (w/w) of PVP)
PVP-Leu (0%)	6	0
PVP-Leu (2.5%)	6	2.5
PVP-Leu (5%)	6	5

PVP-Leu (7.5%)	6	7.5
PVP-Leu (10%)	6	10
PVP-Leu (12.5%)	6	12.5
PVP-Leu (15%)	6	15

4.5.2 Particle size and size distribution

The particle size and size distribution of the spray-dried formulations were determined by laser-light scattering method using the Malvern Mastersizer 2000 (Malvern Instruments Ltd, Malvern, UK) equipped with a Sirocco cell dry powder dispersion unit. A shear pressure of 2.0 bar was used to disperse the powders in air to achieve efficient de-agglomeration. Obscuration was in the range of 2 – 5. The particle size values D_{50} (50% volume median diameter), D_{10} (10% volume below this diameter) and D_{90} (90% volume below this diameter), span and particle size distribution plots were collected and the average values of three measurements reported.

4.5.3 Scanning electron microscopy (SEM)

The surface morphology of the various formulations were imaged by scanning electron microscopy (Phenom^{TM}, FEI Company, Hillsboro, Oregon, USA). A small amount of powder sample was scattered on the aluminium stub mounted with carbon tape and excess powder was removed using air gun. The stubs were then coated with a thin gold film using a sputter coater (Emitech K550X, Quorum Technologies, Kent, UK). The gold coated stubs were then loaded in the instrument and images were captured.

4.5.4 X-ray photoelectron spectroscopy (XPS)

X-ray photoelectron spectroscopy (XPS) analysis was performed using an AXIS Ultra DLD spectrometer (Kratos Analytical Inc., Manchester, UK) with a mono-chromated Al Kα source at a power of 180 W (15 kV × 12 mA), a hemispherical analyser operating in the fixed analyser transmission mode and the standard aperture (analysis area: 0.3 mm × 0.7 mm). The total pressure in the main vacuum chamber during analysis was typically 10^{-8} mbar. Survey spectra were acquired at a pass energy of 160 eV. To obtain more detailed information about chemical structure, oxidation states etc., high resolution spectra were recorded from individual peaks at 20 eV pass energy (yielding a typical peak width for polymers of 1.0 eV). Samples were filled into shallow wells of custom-built sample holders. One lot of each sample was prepared and 2 different locations were analysed on each sample at a nominal photoelectron emission angle of 0º with respect to the surface normal. Since, the actual emission angle is ill-defined in the case of such fine particles (ranging from 0º to 90º) the sampling depth may range from 0 nm to approximately 5 − 10 nm. The atomic concentrations of the detected elements were calculated using integral peak intensities and the sensitivity factors supplied by the manufacturer. Binding energies were referenced to the aliphatic hydrocarbon peak at 285.0 eV.

4.5.5 Time-of-flight secondary ion mass spectrometry (ToF-SIMS)

ToF-SIMS experiments were performed using a PHI TRIFT V nanoTOF instrument (Physical Electronics Inc., Chanhassen, MN, USA) equipped with a pulsed liquid metal $^{79+}$Au primary ion gun (LMIG), operating at 30 kV energy. Dual charge neutralisation was provided by an electron flood gun and 10 eV Ar^+ ions. Experiments were performed under a vacuum of 5 x 10^{-6} Pa or better. “Bunched” Au1 instrumental settings were used to optimise mass resolution for spectra, while “unbunched” Au1 instrumental settings were used to optimise spatial resolution for the collection of images. ToF-SIMS data were collected from 4 areas per sample,

using a raster of 50 x 50 micron and acquisition time of 4 minutes. Sample spectra and images were processed and integrated using WincadenceN software (Physical Electronics Inc., Chanhassen, MN, USA). Integrated peak values of the selected ions were normalized to the total secondary ion intensities. The resulting data were then compared qualitatively by preparing plots of average normalized counts (with 95% confidence intervals) for each species of interest. The percentage normalized counts do not give a measure of absolute coverage, because the specific signals identified were percentages over the total ion signals of all species, but was considered useful for examination of relative changes.

4.5.6 Powder X ray diffraction (P-XRD)

Sample powders were sprinkled onto a quartz sample plate smeared with a thin layer of Vaseline at room temperature. The samples were then analysed by the X-ray diffractometer (Philips 1140 vertical diffractometer, Philips, Holland) for scanning from 2 ˚ to 60 ˚ at 2θ, with an angular increment of 2 ˚/min. The crystalline status of the powders was assessed by examination of the resulting diffraction patterns. The diffraction data was modelled using the rietveld method [18], as implemented in TOPAS (Bruker 2008, Diffracplus TOPAS, Bruker AXS, Karlsruhe, Germany). A previously determined L-leucine structure was used (COD + IUCR) [19]. A model for PVP was determined empirically by fitting two pseudo-voigt peaks to the data, constrained with a single scale factor. The average diffracting domain size was determined by the integral-breadth method [20]. The absolute values of the domain size are not accurate representations of the physical sizes, however the relative changes in the size is of significance, and is indicative of trends in the different formulations.

4.5.7 Shear cell

A Freeman FT4 powder rheometer system (Freeman Technology, Worcestershire, UK) with shear test module was used to characterize bulk cohesion. Briefly, the instrument measures the

powder shear stress at a given consolidating normal stress. For the shear test, the powders (approximately 1 g) were loaded into a 1 mL shear cell module and conditioned. Then, the powder bed was pre-consolidated at a normal stress of 9 kPa using a vented piston, which was then replaced by a shear head. Shear tests were carried out at normal stresses of 3, 4, 5, 6 and 7 kPa. The shear stress at each normal stress was recorded and yield loci were derived as curves to represent the maximum shear stress the sample can support under a certain normal stress. The bulk cohesion forces of each sample were calculated by extrapolating the yield loci to zero normal stress (Eq. 2.1).

$$\tau = C + \sigma \tan \eta \qquad \text{(Eq. 2.1)}$$

Where, τ is the shear stress, σ is the normal stress, η is the angle of friction, and C is the cohesion force. The parameter "cohesion" was calculated by extrapolating the yield loci to a zero normal stress at the intercept. In general, higher bulk cohesion values are considered to correspond to higher cohesive inter-particle forces.

4.5.8 Inverse gas chromatography (IGC)

Surface energies were determined with the use of an inverse gas chromatography (iGC 2000, Surface Measurement Systems Ltd., London, UK) at infinite dilution. All presilanized glass columns and silanized glass wool were purchased from Surface Measurement Systems Ltd., London, UK.

The columns packed with spray-dried formulations exhibited low porosities obstructing the flow of gas through the column. Consequently, column over pressuring was observed. In order to alleviate this, formulations were blended with 80% (w/w) of commercially available 250 µm acid washed pre-silanized glass beads using a smooth mortar and pestle for 5 minutes. Blends were then stored in a humidity controlled environment where

the relative humidity (RH) was less than 20% until column packing. The blends were then packed into pre-silanized glass columns (300 mm × 3 mm) by gentle tapping, until no cracks, hollows, or channels were visible in the powder bed. The columns were loosely stoppered with silanized glass wool at both ends to prevent sample movement. Column packing was performed in a controlled environment with humidity <20% RH.

Before surface energy measurements, packed columns were pre-conditioned with a helium stream at 10 sccm (standard cubic centimetre per minute) for 2 h at 303 K and 0% RH. Dispersive energy measurements were achieved with the use of a series of n-alkanes (chromatography grade decane, nonane, octane, heptane and hexane); while the specific surface energy measurements were achieved with the use of acidic and basic probes – chromatography grade chloroform and ethyl acetate, respectively. For all probes, a concentration of 0.03 p/p0 (where p is the partial pressure and p0 is the saturation vapour pressure) was used. Helium at a flow rate of 10 sccm was used to carry the probes through the stationary phase and the system was kept at 303 K at 0% RH. Dead volumes were based on the retention volume of methane gas at 0.03 p/p0, detection of probes was achieved with a flame ionization detector. Results were analysed with SMS-iGC analysis software v1.3 (Surface Measurement Systems Ltd., London, UK). The values of acidic component (γ^+) and basic component (γ^-) and the molecular cross sectional area of the specific probes are presented in Table 4.2. Three replicated of each sample were measured for all samples and mean values were reported.

Table 4.2 Values of acidic and basic and the molecular cross sectional area of chloroform and ethyl acetate

Probe	**γ^+ (mJ/m^2)**	**γ^- (mJ/m^2)**	**Molecular cross sectional area (m^2)**

Chloroform	3.38	0	4.40×10^{-19}
Ethyl acetate	0	19.2	3.30×10^{-19}

The dispersive surface energy was calculated according to the theory described by Schultz, 1987 [21] while the polar energy was calculated based on the theory proposed by Good-van Oss-Chaudhury, 1987 [22] where the polar energy can be split into two components - an acidic component, γ^+, and a basic component, γ^-. The calculation of the specific energy can be given by equation 2.2 [22, 23].

$$\gamma_s^P = \sqrt{\gamma_S^+ \gamma_S^-} \qquad \text{(Eq. 2.2)}$$

The total surface energy of the material is the sum of the dispersive (γD) and polar (γP) components [24]. Upon determination of the dispersive and polar surface energies, the work of cohesion (w_{co}) for interactions between similar particles can be calculated using the following equation [25, 26]

$$w_{co} = 2\sqrt{\gamma_1^D . \gamma_1^D} + 2\sqrt{\gamma_1^P . \gamma_1^P} \qquad \text{(Eq. 2.3)}$$

4.6 Results

4.6.1 Particle size and size distribution

The particle size of formulations spray-dried with different concentrations of L-leucine is presented in Table 4.3. The particle size of the spray-dried formulations increased slightly with higher L-leucine feed concentration and the change in particle size amongst various formulations was such that particles remain substantially in the 2 to 3 µm median range with similar spread of distribution. Therefore, it was considered unlikely that the particle size would strongly alter particle-particle interaction forces. It was also noted that the spray-dried formulations demonstrated a mono-modal particle size distribution (Figure 4.1).

Table 4.3 – Particle size of spray-dried formulations. Data presented as Mean ±SD (n = 3)

Formulations	Particle Size (µm)			Span
	D_{10}	D_{50}	D_{90}	
PVP-Leu (0%)	1.1 ±0.1	2.1 ±0.1	4.3 ±0.1	1.5 ±0.1
PVP-Leu (2.5%)	1.2 ±0.0	2.4 ±0.0	4.8 ±0.1	1.5 ±0.1
PVP-Leu (5%)	1.2 ±0.0	2.4 ±0.0	4.8 ±0.1	1.5 ±0.1
PVP-Leu (7.5%)	1.3 ±0.0	2.6 ±0.1	5.0 ±0.2	1.5 ±0.1
PVP-Leu (10%)	1.4 ±0.1	2.8 ±0.0	5.5 ±0.1	1.5 ±0.1
PVP-Leu (12.5%)	1.3 ±0.0	2.8 ±0.0	5.5 ±0.1	1.5 ±0.1
PVP-Leu (15%)	1.5 ±0.1	3.00 ±0.0	5.6 ±0.1	1.4 ±0.1

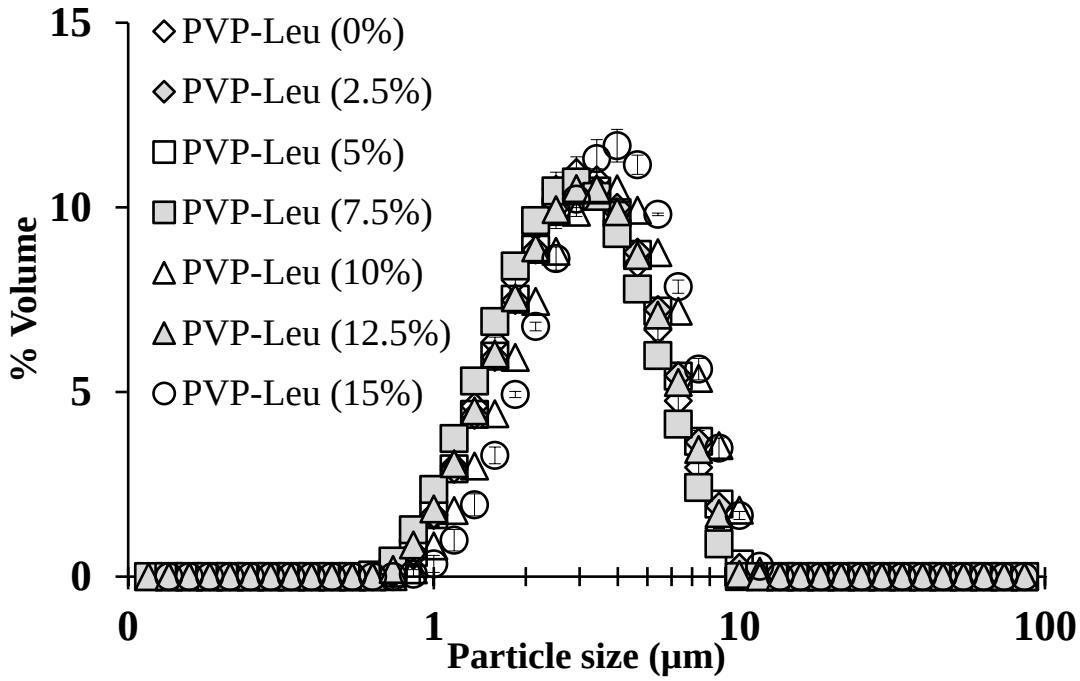

Figure 4.1 – Particle size distribution plots of spray-dried formulations. Data presented as Mean ±SD (n = 3).

4.6.2 Scanning electron microscopy (SEM)

Representative scanning electronic micrographs of the studied formulations are shown in Figure 4.2. Spray-dried PVP (PVP-Leu (0%)) formed small spherical, dimpled and heavily agglomerated particles. The morphology of the spray-dried particles changed with higher L-leucine mass fractions, from smooth-dimpled spheres to increasingly corrugated structures to highly collapsed-sphere particle structures that have folded over into themselves (Figure 4.2). This was consistent with previous observations on the prominent role of L-leucine in determining particle morphology [15]. It was apparent that the highly collapsed particles (as indicated by red arrows in Figure 4.2) were only apparent in formulations with 10% and higher L-leucine feed concentrations.

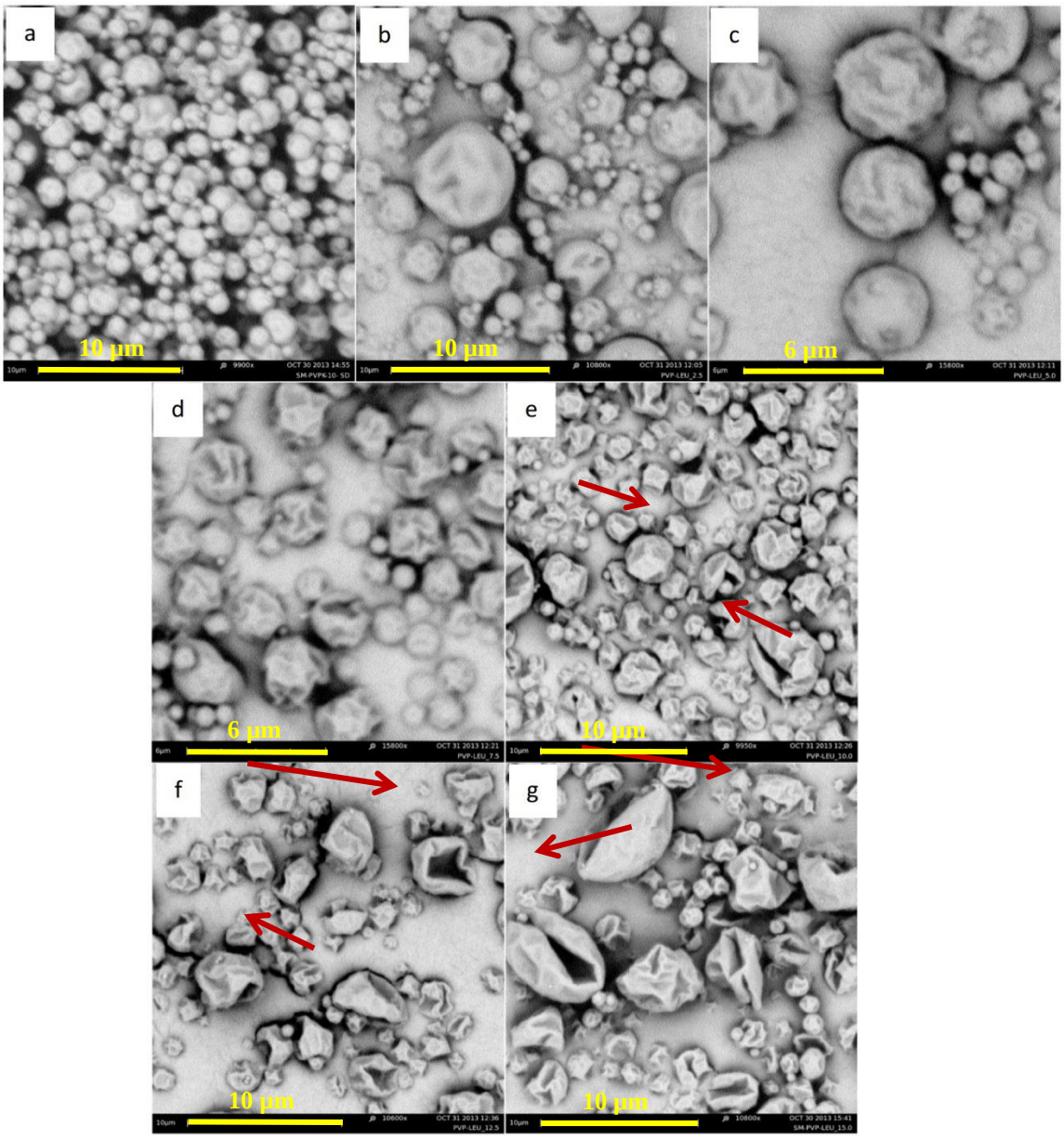

Figure 4.2 – Representative SEM images of various spray-dried formulations; (A) PVP-Leu (0%); (B) PVP-Leu (2.5%); (C) PVP-Leu (5%); (D) PVP-Leu (7.5%); (E) PVP-Leu (10%) (F) PVP-Leu (12.5%) (G) PVP-Leu (15%). Red arrows pointing towards collapsed particles.

4.6.3 X-ray photoelectron spectroscopy (XPS)

Table 4.4 showed the atomic surface composition of various spray-dried formulations as measured by XPS. While the concentration of nitrogen (N) was the same for both compounds

(PVP and L-Leucine) and thus did not vary throughout the series, the concentrations of carbon (C) and oxygen (O) vary systematically between the values for the pure compounds. It was possible to estimate surface fractions of PVP and L-leucine in the formulations based on elemental compositions. However, this was considered unreliable as the compositions were quite similar and there was no element unique to one of the two compounds. Therefore, surface fractions of the two compounds were estimated based on the C 1s and N 1s high resolution spectra (where 1s is the electron orbital). The C 1s and N 1s spectra were distinctly different for PVP and L-leucine because of their different chemical functionality (Appendix 4.1). Reference spectra of the pure compounds were recorded, normalised, and then used as model components to calculate curvefits for the spectra of the spray-dried formulations (Appendix 4.1). The relative peak area of PVP and L-leucine for the co-sprayed formulations therefore represents the relative surface fractions of PVP and L-leucine. The relative surface fractions of PVP and L-leucine were also representative of surface composition as the number of carbon and nitrogen atoms are the same in the case of PVP and L-leucine. The surface compositions were compared against the L-leucine feed concentration in Figure 4.3. There was good agreement between the results obtained using C 1s data and those based on N 1s data.

Table 4.4 – Elemental compositions calculated as relative atomic ratio to carbon for spray-dried formulations as measured by XPS.

S. No.	Formulations	C	N	O
1	PVP-Leu (0%)	76.2 ±0.0	11.7 ±0.0	11.82 ±0.0
2	PVP-Leu (2.5%)	74.6 ±0.0	11.4 ±0.0	13.82 ±0.0
3	PVP-Leu (5%)	73.3 ±0.0	11.4 ±0.1	15.20 ±0.1

4	PVP-Leu (7.5%)	72.0 ±0.1	11.6 ±0.1	16.60 ±0.0
5	PVP-Leu (10%)	71.1 ±0.1	11.3 ±0.1	17.58 ±0.1
6	PVP-Leu (12.5%)	71.1 ±0.1	11.3 ±0.1	17.58 ±0.0
7	PVP-Leu (15%)	70.8 ±0.1	11.2 ±0.1	17.94 ±0.1
8	L-leucine	69.5 ±0.3	11.4 ±0.1	19.12 ±0.3

The data suggested that L-leucine achieve substantially higher surface concentration relative to PVP in all co-spray-dried formulations (Figure 4.3). With 2.5%, L-leucine achieved surface fraction in excess of 33% (w/w), which increased further with higher L-leucine concentration from 2.5% to 10%. This was consistent with previous findings [27]. The surface fraction of PVP similarly diminished with increasing surface L-leucine fraction consistent with the replacement of PVP from the surface of the particles. Further increases in the surface L-leucine concentrations were smaller with further higher feed concentrations (>10%) of L-leucine.

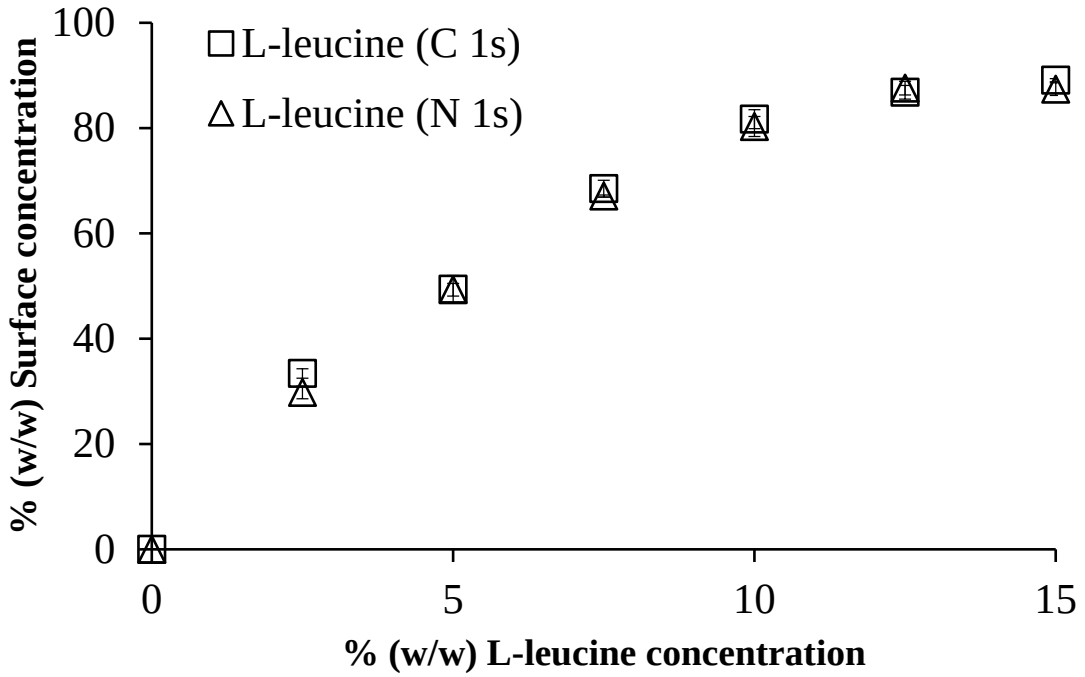

Figure 4.3 – % w/w surface concentrations of L-leucine in spray-dried formulations as calculated by C 1s and N 1s curve-fitting plots using pure components as reference spectra to fit components of spray-dried formulation measured by XPS.

4.6.4 Time-of-flight secondary ion mass spectrometry (ToF-SIMS)

The spray-dried formulations were also subjected to ToF-SIMS analysis in order to further reveal the surface enrichment of L-leucine. The ToF-SIMS spectra of raw PVP and L-leucine are shown in Appendix 4.2. For the pure PVP sample, the fragment $C_8H_{12}NO$ (*m*/*z* 138) was used as the distinguishing signal, while the fragment $C_6H_{14}NO_2$ (*m*/*z* 132) was used as the distinguishing signal for L-leucine (Appendix 4.2). The normalized counts detected for the L-leucine and PVP signals for the spray-dried formulations are given in Figure 4.4 and Figure 4.5).

In PVP-Leu (2.5%), both the PVP and L-leucine signals could be clearly observed indicating the presence of both PVP and L-leucine on the surface of the particles. With higher L-leucine feed concentrations the surface signal of L-leucine increased, while the PVP signal

diminished (Figure 4.4 and Figure 4.5) indicating replacement of PVP by L-leucine from the surface of the particles. The ToF-SIMS data was in general agreement with the XPS data, where an increase in surface L-leucine concentration and a decrease in surface PVP concentration were evident with higher L-leucine feed concentrations.

It is noteworthy that with 5% and higher mass fractions; the L-leucine signal reached a maximum in the ToF-SIMS data, whereas for XPS data the surface L-leucine concentration appeared to maximise with 10% feed concentration. These observed differences in the XPS and ToF-SIMS results may be due to the differences in the depth of detection and surface sensitivity between the two techniques. As a general guide, ToF-SIMS provides chemical information from the top 1 − 2 nm region, whereas XPS provides chemical information from about the top 5 − 10 nm region of the particles.

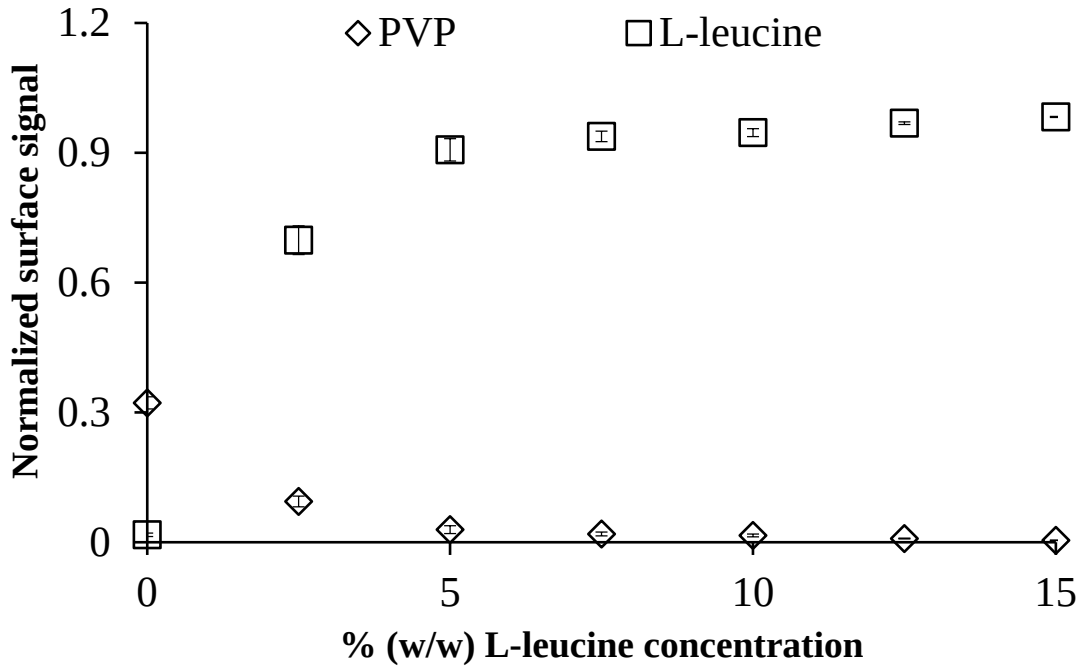

Figure 4.4 – Normalized counts of PVP ($C_8H_{12}NO$; m/z 138) signals and L-leucine ($C_6H_{14}NO_2$; m/z 132) signal over the total spectral peak of spray-dried formulations measured using ToF-SIMS at scan area of 50 µm × 50 µm. For PVP, the normalization was carried out for three

$N^{+}O$ containing peaks ($C_6H_{10}NO$, m/z 112), ($C_6H_{10}NO$, m/z 124), and ($C_8H_{12}NO$, m/z 138). Above figure only presents the normalized signal intensity for ($C_8H_{12}NO$; m/z 138) signal, and thus represent only a fraction of total normalized PVP signals i.e., 1.

∗PVP-Leu (0%) sample was very sticky to load on sample pans, and very difficult to find suitable areas of dispersed particles for analysis, which resulted in poor imaging. Therefore, untreated PVP was considered as control in this study.

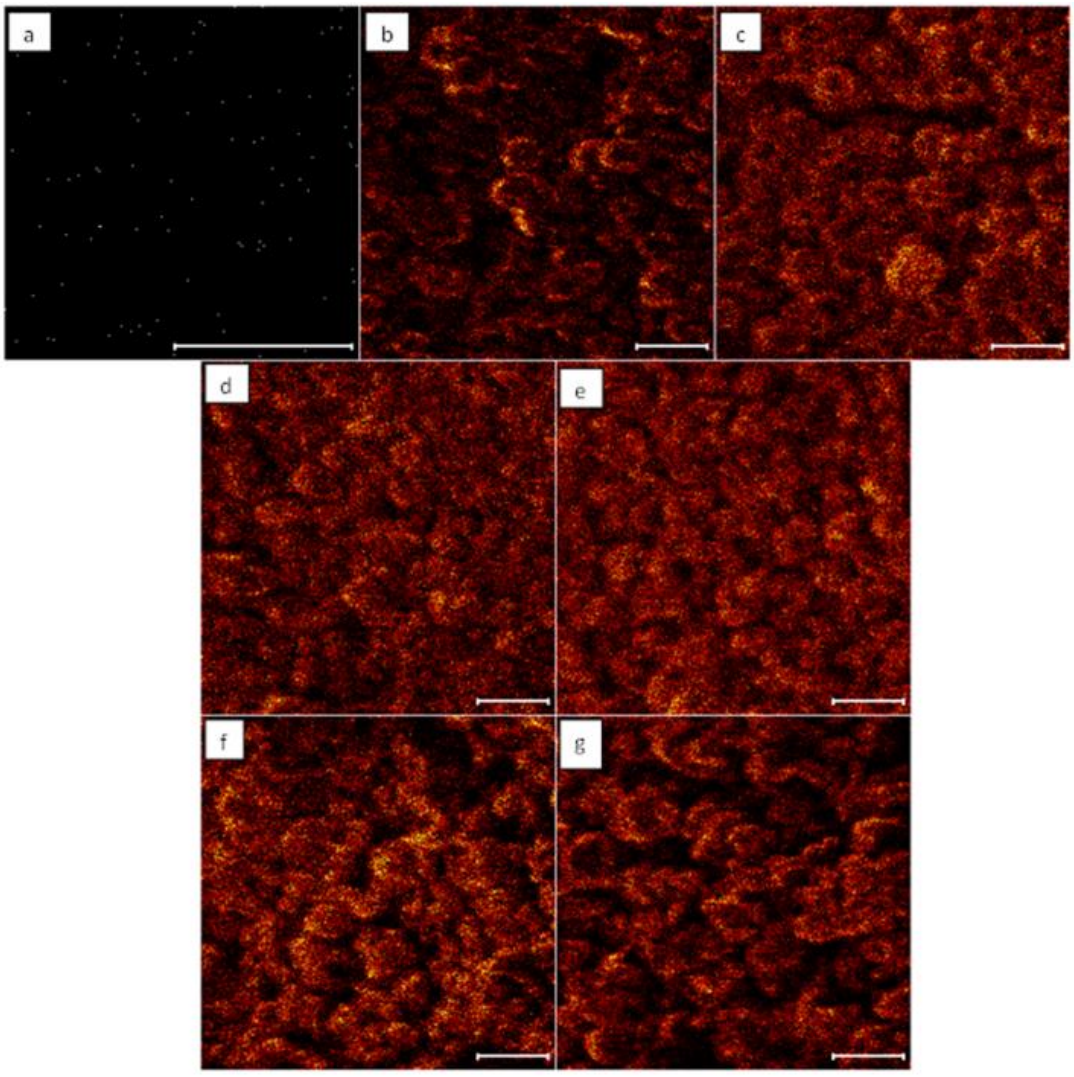

Figure 4.5 – ToF-SIMS micrographs for L-leucine (red) and PVP (black) of samples (a) untreated PVP; (b) PVP-Leu (2.5%); (c) PVP-Leu (5%); (d) PVP-Leu (7.5%); (e) PVP-Leu (10%) (f) PVP-Leu (12.5%) (g) PVP-Leu (15%).

4.6.5 Powder-X ray diffraction (P-XRD)

P-XRD diffractograms of various formulations were collected to study the solid-state characteristics of L-leucine in selected spray-dried formulations. Figure 4.6 provides the combined diffractograms of the spray-dried formulations. The change in solid-state properties of L-leucine in various formulations was investigated by determining its crystallite domain size (Figure 4.6).

The diffraction profiles showed that PVP-Leu (0%) had no clear diffraction peaks and was indicated to be in an amorphous form, while raw L-leucine was crystalline (Appendix 4.3). The combination of low concentration and small domain size rendered the low values of L-leucine, e.g. 2.5% and 5%, difficult to visualise in these spectra. However, it became clear from 7.5% L-leucine that higher order peaks are observed showing that there was three-dimensional L-leucine ordering. The P-XRD pattern observed in L-leucine co-sprayed samples was consistent with literature [15]. The appearance of individual reflections showed a step change in the appearance of the diffraction patterns. For example, the peak at approximately 32.5 °2θ shows a marked increase in intensity in the 7.5% L-leucine sample compared to the 5% L-leucine sample, suggesting that longer range order was becoming more apparent in these samples (Figure 4.6).

Closer inspection of the data revealed that as the intensity of the L-leucine peaks increases, they also appear to sharpen indicating an increase in the average diffracting domain size. Figure 4.6 (as indicated by numbers on the graph) shows the calculated domain size of L-leucine of the various formulations. However, the magnitude of increase in domain size

reduced with 10% or higher L-leucine concentration and so suggests that the rate of growth in domain size was reduced at these concentrations. The peak analysis indicated that L-leucine forms a defined and consistent crystal structure at concentrations as low as 2.5% and subsequently evolves with increasing L-leucine into a nano-crystalline structured layer.

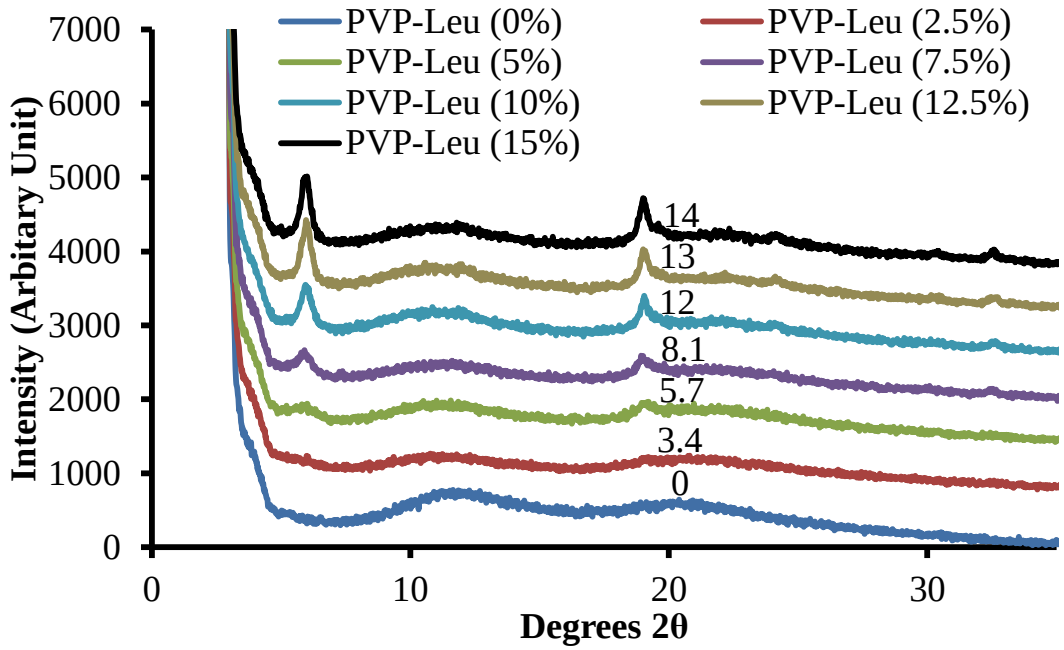

Figure 4.6 –X-ray diffractogram of various spray-dried formulations. Domain size is the average diffracting domain length and the domain size of L-leucine is presented as number over the diffractoram of individual formulation.

4.6.6 Shear cell

The bulk cohesion (Figure 4.7) of the selected formulations was determined using the FT4 rheometer shear cell module. This demonstrated a relationship between surface influence of L-leucine at increasing concentrations and the bulk cohesion properties of the powder. PVP-Leu (0%) showed high cohesion (3.8 kPa). This is consistent with its apparent agglomeration state as noted in the SEM images. No significant reduction in cohesion was seen with 2.5% L-leucine, but with higher L-leucine concentrations, a decline in cohesion was observed. The

cohesion appeared to achieve a stable value at around 10% L-leucine and higher L-leucine concentrations (12.5% and 15%) did not appear to further affect cohesion. Therefore, L-leucine resulted in a reduction in the measured bulk inter-particle cohesion in concentration dependent manner.

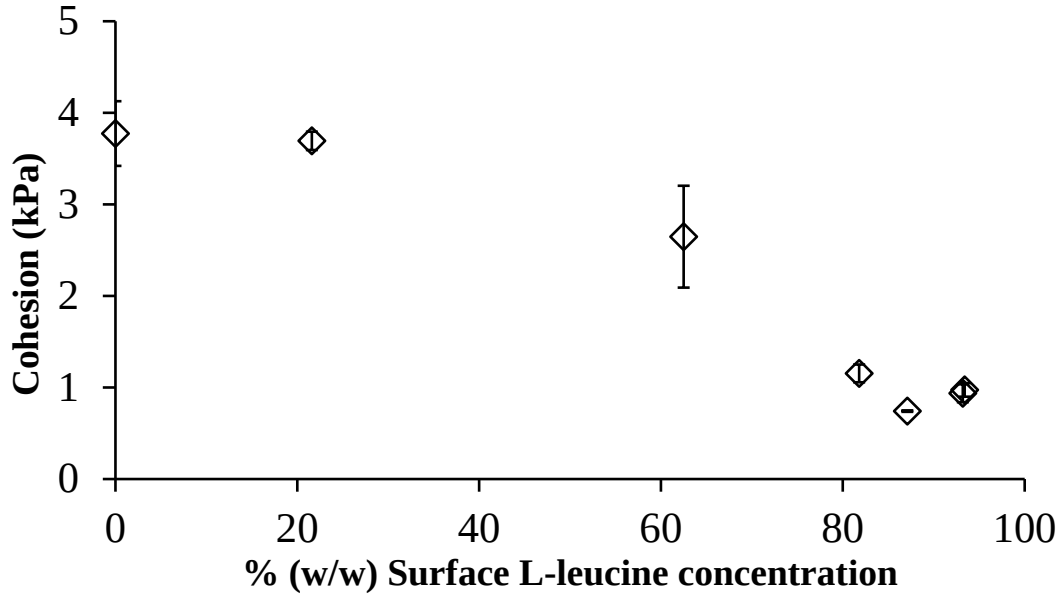

Figure 4.7 – Cohesion of the spray-dried formulations. Data presented as Mean ±SD (n = 3).

4.6.7 Inverse gas chromatography (IGC)

The formulations were analysed using inverse gas chromatography to determine the effect of L-leucine feed concentration on the polar (both acidic and basic components), non-polar and total surface energies (Figure 4.8 and Table 4.5).

The polar surface energy of PVP-Leu (0%) was 96.06 ±8.17 mJ/m^2. At the lowest concentration of L-leucine – the surface of PVP-Leu (2.5%) showed a marked reduction in the polar surface energy and further increase in L-leucine concentration resulted in further reduction in the polar surface energy. The polar surface energy appeared to reduce to 17.43 ±1.15 mJ/m^2 with L-leucine concentration of 7.5%. It appeared that the surface of spray-dried

PVP was more basic than acidic in nature due to a larger γ_S^- (61.5 ±11.01 mJ/m^2) than γ_S^+ (38.0 ±5.98 mJ/m^2) value (Table 4.5). However, when co-spray-dried with L-leucine, the surface of the formulations was more acidic than basic. The basic component of surface energy decreased reaching a value of 4.3 ±0.35 mJ/m2 at 7.5% feed concentration; while the acidic component of surface energy decreased, at a relatively lower rate reaching a value of 17.5 ±0.91 mJ/m2 at 7.5% feed concentration. The higher basicity of PVP may be related to the heterocyclic nitrogen in its structure, whereas higher acidity of PVP-Leu formulations may be attributed to the presence of L-leucine on the surface which exhibits a prominent acidic character [10].

It was proposed that co-spraying a material such as the polymeric PVP with L-leucine leads to rapid mass transport of L-leucine to the air–water interface of a droplet, organizing itself in such a way that its hydrophobic tail (tert–butyl) faces towards the air phase thereby increasing the surface hydrophobicity of the particles, which was recordable in the form of an altered non-polar surface energy [10]. This mass transport appears to be facile, despite the viscosity-modifying character typically associated with PVP. The incorporation of L-leucine resulted in a reduction in both the acidic and basic components of the surface energy, and suggests replacement of polar surface groups of PVP with non-polar chains of L-leucine. However, it was noted that no significant change was observed for the non-polar surface energy of PVP and PVP-Leu. This may be attributed to the limitation of IGC at infinite dilution where only the highest surface energy sites are probed. Consequently, this would suggest that the highest non-polar surface energy of both the hydrophobic portion of PVP and the hydrophobic portion of L-leucine were similar, thus IGC at infinite dilution was unable to reveal any differences in the non-polar surface energy. To overcome this, future work may consider IGC at finite concentration, which allows the determination of a distribution of surface energies across a larger heterogeneous area. Alternatively, the co-spray drying of L-leucine with different materials having varied hydrophobic character may help with the understanding of

the relative changes to the non-polar surface energy that may occur with co-spray drying with L-leucine.

The total surface energy of various spray-dried formulation was shown in Table 4.5. The results indicate that the total surface energy of PVP was relatively high at approximately 140 mJ/m^2 and with 2.5% L-leucine resulted in a reduction in the total surface energy to 85 mJ/m^2. The total surface energy of the formulation dropped with higher L-leucine concentration up to 5%, after which no significant changes were observed. Similarly, the work of cohesion as calculated from the surface energy, suggest that no change in cohesion was observed with 5% L-leucine concentration or higher. This differs slightly to the cohesion values as determined by shear cell method, which indicated a stable cohesion around 10%. Surface energy of solids is not uniformly distributed evenly over the entire surface and IGC at infinite dilution only measures the highest surface energy, which is estimated to be <0.1% of the total surface area available [28]. Therefore, the correlation of surface energy from infinite dilution IGC with other bulk powder properties such as cohesion is likely to have such inconsistencies. Additionally, it may be expected that bulk cohesion is the measure of inter-particle cohesion at normal applied stress and at applied stress; powders may experience other inter-particle forces causing the observed variation to occur.

Table 4.5 – Acidic and basic surface energies and work of cohesion. Data presented as Mean ±SD (n = 3).

Formulations	**Υ^-_s (mJ/m^2)**	**Υ^+_s (mJ/m^2)**	**W_{CO}**
PVP-Leu (0%)	61.5 ±11.0	38.0 ±6.0	280.7 ±21.5
PVP-Leu (2.5%)	20.1 ±7.1	26.6 ±2.0	173.0 ±6.7

PVP-Leu (5%)	6.5 ±1.7	22.4 ±3.8	120.4 ±21.9
PVP-Leu (7.5%)	4.3 ±0.4	17.5 ±0.9	118.9 ±6.3
PVP-Leu (10%)	4.7 ±0.9	17.8 ±0.4	116.9 ±5.5
PVP-Leu (12.5%)	3.6 ±0.3	17.9 ±1.5	115.2 ±2.1
PVP-Leu (15%)	4.3 ±0.9	17.1 ±0.4	109.7 ±3.1

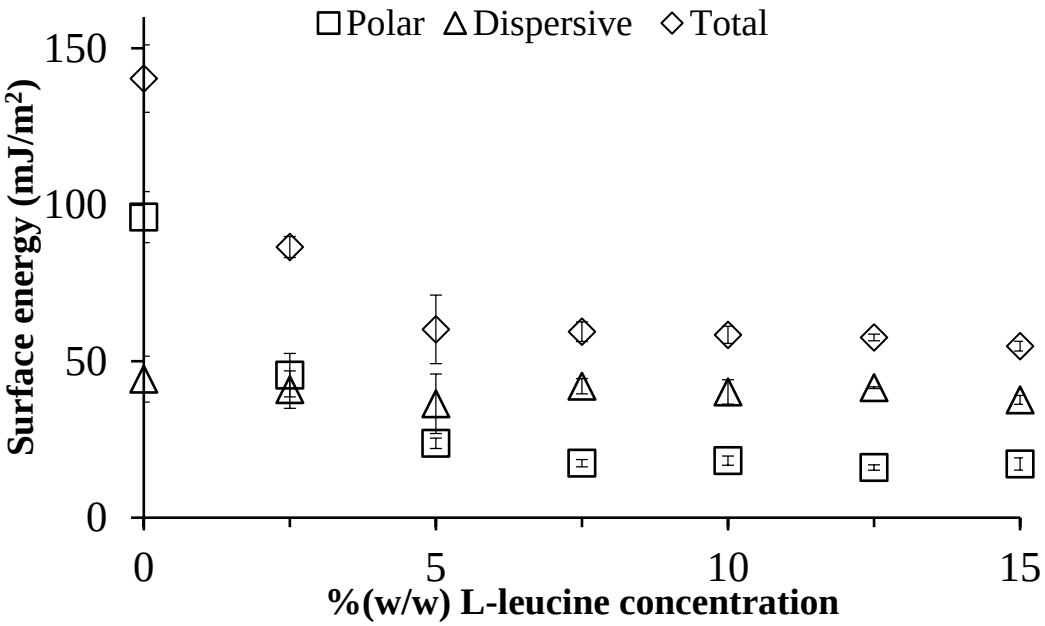

Figure 4.8 – Surface energy (polar, non-polar/dispersive and total) profiles of spray-dried formulations. Data presented as Mean ±SD (n = 3)

4.7 Discussion

Small particle behaviors (<10 µm) are subject to ongoing substantial research and development interest in pharmaceutical formulations given their presence across a range of medicines. Their high cohesion and a tendency to agglomerate limit their functional performance to a

considerable extent [29-31]. Surface modification is considered an effective approach to minimize cohesive forces between such small particles. Co-spraying with L-leucine has been demonstrated to be an effective surface modification strategy to address such inter-particle cohesion and aid optimization of formulation performance particularly in the area of dry powders for inhalation [32]. In this study, we investigated more specifically the effect of surface concentration of L-leucine on the resulting surface morphology, solid-state character of the L-leucine, and provided the examination of both surface energies and the bulk powder cohesion properties. Our aim was to gain further insight into the role of L-leucine on particle formation as well as support a quality-by-design basis of achieving optimum formulation performances.

The modification of particle morphology in response to higher concentrations of L-leucine has been previously reported [8, 33, 34]. We also found the similar trend of increasing surface asperities with higher L-leucine mass fraction. However, it was noted that shrivelled particles and occasionally thin walled and collapsed particles were seen only above a specific L-leucine mass fraction (10% or higher) which was proposed to be a consequence of formation processes specific to PVP used. It was proposed that the combined effect of L-leucine surface enrichment, evaporation and relatively low L-leucine water solubility creates an environment for crystallization and the formation of L-leucine-rich shell early in the drying phase. At and above a specific concentration, L-leucine forms a coherent shell that offers a strong mechanical resistance restricting the escape of water vapour trapped in the core. This results in a plastic expansion of the coherent film as the vapour pressure increases. Ultimately leading to the formation of collapsed thin-walled particles as the vapour pressure is exhausted as illustrated in Figure 4.9. Below this level of L-leucine, an incoherent and semi-permeable L-leucine shell was formed which allows escape of water vapour without leading to the formation of particles with such morphological features.

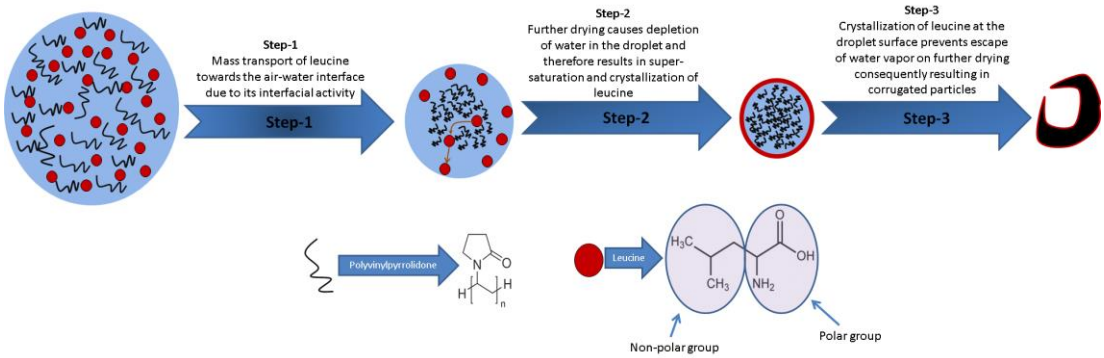

Figure 4.9 – Illustration of sequential events and mass transport of L-leucine in the spray-drying process as proposed in this study.

Investigations of morphological changes and higher L-leucine mass fraction and with solid-state character have previously indicated that the formation of collapsed, thin shell particles may be associated with L-leucine achieving a fully crystalline character which was only achieved >25% L-leucine mass fraction [14]. Alternatively, the formation of a coherent partially ordered L-leucine crust residing on the surface of the particles was also suggested as possible mechanism to explain formation of such particles [15]. It should be noted that the previous work was based on different core materials. However, our study provides evidence that a nano-crystaline L-leucine structure forms on the drying particle surface, even at low concentrations such as 2.5%. The crystallite domain size increased with higher concentration of L-leucine but remained in the order of 5 to 15 nm. This observation of a nano-crystaline structure may help further explain the apparent plasticity of the L-leucine rich shell, which despite its crystallinity, is able to stretch due to the internal vapour pressure. Further work could assess the effect on domain size for different spray-drying conditions with such an approach. This may reveal further information to support understanding of the formation mechanisms. The combination of SEM, XPS, ToF-SIMS and P-XRD revealed new insights into the surface composition, shape and solid-state structure of these composite spray-dried particles.

Another aspect of this work was to better understand the surface energetics and their contribution to the bulk cohesive properties of the resulting powder. The shear test cohesion values provide clear evidence that the bulk cohesion was substantially reduced with higher surface L-leucine concentration and reduce to a relatively stable value at around 10%. This observation indicates that surface concentration also controls the bulk properties of the powder and that a coherent L-leucine surface coverage was effective in minimizing bulk cohesion. The ability of L-leucine to reduce inter-particle cohesion has previously been attributed to its ability to produce corrugated particles [12, 35]. However, the effect of L-leucine on the surface energy of the spray-dried formulation was relatively unexplored. This was mainly due to past efforts to investigate the effect of L-leucine on surface energy of spray-dried formulations that did not result in a meaningful outcome [36]. This was considered to be associated with the difficulty in packing the fine powders in the column in reproducible manner and controlling the factors affecting surface energy such as humidity, which can potentially affect the reproducibility and reliability of the obtained data.

In this study, we were able to overcome such difficulties and achieve more reliable and reproducible results by mixing the spray-dried powder with inert glass beads (to achieve efficient column packing) as well as by storing and packing the powder in a controlled humidity environment. Surface energy data indicated that a consistent drop in the polar surface energy of the formulation was noted with higher surface L-leucine concentration. This observation supports the conclusion that non-polar groups are dominant at the surface. Therefore, we propose that the orientation of the L-leucine likely appears to be with the hydrophobic, hydrocarbon chains oriented to the surface, rather than the polar amine and acid groups, and assembled in an ordered crystalline array. This study therefore provides the first direct support for such molecular concentration, crystalline structure and molecular orientation specific to the surface of such spray-dried particles.

Thus, a combination of both surface saturation and a defined solid-state character was collectively needed to achieve effective L-leucine functionality. Thus, the surface concentration of L-leucine dictates surface properties, which consequently controls bulk performance of the spray-dried formulations.

These findings can be used as a guide to optimize particle design for achieving a desired formulation performance of the bulk powder. In the context of their application, we can better understand for example, the minimum L-leucine level required to give an effective surface property, representing a coherent, crystalline, suitably oriented molecular structure. This can then be employed to optimise the powder for formation of interactive and other structured mixtures, fluidisation and aerosolisation. It may also aid in optimisation of dissolution or moisture protection of the powder as a result of a hydrophobic L-leucine coating, or minimise the need for excess L-leucine that may compromise physical behaviour of the particle core in process such as compaction in multifunctional excipients application for tablet formulations [16].

4.8 Conclusion

L-leucine has been shown to have an important role in both current and potential future pharmaceutical formulations. The present work investigated the effect of surface L-leucine concentration on particle morphology, crystallinity, surface energy and bulk powder cohesion to understand the relationship between surface L-leucine concentration, resultant surface physico-chemical properties and bulk powder properties. This study has substantially clarified our understanding of the role of L-leucine in particle formation, indicating that the L-leucine enriches the surface of the droplets early in the drying phase, which is followed by its crystallization into nano-sized domains on the surface. This affects the subsequent drying and plastic behaviour of the surface composition and controls powder surface properties such as

morphology and surface energy, which consequently dictates the bulk behaviour of the spray-dried formulations. Thus, optimum surface L-leucine concentration is required to achieve optimum surface as well as bulk properties of the spray-dried formulations and this understanding may be employed for future formulation studies to optimize performance of a range of spray-dried formulations.

4.9 Acknowledgments

Sharad Mangal is thankful to Monash Institute of Graduate Research (MIGR) for providing Monash Graduate Scholarship (MGS) and Monash International Postgraduate Research Scholarship (MIPRS).

4.10 References

[1] Zhou Q, Qu L, Gengenbach T, Larson I, Stewart P, Morton DV. Effect of surface coating with magnesium stearate via mechanical dry powder coating approach on the aerosol performance of micronized drug powders from dry powder inhalers. AAPS PharmSciTech 2013; 14(1): 38-44.

[2] Han X, Ghoroi C, To D, Chen Y, Dave R. Simultaneous micronization and surface modification for improvement of flow and dissolution of drug particles. Int J Pharm 2011; 415(1-2): 185-95.

[3] Mao C, Thalladi VR, Kim DK, Ma SH, Edgren D, Karaborni S. Harnessing ordered mixing to enable direct-compression process for low-dose tablet manufacturing at production scale. Powder Technol 2013; 239(0): 290-299.

[4] Zhou QT, Qu L, Larson I, Stewart PJ, Morton DAV. Improving aerosolization of drug powders by reducing powder intrinsic cohesion via a mechanical dry coating approach. Int J Pharm 2010; 394(1–2): 50-59.

[5] Kendall K, Stainton C. Adhesion and aggregation of fine particles. Powder Technol 2001; 121(2-3): 223-229.

[6] Morton DAV, Green M, Staniforth JN, Begat P, Price R, Young PM. The study of force control aditives in creating high-performance dry powder inhaler formulations. In, Respiratory Drug Delivery VIII: Arizona, USA, 2002.

[7] Staniforth JN, Morton DAV, inventor, assignee Magnesium stearate, a phospholipid, or an amino acid in preparation of pharmaceutical particles for inhalation. 2002.

[8] Lucas P, Anderson K, Potter UJ, Staniforth JN. Enhancement of small particle size dry powder aerosol formulations using an ultra low density additive. Pharm Res 1999; 16(10): 1643-1647.

[9] Lechuga-Ballesteros D, Charan C, Stults CLM, Stevenson CL, Miller DP, Vehring R, Tep V, Kuo M-C. Trileucine improves aerosol performance and stability of spray-dried powders for inhalation. J Pharm Sci 2008; 97(1): 287-302.

[10] Chew NYK, Shekunov BY, Tong HHY, Chow AHL, Savage C, Wu J, Chan HK. Effect of amino acids on the dispersion of disodium cromoglycate powders. J. Pharm. Sci. 2005; 94(10): 2289-2300.

[11] Vehring R. Pharmaceutical particle engineering via spray drying. Pharm Res 2008; 25(5): 999-1022.

[12] Castellanos A. The relationship between attractive interparticle forces and bulk behaviour in dry and uncharged fine powders. Adv Phys 2005; 54(4): 263-376.

[13] Chew NYK, Tang P, Chan HK, Raper JA. How much particle surface corrugation is sufficient to improve aerosol performance of powders? Pharm Res 2005; 22(1): 148-152.

[14] Feng AL, Boraey MA, Gwin MA, Finlay PR, Kuehl PJ, Vehring R. Mechanistic models facilitate efficient development of leucine containing microparticles for pulmonary drug delivery. Int J Pharm 2011; 409(1–2): 156-163.

[15] Sou T, Kaminskas LM, Nguyen T-H, Carlberg R, McIntosh MP, Morton DAV. The effect of amino acid excipients on morphology and solid-state properties of multi-component spray-dried formulations for pulmonary delivery of biomacromolecules. Eur J Pharm Biopharm 2013; 83(2): 234-243.

[16] Sharad. M, Felix. M, Lakio S, AV. MD, Ian. L. The role of physico-chemical and bulk characteristics of interactive excipients on binder and flow additive properties. Int. J. Pharm. 2014; Submitted.

[17] Mangal S, Meiser F, Lakio S, Morton D, Larson I. The role of physico-chemical and bulk characteristics of co-spray dried l-leucine and polyvinylpyrrolidone on glidant and binder properties in interactive mixtures. Int J Pharm 2015; 479(2): 338-348.
[18] Rietveld H. A profile refinement method for nuclear and magnetic structures. J Appl Crystallogr 1969; 2(2): 65-71.
[19] Gorbitz CH, Dalhus B. Redetermination of L-Leucine at 120K. Acta Crystallogr 1996; 52(7): 1754-1756.
[20] Balzar D, Ledbetter H. Accurate modeling of size and strain broadening in the rietveld refinement: the "Double-Voigt" approach. Adv X Ray Anal 1995; 38: 397-404.
[21] Schultz J, Lavielle L, Martin C. The role of the interface in carbon fibre-epoxy composites. J Adhes 1987; 23(1): 45-60.
[22] van Oss CJ, Chaudhury MK, Good RJ. Monopolar surfaces. Advances in Colloid and Interface Science 1987; 28(1): 35-64.
[23] Traini D, Young PM, Thielmann F, Acharya M. The Influence of Lactose Pseudopolymorphic Form on Salbutamol Sulfate–Lactose Interactions in DPI Formulations. Drug Development and Industrial Pharmacy 2008; 34(9): 992-1001.
[24] Fowkes FM. Attractive forces at interfaces. Ind Eng Chem Res 1964; 56(12): 40-52.
[25] van Oss CJ. Acid—base interfacial interactions in aqueous media. Colloids Surf A 1993; 78: 1-49.
[26] Van Oss CJ, Good RJ, Chaudhury MK. Additive and nonadditive surface tension components and the interpretation of contact angles. Langmuir 1988; 4(4): 884-891.
[27] Raula J, Thielmann F, Kansikas J, Hietala S, Annala M, Seppala J, Lahde A, Kauppinen EI. Investigations on the humidity-induced transformations of salbutamol sulphate particles coated with L-leucine. Pharm Res 2008; 25(10): 2250-61.
[28] Yla-Maihaniemi P, Heng J, Thielmann F, Williams D. Inverse gas chromatographic method for measuring the dispersive surface energy distribution for particulates. Langmuir 2008; 24(17): 9551-9557.
[29] de Villiers MM. Influence of cohesive properties of micronized drug powders on particle size analysis. J Pharm Biomed Anal 1995; 13(3): 191-198.
[30] Hartley PA, Parfitt GD, Pollack LB. The role of the van der Waals force in the agglomeration of powders containing submicron particles. Powder Technol 1985; 42(1): 35-46.
[31] Mullarney MP, Beach LE, Davé RN, Langdon BA, Polizzi M, Blackwood DO. Applying dry powder coatings to pharmaceutical powders using a Comil for improving powder flow and bulk density. Powder Technol 2011; 212(3): 397-402.
[32] Ganderton D, Morton DAV, Lucas P, inventor, assignee Improvements in or relating to powders. 2000.
[33] Li HY, Neill H, Innocent R, Seville P, Williamson I, Birchall JC. Enhanced dispersibility and deposition of spray-dried powders for pulmonary gene therapy. J Drug Target 2003; 11(7): 425-432.
[34] Seville PC, Learoyd TP, Li HY, Williamson IJ, Birchall JC. Amino acid-modified spray-dried powders with enhanced aerosolisation properties for pulmonary drug delivery. Powder Technol 2007; 178(1): 40-50.
[35] Vehring R. Pharmaceutical particle engineering via spray drying. Pharm. Res. 2008; 25(5): 999-1022.
[36] Chew NY, Shekunov BY, Tong HH, Chow AH, Savage C, Wu J, Chan HK. Effect of amino acids on the dispersion of disodium cromoglycate powders. J Pharm Sci 2005; 94(10): 2289-300.

4.11 Appendix

4.11.1 Appendix 4.1 – Example of a C 1s fitted using reference spectra of PVP and Leu.

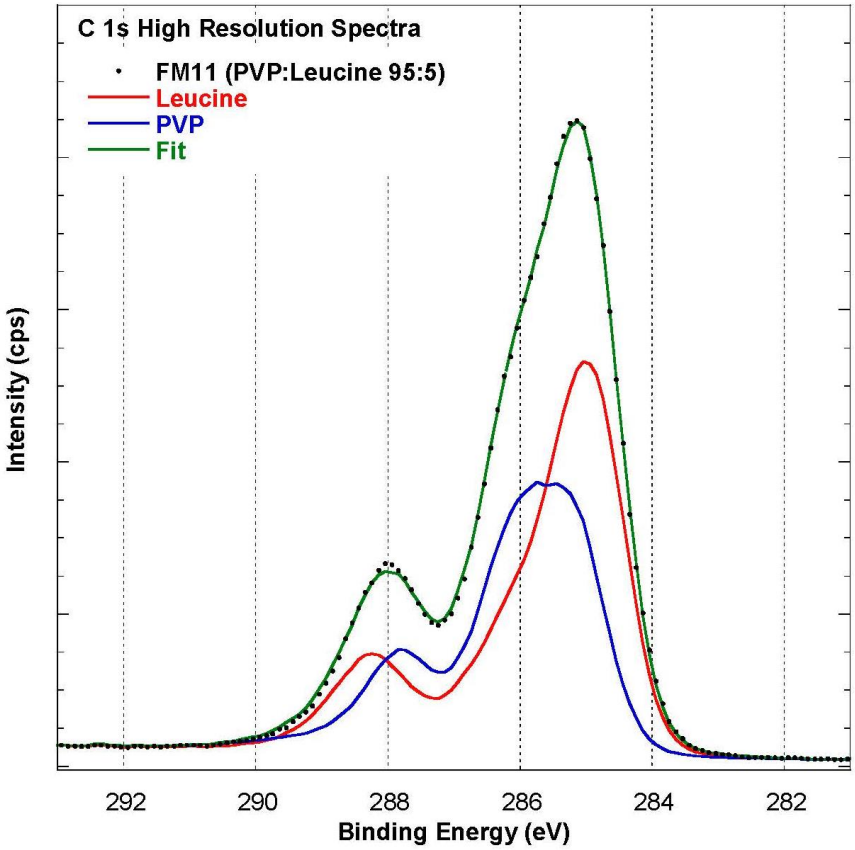

4.11.2 Appendix 4.2 – ToF-SIMS spectra of A-PVP and B-L-leucine. Arrows showing diagnostic peaks used in this study.

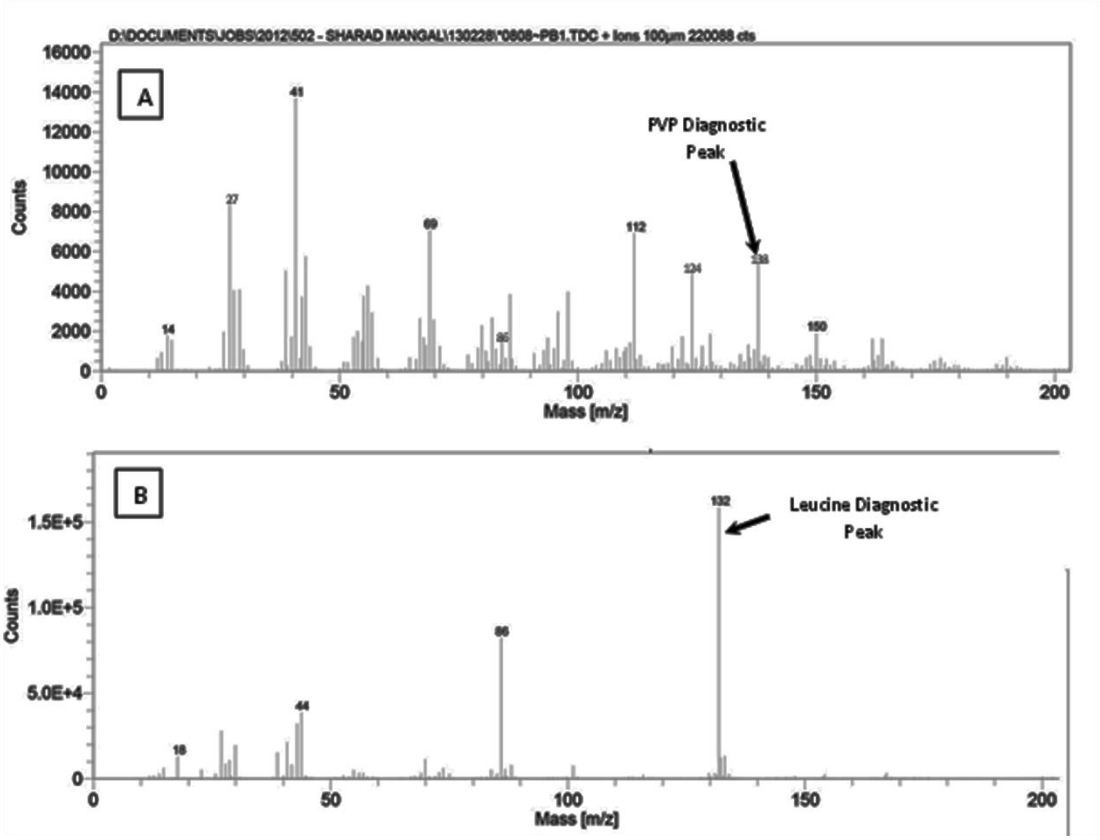

4.11.3 Appendix 4.3 – X-ray diffractogram of L-leucine.

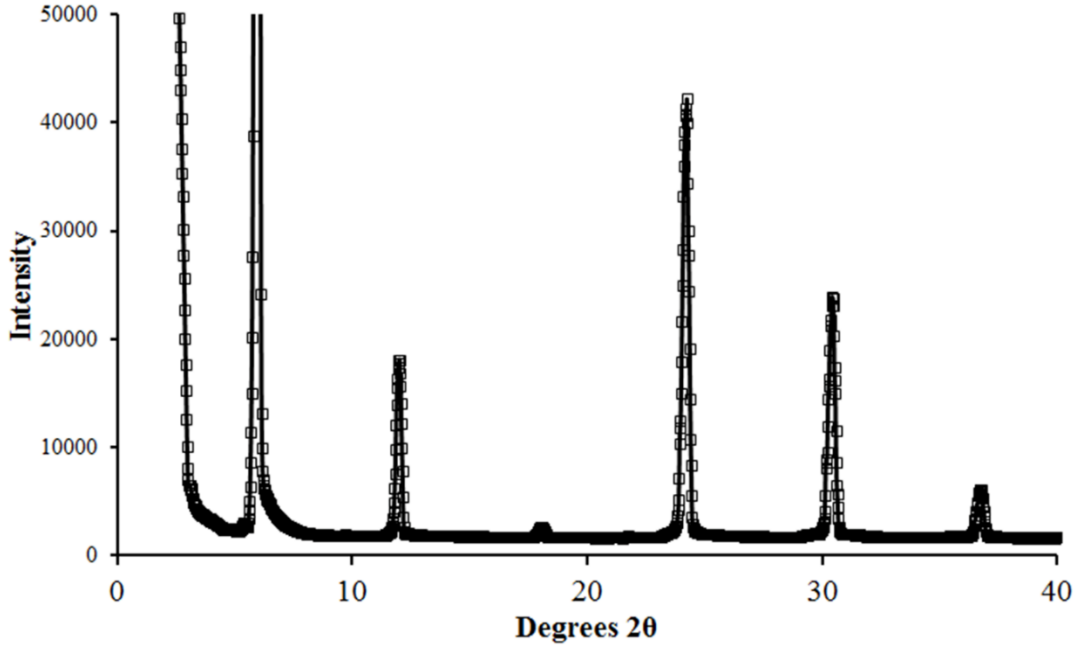

4.11.4 Appendix 4.4 – Shear cell data of spray dried formulations demonstrating shear stress as a function of applied normal stress.

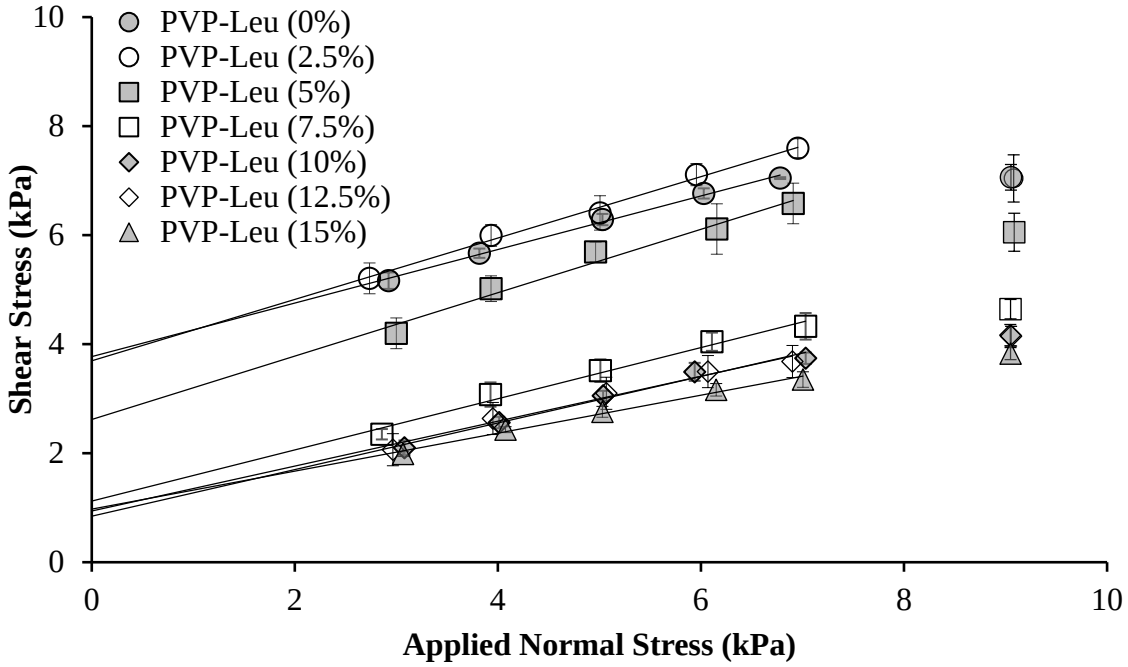

Chapter 5

Applying surface energy derived cohesive-adhesive balance model in predicting the mixing, flow and compaction behaviour of interactive mixtures

Sharad Mangal[1], Felix Meiser[1], Geoffrey Tan[1], Thomas Gengenbach[2], David AV Morton[1]*, Ian Larson[1]*

[1] Drug Delivery, Disposition and Dynamics, Monash University, 381 Royal Parade, Parkville, VIC-3052, Australia
[2] CSIRO Materials Science and Engineering, Bayview Avenue, Clayton, VIC-3168, Australia
* Corresponding Authors

*** Submitted as:**
Mangal S, Meiser F, Geoffrey Tan, Thomas Gengenbach, Morton DA, Larson I. Improving the functional performance of composite excipients through particle engineering and optimized interactive mixing. Special issue of Eur J Pharm Biopharm. Dedicated to 7th Granulation Conference; Reviewer's comments received.

5 Declaration for Thesis Chapter 5

Declaration by candidate

In the case of Chapter 5, the nature and extent of my contribution to the work was the following:

Nature of contribution	**Extent of contribution (%)**
Study initiation, formation of hypothesis, laboratory work, data collection, analysis and interpretation and writing the manuscript	65%

The following co-authors contributed to the work. If co-authors are students at Monash University, the extent of their contribution in percentage terms must be stated:

Name	**Nature of contribution**	**Extent of contribution (%) for student co-authors only**
Felix Meiser	Supervision and manuscript revision	5%
Geoffrey Tan	IGC characterization and proofreading	5%
Thomas Gengenbach	XPS characterization and proofreading	5%
David AV Morton	Supervision and manuscript revision	10%
Ian Larson	Supervision and manuscript revision	10%

The undersigned hereby certify that the above declaration correctly reflects the nature and extent of the candidate's and co-authors' contributions to this work*.

Candidate's Signature	[redacted]	**Date 23.11.2015**
Main Supervisor's Signature	[redacted]	**Date 24/11/15**

*Note: Where the responsible author is not the candidate's main supervisor, the main supervisor should consult with the responsible author to agree on the respective contributions of the authors.

5.1 Commentary

In the chapter 1, we selected two small particle formulations (a low cohesion and a high cohesion small particle formulation) and investigated the effect of relative cohesion on their interactive mixing behaviour as well as binder and flow additive actions. In this study, we address objective 3 " to investigate the relationship between interactive mixing behaviour with binder and flow additive action of small binder particles' For this study, five small particle binder formulations with varying cohesions (as shown in chapter 2), were selected. The interactive mixing behaviour was predicted using a cohesion-adhesion balance approach and compared with observed interactive mixing behaviour. Moreover, the relationship between the interactive mixing behaviour and functional performance i.e., binder and flow additive action was investigated.

5.2 Abstract

Objective

In this study, we investigated the applicability of cohesive-adhesive balance (CAB) model to predict the interactive mixing behaviour of small excipient particles. Further, we also investigated the application of this CAB model to predict the flow and compactability of resultant blends.

Methods

Excipients created by co-spraying polyvinylpyrrolidone (PVP, a model pharmaceutical binder) with various L-leucine concentrations were used for this study. Paracetamol was used as model active pharmaceutical ingredient (API). The surface energy was used to derive the work of cohesion (w_{co}) and work of adhesion (w_{ad}) to predict the interactive mixing behaviour of the excipients with paracetamol. The blends were visualized under a scanning electron microscopy microscope to assess the interactive mixing behaviour. In addition, the flow performance and tabletting behaviour of various blends were characterized.

Results

The surface-energy derived work of adhesion (w_{ad}) between excipient and paracetamol particles increased, while the corresponding work of cohesion (w_{co}) between excipient particles decreased, with increasing L-leucine concentrations. In blends for which the work of cohesion was higher than the work of adhesion ($w_{co} > w_{ad}$), small excipient particles were apparent as agglomerates. For excipients with 5% and higher L-leucine concentrations, the work of adhesion between excipient and paracetamol particles was higher than or equivalent to the work of cohesion between excipient particles ($w_{ad} \geq w_{co}$) and agglomerates were less apparent. This is an indicator of formation of homogeneous interactive mixtures. At 5% (w/w) excipient proportions, blends for which $w_{ad} \geq w_{co}$ demonstrated higher compactability than

other blends. Furthermore, at 10% (w/w) and higher excipient proportions, these blends also demonstrated better flow performance than other blends.

Conclusion

In conclusion, this is the first reported study to demonstrate that surface-energy derived CAB data effectively predicted the interactive mixing behaviour of small excipient particles. Furthermore, at certain proportions of small excipient particles this CAB balance also predicted the flow and compaction behaviour of the API/excipient blends.

Keywords: Polyvinylpyrrolidone; L-leucine; cohesion-adhesion balance, paracetamol, surface energy, work of cohesion, work of adhesion, high-dose API, direct compression, flow, compactability

5.3 Graphical abstract

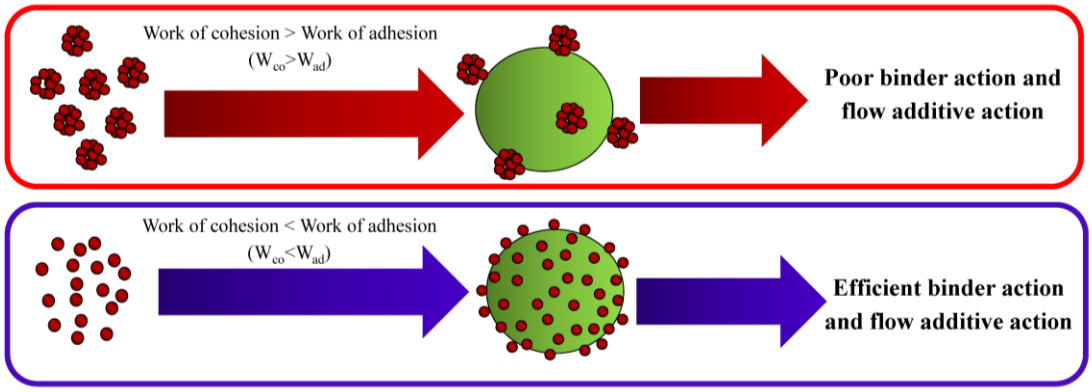

5.4 Excipients for Powder Flow or for Powder Compaction

Flowability and compactibility are essential material attributes for efficient tablet manufacturing [1-4]. However, the majority of APIs lack the flow and/or compactability needed for direct tablet manufacturing [5]. Excipients (binders and flow additives) are incorporated to improve the compactibility and flow. Therefore, the success of tablet formulation critically depends on these excipients [6, 7].

Both flowability and compactibility depend on inter-particle forces [8]. In practice, flow additives improve flow by reducing inter-particle forces [9], while binders improve compactability by increasing inter-particle forces [10]. Thus, from a fundamental perspective, flow additives and binders have opposite impacts on powder blends and would be expected to conflict with each other's performance.

5.5 Interactive Mixing and Control of Cohesion

The concept of interactive mixing involves the adhesion of small particles (typically <10 μm) to larger particles resulting in formation of a homogeneous and segregation resistant powder mix [11]. The formation of interactive mixture depends on the magnitude of forces acting between the small and large particles. Efficient de-agglomeration and preferential adhesion of small particles to large particles is energetically favoured when the forces of adhesion acting between small and large particles are stronger than the forces of cohesion acting between the small particles [12, 13]. This concept is known as the cohesive-adhesive balance (CAB) [12, 13].

Glidants/flow additives are nanometric in size and improve the flow of cohesive particles by adhering to them consequently forming interactive mixtures [14-16]. However, due to their small size, most flow additives are highly cohesive in nature. Low shear mixing is unable to efficiently de-agglomerate these cohesive structures resulting in non-homogeneous

mixtures and consequently poor flow [10, 17-19]. High shear mixing facilitates de-agglomeration and the formation of a more homogeneous interactive mixture, and consequently optimum flow improvement [15, 20, 21]. This suggests that the interactive mixing behaviour of small excipient particles affect the flow performance of the resulting interactive mixtures.

Theoretically, a monolayer of binder particles facilitates optimum gain in tensile strength [22, 23]. This can be explained by percolation theory, which predicts that a three-dimensional continuous bonding network of the excipient must be present in order for the tablet to achieve optimal tensile strength [24, 25]. It has been demonstrated that small binder particles with the ability to form efficient interactive mixtures also express an efficient binder action [26]. This suggests that cohesive adhesive balance of small excipient particles also affects the compaction behavior of the resulting interactive mixtures.

Clearly, both flow and compaction behavior of blends depend on the dispersibility of small excipient particles, In this study, we used the cohesive-adhesive balance (CAB) model with surface energy-derived cohesion and adhesion data to predict the dispersibility and therefore the interactive mixing behaviour of small excipient particles with paracetamol. In addition, the applicability of CAB to predict the flow and compaction behaviour of the resultant blends was investigated. Small, micron-sized excipients (PVP spray-dried with L-leucine) were compacted into tablets and their tensile strength determined. Paracetamol was selected as a poorly compressible cohesive API model [27]. The surface energies of spray-dried excipients and paracetamol were determined using an inverse gas chromatography, and the cohesion-adhesion balance was derived from these surface energy data [28, 29]. The applicability of the CAB model to predict the dispersibility and therefore the interactive mixing behaviour of small excipient particle was then qualified by inspection of the API/excipient blends under a scanning

electron microscope. Powder blends were then characterized for their tableting behaviour and flow performance.

5.6 Materials and Methods

In this study, we used previously prepared PVP (molecular weight ~10 kDa, as per supplier's specifications) and L-leucine spray-dried formulations [30]. The mean particle diameter (D_{50}) of various spray-dried formulations was in the range of 2-3 µm with narrow particle size distributions. Paracetamol of analytical grade was procured from Sigma-Aldrich (St. Louis, MO, USA). The particle diameters of paracetamol were D_{10} – 3.7 ±0.1 µm, D_{50} – 21.4 ±0.3 µm, and D_{90} – 151.5 ±5.0 µm.

5.6.1 Inverse gas chromatography

The surface energy of paracetamol was determined with an inverse gas chromatography (iGC 2000, Surface Measurement Systems Ltd., London, UK) at infinite dilution. Briefly, paracetamol powder was packed into pre-silanized glass columns (300 mm × 3 mm internal diameter) by gentle tapping, until no cracks, hollows, or channels were visible in the powder bed. The columns were loosely stoppered with silanized glass wool at both ends to prevent sample movement.

Before measurement, the packed columns were pre-conditioned with a helium stream at 10 standard cubic centimetre per minute (sccm) for 2 h at 303 K and 0% RH. Dispersive energy measurements were achieved with the use of a series of n-alkanes (chromatography grade decane, nonane, octane, heptane and hexane (Sigma-Aldrich, St. Louis, MO, USA)), while the specific surface energy measurements were achieved with the use of acidic (chromatography grade chloroform (Sigma-Aldrich, St. Louis, MO, USA)) and basic probes (chromatography grade ethyl acetate (Sigma-Aldrich, St. Louis, MO, USA)), respectively. For all probes, a concentration of 0.03 p/p0 (where p is the partial pressure and p0 is the saturation

vapour pressure) was used. Helium at a flow rate of 10 sccm was used to carry the probes through the stationary phase and the system was maintained at 303 K at 0% RH. Dead volumes were based on the retention volume of methane gas at 0.03 p/p0, detection of probes was achieved with a flame ionization detector. Replicates of 3 were conducted for all samples.

The dispersive surface energy was calculated according to the theory described by Schultz [31] while the specific energy was calculated based on the theory proposed by Good-van Oss-Chaudhury [32] where the specific energy can be split into two components - an acidic component, γ^+, and a basic component, γ^-. The calculation of the specific energy is given by the following equation [32, 33]:

$$\gamma_s^P = \sqrt{\gamma_S^+ \gamma_S^-} \qquad \text{Eq. (3.1)}$$

The total surface energy of the material is the additive effect of both the dispersive (γ^D) and polar (γ^P) components [34]. Upon determination of the dispersive and polar surface energies, the work of adhesion (w_{ad}) for interactions between dissimilar particles and the work of cohesion (w_{co}) for interactions between similar particles can be calculated using the following equations [28, 29]:

$$w_{co} = 2\sqrt{\gamma_1^D . \gamma_1^D} + 2\sqrt{\gamma_1^P . \gamma_1^P} \qquad \text{Eq. (3.2)}$$

$$w_{ad} = 2\sqrt{\gamma_1^D . \gamma_2^D} + 2\sqrt{\gamma_1^P . \gamma_2^P} \qquad \text{Eq. (3.3)}$$

Where, γ_1^D and γ_1^P represent the dispersive and polar energies of particles of solid 1, and γ_2^D and γ_2^P represent the dispersive and polar energies of particles of solid 2.

5.6.2 Blending

To minimize the effect of humidity related variations, all the excipients were stored in a controlled humidity (42 ± 2 % RH) environment until equilibration. When the gain in mass was <10 mg (per ~50 g excipient batch) on three consecutive measurements (with 24 hours

between each measurement), the mass was considered to have attained equilibrium. A total of 50 g blend was prepared by mixing paracetamol with predetermined ratios (5, 10, 15 and 20% (w/w)) of spray-dried excipients in a 250 mL glass jar using a Turbula mixer (Willy A. Bachofen, Muttenz, Switzerland) at 72 rpm for 5 min.

5.6.3 Scanning electron microscopy (SEM)

The interactive mixing behaviour of the spray-dried excipients with paracetamol was visualised by SEM (Phenom, FEI Company, Hillsboro, OR, USA). Double-sided adhesive tape was placed on an aluminium stub and after stripping off the upper side of the adhesive, a small amount of sample was scattered on the stub and dispersed by tapping lightly on the edge of the stub. The stubs were then coated with a fine gold film using a sputter coater (Emitech K550X, Quorum Technologies, Kent, UK) using an electrical potential of 2.0 kV at 25 mA for 3 min. The coated stubs were then loaded into the SEM docking bay and images were captured at various magnifications.

5.1.1 Tensile strength

Powder formulations, 105 ± 5 mg, were manually filled in the tablet die; the tablets were produced in a computer-controlled tablet press (Gamlen Tableting Ltd., Nottingham, UK). The powder formulations were compressed at 80, 120 and 154 MPa with a punch speed of 1 mm/s using a flat punch and die measuring 6 mm in diameter. The die and punch were lubricated with a trace dusting of magnesium stearate prior to each compression [35, 36]. The dimensions (diameter and thickness) of each tablet were measured. The breaking force of the tablets was measured using an Erweka hardness tester (TBH-30, Erweka, Heusenstamm, Germany). The tensile strength of the tablets was calculated according to the following equation [37];

$$6 \quad \sigma = \frac{2F}{\pi DH} \qquad \text{Eq. (3.4)}$$

where σ is tensile strength, F is the breaking force, D is the tablet diameter, and H is the tablet thickness.

5.6.4 Evaluation of flow

Bulk and tapped density were determined to assess the effect of various added spray-dried excipients on the flow of paracetamol. A 10 mL glass measuring cylinder was placed onto a calibrated balance (B1-205, Sartorius AG, Goettingen, Germany) and tared. Powder was then gently transferred into the measuring cylinder by allowing the powder to fall from a fixed height of 10 cm into the cylinder without any agitation. Each sample was tested in triplicate and the bulk density was calculated from the ratio of mass and volume. The tapped density (ρ_{tap}) was determined by mechanically tapping a graduated cylinder containing the powder for 1250 taps using a tapped density analyser (Autotap™, Quantachrome Instruments, Boynton Beach, FL, USA). The powder volume was noted after tapping and the tapped density was calculated as mass divided by the tapped volume of the powders. The bulk and tapped densities were used to calculate the Carr's index and Hausner's ratio calculated according to the following equations [38, 39]:

$$Carr's\ Index = \frac{\rho_{tap} - \rho_{bulk}}{\rho_{tap}} \times 100 \qquad \text{Eq. (3.5)}$$

$$Hausner's\ Ratio = \frac{\rho_{tap}}{\rho_{bulk}} \times 100 \qquad \text{Eq. (3.6)}$$

5.6.5 Statistical analysis

The results were expressed as Mean ±SD (standard deviation) and the statistical analysis was preformed via one-way analysis of variance (ANOVA) with Tukey–Kramer multiple comparison post-hoc tests using SPSS™ software (SPSS Inc., IBM Corporation, New York, USA).

5.7 Results

5.7.1 Tensile strength-Binders

The compactability of the spray-dried excipients was determined by compacting them alone and testing the tensile strength of the resulting tablets. PVP spray-dried with no L-leucine showed the highest tensile strength (Figure 5.1). Incorporation of L-leucine reduced the tablet tensile strength indicating that L-leucine compromised the compactability of the PVP. This may be attributed to the coating of PVP with L-leucine. L-leucine is known as a low-bonding lubricant material [40]. The detrimental effect of lubricant on material compactability is well-known. It was proposed that lubricant reduces inter-particle bonding and allows greater tablet relaxation, and consequently reduces compactability [41-44]. It is interesting that despite a change in surface coverage a change in compactability was not observed between PVP spray dried with different L-leucine concentrations. We propose that with as low as 2.5% feed L-leucine concentration, majority of PVP surfaces were covered by L-leucine, thus further increase in surface L-leucine concentration (with increasing L-leucine feed concentration) was an indication of deposition of L-leucine in deeper surface, which did not further reduce PVP bonding.

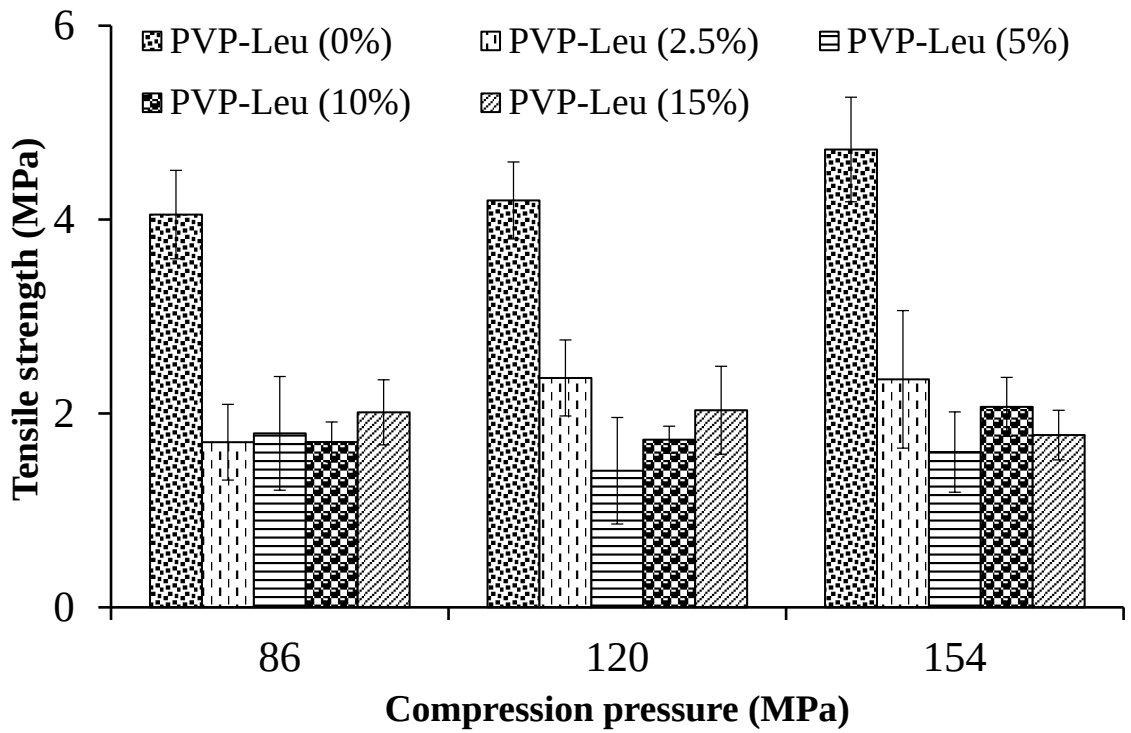

Figure 5.1 – Tensile strength of tablets prepared from different spray-dried formulations. Data presented as Mean ±SD (n = 5).

5.7.2 Cohesion-adhesion balance

The surface energy data were used to calculate the work of cohesion (w_{co}) and work of adhesion (w_{ad}) (Table 5.1). The results indicated that the work of cohesion of PVP-Leu (0%) and PVP-Leu (2.5%) was higher than the corresponding work of adhesion to paracetamol. Therefore, the self-agglomeration of the small spray-dried particles was more energetically favoured than their adhesion to paracetamol. The work of cohesion reduced with higher feed L-leucine concentrations, such that for PVP-Leu (5%), PVP-Leu (10%) and PVP-Leu (15%), the work of cohesion was approximately equivalent to the work of adhesion to paracetamol. Thus, the adhesion of the small particles to the paracetamol particles was anticipated to be more energetically favoured than the respective cohesion (agglomeration) of small excipient particles.

Table 5.1 – Cohesive-adhesive balance (CAB) data for API/excipient interactive mixtures. Data presented as Mean ±SD (n = 3).

Formulations	w_{co} (mJ/m^2)*	w_{ad} (mJ/m^2)	w_{co} Vs w_{ad}
PVP-Leu (0 %)	280.7 ±21.5	165.8 ±8.1	$w_{co} > w_{ad}$
PVP-Leu (2.5%)	173.0 ±6.7	139.5 ±3.5	$w_{co} > w_{ad}$
PVP-Leu (5%)	120.4 ±21.9	120.1 ±12.6	$w_{ad} \approx w_{co}$
PVP-Leu (10%)	116.9 ±5.5	120.3 ±3.3	$w_{ad} \geq w_{co}$
PVP-Leu (15%)	109.7 ±3.1	116.6 ±1.5	$w_{ad} \geq w_{co}$

*from [30].

5.7.3 Scanning electron microscopy (SEM): Blends

The interactive mixing behaviour of the spray-dried powders with paracetamol was qualitatively assessed by visual inspection of SEM images of these blends (Figure 5.2). It was observed that the PVP-Leu (0%) particles were agglomerated and poorly dispersed over the surface of paracetamol (as indicated by the arrows in Figure 5.2 (A)). SEM images of the PVP-Leu (2.5%)/Paracetamol blends showed some agglomerates on the surface of the paracetamol particles (as indicated by arrows in Figure 5.2 (B)). With 5% and higher L-leucine feed concentrations, little sign of these agglomerates was evident on the surfaces of the paracetamol particles, indicating de-agglomeration and distribution of the excipient particles across the surface of the paracetamol particles. This observed interactive mixing behaviour of excipient particles with paracetamol was consistent with the above CAB predictions based on the work of adhesion and the work of cohesion.

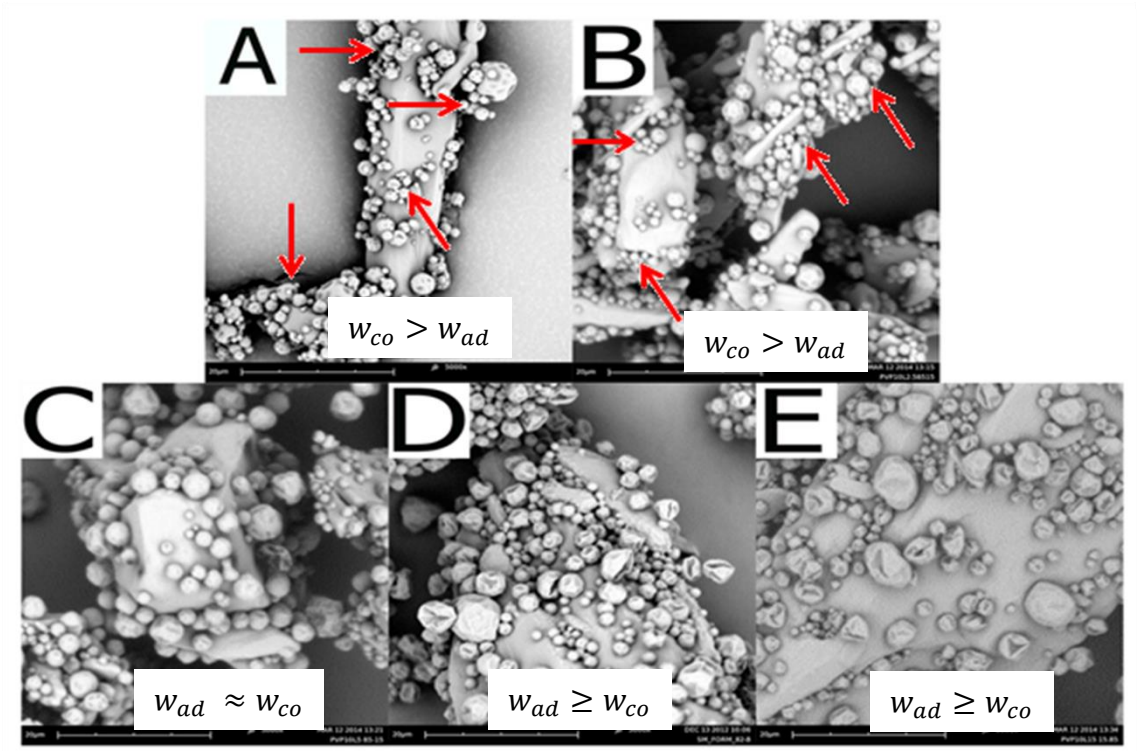

Figure 5.2 – Representative SEM images of API/excipient (85% (w/w) /15% (w/w)) blends: (A) PVP-Leu (0%)/Para, (B) PVP-Leu (2.5%)/Para, (C) PVP-Leu (5%)/Para, (D) PVP-Leu (10%)/Para and (E) PVP-Leu (15%)/Para.

5.7.4 Compactability

API/excipient blends were compacted into tablets and tensile strength was determined. This data was used as a measure of the binder activity of the spray-dried powder formulations (Figure 5.3). At the lowest excipient level of 5% (w/w) spray-dried powders added to paracetamol, both blends of API with PVP-Leu (0%) and PVP-Leu (2.5%) resulted in the formation of substantially weaker tablets compared to the API blended with spray-dried powders of 5% L-Leucine and above. These powder blends are indicated by arrows. These results show that with the low level of excipient (5% (w/w)), it was possible to make tablets with tensile strength of > 1.7 MPa, which is considered to be a strength acceptable for large scale pharmaceutical manufacturing [45]. In contrast, at higher spray-dried powder levels with

API, the PVP-Leu (0%) blend resulted in substantially higher tensile strength compared to the blends of API with PVP of all L-leucine contents.

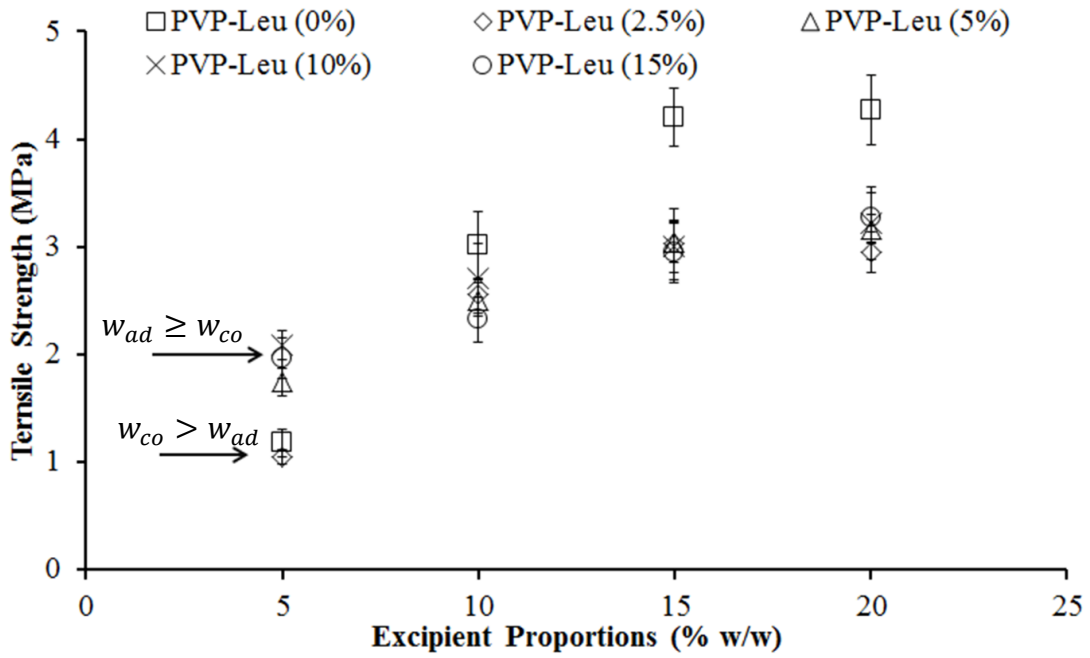

Figure 5.3 – Tensile strength of tablets produced from various API/excipient blends compacted at 154 MPa. Data presented as Mean ±SD (n = 5).

5.7.5 Evaluation of flow

The bulk and tapped densities, Carr's index and Hausner's ratio are presented in Figure 5.4.

Powders with good flowability achieve better packing thereby they typically have higher bulk densities than powders with poor flowability [46, 47]. Paracetamol had a low bulk density (0.31 g/mL). Adding PVP-Leu (0%) or PVP-Leu (2.5%), did not significantly ($p>0.05$) increase its bulk density (Figure 5.4 A). However, addition of PVP-Leu (5%), PVP-Leu (10%) and PVP-Leu (15%) resulted in a significant increase in the bulk density ($p<0.05$). This effect was more evident and pronounced at higher excipient proportions. Again, as predicted by CAB data, the work of cohesion ($\boldsymbol{w_{co}}$) was higher than the work of adhesion ($\boldsymbol{w_{ad}}$) for PVP-Leu (0%) and PVP-Leu (2.5%) blends. while the work of adhesion ($\boldsymbol{w_{ad}}$) was higher/equivalent to

the respective work of cohesion ($\boldsymbol{w_{co}}$) for other API/excipient blends. This suggests that CAB can also effectively predict the flow performance of interactive mixtures. This may be attributed to the efficient coverage of host particles by more flowable guest particles reducing direct inter-particle interactions between cohesive host particles. In essence, the surfaces of the poorly flowing API are now covered with better flowing (less cohesive) guest particles hence the blends have better flow. Interestingly, the interactive mixtures with CAB supporting homogeneous interactive mixing also demonstrated varying bulk density. The bulk density of blends of PVP-Leu (10%) and PVP-Leu (15%) was significantly higher than PVP-Leu (5%) ($p<0.05$). Tapped density data was in good accordance with bulk density data indicating similar powder flow behaviour (Figure 5.4 B).

The Carr's Index and Hausner's ratio API/excipient blends are presented in Figure 5.4 C and D. In general, the Carr's index and Hausner's ratio data were in good agreement with bulk and tapped density data except for PVP-Leu (0%)/API blends. This deviation in Carr's index and Hausner ratio data may be attributed to cohesive nature of PVP-Leu (0%)/API blends. We propose that the energy supplied by the tapping machine was insufficient to disrupt the cohesive blend structure, which reduces the degree of powder volume reduction achieved upon tapping. Other researchers have also reported similar observation [8, 47]. Thus, Carr's index and Hausner's ratio are not universal flow indicators, and are deemed unsuitable for highly cohesive powders.

Typically, a Carr's index between 21–25 and Hausner's ratio between 1.26–1.34 is considered suitable for industrial scale tablet manufacturing [48]. Notably, none of the API/excipient blends (for which Carr's index and Hausner's ratio were considered applicable) could achieve a suitable Carr's index or Hauner's ratio. Therefore, these excipients are relatively weak flow additives. The limitation of these excipients compared to silicon dioxide has also been demonstrated and was attributed to their relatively large particle size compared

to silicon dioxide [19, 26]. It should, however, be highlighted that the host particle size also controls the flow additive action of small excipients [16, 19, 49]. Thus, the flow improvement achieved using these excipients may vary depending on host particle size. However, further studies are being conducted to specifically investigate how the flow additive action of these excipients changes with host particle size.

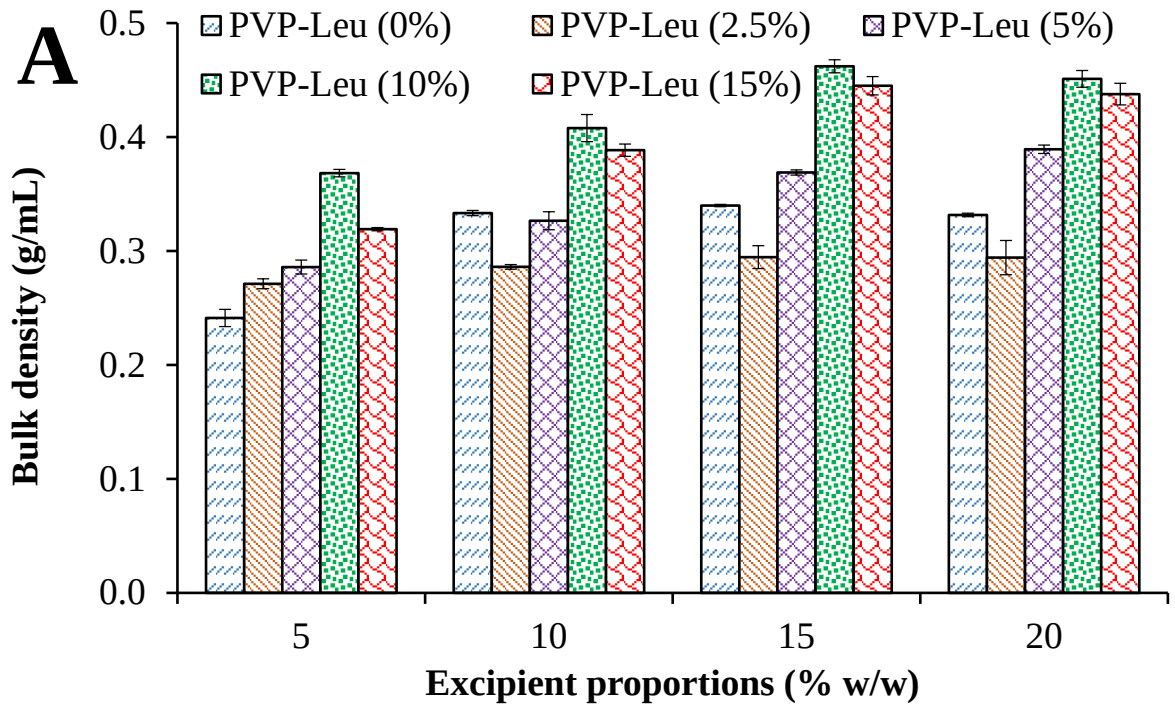
A
PVP-Leu (0%)
PVP-Leu (2.5%)
PVP-Leu (5%)
PVP-Leu (10%)
PVP-Leu (15%)
Bulk density (g/mL)
0.5
0.4
0.3
0.2
0.1
0.0
5
10
15
20
Excipient proportions (% w/w)

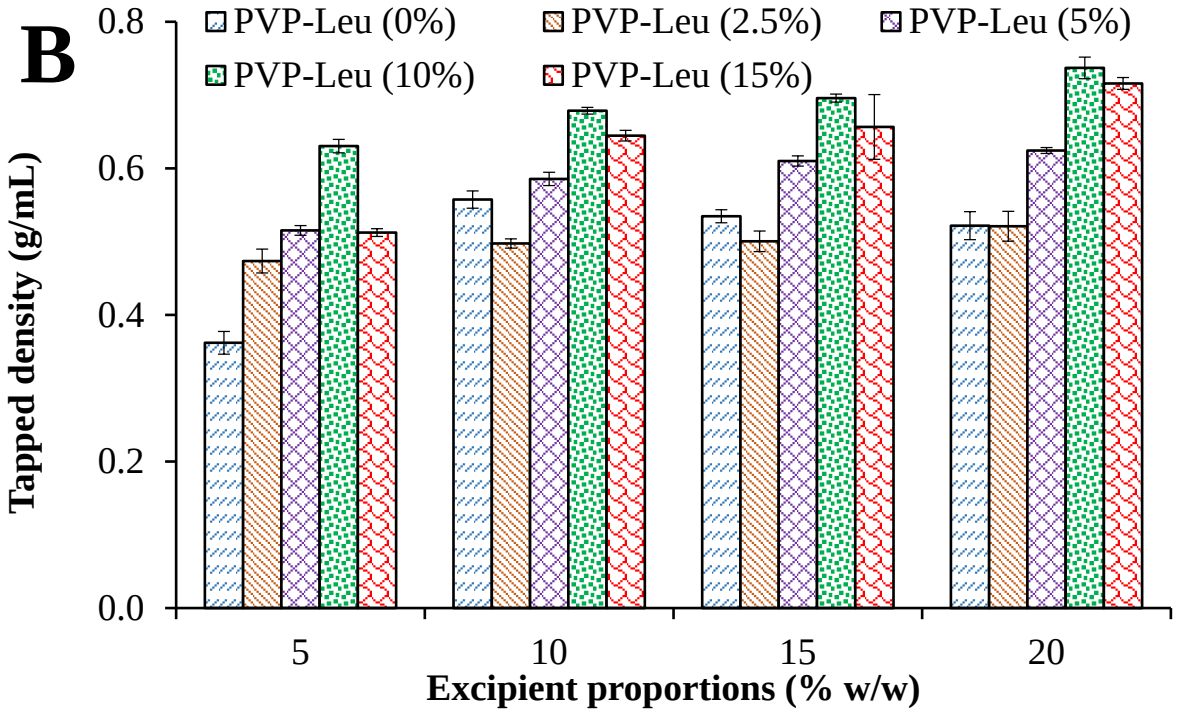
B
PVP-Leu (0%)
PVP-Leu (2.5%)
PVP-Leu (5%)
PVP-Leu (10%)
PVP-Leu (15%)
Tapped density (g/mL)
0.8
0.6
0.4
0.2
0.0
5
10
15
20
Excipient proportions (% w/w)

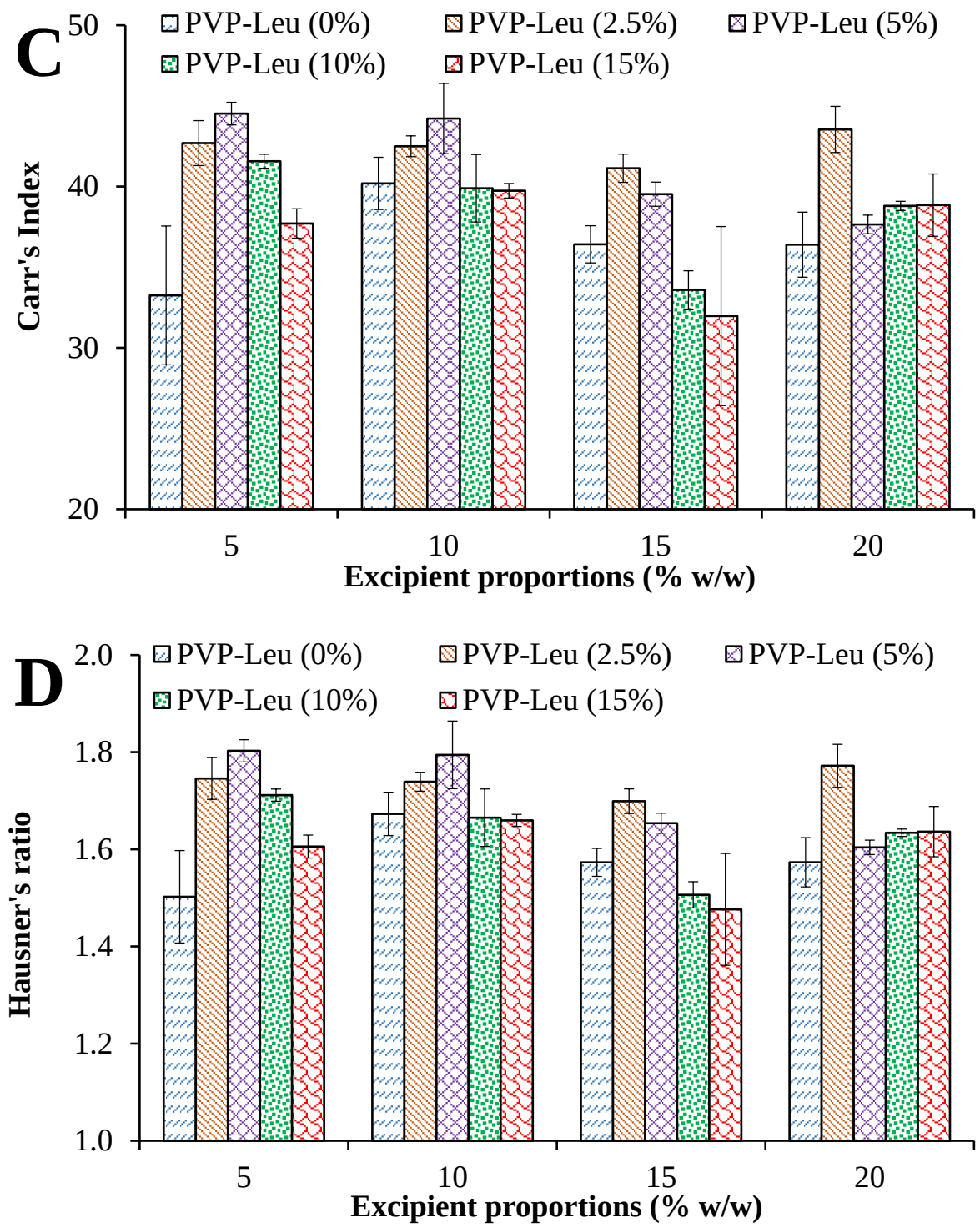

Figure 5.4 – Bulk density (A), Tapped density (B), Carr's Index (C) and Hausner's ratio (D) data of API/excipient blends. Data represented as Mean ±SD (n = 3).

5.8 Discussion

The concept of interactive mixtures has been shown to be effective in achieving uniform mixing of small dose APIs in powder blends where small particles adhere to the surface of large particles [50]. In addition, the gold standard flow additive silica has been shown to improve flow by adhering to large particles and forming interactive mixtures [10]. Thus, interactive mixing finds significant commercial application in pharmaceutical tablet formulations. We have shown that a small binder particle excipient exhibits binder and as well as a weak flow additive action and forms interactive mixtures [26]. Such improvements in binder and flow additive action were previously attributed to efficient interactive mixing behaviour of small excipient particles [26]. This is the first study to employ surface-energy derived cohesion-adhesion balance (CAB) data to predict the interactive mixing behaviour of small excipient particles with a cohesive API, as well as the flow and compaction behaviours of the API/excipient blends.

The formation of an interactive mixture is energetically favoured if forces of adhesion are similar or stronger than the forces of cohesion. Previous studies used a colloid probe AFM technique to measure the relative magnitude of adhesive and cohesive interactions and consequently predict interactive mixing behaviour [13]. To the author's knowledge, this present study is the first to use surface energy data from IGC measurements to enable the characterization of the adhesive and cohesive interactions, and then predict interactive mixing behaviour. However, further studies investigation the surface coverage achieved by small particles and its relationship with CAB data would be required to gain an in-depth understanding and effective implication of this predictive model.

Previous studies have investigated the interactive mixing behaviour of excipient can affect the compactability of interactive powder mixtures [26]. At low excipient proportions, interactive mixtures with CAB predicted homogeneous interactive mixing behaviour (i.e., with

work of adhesion (w_{ad}) greater than or equal to the work of cohesion (w_{co})) demonstrated better compactability than CAB predicted inhomogeneous mixtures (i.e., with work of adhesion (w_{ad}) less than the work of cohesion (w_{co})). This indicated that the CAB model may also be effectively employed to predict the compaction behaviour of API/excipient blends. Excipients, which are effective at improving the compaction at low proportions, may find applications in tabletting of high-dose difficult to compact APIs [3].

We also observed that the compaction behaviour of interactive mixture with high excipient proportions deviated significantly form CAB predicted model behaviour i.e., the interactive mixtures demonstrated a high compactability despite CAB predicted inhomogeneous mixing of the small excipients. This may be attributed to an excess of excipient particles in the blend, allowing them to effectively cover host particles despite poor dispersion, thus offsetting the effect of dispersion/mixing behaviour. Thus, we proposed that there are two important factors, which govern the compactability of interactive mixtures. At low levels of excipient, the compactability of the blend is dependent on the interactive mixing behaviour of the excipients where a more homogenous dispersion of the excipient over the surfaces of the API allows it to express greater binder action. However, at higher levels of excipient, the compactability of API/excipient blend is no longer governed by the dispersibility of the excipient particles rather it is determined by their intrinsic compactability. This is perhaps because at higher levels of excipient, there is an excess availability of the binder particle, thus the binder particles are likely to sufficiently cover the surface of the API regardless of how well the binder particles de-agglomerate.

Flow additives improve flow by adhering to cohesive particles and thus acting as spacers and by reducing inter-particle forces [14, 19, 21]. This suggests that the small particles improve flow by forming interactive mixtures. Previous studies have suggested that particles size, surface coverage, chemical nature, as well as mixing behaviour of small excipients can

significantly influence the flow performance of interactive mixtures [14, 16, 19, 21, 51-53]. In this study, we investigated if the CAB model can also predict the flow performance of powder blends. It was noted that the flow improvement was only evident in case of CAB predicted homogeneous interactive mixing behaviour (i.e., with work of adhesion (w_{ad}) greater than or equal to the work of cohesion (w_{co})). This improvement was more pronounced and distinct at higher excipient proportions. This may be attributed to greater surface coverage of paracetamol particles by small excipient particles, which significantly reduces inter-particle interactions between paracetamol particles offering greater flow improvements, which is consistent with earlier observations [16, 19, 21]. Notably, optimal flow additive action was observed with excipients containing higher proportions of L-leucine indicating that not only interactive mixing behaviour but also other particle properties of small particles may also play an important role in determining flow of interactive mixtures. This may be attributed to the reduction in cohesion of excipient particles with higher L-leucine concentrations, as previously reported. Since, the small excipient particles covers the surface of host particles in interactive mixtures, these particulate structures act as core-shell agglomerates, where inter-particle interactions of shell (excipient particles) i.e., cohesion becomes the leading factor controlling the flow of the core (host particles). Thus, excipients with lower cohesion allows better flow improvements, if the effect of mixing behaviour is disregarded. Further studies are being conducted to look into this aspect of flow improvements.

5.9 Conclusion

In conclusion, the surface energy derived cohesive-adhesive balance (CAB) model can effectively predict the interactive mixing behaviour of small particles. This data could also effectively predict the compactability and flow behaviour of resultant interactive mixtures at certain excipient proportions. Overall, this knowledge may help provide significant insight into

the mixing, flow and compaction behaviour of interactive mixture, and thus create optimum interactive powder mixtures for tablet manufacturing.

5.10 Acknowledgements

Sharad Mangal is thankful to Monash Institute of Graduate Research (MIGR) for providing Monash Graduate Scholarship (MGS) and Monash International Postgraduate Research Scholarship (MIPRS). Authors would like to acknowledge Dr. Shyamal Das from University of Otago for his help.

5.11 References

[1] Staniforth JN. Powder flow. In: Aulton ME, Ed., Pharmaceutics: The science of dosage form design. 2nd ed., Edinbergh, UK: Churchill Livingstone, 2002; pp. 197–210.

[2] Sun CC. Decoding powder tabletability: Roles of particle adhesion and plasticity. J Adhes Sci Technol 2011; 25(4-5): 483-499.

[3] Mangal S, Meiser F, Morton D, Larson I. Particle engineering of excipients for direct compression: Understanding the role of material properties. Curr Pharm Des 2015.

[4] Mangal S, Larson I, Meiser F, Morton DAV. Particle Engineering of Polymers into Multifunctional Interactive Excipients. In, Handbook of Polymers for Pharmaceutical Technologies. John Wiley & Sons, Inc., 2015; pp. 1-31.

[5] Rojas J, Buckner I, Kumar V. Co-proccessed excipients with enhanced direct compression functionality for improved tableting performance. Drug Dev Ind Pharm 2012; 38(10): 1159-1170.

[6] Bolhius GK, Waard Hd. Materials for direct compaction. In: Alderborn G, Nystrom C, eds., Pharmaceutical Powder Compaction Technology. Informa Healthcare: New York, 1996; pp. 419-500.

[7] Bolhuis GK, Armstrong NA. Excipients for direct compaction—an update. Pharm Dev Technol 2006; 11(1): 111-124.

[8] Li Q, Rudolph V, Weigl B, Earl A. Interparticle van der Waals force in powder flowability and compactibility. Int J Pharm 2004; 280(1–2): 77-93.

[9] Nyström C, Alderborn G, Duberg M, Karehill P-G. Bonding surface area and bonding mechanism-two important factors for the understanding of powder comparability. Drug Dev Ind Pharm 1993; 19(17-18): 2143-2196.

[10] Han X, Jallo L, To D, Ghoroi C, Dave R. Passivation of high-surface-energy sites of milled ibuprofen crystals via dry coating for reduced cohesion and improved flowability. J Pharm Sci 2013; 102(7): 2282-96.

[11] Hersey JA. Ordered mixing: a new concept in powder mixing practice. Powder Technol 1975; 11(1): 41-44.

[12] Begat P, Morton DAV, Staniforth J, Price R. The cohesive-adhesive balances in dry powder inhaler formulations II: influence on fine particle delivery characteristics. Pharm Res 2004; 21(10): 1826-1833.

[13] Begat P, Morton DV, Staniforth J, Price R. The cohesive-adhesive balances in dry powder inhaler formulations I: direct quantification by atomic force microscopy. Pharm Res 2004; 21(9): 1591-1597.

[14] Jonat S, Hasenzahl S, Drechsler M, Albers P, Wagner KG, Schmidt PC. Investigation of compacted hydrophilic and hydrophobic colloidal silicon dioxides as glidants for pharmaceutical excipients. Powder Technol 2004; 141(1–2): 31-43.

[15] Yang L, Venkatesh G, Fassihi R. Characterization of Compressibility and Compactibility of Poly(ethylene oxide) Polymers for Modified Release Application by Compaction Simulator. Journal of Pharmaceutical Sciences 1996; 85(10): 1085-1090.

[16] Chen Y, Yang J, Dave RN, Pfeffer R. Fluidization of coated group C powders. AIChE J 2008; 54(1): 104-121.

[17] Meyer K, Zimmermann I. Effect of glidants in binary powder mixtures. Powder Technology 2004; 139(1): 40-54.

[18] Zimmerman I, Eber M, Meyer K. Nanomaterials as flow regulators in dry powders. Z Phys Chem 2004; 218: 51-102.

[19] Yang J, Sliva A, Banerjee A, Dave RN, Pfeffer R. Dry particle coating for improving the flowability of cohesive powders. Powder Technol 2005; 158(1–3): 21-33.
[20] Chen Y, Yang J, Dave RN, Pfeffer R. Fluidization of coated group C powders. AIChE Journal 2008; 54(1): 104-121.
[21] Chen Y, Quintanilla MA, Yang J, Valverde JM, Dave RN. Pull-off force of coated fine powders under small consolidation. Phys Rev E Stat Nonlin Soft Matter Phys 2009; 79(4 Pt 1): 1-14.
[22] Nyström C, Mazur J, Sjögren J. Studies on direct compression of tablets II. The influence of the particle size of a dry binder on the mechanical strength of tablets. Int J Pharm 1982; 10(3): 209-218.
[23] Mattsson S, Nyström C. Evaluation of strength-enhancing factors of a ductile binder in direct compression of sodium bicarbonate and calcium carbonate powders. Eur J Pharm Biopharm 2000; 10(1): 53-66.
[24] Leuenberger H. The application of percolation theory in powder technology. Adv Powder Technol 1999; 10(4): 323-352.
[25] Blattner D, Kolb M, Leuenberger H. Percolation theory and compactibility of binary powder systems. Pharm Res 1990; 7(2): 113-117.
[26] Mangal S, Meiser F, Lakio S, Morton D, Larson I. The role of physico-chemical and bulk characteristics of co-spray dried l-leucine and polyvinylpyrrolidone on glidant and binder properties in interactive mixtures. Int J Pharm 2015; 479(2): 338-348.
[27] Minchom CM, Armstrong NA. A proposed technique for expressing the capacity of directly compressible tablet diluents. J Pharm Pharmacol 1989; 39: 69.
[28] van Oss CJ. Acid—base interfacial interactions in aqueous media. Colloids Surf A 1993; 78: 1-49.
[29] Van Oss CJ, Good RJ, Chaudhury MK. Additive and nonadditive surface tension components and the interpretation of contact angles. Langmuir 1988; 4(4): 884-891.
[30] Mangal S, Meiser F, Tan G, Gengenbach T, Denman J, Rowles MR, Larson I, Morton DAV. Relationship between surface concentration of l-leucine and bulk powder properties in spray dried formulations. Eur J Pharm Biopharm 2015; 94: 160-169.
[31] Schultz J, Lavielle L, Martin C. The role of the interface in carbon fibre-epoxy composites. J Adhes 1987; 23(1): 45-60.
[32] van Oss CJ, Chaudhury MK, Good RJ. Monopolar surfaces. Adv Colloid Interface Sci 1987; 28(1): 35-64.
[33] Traini D, Young PM, Thielmann F, Acharya M. The influence of lactose pseudopolymorphic form on salbutamol sulfate-lactose interactions in DPI formulations. Drug Dev Ind Pharm 2008; 34(9): 992-1001.
[34] Fowkes FM. Attractive forces at interfaces. Ind Eng Chem Res 1964; 56(12): 40-52.
[35] Gharaibeh SF, Aburub A. Use of first derivative of displacement vs. force profiles to determine deformation behavior of compressed powders. AAPS PharmSciTech 2013; 14(1): 398-401.
[36] Gupta A, Hamad M, Tawakkul M, Sayeed V, Khan M. Difference in the lubrication efficiency of bovine and vegetable-derived magnesium stearate during tabletting. AAPS PharmSciTech 2009; 10(2): 500-504.
[37] Fell JT, Newton JM. Determination of tablet strength by the diametral-compression test. J Pharm Sci 1970; 59(5): 688-691.
[38] Carr R. Evaluating flow properties of solids. Chemical Engineering Science 1965; 72: 163-168.
[39] Shah RB, Tawakkul MA, Khan MA. Comparative Evaluation of Flow for Pharmaceutical Powders and Granules. AAPS PharmSciTech 2008; 9(1): 250-258.

[40] Staniforth JN, Morton DAV, inventor, assignee Magnesium stearate, a phospholipid, or an amino acid in preparation of pharmaceutical particles for inhalation. 2002.
[41] van der Voort Maarschalk K, Zuurman K, Vromans H, Bolhuis GK, Lerk CF. Porosity expansion of tablets as a result of bonding and deformation of particulate solids. Int J Pharm 1996; 140(2): 185-193.
[42] Rees JE, Tsardaka KD. Some effects of moisture on the viscoelastic behaviour of modified starch during powder compaction. Eur J Pharm Biopharm 1994; 40(4): 193-197.
[43] van Veen B, van der Voort Maarschalk K, Bolhuis GK, Zuurman K, Frijlink HW. Tensile strength of tablets containing two materials with a different compaction behaviour. Int J Pharm 2000; 203(1–2): 71-79.
[44] van Veen B, van der Voort Maarschalk K, Bolhuis GK, Visser MR, Zuurman K, Frijlink HW. Pore formation in tablets compressed from binary mixtures as a result of deformation and relaxation of particles. European Journal of Pharmaceutical Sciences 2002; 15(2): 171-7.
[45] Pitt KG, Heasley MG. Determination of the tensile strength of elongated tablets. Powder Technol 2013; 238: 169-175.
[46] Castellanos A. The relationship between attractive interparticle forces and bulk behaviour in dry and uncharged fine powders. Adv Phys 2005; 54(4): 263-376.
[47] Abdullah EC, Geldart D. The use of bulk density measurements as flowability indicators. Powder Technol 1999; 102(2): 151-165.
[48] Leane M, Pitt K, Reynolds G. A proposal for a drug product Manufacturing Classification System (MCS) for oral solid dosage forms. Pharm Dev Technol 2015; 20(1): 12-21.
[49] Chen Y, Quintanilla MAS, Yang J, Valverde J, Dave R. Pull-off force of coated fine powders under small consolidation. Phys Rev E Stat Nonlin Soft Matter Phys 2009; 79(4): 041305-041305.
[50] Lai F, Hersey JA, Staniforth JN. Segregation and mixing of fine particles in an ordered mixture. Powder Technol 1981; 28(1): 17-23.
[51] Chen Y, Jallo L, Quintanilla MAS, Dave R. Characterization of particle and bulk level cohesion reduction of surface modified fine aluminum powders. Colloids and Surfaces A: Physicochemical and Engineering Aspects 2010; 361(1–3): 66-80.
[52] Chen Y, Jallo L, Quintanilla MAS, Dave R. Characterization of particle and bulk level cohesion reduction of surface modified fine aluminum powders. Colloid Surface A 2010; 361(1–3): 66-80.
[53] Jonat S, Hasenzahl S, Gray A, Schmidt PC. Mechanism of glidants: investigation of the effect of different colloidal silicon dioxide types on powder flow by atomic force and scanning electron microscopy. J Pharm Sci 2004; 93(10): 2635-2644.

Chapter 6

To investigate the relationship between the cohesion and flow additive action of small binder particles

Sharad Mangal[1], Thomas Gengenbach[2], Doug Millington-Smith[3], Brian Armstrong[3], David AV Morton[1]*, Ian Larson[1]*

[1] Drug Delivery, Disposition and Dynamics, Monash University, 381 Royal Parade, Parkville, VIC-3052, Australia
[2] CSIRO Materials Science and Engineering, Bayview Avenue, Clayton, VIC-3168, Australia
[3] Freeman Technology, Miller Court, Tewkesbury Business Park, Severn Dr, Tewkesbury, Gloucestershire GL20 8DN, United Kingdom
* Corresponding Authors

***Submitted as:**
Mangal S, Gengenbach T, Millington-Smith D, Armstrong B, Morton DAV, Larson I. Relationship between the cohesion of guest particles and the flow performance of interactive mixtures. Eur J Pharm Biopharm. Accepted for publication. doi: 10.1016/j.ejpb.2016.03.012.

6 Declaration for Thesis Chapter 6

Declaration by candidate

In the case of Chapter 6, the nature and extent of my contribution to the work was the following:

Nature of contribution	**Extent of contribution (%)**
Study initiation, formation of hypothesis, laboratory work, data collection, analysis and interpretation and writing the manuscript	60%

The following co-authors contributed to the work. If co-authors are students at Monash University, the extent of their contribution in percentage terms must be stated:

Name	**Nature of contribution**	**Extent of contribution (%) for student co-authors only**
Brian Armstrong	Manuscript revision and flow data assessment	10%
Doug Millington-Smith		
Thomas Gengenbach	XPS characterization and proofreading	10%
David AV Morton	Supervision and manuscript revision	10%
Ian Larson	Supervision and manuscript revision	10%

The undersigned hereby certify that the above declaration correctly reflects the nature and extent of the candidate's and co-authors' contributions to this work*.

Candidate's Signature	[redacted]	**Date 23.11.2015**
Main Supervisor's Signature	[redacted]	**Date 24/11/15**

*Note: Where the responsible author is not the candidate's main supervisor, the main supervisor should consult with the responsible author to agree on the respective contributions of the authors.

6.1 Commentary

In the previous chapter, the flow of interactive mixtures improved with efficient interactive mixing as well as reducing cohesion of small binder particles. In this study, we address the specific objective 4 "to investigate the relationship between the cohesion of small particles and the flow of interactive mixture". In interactive mixtures, the guest particles are present at the interfaces of the host particles. At sufficient surface coverage, the inter-particle interactions between the guest particles are the dominant particle-particle interaction, hence the flow of such interactive mixture would depend on inter-particle interactions between guest particles. Thus, we hypothesized that the cohesion of guest particles governs the flow behaviour of interactive mixtures and consequently their flow additive action.

6.2 Abstract

In this study, we aimed to investigate the effects cohesion of small surface-engineered guest binder particles on the flow behaviour of interactive mixtures. Polyvinylpyrrolidone (PVP) - a model pharmaceutical binder - was spray-dried with varying L-leucine feed concentrations to create small surface-engineered binder particles with varying cohesion. These spray-dried formulations were characterized by their particle size distribution, morphology and cohesion. Interactive mixtures were produced by blending these spray-dried formulations with paracetamol. These blends were visualized under scanning electron microscope to confirm formation of interactive mixtures. Surface coverage of paracetamol by guest particles as well as the flow behaviour of these mixtures were examined. The flow performance of interactive mixtures was evaluated using measurements of conditioned bulk density, basic flowability energy, aeration energy and compressibility. With higher feed L-leucine concentrations, the surface roughness of small binder particles increased, while their cohesion decreased. Visual inspection of the SEM images of the blends indicated that the guest particles adhered to the surface of paracetamol resulting in effective formation of interactive mixtures. These images also showed that the low-cohesion guest particles were better de-agglomerated consequently formed a more homogeneous interactive mixture with paracetamol compared with high cohesion formulations. The flow performance of interactive mixtures changed as a function of the cohesion of the guest particles. Interactive mixtures with low-cohesion guest binder particles showed notably improved bulk flow performance compared to those containing high-cohesion guest binder particles. Thus, our study suggests that the cohesion of guest particles dictates the flow performance of interactive mixtures.

Keywords: FT4, bulk density; interactive mixture; paracetamol; polyvinylpyrrolidone; L-leucine; particle engineering, surface coverage, X-ray photoelectron spectroscopy, shear cell

6.3 Graphical abstract

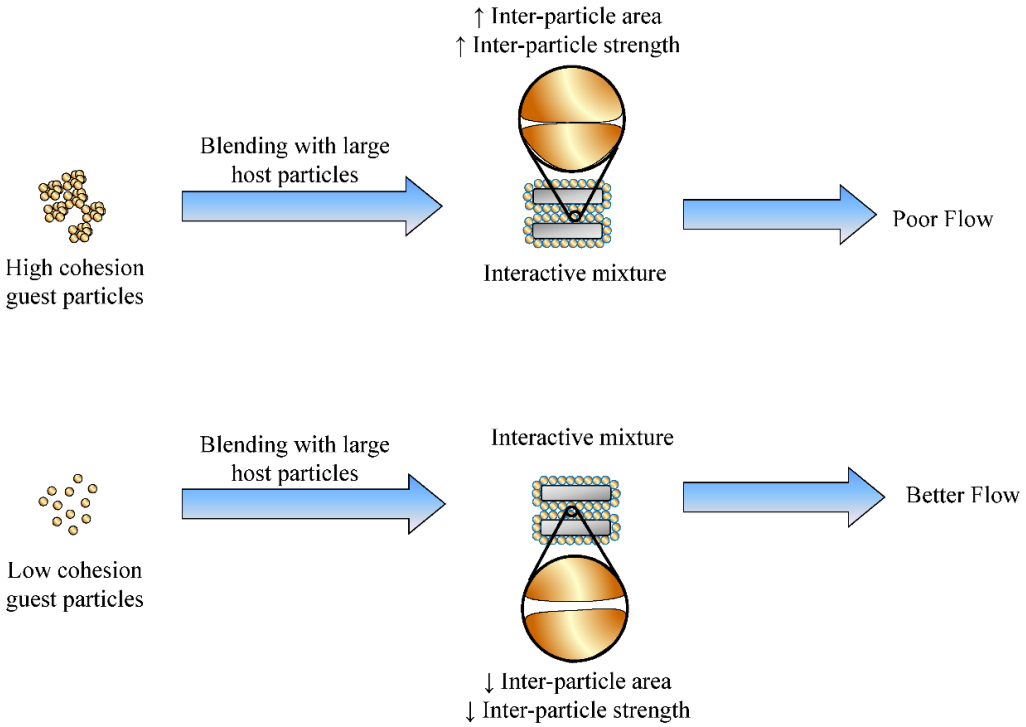

6.4 Introduction

In general, powder flow can be defined as the movement of particles relative to adjacent particles and/or surfaces [1]. The manufacturing of pharmaceutical solid dosage forms involves several processes, which are highly sensitive to powder flow [2, 3]. For example, the delivery of a consistent dose into a tablet die during tablet manufacturing. Thus, predictable and reproducible flow is an important powder characteristic for successful manufacturing [4, 5].

Many pharmaceutical powders exhibit poor flow and hence are inherently unsuitable for manufacturing process. Poor flowability is a result of strong inter-particles cohesive forces (between particles of similar chemical natures) arising mainly from van der Waals attraction. The magnitude of these forces increase as the particle size is reduced and hence they become the dominant factor controlling the flow of small particles.

Coating cohesive particles with small guest particles (silicon dioxide is often regarded as a flow additive or glidant) is a commonly used method of improving flow [6-10]. These guest particles act as nano-surface roughness on the cohesive host particles, reducing interactions between them and improving their flow. [11]. This suggests that these flow additives (small guest particles) mainly act by adhering to the surfaces of cohesive host particles [6, 12].

Interactive mixing also describes the adhesion of small particles (<10 μm) to relatively large particles [13], which implies that the flow additives also work of the principle of interactive mixing [5]. Cohesive forces (or work of cohesion, w_{co}) act between similar particles, while adhesion forces (or work of adhesion, w_{ad}) act between dissimilar particles. Cohesive-adhesive balance or CAB describes the relative magnitude of these different forces [14, 15]. Previously, surface energy has been used to calculate the magnitude of forces acting

between particles [16]. The surface energies of two interacting particles can be utilised to calculate w_{ad} and w_{co} [17, 18]:

$$w_{co} = 2\sqrt{\gamma_1^D.\gamma_1^D} + 2\sqrt{\gamma_1^P.\gamma_1^P} \qquad \text{Eq. (6.1)}$$

$$w_{ad} = 2\sqrt{\gamma_1^D.\gamma_2^D} + 2\sqrt{\gamma_1^P.\gamma_2^P} \qquad \text{Eq. (6.2)}$$

where, γ_1^D and γ_1^P represent the dispersive and polar energies of particles of solid 1, and γ_2^D and γ_2^P represent the dispersive and polar energies of particles of solid 2.

For interactive mixtures to form, adhesion of guest particles to host particles must be preferred to cohesive forces, i.e. $w_{ad} > w_{co}$ [14, 15]. However, small particles (<10 µm) can be highly cohesive [19]. These relatively strong cohesive forces inhibit de-agglomeration and the dispersion of these small particles over host particles, which compromise their ability to form interactive mixtures (as $w_{ad} < w_{co}$) and consequently their flow additive ability [5, 8].

In theory, there are two main approaches to maximize the de-agglomeration and surface coating quality of such small particles. Firstly, the deliberate de-agglomeration and dispersion of guest particles using high shear mixing processes (dry powder coating) and secondly, engineering particles with reduced forces of cohesion, thus making them inherently more adhesive than cohesive.

Dry powder coating approaches have been found to enhance the de-agglomeration and dispersion of small flow additives over host particles, thus improving their flow additive ability. Dry coating approaches include mechanofusion [8-10], hybridizer [20], comil [21, 22], fluid energy mills [23] and the magnetically assisted impaction coater (MAIC) [23, 24]. The enhanced flow additive action following dry coating was attributed to greater host surface

coverage, implying the relationship between de-agglomeration and flow additive action [12, 24].

Particle engineering utilising L-leucine is an effective strategy to control the cohesion of small particles [25, 26]. Upon co-spraying, L-leucine enriches the surface of small particles, increase surface corrugation [26, 27] and reduce surface energy [25] , thus reduce the cohesion [25]. We have recently demonstrated that L-leucine surface enriched small binder particles exhibit efficient de-agglomeration and dispersion over host particles even using low shear mixing [19, 28]. Such improved dispersion behaviour also allowed low-cohesion guest binder particles to express a flow additive action [19, 28].

In interactive mixtures, the guest particles are present at the interfaces of the host particles. At surface coverages of approximately >40%, guest-guest interactions are the dominant inter-particles interactions, while host-host interactions are negligible [29, 30]. In such mixtures, the flow would be expected to mainly depend on the nature of guest particles. In this context, guest particle properties i.e., size, surface coverage and chemical nature have been shown to strongly affect the flow performance of interactive mixtures [6, 11, 12, 24, 31]. In this study, we have extended an ongoing investigation into the potential design of an engineered small binder particles with the aim to investigate the relationship between the cohesion of guest particles and the flow performance on interactive mixtures. We investigated the change in surface coverage as well as the flow performance of interactive mixtures with respect to the cohesion of guest particles. This was done to gain further insight into the effect of nature of guest particles on their flow additive action.

6.5 Materials and methods

Paracetamol of analytical grade and PVP (molecular weight ~ 30 kDa, as per supplier's specifications) were procured from Sigma–Aldrich (St. Louis, Missouri, MO, USA). L-leucine was purchased from Ajinomoto Co. Inc. (Tokyo, Japan).

6.5.1 Method of preparation

Aqueous solutions of PVP (6 % (w/v)) and predetermined proportions of L-leucine were spray-dried using the method as described previously [16]. Briefly, PVP and L-leucine were accurately weighed and dissolved in water with the aid of magnetic stirring. The resultant solutions (approximately 500 mL) were spray-dried using a laboratory scale spray-dryer (Buchi-190 mini, Buchi Laboratory Equipment, Flawil, Switzerland) with a 0.5 mm two-fluid nozzle. The standard operating conditions employed during spray-drying were: inlet temperature, 125 ±5 °C; spray air flow rate, 800 L/h; and liquid solution feed rate, 10 mL/min. These conditions resulted in an outlet temperature of 70 ±2 °C. The powders were collected immediately and stored in a resealable aluminium foil bag to prevent moisture uptake.

6.5.2 Particle size and size distribution

The particle size measurements were performed using a Malvern Mastersizer 2000 (Malvern Instruments Ltd., Malvern, UK). Powder samples were spread along the sample feed tray. Particle size measurements were performed at a shear pressure of 2.0 bar and the feeder setting of 50%. Measurements for each formulation were performed in triplicate.

6.5.3 Scanning electron microscopy (SEM)

The morphology and blending behaviour of the spray-dried formulations were visualised by SEM (Phenom^{TM}, FEI Company, Hillsboro, OR, USA). Double-sided adhesive tape was placed

on an aluminium stubs and a small amount of sample was placed on the tape followed by gentle tapping to disperse the sample evenly. The stubs were then coated with a fine gold film using a sputter coater (Emitech K550X, Quorum Technologies, Kent, UK) at an electrical potential of 2.0 kV at 25 mA for 3 min. The coated stubs were then loaded into the SEM and images captured.

6.5.4 Evaluation of cohesion of binder powders

A Freeman FT4 Powder Rheometer® system (Freeman Technology, Gloucestershire, UK) with a shear test module was used to characterize bulk cohesion. Briefly, the instrument measures the powder shear stress at a given consolidating normal stress. For the shear test, the powders (approximately 1 g) were loaded into a 1 mL shear cell module and conditioned. The powder bed was pre-consolidated at a normal stress of 9 kPa using a vented piston, which was then replaced by a shear head. Shear tests were carried out at normal stresses of 7, 6, 5, 4 and 3 kPa. The shear stress at each normal stress was recorded and yield loci were derived as curves to represent the maximum shear stress the sample can support under a certain normal stress following a specific pre-consolidating stress. The bulk cohesion forces of each sample were calculated by extrapolating the yield locus to zero normal stress (Eq. 6.3).

$$\tau = C + \sigma \tan \eta \qquad \text{(Eq. 6.3)}$$

where, τ is the shear stress, σ is the normal stress, η is the angle of internal friction, and C is the cohesion. The cohesion was calculated by extrapolating the yield loci to a zero normal stress at the intercept. In general, higher cohesion values are considered to correspond to higher cohesive inter-particle forces [10, 28].

6.5.5 Blending

A total of 50 g of blended samples were prepared by mixing paracetamol with predetermined amounts of each spray-dried formulation in a 250 mL glass jar using a Turbula T2 mixer (Willy A. Bachofen, Muttenz, Switzerland) at 72 rpm for 5 min.

6.5.6 Blending behaviour

X-ray photoelectron spectroscopy (XPS) analysis was performed using an AXIS Ultra DLD Spectrometer (Kratos Analytical Ltd., Manchester, U.K.), equipped with a monochromated Al Kα source at a power of 180 W (12 mA, 15 kV). A small quantity of each sample was filled into the shallow wells of custom-made powder sample holders [29]. Sample charging during irradiation was compensated for by an electron flood gun in combination with a magnetic immersion lens. A reference binding energy of 285.0 eV for the aliphatic hydrocarbon C 1s component was used to correct for any remaining offsets due to charge neutralisation of specimens under irradiation [30]. The pressure in the main vacuum chamber during analysis was typically 10^{-6} Pa. Spectra were recorded with the nominal photoelectron detection normal to the sample surface. In the case of powders of random orientations, the microscopic emission angle is ill-defined. Consequently, the sampling depth might vary between 0 nm and 5 - 10 nm, depending on the kinetic energy of the measured photoelectrons. The area analysed on each sample had approximate dimensions of 0.3 mm × 0.7 mm. The elemental composition of the samples was obtained from survey spectra (160 eV pass energy) using integral peak intensities and the sensitivity factors supplied by the manufacturer. High-resolution spectra of individual peaks were recorded at 20 eV pass energy which results in a peak width (full width at half maximum) of typically 0.9 - 1.1 eV for organic polymeric materials.

In order to determine relative fractions of PVP, L-leucine (Leu) and Paracetamol (Para), reference data were acquired for the three pure compounds. By comparing the data

obtained from the interactive mixtures to the reference data, one can estimate surface fractions of the individual compounds using two methods. The first is based on observed variations in elemental surface composition. The elemental composition (C, N, O) of the interactive mixtures is assumed to be a linear combination of the compositions of the three pure constituents (PVP, Leu, Para) which can be expressed as a system of three linear equations. The resulting 3 x 3 matrix can then be solved to calculate relative fractions of the three constituents in a particular blend [31]. The second method involves comparing high-resolution spectra, specifically carbon (C) 1s, spectra since they are significantly different for PVP, Leu and Para because of their different chemical structures. This allows the surface fractions of the three compounds in the blends to be estimated using curve fitting: the reference spectra of PVP, Leu, and Para can be used as three fit components to calculate optimised curve fits of the spectra of the interactive mixture (Figure 6.1). This yields the relative number of C atoms which are present as part of either PVP, Leu or Para [29]. Scaled using the respective number of C atoms in one molecule of the pure compound, these fractions can be converted to relative molar fractions of PVP, Leu or Para.

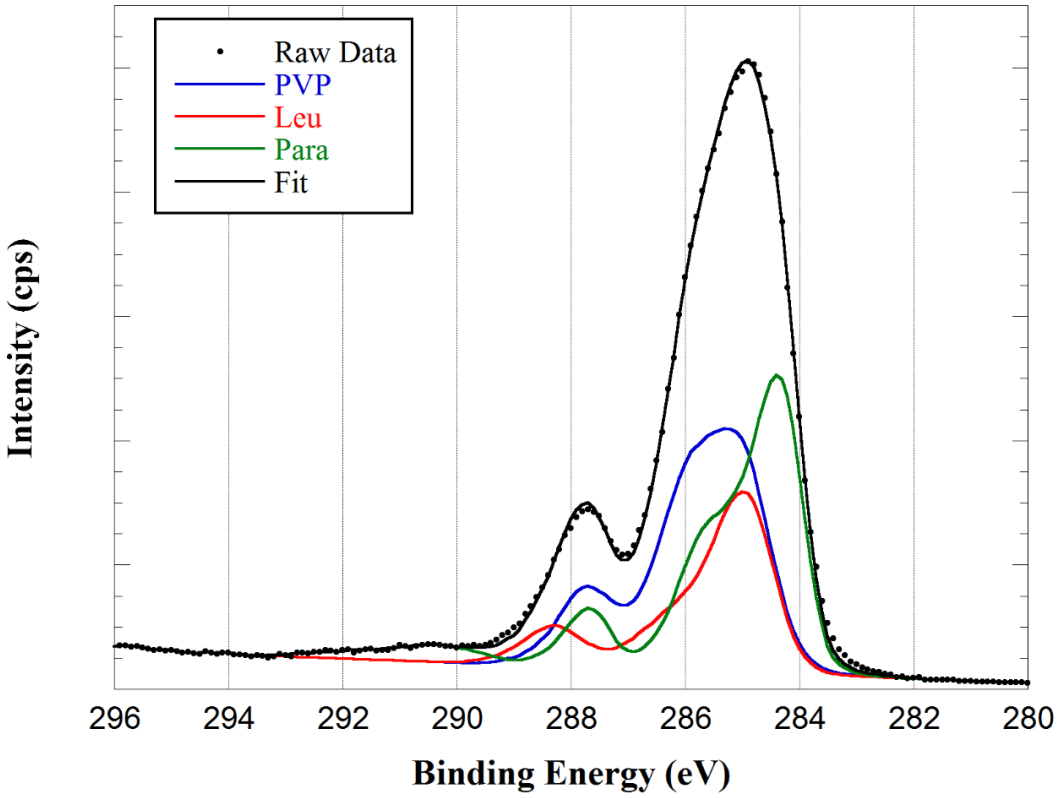

Figure 6.1 – Example of a C 1s fitted using reference spectra of PVP, Leu and Para.

Molar fractions thus derived from XPS data are presented with uncertainties based simply on two measurements per sample. The overall uncertainty in determining molar surface fractions is a combination of instrument-related experimental uncertainty (XPS) as well as uncertainties involved in estimating fractions using the two methods described, and is therefore difficult to estimate. Since XPS-derived results will only be discussed in qualitative terms, a comprehensive error analysis was deemed unnecessary.

6.5.7 Evaluation of flow performance of interactive mixtures

The effect of cohesion of guest particle on flow of interactive mixtures was evaluated using: (i) conditioned bulk density (CBD), (ii) basic flowability energy (iii) aeration and (iv) compressibility using the FT4 Powder Rheometer.

6.5.7.1 Conditioned bulk density (CBD)

The CBD test involves a powder conditioning cycle to reduce the operator-induced packing errors associated with conventional methods, hence it is considered more reproducible [32, 33]. The CBD of different blends was assessed using the method described in detail elsewhere [34]. Approximately 12 g powder samples were gently filled into a 25 cm^3 cylindrical vessel fitted with a 10 cm^3 extension vessel with a splitting assembly. The samples were conditioned to create a uniform powder bed in a low stress packing state. The cylindrical vessel was then split which allowed the excess powder to be removed leaving only the powder in 25 cm^3 cylindrical vessel. The weight of the powder was recorded automatically and the conditioned bulk density was calculated by dividing the weight of the powder by the volume of the vessel.

6.5.7.2 Basic flowability energy (BFE)

Basic flow energy (BFE) is defined as the amount of energy needed to move a conditioned powder in a defined flow pattern [34]. BFE is derived from measurements of both the axial and rotational forces acting on the shear blade as it passes through the powder. The basic flowability energy (BFE) was measured during downward movement of the blade at a tip speed 100 mm/s through the powder bed.

6.5.7.3 Aeration

The aeration energy (AE) is intended to measure changes in the flow of the powder under the influence of an air stream at a range of velocities [34]. The aeration test was performed in a 35 cm^3 cylindrical vessel mounted on a base comprising a perforated mesh fitted to a plenum chamber that acted as an air inlet port [35]. These tests were carried out at air velocities of 0, 2, 4, 6, 8 and 10 mm/s. At each velocity, the energy required to move the rotating blade from the top to the bottom of the vessel was determined. The energy required to move the blade

through the powder bed at the highest air flow rate used in these tests i.e., 10 mm/s, was used to distinguish the flow behaviour of different interactive powder blends. In all the test cycles, the tip speed of the blade was 100 mm/s.

8.1.1.1 Compressibility

The compressibility test is a measurement of changes in volume of a powder as a function of applied stress (range from 1 to 15 kPa) [34]. It is an indicator of packing and flow behaviour [33, 36, 37]. Cohesive powders typically exhibit high compressibility compared to free-flowing powders [36]. The change in volume i.e., the compressibility, of different blends at 15 kPa was used for comparison. For each test, all powder samples were tested in triplicate and average values were reported.

6.6 Results

6.6.1 Particle size and size distribution

Table 6.1 presents the particle size distributions of the spray-dried guest particles. The sizes of the various spray-dried particles were relatively similar to each other, implying that L-leucine had a negligible impact on particle size. The spray-dried formulations also demonstrated a mono-modal particle size distribution (Figure 6.2). This is consistent with our previous observations [22].

Table 6.1 – Particle size of various spray-dried formulations and paracetamol. Data presented as Mean ±SD (n = 3).

Materials	Particle Size (µm)			Span
	D_{10}	D_{50}	D_{90}	
PVP-Leu (0%)	1.5 ±0.0	3.2 ±0.1	6.1 ±0.11	1.5 ±0.01
PVP-Leu (2.5%)	1.3 ±0.0	2.7 ±0.0	5.2 ±0.01	1.4 ±0.01
PVP-Leu (5%)	1.5 ±0.0	3.3 ±0.0	6.6 ±0.06	1.5 ±0.01
PVP-Leu (10%)	1.4 ±0.1	3.0 ±0.0	5.9 ±0.12	1.5 ±0.07
PVP-Leu (15%)	1.6 ±0.1	3.4 ±0.0	6.7 ±0.14	1.5 ±0.07
Paracetamol	3.7 ±0.1	21.4 ±0.3	151.5 ±5.0	6.8 ±0.1

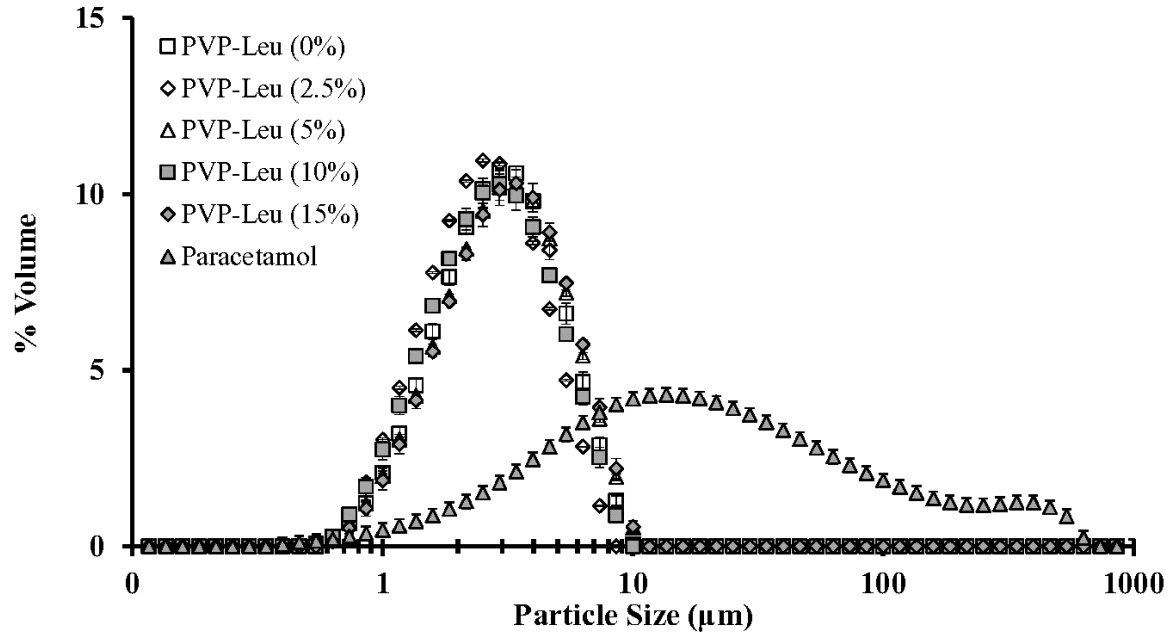

Figure 6.2 – Particle size distribution of various spray-dried formulations and paracetamol. Data presented as Mean ±SD (n = 3).

6.6.2 Surface morphology

Representative SEM images of the spray-dried formulations are shown in Figure 6.3. PVP spray-dried alone (Figure 6.3 A) formed spherical, dimpled and agglomerated particles. Incorporation of L-leucine at as low as 2.5% (w/w) resulted in reduced agglomeration (Figure 6.3 B). As the feed concentration of L-leucine was increased, the surface roughness of these spray-dried particles increased (Figure 6.3). This is consistent with previous observations suggesting the role of L-leucine in influencing the morphology [38]. Increasing surface roughness in such particles is typically claimed to result in reduced inter-particle contact area and therefore powders tend to exhibit relatively lower cohesion [12, 21, 39].

Such change in particle morphology has in several studies been proposed to be a result of surface L-leucine enrichment during droplet drying [26, 27, 43]. It was proposed that low water solubility of L-leucine [26, 27, 43] allows it to reach saturation early during droplet

drying, which is followed by its precipitation first at the droplet interface. It was also speculated that L-leucine first enriches the surface of the droplets due to its interfacial activity [44]. Crystalline character of L-leucine precipitate in spray-dried formulations has been shown from powder diffraction [25, 42], and indicates that a degree of self-assembly occurs during the particle formation process. Researchers have also attempted to model this mass transport behaviour of L-leucine during droplet drying process, notably via the use of the Peclet number [27].

It is generally agreed that as droplet drying progresses, the growing surface L-leucine enriched shell becomes stressed by the increasing vapour pressure of evaporating water, in a manner well documented in the spray drying industry [45]. A common result in this situation is the "blowing" of the shell as it stretches, followed by eventual collapse or rupture of the shell, resulting in the characteristic textured surface morphology of the resultant particles. Thus, the morphology of particles depends on the thickness of L-leucine shell, which determines the resistance that the shell offers to the escape of vapour. The shell thickness is governed by its feed concentration and hence the morphology of spray-dried particles depends on its feed concentration [25]. Morphology changes such as this are claimed to result in reduced inter-particle contact area and therefore lower cohesion [12, 24, 46].

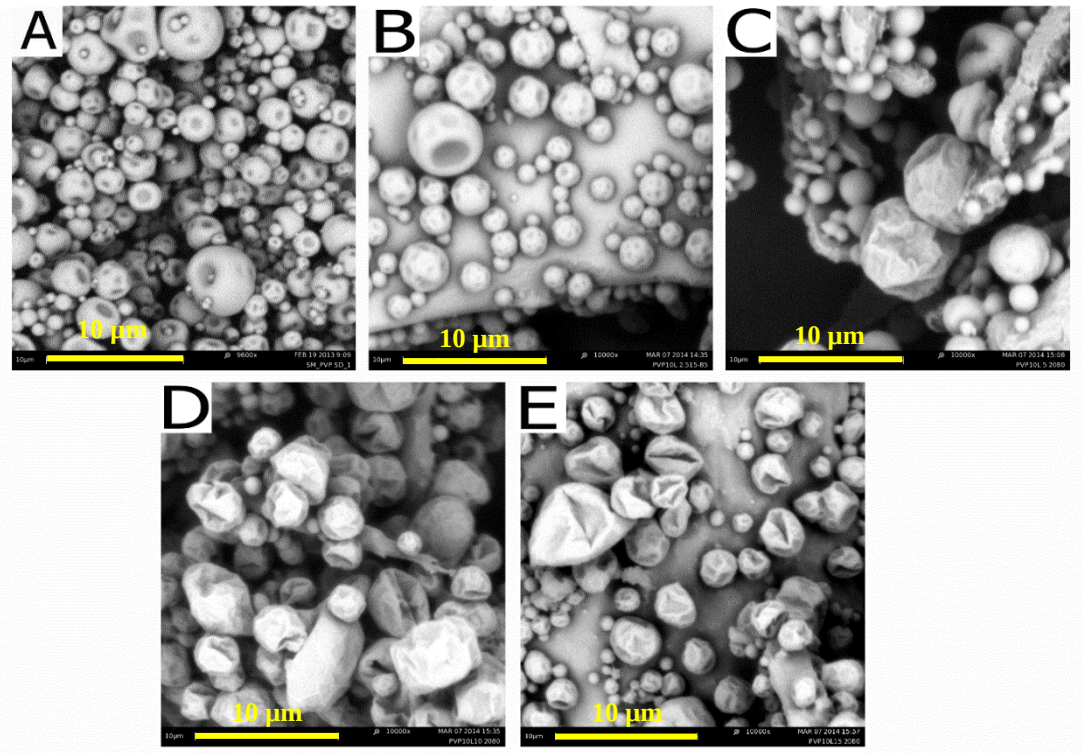

Figure 6.3 – SEM images of spray-dried formulations; (A) PVP-Leu (0%); (B) PVP-Leu (2.5%); (C) PVP-Leu (5%); (D) PVP-Leu (10%) and (E) PVP-Leu (15%).

6.6.3 3.3 Cohesion of binder powders

The cohesion of the spray-dried formulations was determined using the FT4 rheometer shear cell module. The results indicated that the PVP spray-dried alone exhibits higher cohesion (Figure 6.4), while co-spraying with L-leucine resulted in a significant reduction in cohesion. Decreasing cohesion was evident with increasing L-leucine feed concentrations. The cohesion appeared to achieve a minimum level at the 10% L-leucine level, and higher. Our previous findings (which used PVP of a different molecular weight) indicated that the surface L-leucine concentration controls the cohesion of small composite particles, where with approximately 10% feed L-leucine concentration, spray-dried particles are proposed to be coherently coated with L-leucine and exhibit lowest cohesion [22].

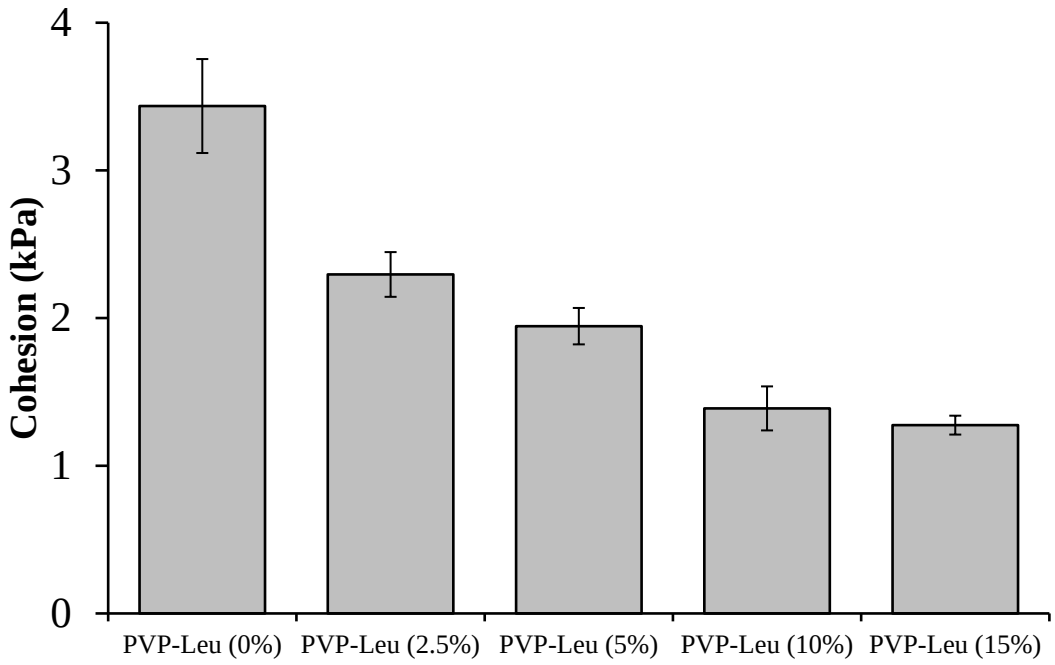

Figure 6.4 – Cohesion of the spray-dried formulations. Data presented as Mean ±SD (n = 3).

6.6.4 Blending behaviour

6.6.4.1 SEM imaging

Representative SEM images of powder formulations are presented in Figure 6.5. PVP spray-dried alone appeared substantially as agglomerates adhered to the surface of paracetamol particles, indicating poor dispersion. In contrast, PVP spray-dried with L-leucine appeared mostly as individual discrete particles (with few agglomerates) adhered to the surface of paracetamol particles. This implies that L-leucine facilitates de-agglomeration (due to reduced cohesion) and the dispersion of guest particles over large host particles during mixing.

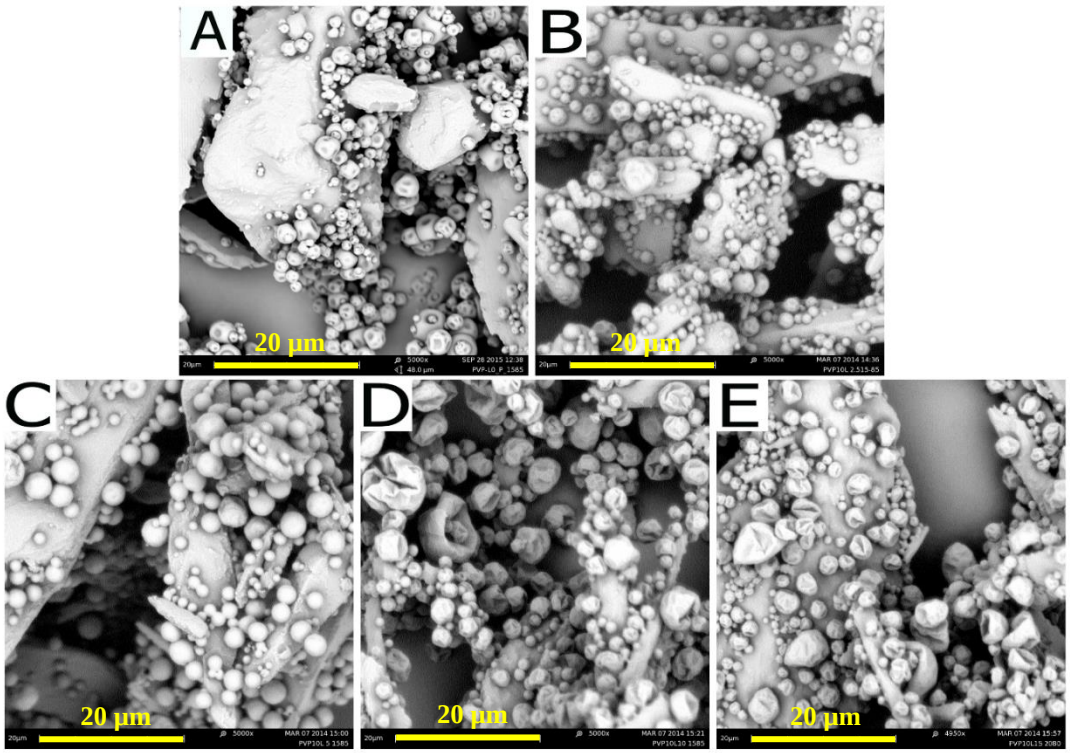

Figure 6.5 – Representative SEM images of interactive powder formulations. (A) PVP-Leu (0%)/Para; (B) PVP-Leu/Para (2.5%); (C) PVP-Leu (5%)/Para; (D) PVP-Leu (10%)/Para and (E) PVP-Leu (15%).

6.6.4.2 XPS analysis

XPS study was conducted to semi-quantitatively assess the surface fraction of exposed paracetamol detected in blends. This data, expressed as a fraction of the total surface area, is presented in Table 6.2. Incorporation of guest particles resulted in a reduction in the level of paracetamol signal, indicating paracetamol particle surface being covered by guest particles. With 10% guest particle fraction, the paracetamol signal reduced to approximately 40% of the original un-blended level. With higher guest particle mass added to the blend (regardless of their cohesion), the paracetamol signal reduced further indicating greater surface coverage.

However, comparison of the interactive mixtures of paracetamol with PVP spray-dried without L-leucine showed relatively higher paracetamol signals, indicating a lower

surface coverage by these guest particles compared with formulations spray-dried with L-leucine. This XPS-based assessment is consistent with the SEM images described earlier, which indicated the presence of L-leucine allowed greater dispersion of the guest particles over paracetamol. Despite having lower cohesion, the PVP-Leu (10%) and PVP-Leu (15%) provided lower coverage compared with PVP-Leu (5%). It is suggested if the reduction of the forces of adhesion between guest particles and paracetamol is too great, it may allow the guest particles to detach from the surface of the paracetamol particles reducing surface coverage. The surface coverages calculated from the elemental compositions of the blends also showed similar trends, supporting the robustness of these measurements (Appendix 6.1).

Table 6.2 – % surface fraction of paracetamol (based on C 1s curvefits) at corresponding guest particle fractions. See text for details.

Formulations	**Surface fraction of paracetamol (as calculated by C 1s curvefits) at corresponding guest particle fractions**			
	5%	**10%**	**15%**	**20%**
PVP-Leu (0%)	68.3 ±3.3 %	55.9 ±5.6 %	48.2 ±4.1 %	43.7 ±4.7 %
PVP-Leu (2.5%)	65.6 ±1.0 %	48.8 ±2.7 %	48.6 ±0.6 %	34.1 ±2.1 %
PVP-Leu (5%)	51.5 ±0.5 %	35.6 ±0.3 %	27.5 ±2.6 %	22.9 ±0.2 %
PVP-Leu (10%)	60.3 ±3.3 %	50.6 ±0.1 %	35.7 ±0.7 %	33.1 ±1.6 %
PVP-Leu (15%)	66.4 ±0.3 %	49.9 ±2.2 %	39.6 ±0.5 %	28.8 ±0.2 %

6.6.5 Flow performance of interactive mixtures

6.6.5.1 Conditioned bulk density (CBD)

Better flowability is typically associated with higher bulk density [33, 40-42]. The CBD values of the powder blends as a function of cohesion and guest particle fraction are shown in Figure 6.6. The bulk density of paracetamol was lowest (0.3 ± 0.0 g/mL), while interactive mixtures showed relatively higher bulk densities. At 5% (w/w) guest particle fraction, the cohesion of guest particles had no observable effect on the bulk density of the interactive mixtures. At higher guest particle fractions (10%, 15% and 20% (w/w)), an increase in bulk density was observed, indicating the modified inter-particle interactions between guest particles was positively affecting the flow behaviour. At guest particles fractions of 10% (w/w) and higher, the flow behaviour of interactive mixtures improved with reducing cohesion of guest particles.

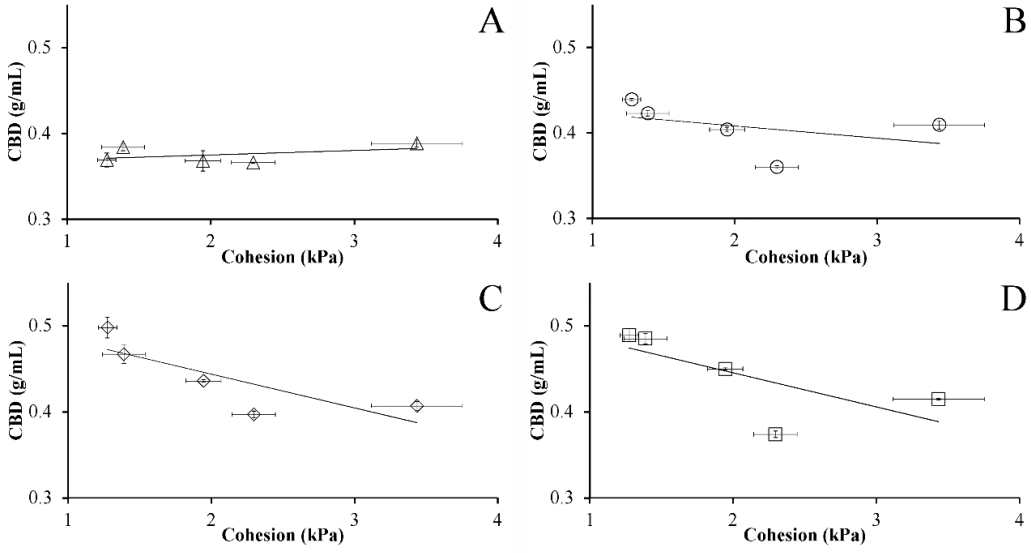

Figure 6.6 – Conditioned bulk density (CBD) of interactive mixture as a function of cohesion of guest particles. Four graph represent different guest to host ratio, (A) 5% (w/w) / 95% (w/w); (B) 10% (w/w) / 90% (w/w); (C) 15% (w/w) / 85% (w/w) and (D) 20% (w/w) / 80% (w/w). Data presented as Mean ±SD (n = 3).

6.6.5.2 Basic flowability energy (BFE)

The basic flowability energy is the energy required to establish a particular flow pattern in a precise volume of conditioned powder. The BFE has been proposed as useful tool for measuring the effect of flow additives on uncompressed powder's flowability [34]. In this case, a lower BFE should represent improved powder flow. It was observed that paracetamol demonstrated the highest BFE (110.6 ± 0.9). The BFE of interactive mixtures was substantially lower than of the pure paracetamol. The BFE of interactive mixtures with low guest particle fractions (5% (w/w), Figure 6.7A) did not change significantly on changing cohesion. However, interactive mixtures with higher guest particle fractions (10% (w/w), 15% (w/w) and 20% (w/w)) showed a notable decline in the BFE indicating flow improvement as a function of reducing guest particle cohesion. In general, the trends observed in the BFE data were in agreement with the trends seen in the CBD data.

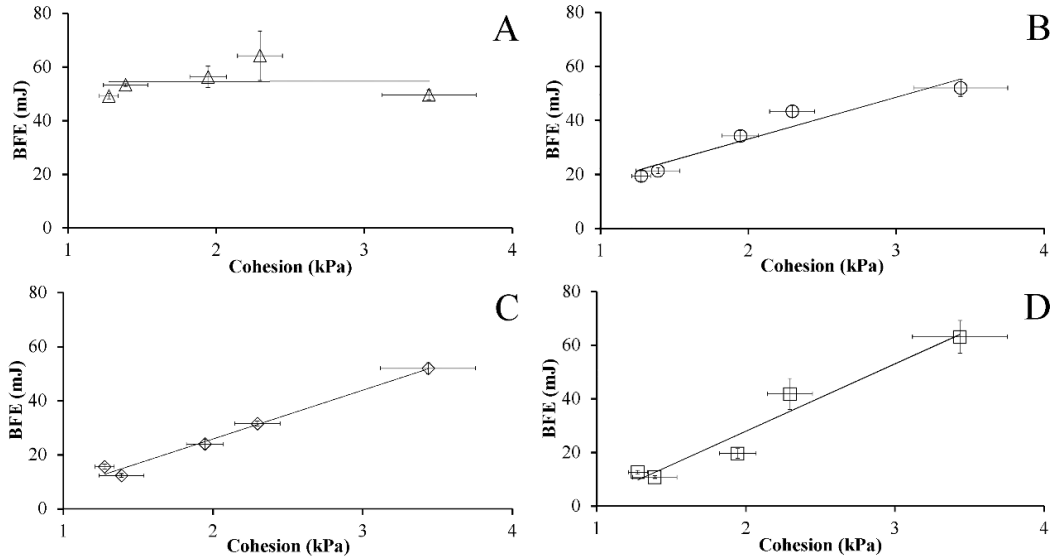

Figure 6.7 – Basic flowability energy (BFE) of interactive mixture as a function of cohesion of guest particles. Four graph represent different guest to host ratio, (A) 5% (w/w) / 95% (w/w);

(B) 10% (w/w) / 90% (w/w); (C) 15% (w/w) / 85% (w/w) and (D) 20% (w/w) / 80% (w/w). Data presented as Mean ±SD (n = 3).

6.6.5.3 Aerated Energy (AE)

It is believed that cohesive powders exhibit lower sensitivity to fluidising air than free flowing powders [43]. Therefore, the energy required to fluidise and convey the cohesive powders in an air stream may be considered to be an indicator of flow of unconsolidated powders [43]. The aeration energy of pure paracetamol was high (92.9 ±5.5 mJ) and was relatively insensitive to air velocity indicating paracetamol's cohesive nature (Appendix 6.2) [26]. The aeration energy of the interactive mixtures was lower compared to pure paracetamol. The aeration energy of interactive mixtures consisting of lower guest particle fraction (5% (w/w)) remained relatively unchanged as a function of the cohesion of guest particles formulations. However, at relatively higher guest particle fractions (10%, 15% and 20% (w/w)), a sharp decline in the aeration energy was recorded as a function of guest particle cohesion.

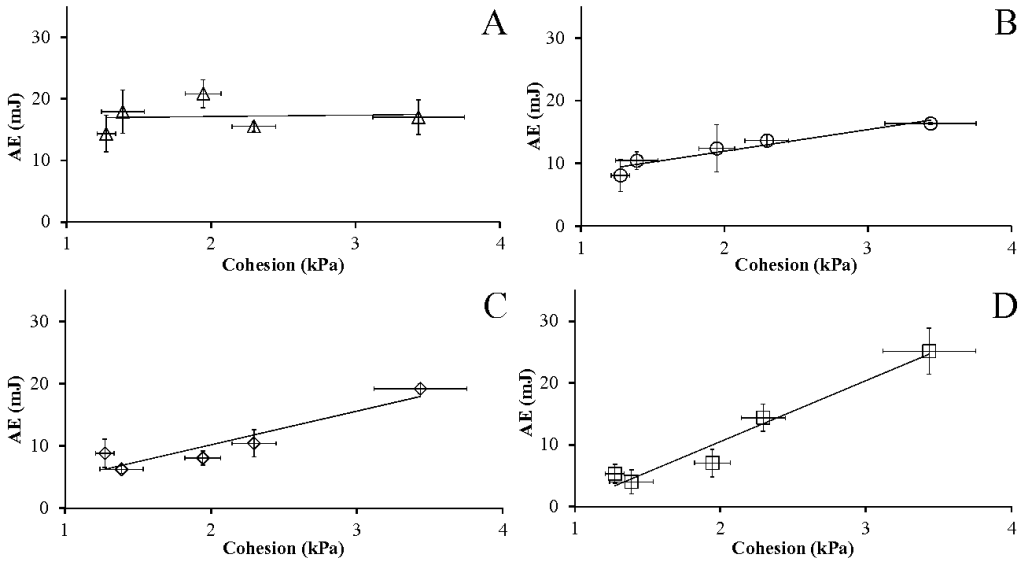

Figure 6.8 – Aeration energy (AE) of interactive mixture as a function of cohesion of guest particles. Four graph represent different guest to host ratio, (A) 5% (w/w) / 95% (w/w); (B)

10% (w/w) / 90% (w/w); (C) 15% (w/w) / 85% (w/w) and (D) 20% (w/w) / 80% (w/w). Data presented as Mean ±SD (n = 3).

6.6.5.4 Compressibility

A compressibility test offers a further indication of the ability of the powders to pack efficiently [33]. In powders with poor flowability, relatively large voids are formed due to the high inter-particle interaction forces, whereas free-flowing powders exhibit low inter-particle cohesion and therefore pack more efficiently. Thus, it is expected that poorly flowing powders will be more compressible than free-flowing powders [33, 36, 37, 44]. Pure paracetamol exhibited high compressibility (48.6 ±2.0 %) while interactive mixtures showed a relatively lower compressibility (Figure 6.9). The compressibility of the interactive mixtures was similar at lower guest particle fraction (5% (w/w)), while at higher guest particle fractions (10%, 15% and 20% (w/w)) a sharp decline in compressibility was noted as a function of guest particle cohesion. The correlation between compressibility and cohesion of guest particles improved with increasing guest particle fractions up to 15% (w/w), but decreased at higher guest particle fraction (Figure 6.9). This may be attributed to an excess of guest particles in the mixtures, which was also evident by the higher compressibility of interactive mixture with 20% (w/w) guest particles fraction compared with the mixtures with 15% (w/w) guest particle fraction.

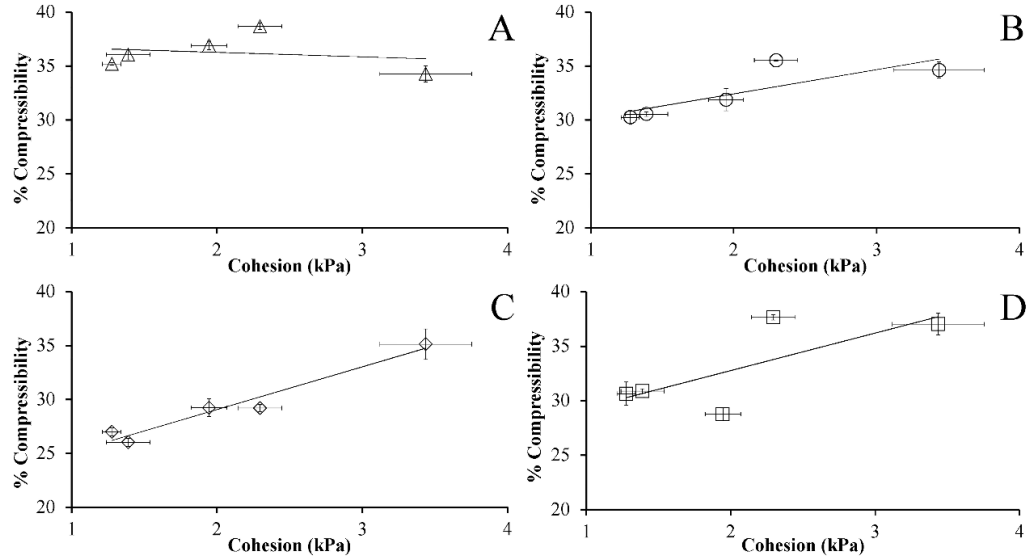

Figure 6.9 – % Compressibility of interactive mixture as a function of cohesion of guest particles. Four graph represent different guest to host ratio, (A) 5% (w/w) / 95% (w/w); (B) 10% (w/w) / 90% (w/w); (C) 15% (w/w) / 85% (w/w) and (D) 20% (w/w) / 80% (w/w). Data presented as Mean ±SD (n = 3).

6.7 Discussion

Improving the flow of poor flowing powders is a common practice in pharmaceutical industry [3]. The most common approach is to blend the poorly flowing powder with glidants (guest particles) such as colloidal silicon dioxide and its derivatives [6, 52]. A number of models have been proposed to explain how particle-particles contacts influence the magnitude of inter-particle forces and hence powder flow [53-55]. Recently, Chen et al. proposed a multi-asperity particle contact model accounting for the impact of guest particles on the magnitude of inter-particle force between host particles [12].

According to this model, the magnitude of the host particle cohesion depends on the guest particles size and their surface area coverage. It has also been shown experimentally that

smaller guest particles and greater guest particle coverage are associated with decreasing inter-particle forces between host particles and hence better flow improvements [12, 29, 56, 57]. In this context, guest particle sizes of 10-20 nm and surface coverages of more than 40% were proposed to facilitate optimal reduction in inter-particle forces and hence ensure optimal flow improvements [12, 24, 29, 31].

Another study suggested that hydrophobic colloidal silica particles exhibit better flow additive action than hydrophilic colloidal silica particles. This was attributed to the ability of hydrophobic silica particles to cause greater reduction in inter-particle forces (as measured by atomic force microscopy) between host particles [11, 24]. This suggests that the nature of guest particles can have an effect on the flow performance interactive mixtures. Clearly surface chemistry of guest particles is important apart from size and surface coverage.

It should be highlighted that when host particles are sufficiently coated with guest particles, the guest-guest interactions represent the dominating particle interactions [29, 30]. Thus, it would be reasonable to assume that the inter-particle forces acting between guest particles would also contribute significantly to the flow performance in such interactive powder mixtures. Since, surface properties such as morphology, surface energy and chemical nature etc. govern the magnitude of inter-particle forces [25, 33, 58], the flow performance of interactive mixtures may change as a function of morphology, surface energy and chemical nature of guest particles.

Cohesion is a bulk powder property, which represents the net inter-particles forces [10, 25, 33], and it would be reasonable to assume that the cohesion of guest particles would also affect the flow performance of interactive mixtures.

The cohesion of studied spray-dried formulations was quantified using a shear cell. The measured cohesion of the guest particles reduced with higher feed L-leucine concentration,

consistent with previous research [25]. The most cohesive guest particles i.e., PVP-Leu (0%), blended the least homogeneously and coherently with paracetamol particles, as visualized by the presence of agglomerates of the small particles. This is consistent with previous studies indicating that cohesive particles are more difficult to de-agglomerate via low shear mixing and thus disperse less homogeneously over large particles [12, 29, 57]. In contrast, the guest particles containing L-leucine de-agglomerated more efficiently and dispersed more homogeneously on the surface of paracetamol particles, such that reduction in cohesion facilitates de-agglomeration and formation of homogeneous interactive mixtures. This provides a substantiation of more speculative observations from our previous research [28].

Our results indicate that the cohesion of guest particles had negligible impact on the flow performance indicators of interactive mixtures at lower guest particle fraction (i.e., 5% (w/w) to host particle fraction). This may be attributed to the lower coverage of paracetamol particles (at such low guest particle fraction), which allowed host particle interactions to dominate and govern the flow performance [29, 30].

At increasing guest particle fractions, the surface coverages increased (as supported by XPS), and the flow performance of interactive mixtures improved as a function of reducing guest particle cohesion. There was an indication that guest particles with lower cohesion resulted in interactive mixtures with better absolute flow performance than high cohesion guest particles. Most flow descriptors showed a significant relationship between the cohesion of guest particles and the flow performance of interactive mixtures. At higher guest particle fractions, and estimated surface coverages, the relationship between the cohesion of guest particle and the flow improvement was more marked. This is consistent with previous studies suggesting that the extent of surface coverage of host particles (by guest particles) has an impact on the flow behaviour of interactive mixtures [29, 30].

The mechanism of action of flow additives such as small guest particles is not yet fully understood. However, three potential theories have been proposed to explain this. The first theory suggests that the adhesion of guest particles to host particles allow them to roll over each other referred to as "ball bearing action" leading to improved flow [31]. A second theory suggests that the adhesion of small guest particles to host particles increase the inter-particle separation (also referred to as "spacer effect"), which reduces inter-particle forces and improves their flow [31]. A more recent theory suggests that the small guest particles acts as "nano-surface roughness" and reduce the inter-particle forces between host particles leading to improved flow [24, 57, 59]. This theory also suggests that the reduction in the inter-particles force between host particles is inversely proportional to guest particle size (as described earlier) and hence smaller guest particles are more effective at improving flow than larger guest particles [12, 24]. It should be highlighted that silicon dioxide (a benchmark flow additive) effectively improves the flow of host particles at low fractions (1-2% (w/w)) [12, 19, 24]. However, in our study a notable flow improvement was achieved at higher guest particle fractions (10-20% w/w). Thus, the lesser flow additive activity of guest particles in our study (particularly at low guest particle fractions) may be attributed to their larger size relative to silicon dioxide (which is typically nano-sized [31]) compared with micron-sized particles as used in current study. Additionally, larger guest particles possess lower surface area compared to smaller particles, thus are required in greater fractions for sufficient host surface coverage typically required to cause a notable flow improvement [12, 24].

A previous study has shown that guest particles greater than 0.5 µm exhibit negligible effect on the flow performance of host particles [24]. However, our study suggested that much larger guest particles (1-10 µm) that have low cohesion due to lubricated surfaces could substantially improve the flow of host particles. Further studies are recommended to investigate

the effect of cohesion and surface compositions of guest particles on the flow of host particles with varying properties such as particle size, shape etc.to put further light on this relationship.

Overall, these findings support our hypothesis that the cohesion of guest particles governs the flow performance of interactive mixtures. This indicates that the guest particles properties that dictate their cohesion such as surface morphology and surface energy etc. can have a marked impact on the flow performance of interactive mixtures. Since these particle properties are difficult to control at such small particle size levels, it difficult to investigate their impact (individually or otherwise) on the flow performance of interactive mixtures. However, cohesion -which can be determined relatively easily- takes into account the impact of these surface properties on net inter-particle forces. Therefore, we propose that considering the effect of cohesion of guest particles may help us effectively estimate inter-particle forces and thus predict the flow performance of resultant interactive mixtures.

For low dose powder formulations, small API particles (typically 1-10 μm) are often mixed with large particles to achieve homogeneous mixtures and where good content uniformity is achieved via interactive mixing [60-63]. It has been shown that the addition of small cohesive APIs generally decreases the flow performance of the resulting blends [64]. Our study suggests that the flow performance of such blends/mixtures can be controlled by understanding and optimizing the cohesion of guest particles via particle engineering.

6.8 Conclusion

In this study, we have demonstrated relationships between the cohesion of composite binder guest particles and the flow performance of resulting interactive mixtures. We have shown that low-cohesion guest particles can exhibit better flow additive action than high-cohesion guest particles, and deeper understanding of this relationship may help in adopting a more informed and targeted approach to design guest particles for producing efficient interactive mixtures.

This knowledge is proposed to be valuable in design of industrial powder formulations, which involve interactive mixing such as tablets and for dispersible powders in dry powder inhalers.

6.9 Acknowledgements

Sharad Mangal is thankful to Monash Institute of Graduate Research (MIGR) for providing Monash Graduate Scholarship (MGS) and Monash International Postgraduate Research Scholarship (MIPRS).

6.10 References

[1] Peleg M. Flowability of food powders and methods for its evaluation — A review. J Food Process Eng 1977; 1(4): 303-328.

[2] Guerin E, Tchoreloff P, Leclerc B, Tanguy D, Deleuil M, Couarraze G. Rheological characterization of pharmaceutical powders using tap testing, shear cell and mercury porosimeter. Int J Pharm 1999; 189(1): 91-103.

[3] Staniforth J. Powder flow. In: Aulton ME, ed., Pharmaceutics: The Science of Dosage Form Design: Churchill Livingstone, 2002; pp. 197–210.

[4] Teunou E, Fitzpatrick JJ, Synnott EC. Characterisation of food powder flowability. J Food Eng 1999; 39(1): 31-37.

[5] Meyer K, Zimmermann I. Effect of glidants in binary powder mixtures. Powder Technol 2004; 139(1): 40-54.

[6] Jonat S, Albers P, Gray A, Schmidt PC. Investigation of the glidant properties of compacted colloidal silicon dioxide by angle of repose and X-ray photoelectron spectroscopy. Eur J Pharm Biopharm 2006; 63(3): 356-359.

[7] Zimmerman I, Eber M, Meyer K. Nanomaterials as flow regulators in dry powders. Z Phys Chem 2004; 218: 51-102.

[8] Qu L, Zhou Q, Gengenbach T, Denman JA, Stewart PJ, Hapgood KP, Gamlen M, Morton DAV. Investigation of the potential for direct compaction of a fine ibuprofen powder dry-coated with magnesium stearate. Drug Dev Ind Pharm 2014: 1-13.

[9] Zhou Q, Qu L, Gengenbach T, Larson I, Stewart P, Morton DV. Effect of surface coating with magnesium stearate via mechanical dry powder coating approach on the aerosol performance of micronized drug powders from dry powder inhalers. AAPS PharmSciTech 2013; 14(1): 38-44.

[10] Zhou QT, Qu L, Larson I, Stewart PJ, Morton DAV. Improving aerosolization of drug powders by reducing powder intrinsic cohesion via a mechanical dry coating approach. Int J Pharm 2010; 394(1–2): 50-59.

[11] Jonat S, Hasenzahl S, Gray A, Schmidt PC. Mechanism of glidants: Investigation of the effect of different colloidal silicon dioxide types on powder flow by atomic force and scanning electron microscopy. J Pharm Sci 2004; 93(10): 2635-2644.

[12] Chen Y, Yang J, Dave RN, Pfeffer R. Fluidization of coated group C powders. AIChE J 2008; 54(1): 104-121.

[13] Hersey JA. Ordered mixing: A new concept in powder mixing practice. Powder Technol 1975; 11(1): 41-44.

[14] Begat P, Morton DAV, Staniforth J, Price R. The cohesive-adhesive balances in dry powder inhaler formulations II: influence on fine particle delivery characteristics. Pharm Res 2004; 21(10): 1826-1833.

[15] Begat P, Morton DV, Staniforth J, Price R. The cohesive-adhesive balances in dry powder inhaler formulations I: direct quantification by atomic force microscopy. Pharm Res 2004; 21(9): 1591-1597.

[16] Mangal S, Meiser F, Lakio S, Morton D, Larson I. The role of physico-chemical and bulk characteristics of co-spray dried l-leucine and polyvinylpyrrolidone on glidant and binder properties in interactive mixtures. Int J Pharm 2015; 479(2): 338-348.

[17] Galet L, Ouabbas Y, Chamayou A, Grosseau P, Baron M, Thomas G. Surface analysis of silica gel particles after mechanical dry coating with magnesium stearate. Kona Powder Part J 2010; 28: 209-218.

[18] Mullarney MP, Beach LE, Davé RN, Langdon BA, Polizzi M, Blackwood DO. Applying dry powder coatings to pharmaceutical powders using a Comil for improving powder flow and bulk density. Powder Technol 2011; 212(3): 397-402.
[19] Chattoraj S, Shi L, Sun CC. Profoundly improving flow properties of a cohesive cellulose powder by surface coating with nano-silica through comilling. J Pharm Sci 2011; 100(11): 4943-4952.
[20] Ghoroi C, Han X, To D, Jallo L, Gurumurthy L, Davé RN. Dispersion of fine and ultrafine powders through surface modification and rapid expansion. Chem Eng Sci 2013; 85(0): 11-24.
[21] Yang J, Sliva A, Banerjee A, Dave RN, Pfeffer R. Dry particle coating for improving the flowability of cohesive powders. Powder Technol 2005; 158(1–3): 21-33.
[22] Mangal S, Meiser F, Tan G, Gengenbach T, Denman J, Rowles MR, Larson I, Morton DAV. Relationship between surface concentration of l-leucine and bulk powder properties in spray dried formulations. Eur J Pharm Biopharm 2015; 94: 160-169.
[23] Vehring R. Pharmaceutical particle engineering via spray drying. Pharm Res 2008; 25(5): 999-1022.
[24] Mangal S, Meiser F, Tan G, Gengenbach T, Larson I, Morton DAV. Improving the functional performance of composite excipients through particle engineering and optimized interactive mixing. Eur J Pharm Biopharm 2015; Submitted.
[25] Chen Y, Quintanilla MA, Yang J, Valverde JM, Dave RN. Pull-off force of coated fine powders under small consolidation. Phys Rev E Stat Nonlin Soft Matter Phys 2009; 79(4 Pt 1): 1-14.
[26] Han X, Jallo L, To D, Ghoroi C, Dave R. Passivation of high-surface-energy sites of milled ibuprofen crystals via dry coating for reduced cohesion and improved flowability. J Pharm Sci 2013; 102(7): 2282-96.
[27] Jonat S, Hasenzahl S, Drechsler M, Albers P, Wagner KG, Schmidt PC. Investigation of compacted hydrophilic and hydrophobic colloidal silicon dioxides as glidants for pharmaceutical excipients. Powder Technol 2004; 141(1–2): 31-43.
[28] Han X, Ghoroi C, To D, Chen Y, Dave R. Simultaneous micronization and surface modification for improvement of flow and dissolution of drug particles. Int J Pharm 2011; 415(1-2): 185-95.
[29] Zhou Q, Denman JA, Gengenbach T, Das S, Qu L, Zhang H, Larson I, Stewart PJ, Morton DAV. Characterization of the surface properties of a model pharmaceutical fine powder modified with a pharmaceutical lubricant to improve flow via a mechanical dry coating approach. J Pharm Sci 2011; 100(8): 3421-3430.
[30] Beamson G, Briggs D. High resolution XPS of organic polymers. In, 1st ed. Chichester: John Wiley & Sons 1993; pp.
[31] Gaiani C, Morand M, Sanchez C, Tehrany EA, Jacquot M, Schuck P, Jeantet R, Scher J. How surface composition of high milk proteins powders is influenced by spray-drying temperature. Colloid Surface B 2010; 75(1): 377-384.
[32] Freeman R. Predicting flowability and characterizing powders. Pharm Dev Technol Eur 2004; 16(1): 41.
[33] Schulze D. Powders and bulk solids: Behavior, characterization, storage and flow In. Springer: Berlin–Heidelberg–NewYork–Tokyo, 2008.
[34] Freeman R. Measuring the flow properties of consolidated, conditioned and aerated powders — A comparative study using a powder rheometer and a rotational shear cell. Powder Technol 2007; 174(1–2): 25-33.
[35] Freeman T, Price R. Dynamic powder characterization for DPI formulation. Drug Del Technol 2009; 9(5): 50–55.

[36] Fu X, Huck D, Makein L, Armstrong B, Willen U, Freeman T. Effect of particle shape and size on flow properties of lactose powders. Particuology 2012; 10(2): 203-208.
[37] Turki D, Fatah N. Behavior and fluidization of the cohesive powders: Agglomerates sizes approach. Braz J Chem Eng 2008; 25(4): 697-711.
[38] Sou T, Kaminskas LM, Nguyen T-H, Carlberg R, McIntosh MP, Morton DAV. The effect of amino acid excipients on morphology and solid-state properties of multi-component spray-dried formulations for pulmonary delivery of biomacromolecules. Eur J Pharm Biopharm 2013; 83(2): 234-243.
[39] Chew NYK, Tang P, Chan HK, Raper JA. How much particle surface corrugation is sufficient to improve aerosol performance of powders? Pharm Res 2005; 22(1): 148-152.
[40] Castellanos A. The relationship between attractive interparticle forces and bulk behaviour in dry and uncharged fine powders. Adv Phys 2005; 54(4): 263-376.
[41] Abdullah EC, Geldart D. The use of bulk density measurements as flowability indicators. Powder Technol 1999; 102(2): 151-165.
[42] Zhou Q, Qu L, Gengenbach T, Denman JA, Larson I, Stewart PJ, Morton DAV. Investigation of the extent of surface coating via mechanofusion with varying additive levels and the influences on bulk powder flow properties. Int J Pharm 2011; 413(1–2): 36-43.
[43] Zhou QT, Armstrong B, Larson I, Stewart PJ, Morton DAV. Understanding the influence of powder flowability, fluidization and de-agglomeration characteristics on the aerosolization of pharmaceutical model powders. Eur J Pharm Sci 2010; 40(5): 412-421.
[44] Turki D, Fatah N. Description of consolidation forces on nanometric powders. Brazilian Journal of Chemical Engineering 2010; 27(4): 555-562.
[45] Chen Y, Jallo L, Quintanilla MAS, Dave R. Characterization of particle and bulk level cohesion reduction of surface modified fine aluminum powders. Colloid Surface A 2010; 361(1–3): 66-80.
[46] Thiel WJ, Nguyen LT, Sberna FJ. Content uniformity of microdose tablets (dosage 1 microgram--10 mg) produced by fluid bed granulation of interactive mixtures. J Pharm Pharmacol 1986; 38(5): 335-43.
[47] Swaminathan V, Kildsig DO. Polydisperse powder mixtures: effect of particle size and shape on mixture stability. Drug Dev Ind Pharm 2002; 28(1): 41-8.
[48] Zhao FY, Stewart PJ. Modeling the deagglomeration of micronized benzodiazepines from powder mixtures added to dissolution media. J Pharm Sci 2004; 93(6): 1618-27.
[49] Adi H, Larson I, Stewart PJ. Adhesion and redistribution of salmeterol xinafoate particles in sugar-based mixtures for inhalation. Int J Pharm 2007; 337(1-2): 229-38.
[50] More PK, Khomane KS, Bansal AK. Flow and compaction behaviour of ultrafine coated ibuprofen. Int J Pharm 2013; 441(1-2): 527-34.

6.11 Appendix

6.11.1 **Appendix 6.1 –** % surface fraction of paracetamol (based on elemental composition) at corresponding guest particle fractions. See text for details.

Formulations	**Surface fraction of paracetamol (as calculated by elemental composition) at corresponding guest particle fractions**			
	5%	**10%**	**15%**	**20%**
PVP-Leu (0%)	68.5 ±5.0 %	55.3 ±2.3 %	43.2 ±4.2 %	35.7 ±1.5 %
PVP-Leu (2.5%)	48.8 ±6.6 %	31.4 ±3.2 %	36.6 ±0.4 %	22.0 ±1.2 %
PVP-Leu (5%)	35.7 ±6.6 %	18.0 ±0.7 %	17.3 ±6.3 %	8.7 ±1.3 %
PVP-Leu (10%)	56.7 ±3.7 %	38.9 ±0.4 %	25.0 ±5.0 %	21.6 ±4.8 %
PVP-Leu (15%)	47.9 ±3.2	39.2 ±2.8	28.2 ±4.8 %	19.6 ±2.1 %

6.11.2 **Appendix 6.2 –** Aeration energy profiles of studied powder formulations as a function of air velocity. Four graph represent different guest to host ratio, (A) 5% (w/w) / 95% (w/w); (B) 10% (w/w) / 90% (w/w); (C) 15% (w/w) / 85% (w/w) and (D) 20% (w/w) / 80% (w/w). Data presented as Mean ±SD (n = 3).

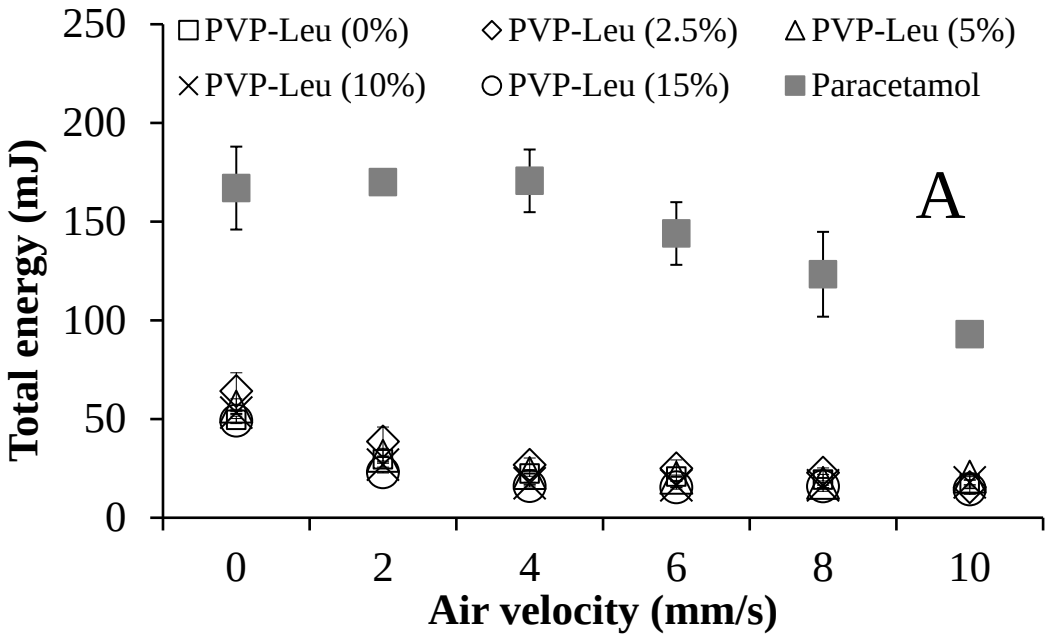

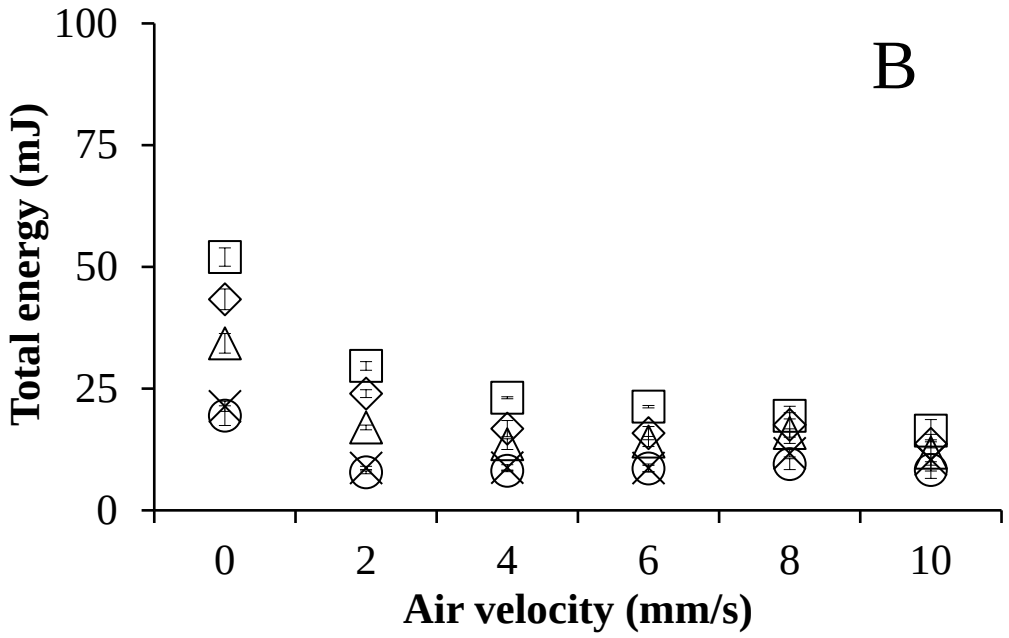

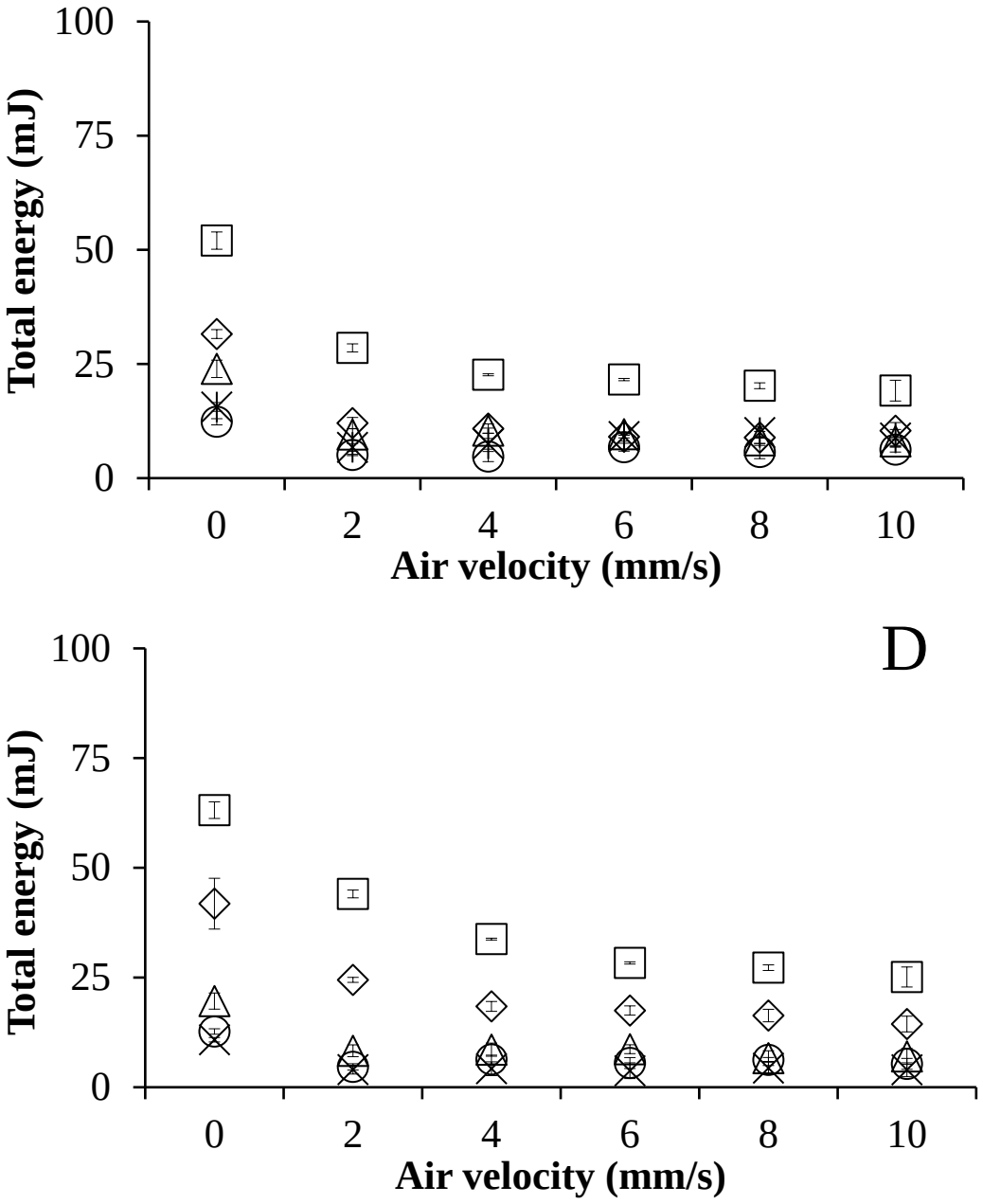
C
100
75
50
25
0
Total energy (mJ)
0
2
4
6
8
10
Air velocity (mm/s)
D
100
75
50
25
0
Total energy (mJ)
0
2
4
6
8
10
Air velocity (mm/s)

6.11.3 Appendix 6.3 – Shear cell data of spray-dried formulations demonstrating shear stress as a function of applied normal stress.

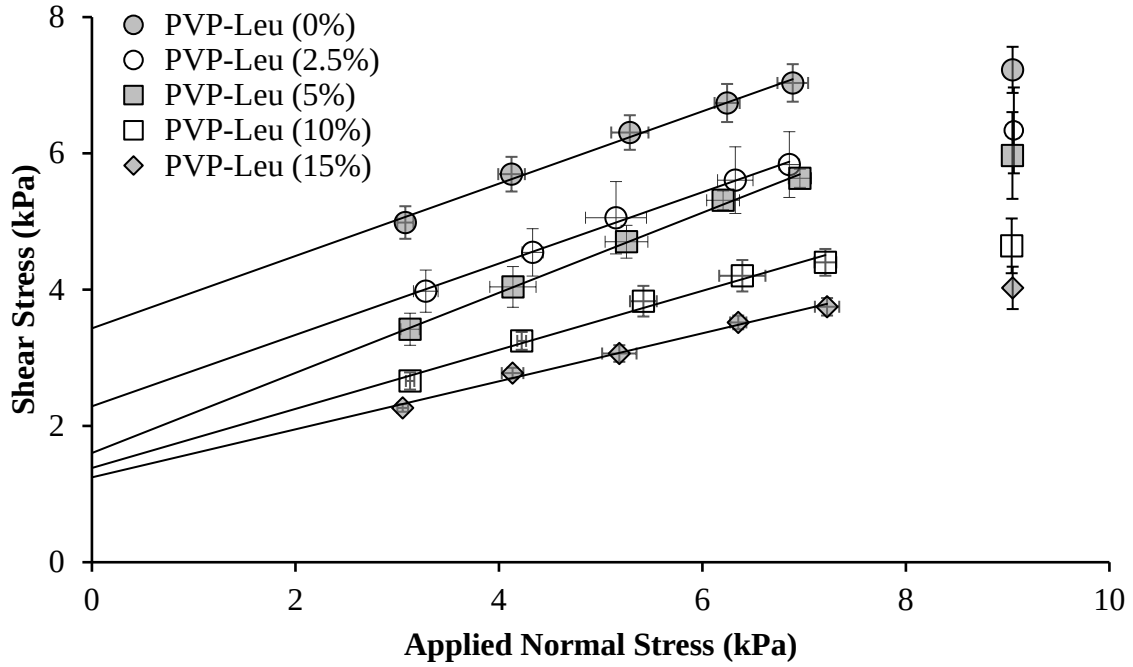

Chapter 7
To investigate the effect of mechanical properties of surface engineered small particles on their binder activity

Sharad Mangal[1], Satu Lakio[2], Thomas Gengenbach[3], David AV Morton[1]*, Ian Larson[1]*

[1] Drug Delivery, Disposition and Dynamics, Monash Institute of Pharmaceutical Science, 381 Royal Parade, Parkville, VIC 3052, Australia
[2]AstraZeneca R&D, Pepparedsleden 1, 43150 Mölndal, Sweden
[3] CSIRO Materials Science and Engineering, Bayview Avenue, Clayton, VIC-3168, Australia
* Corresponding Authors

***Submitted as:**
Mangal S, Lakio S, Gengenbach T, Morton DAV, Larson I. Effect of the deformability of guest particles on the tensile strength of tablets from interactive mixtures. Int J Pharm. Accepted for publication.

7 Declaration for Thesis Chapter 7

Declaration by candidate

In the case of Chapter 7, the nature and extent of my contribution to the work was the following:

Nature of contribution	**Extent of contribution (%)**
Study initiation, formation of hypothesis, laboratory work, data collection, analysis and interpretation and writing the manuscript	65%

The following co-authors contributed to the work. If co-authors are students at Monash University, the extent of their contribution in percentage terms must be stated:

Name	**Nature of contribution**	**Extent of contribution (%) for student co-authors only**
Felix Meiser	Supervision and manuscript revision	5%
Satu Lakio	Supervision and manuscript revision	5%
Thomas Gengenbach	XPS characterization and proofreading	5%
David AV Morton	Supervision and manuscript revision	10%
Ian Larson	Supervision and manuscript revision	10%

The undersigned hereby certify that the above declaration correctly reflects the nature and extent of the candidate's and co-authors' contributions to this work*.

Candidate's Signature	[redacted]	**Date 23.11.2015**
Main Supervisor's Signature	[redacted]	**Date 24/11/15**

*Note: Where the responsible author is not the candidate's main supervisor, the main supervisor should consult with the responsible author to agree on the respective contributions of the authors.

7.1 Commentary

In chapter 1 and 3, it was demonstrated that the surface cohesion properties of small binder particles affect their binder activity. In this study, we address specific objective 5 "to investigate the effect of mechanical properties of low cohesion small particles on their binder activity". Given that mechanical properties such as plastic/elastic behaviour of binder particles can also affect their ability to facilitate inter-particle bonding between other formulation components, the mechanical properties of small binder particles may also affect their binder activity. Thus, we hypothesized that the small binder particles with higher deformability will express greater binder activity, when compared to the small binder particles with lower deformability.

7.2 Abstract

In this study, we investigated the influence of deformability of specifically-engineered guest particles on the tensile strength of tablets of interactive mixtures. The binder polyvinylpyrrolidone (PVP) of different molecular weights were spray dried with L-leucine to create guest particle formulations. The guest particle formulations were characterized by their particle size, surface L-leucine concentration and glass transition temperature (Tg). These spray-dried particles were then blended with paracetamol to form interactive mixtures, which were compacted into tablets and tablet tensile strength and elastic recovery were determined. The guest particles had particle diameters in the range of 1 – 10 μm, and surfaces that were L-leucine enriched. The Tg of guest particle formulations increased with increasing molecular weight of the PVP. All the guest particle formulations formed an observed homogeneous interactive mixture with paracetamol. The tensile strength of the tablets of interactive mixtures increased with decreasing Tg of the guest particles. In these interactive mixtures, higher tensile strength was also associated with lower tablet elastic recovery. The elastic recovery of the tablets showed a correlation with the elastic recovery of the tablets of guest particles. Thus, our results indicated that the deformability of guest particles dictates the tensile strength of the tablets of these interactive mixtures.

Keywords: Paracetamol, tabletting, binder, L-leucine, spray drying, polyvinylpyrrolidone, elasticity, interactive mixing, host particles

7.3 Introduction

In interactive mixtures, small guest particles (typically < 10 μm) adhere to the surfaces of larger host particles [1-4]. However, strongly cohesive nature impedes the de-agglomeration

of small particles and is thus a major impediment in the formation of homogeneous interactive mixtures [5]. Homogeneous interactive mixtures forms, when guest particles de-agglomerates efficiently and preferentially adheres to large particles upon mixing. It is generally accepted that preferential adhesion of small particles to large particle occur, when the forces of adhesion between guest particles and host particles are stronger than the forces of cohesion between guest particles. This concept is referred to as cohesive-adhesive balance [6, 7].

Surface properties strongly influence the forces of inter-particle interaction and hence cohesion [8, 9]. Previous studies have suggested surface manipulation by increasing surface asperity [10-12], reducing surface energy [13, 14] and coating with nanometric sized particles [15, 16] can efficiently reduce the cohesion of small particles. Co-spraying with L-leucine is a promising strategy to reduce the cohesion of small particles [17-19]. The exact mechanism by which L-leucine reduces cohesion is a subject of active debate [19-21]. However, L-leucine is proposed to enrich into the surface of the spray-dried particles owing to its interfacial activity [22] and low water solubility [23, 24] and form L-leucine film/shell [20, 21, 24]. The L-leucine film/shell increases the surface asperity of the particles reducing inter-particles forces acting between such L-leucine coated small particles [17, 19].

We demonstrated that co-spraying a model binder (PVP) with L-leucine forms L-leucine surface enriched small particles with low bulk cohesion [25]. These L-leucine coated small binder particles formed a homogeneous interactive mixture with a model API and improved its flow and compactability [25]. It was proposed that this could be a potential excipient technology platform to improve the flow and compaction behaviour of cohesive and poorly compactable APIs. In this study, we aim to gain insight into the mechanism which facilitates such surface engineered binder particles to express binder action.

L-leucine is a weakly bonding material with the ability to reduce inter-particle interactions [18, 26-28], thus it is unlikely that L-leucine would facilitate bonding between host particles and improve the compaction behaviour of the resultant interactive mixture. We proposed that deformability of binder at the core allows the L-leucine shell to stretch and eventually rupture, leading to creation of PVP surfaces, which participate in inter-particle bonding between host particles, improving the compactability of interactive mixtures. Thus, it would be reasonable to hypothesize that the deformability of the L-leucine coated guest particles would correlate with the compactability of interactive mixtures. In this study, we for the first time investigate the effect of deformability of L-leucine coated guest binder particles on the compactability of the resultant interactive mixtures.

In general, the plastic/elastic deformation that a material undergoes depends on its resistance to the deformation such as under compression; this represents its mechanical behaviour [29]. Materials with lower resistance, deform more creating larger areas for inter-particle bonding, and hence form tablets with higher tensile strength [30, 31]. The glass transition temperature (Tg) of amorphous material can determine their resistance to deformation under compression [29-31]. When the Tg of such materials is close to compression temperature, the resistance to deformation is relatively low, which results in greater deformation and formation of tablets with higher tensile strength [30-32]. We hypothesized that the Tg of the guest particles would also dictate their deformability, and hence the tensile strength of tablets of the resultant interactive mixture (Figure 7.1).

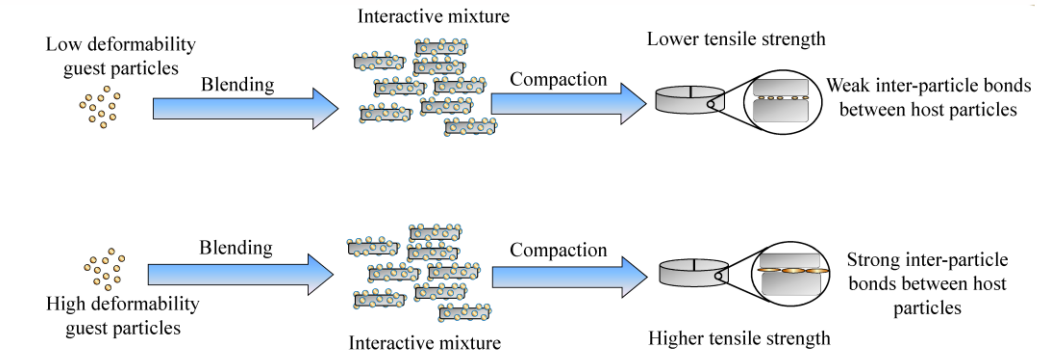

Figure 7.1 – Schematic showing effect of deformation of guest particles on inter-particle bonding between host particles and tensile strength.

In this study, PVP was selected as an amorphous material with a characteristic plastic deformation behaviour [33]. PVP with different molecular weights were selected to create guest particle formulations with varying Tg [34]. PVPs (of different molecular weight) were spray-dried with L-leucine to form L-leucine coated small guest particles. The guest particle formulations were characterised for their particle size, surface morphology, surface L-leucine concentrations, and Tg. Interactive mixtures were created by mixing the guest particle formulations with paracetamol, which were then compacted into the tablets. The tensile strength and elastic recovery of tablets of pure guest particle and interactive mixtures were determined.

7.4 Materials and methods

7.1.1 Materials

Paracetamol and polyvinylpyrrolidone (PVP) with different average molecular weight grades (K-10, K-40 and K-90 average molecular weight ~ 10, ~ 30 and ~ 360 kDa, respectively, as per supplier's specifications) were procured from Sigma-Aldrich (St. Louis, MO, USA). L-leucine was purchased from Ajinomoto Co. Inc. (Tokyo, Japan). Magnesium stearate was procured from Mallinckrodt Pharmaceuticals (St. Louis, MO, USA).

7.1.2 Method of preparation

Aqueous solutions of PVP and L-leucine were spray-dried using the procedure previously described by Mangal et al. [21, 25]. Briefly, PVP (6% w/v) and L-leucine (10% (w/w) of PVP) were weighed accurately and dissolved in 500 mL of purified water with the aid of magnetic stirring. The resultant solution was then spray-dried using a Buchi B-190 spray dryer (Buchi Laboratory Equipment, Flawil, Switzerland) with a 0.5 mm two-fluid nozzle. The standard operating conditions employed during spray drying were: inlet temperature 125 ±5 °C; spray air flow rate 800 L/h and solution pump setting 10 mL/min. These conditions resulted in an outlet temperature of 70 ±2 °C. The aqueous solution of 6% (w/v) high molecular weight PVP (360 kDa) was very viscous, which resulted in fusion of particles at the spray nozzle exit. Therefore, the PVP was reduced to 4.5% w/v for this molecular weight, while the proportion of L-leucine was kept at the same proportion to other formulations i.e., 10% (w/w) respective of PVP. The PVP spray-dried formulations were denoted as PVP10-Leu, PVP40-Leu and PVP90-Leu. The yield of spray-dried excipients was between 40-60% w/w.

All the spray-dried formulations were equilibrated in a desiccator of saturated potassium carbonate solution (which resulted in % relative humidity of 42 ±2 %RH), until a constant mass was achieved, prior to use. This was done to ensure that the spray-dried formulation were equilibrated to ambient humidity conditions before experiments to minimize humidity related variations in this study.

7.1.3 Particle size and size distribution

Particle size measurements were performed using a Malvern Mastersizer 2000 (Malvern Instruments Ltd., Malvern, UK) dry cell. An optimised shear pressure of 2.0 bar was established and used to result in efficient dispersion of small particles during measurements at a feeder setting of 50% [25]. The in-built software provided values of D_{50} (volume median

diameter), D_{10} (10% volume below this diameter) and D_{90} (90% volume below this diameter). The particle size distribution was presented as span, which represents the width of the size distribution based on the D_{10}, D_{50} and D_{90} quantile.

$$Span = \frac{D90-D10}{D50} \qquad \text{(Eq. 7.1)}$$

7.1.4 Scanning electron microscopy

The morphology and blending behaviour of the spray-dried formulations were visualised by scanning electron microscopy (SEM) (Phenom™, FEI Company, Hillsboro, OR, USA). Double-sided adhesive tape was placed on aluminium stubs and a small amount of sample added, followed by gentle tapping to disperse the sample evenly. The stubs were then coated with a fine gold film using a sputter coater (Emitech K550X, Quorum Technologies, Kent, UK) at an electrical potential of 2.0 kV at 25 mA for 3 min. The coated stubs were then loaded into the SEM and images were captured.

7.1.5 X-ray photoelectron spectroscopy

X-ray photoelectron spectroscopy (XPS) analysis was performed using an AXIS Ultra DLD spectrometer (Kratos Analytical Inc., Manchester, UK) with a mono-chromated Al K_α source at a power of 180 W (15kV × 12mA), a hemispherical analyser operating in the fixed analyser transmission mode and the standard aperture (analysis area: 0.3 mm × 0.7 mm). The total pressure in the main vacuum chamber during analysis was typically 10^{-8} mbar. Survey spectra were acquired at a pass energy of 160 eV. To obtain more detailed information about chemical structure, high resolution spectra were recorded from individual peaks at 20 eV pass energy (yielding a typical peak width for polymers of 1.0 eV). Samples were filled into shallow wells of custom-built sample holders. One well of each sample was prepared and 2 different locations were analysed on each sample at a nominal photoelectron emission angle of 0º with respect to

the surface normal. Since the actual emission angle is ill-defined in the case of such micro-particles (ranging from 0º to 90º) the sampling depth may range from 0 nm to approximately 5 – 10 nm. Binding energies were referenced to the aliphatic hydrocarbon peak at 285.0 eV. Reference spectra of the pure PVP and L-leucine were recorded, normalised and then used as model components to calculate curve-fits for the spectra of the spray-dried formulations. Therefore the relative peak area of PVP and L-leucine for the co-sprayed PVP-Leu particles approximates to the relative surface atomic fractions (or mass fraction given the number of atoms are same) of L-leucine and PVP in the formulations.

7.1.6 Time-of-flight secondary ion mass spectrometry

Time-of-flight secondary ion mass spectrometry (ToF-SIMS) experiments were performed using a nanoToF instrument (Physical Electronics Inc., Chanhassen, MN, USA) equipped with a pulsed liquid metal $^{79+}$Au primary ion gun (LMIG), operating at 30 kV energy. Dual charge neutralisation was provided by an electron flood gun and 10 eV Ar+ ions. Experiments were performed under a vacuum of 5 x 10^{-6} Pa. "Bunched" Au1 instrumental settings were used to optimise mass resolution for spectra, while "unbunched" Au1 instrumental settings were used to optimise spatial resolution for the collection of images. ToF-SIMS data were collected from 4 areas per sample, using a raster of 50 x 50 µm and acquisition time of 4 min. Sample spectra and images were processed and integrated using WincadenceN software (Physical Electronics Inc., Chanhassen, MN, USA). Integrated peak values of the selected ions were normalized to the total secondary ion intensities. The resulting data were then compared qualitatively by preparing plots of average normalized counts (with 95 % confidence intervals) for each species of interest. The percentage normalized counts do not give a measure of absolute coverage, because the specific signals identified were percentages over the total ion signals of all species, but are considered useful for examination of relative changes.

7.1.7 Dynamic vapour sorption (DVS)

Moisture sorption characteristics of spray dried formulations was determined at a constant temperature of 25 ±0.1 °C using DVS Intrinsic (Surface Measurement Systems, UK). The DVS Intrinsic measures uptake of water vapour gravimetrically with a mass resolution of ±0.1 μg. All samples were exposed to a stepwise increase in relative humidity (RH %) (0%, 30%, 40%, 50% and 60%). At each stage, the equilibrium behaviour was defined when the mass variation versus time dm/dt was ≤0.005 mg/min.

7.1.8 Differential scanning calorimetry (DSC)

The Tg of spray-dried formulations was determined by thermal analysis (DSC 8500, PerkinElmer, Waltham, MA, USA). To determine the Tg, the humidity conditioned samples were directly weighed (5 – 10 mg) into aluminium pans. The pans were immediately crimped hermetically. The following program was used to run the experiments:

Hold for 3 min at 30 °C,

Heat from 30 to 120 °C at a rate of 20 °C/min,

Hold for 120 °C for 5 min,

Cool from 120 °C to −40 °C at a rate of 20 °C/min,

Heat from −40 °C to 120 °C at a rate of 20 °C/min.

The Tg was detected as a change in heat capacity (Cp) of the material. A thermal event was easily identified in step 5 and hence this step was used to calculate the Tg. The Tg was calculated by using the midpoint based on half Cp, which was determined by drawing tangents on the heat flow curve at temperatures above and below the Tg. All the measurements were performed in triplicate and against a blank reference aluminium pan.

7.1.9 Blending

Interactive mixtures were prepared by blending spray-dried guest particle formulations with paracetamol using a Turbula mixer T2F (Willy A. Bachofen, Muttenz, Switzerland). Briefly, a 10 g blend was prepared by mixing paracetamol with varying proportions of guest particle formulations in a 100 mL glass jar at 72 rpm for 5 min.

7.1.10 Tableting

The interactive mixtures weighing 105 ±5 mg were manually filled into the die and the tablets were manufactured using a computer-controlled tablet press (Gamlen Tableting Ltd., Nottingham, UK). Flat 6 mm punch was used and powders were compressed using forces of 86, 120 and 154 MPa. The die and punch were lubricated with magnesium stearate prior to each compression to reduce the friction between the die wall and tablet edges [35, 36]. The punch speed was 1 mm/s. The dimensions (diameter and thickness) of each tablet were measured after compression.

7.1.11 Tensile strength

The breaking force of the tablets was measured using a hardness tester (TBH-30, Erweka, Heusenstamm, Germany). The tensile strength of the tablets was calculated according to the following equation [37]:

$$\sigma = \frac{2F}{\pi DH} \qquad \text{(Eq. 7.2)}$$

where σ is tensile strength, F is the breaking force, D is the tablet diameter, and H is the tablet thickness.

7.1.12 Elasticity factor (%)

The extent of elastic deformation of the powders during compression can also be assessed by measuring tablet height during and after compression [38]. Force-displacement curves were recorded to determine the elasticity recovery of tablets. The elasticity recovery of the tablets was calculated by using below equation [39]:

$$\%\ \text{Elasticity factor (EF)} = \frac{(S_{max} - S_{od})}{(S_{max} - S_o)} * 100\% \qquad \text{(Eq. 7.3)}$$

where S_{max} is the maximum upper punch displacement, S_o is the displacement of the upper punch when force is first registered and S_{od} is the displacement of the upper punch in the decompression phase (Appendix 7.1).

7.1.13 Statistical analysis

The statistical analysis was performed on tensile strength of guest paarticle formulations via by one-way analysis of variance (ANOVA) with Tukey–Kramer multiple comparison post-hoc tests using Graphpad instat software (GraphPad Software, Inc, CA, USA). A p value of < 0.05 was considered as significant.

7.5 Results

7.5.1 Particle size and size distribution

Table 7.1 shows the particle sizes of the commercial PVPs, spray-dried guest particle formulations and paracetamol. The particles sizes of commercial PVP was very high (>10 µm as typically desirable for interactive mixing) and hence were believed not to form interactive mixtures, as such. Aqueous solutions of PVP of different molecular weight and L-leucine were spray dried to create small particles. The particle sizes of spray-dried particles were typically < 10 µm, which is considered suitable for the formation of interactive mixtures. In addition, spray dried formulations exhibited similar sizes with and a mono-modal particle size distribution (Appendix 7.2). Paracetamol was used as the host material, and the particles size of paracetamol was higher than the size of guest particle formulations Table 7.1. The particle size distribution of paracetamol was broad (Appendix 7.2).

Table 7.1 – Particle size of spray-dried guest particle formulations and Paracetamol. Data presented as Mean ±SD (n = 3).

Formulations	**Particle Size (µm)**			**Span**
	D_{10}	**D_{50}**	**D_{90}**	
PVP10	8.2 ±0.1	26.6 ±0.2	56.7 ±0.6	1.8 ±0.0
PVP40	19.6 ±0.1	68.6 ±0.6	179.6 ±1.5	2.3 ±0.0
PVP90	133.4 ±12.9	393.4 ±34.3	890.7 ±47.4	1.9 ±0.1
PVP10-Leu	1.4 ±0.0	2.8 ±0.0	5.5 ±0.1	1.5 ±0.1
PVP40-Leu	1.4 ±0.1	3.0 ±0.0	5.9 ±0.1	1.5 ±0.1
PVP90-Leu	1.1 ±0.0	2.6 ±0.1	5.7 ±0.1	1.8 ±0.0
Paracetamol	3.7 ±0.1	21.4 ±0.3	151.5 ±5.0	6.8 ±0.1

7.5.2 Surface morphology

The SEM images showed that the commercial PVP10 and PVP40 were near-spherical, whereas PVP90 appeared as flakes (Figure 2). The spray-dried composite guest particles appeared near spherical but rough and corrugated. This was proposed to be due to the previously reported tendency of L-leucine to enrich and crystalize on the surface of the drying droplets leading to formation of L-leucine enriched surface shells [20, 21, 24]. These surface shells interfered with the evaporation rate of water vapour, and on further drying result in pressure build up affecting shell stretching, integrity and collapse seen as particle morphology variations [24].

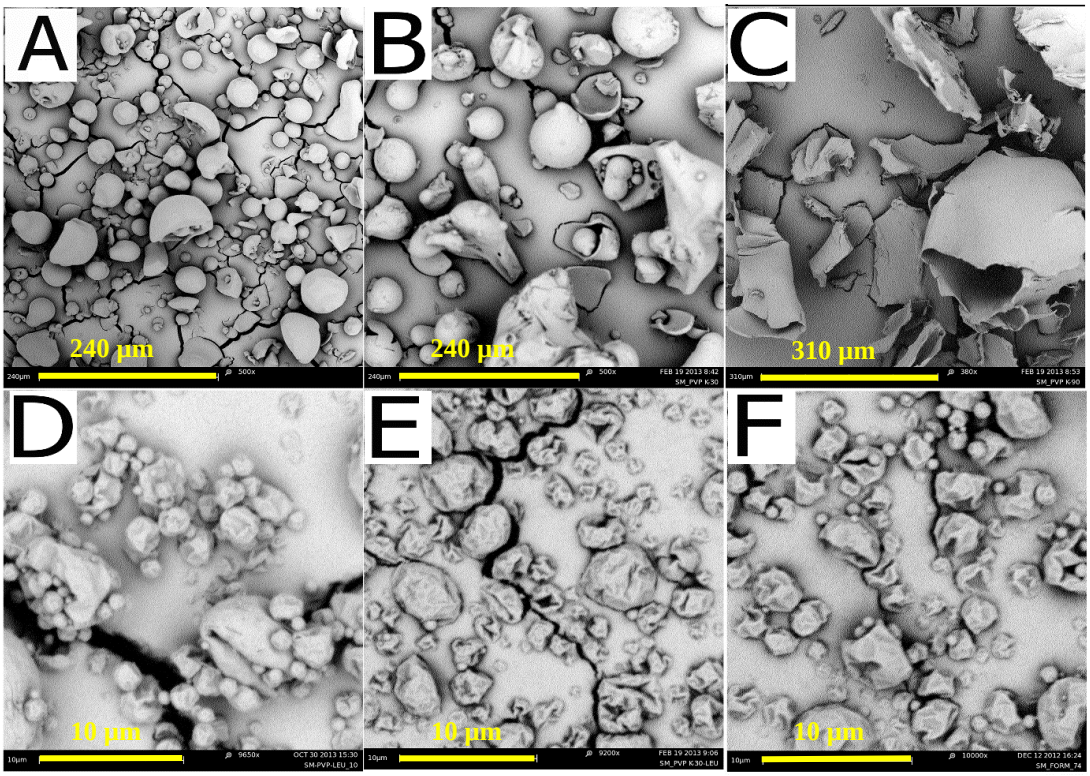

Figure 7.2 – Representative SEM images of A – PVP10; B – PVP40; C – PVP90; D – PVP10-Leu; E – PVP40-Leu and F – PVP90-Leu.

7.5.3 X-ray photoelectron spectroscopy (XPS)

Figure 3 shows the surface chemical composition of composite spray-dried guest particles from XPS study. Notably, approximately 80% of the surface composition was found to be L-leucine (Figure 3), indicating formation of surface L-leucine enriched particles with substantially lower PVP levels relative to composition ratio.

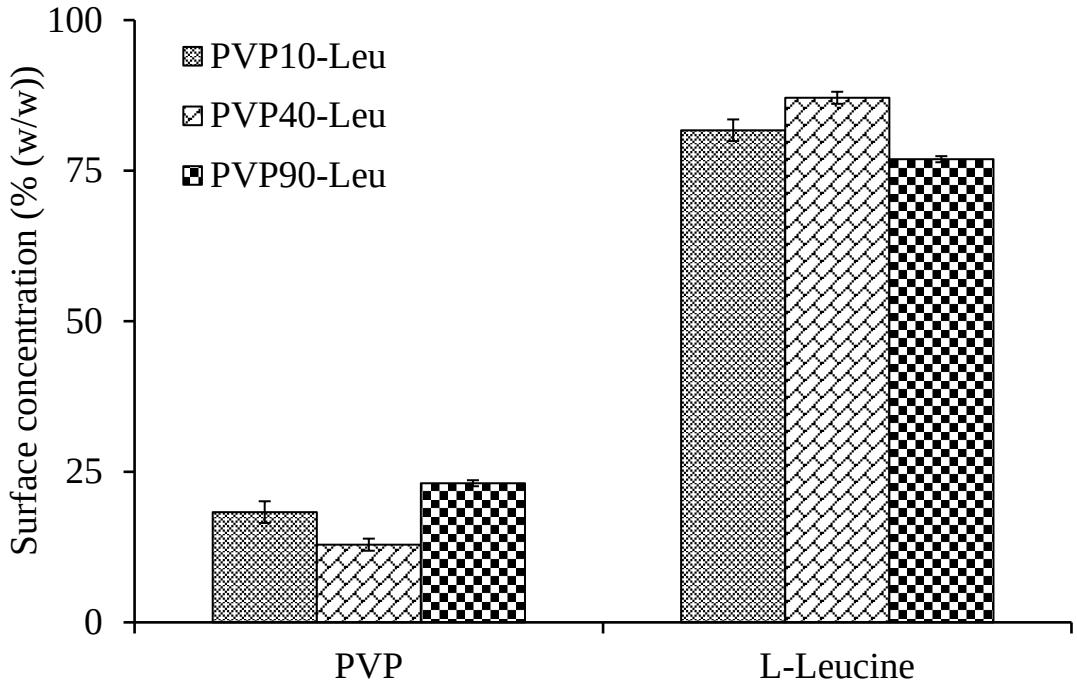

Figure 7.3 – Surface composition (% w/w) of PVP and L-leucine in spray-dried guest particle formulations as determined using XPS. Data presented as mean ±SD (n = 3).

7.5.4 Time-of-flight secondary ion mass spectrometry (ToF-SIMS)

For PVP sample, fragments $C_6H_{10}NO$ (m/z 112), $C_6H_{10}NO$ (m/z 124), and $C_8H_{12}NO$ (m/z 138) were used as distinguishing signals, while the fragment $C_6H_{14}NO_2$ (*m/z* 132) was used as the distinguishing signal for L-leucine [21]. Consistent with XPS study, the ToF-SIMS data also indicated that the surface of spray-dried guest particles was L-leucine enriched with reduced PVP (Table 7.2). The intensity of the surface L-leucine signal was similar in all composite

formulations indicating molecular weight did not interfere the mass transport of L-leucine on particle formation. This further supports a nearly complete surface coverage of PVP by the L-leucine, and indicates that the surface composition of all the guest particle formulations were similar. The tendency of L-leucine to enrich surfaces upon co-spraying is a well-known phenomenon. Some researchers believe that the low water solubility of L-leucine [23, 24] allows it to reach saturation early during droplet drying, that causes precipitation at the droplet interface [20, 24]. While others believe, that L-leucine first enriches the surface of the droplets due to its interfacial activity [19, 21, 22] and then crystalizes due to its low water solubility [19, 21]. However, the exact mechanism is not yet clear and debatable [19-21, 24, 40]. Detailed discussion on the droplet drying kinetics and factors affecting solute mass transfer in drying droplets can be found elsewhere [23, 24].

Table 7.2 – Normalized counts of PVP $C_6H_{10}NO$ (m/z 112), $C_6H_{10}NO$ (m/z 124), and $C_8H_{12}NO$ (m/z 138), and L-leucine ($C_6H_{14}NO_2$; m/z 132) signals over the total spectral peak of samples measured using ToF-SIMS at scan area of 50 µm × 50 µm.

Chemical Fragment	**PVP**			**L-leucine**
	$C_6H_{10}NO$	**$C_7H_{10}NO$**	**$C_8H_{12}NO$**	**$C_6H_{14}NO_2$**
PVP10	0.4 ± 0.0	0.3 ± 0.0	0.3 ± 0.0	0.0 ± 0.0
PVP30	0.3 ± 0.0	0.3 ± 0.0	0.4 ± 0.0	0.0 ± 0.0
PVP90	0.3 ± 0.0	0.3 ± 0.0	0.4 ± 0.0	0.0 ± 0.0
PVP10-Leu	0.0 ± 0.0	0.0 ± 0.0	0.0 ± 0.0	0.9 ± 0.0
PVP30-Leu	0.0 ± 0.0	0.0 ± 0.0	0.0 ±0.0	1.0 ±0.0
PVP90-Leu	0.0 ± 0.0	0.0 ± 0.0	0.0 ± 0.0	1.0 ± 0.0

7.5.5 Dynamic vapour sorption (DVS)

DVS data indicated that guest particle formulations took up substantial amount of moisture (Figure 7.4) indicating that surface L-leucine film does not interfere with moisture transport and hence the hygroscopicity of PVP. This may be attributed to the formation of a semi-permeable shell on the surface of PVP, which allowed the cross-transport of moisture.

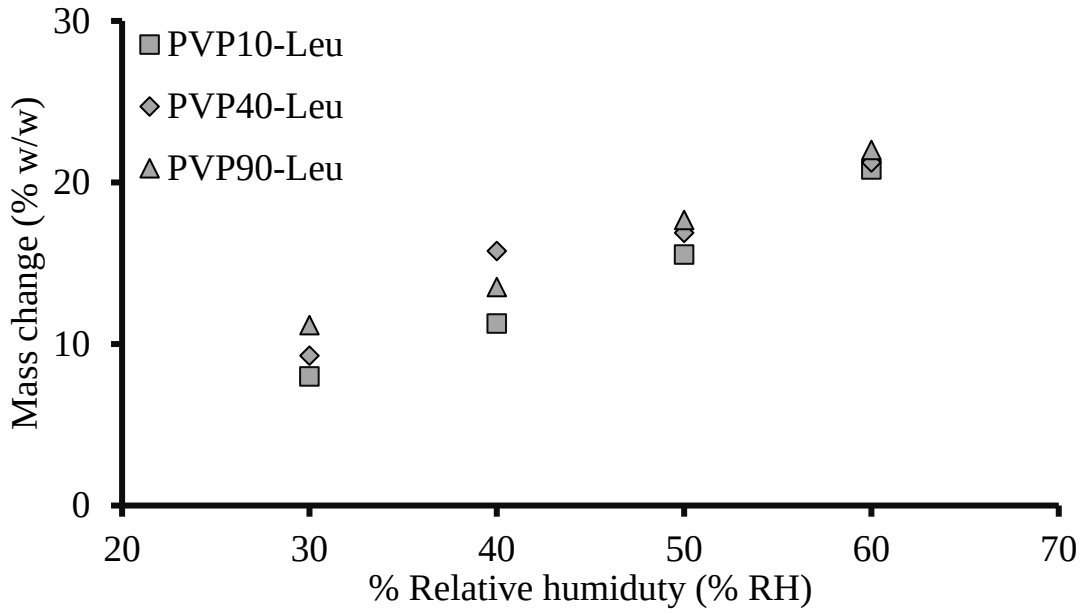

Figure 7.4 – Moisture sorption profiles of spray-dried formulations.

7.5.6 Differential scanning calorimetry (DSC)

The Tg of spray-dried guest particles as a function of PVP molecular weight is presented in Figure 7.5. Results indicated that the Tg of spray-dried particles increased as a function of the PVP molecular weight. This is consistent with previous studies suggesting that the low molecular weight polymers exhibit a lower Tg resulting from larger proportion of chain ends [34, 41, 42].

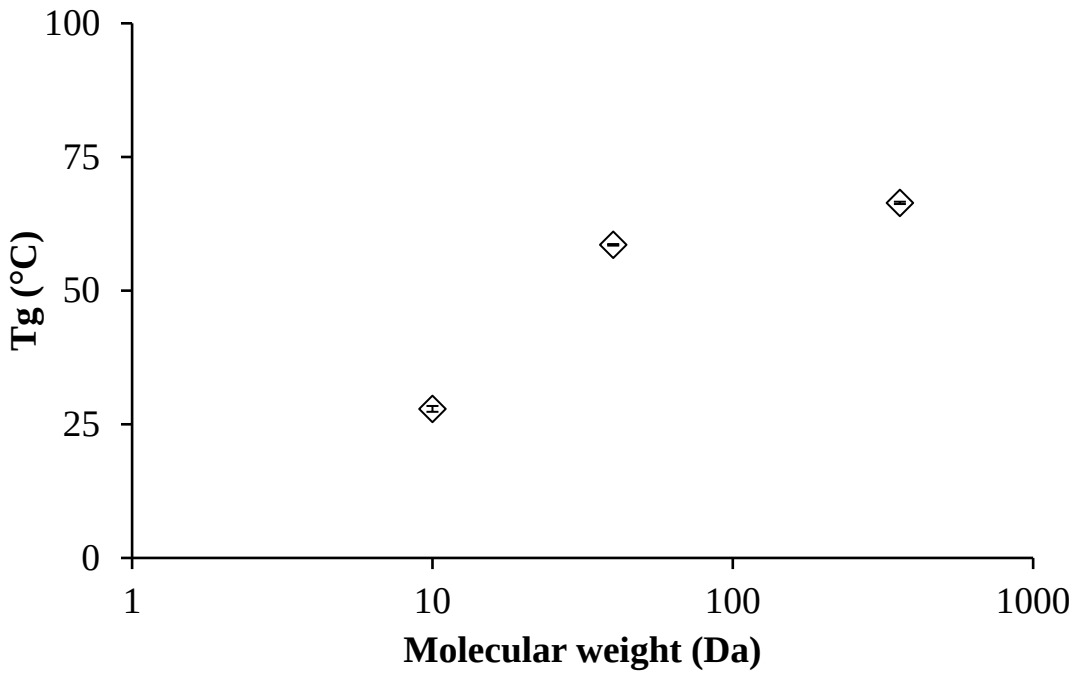

Figure 7.5 – Glass transition temperature (Tg) of spray-dried guest particle formulations as a function of log molecular weight of PVP (Log Da). Data presented as mean ±SD (n = 3).

7.5.7 Interactive mixing behaviour

The mixtures of spray-dried formulations and paracetamol were imaged to visually assess the quality of blend structure. Representative SEM images of all formulations show that the small guest particles adhered to paracetamol particles indicating the formation of interactive mixtures (Figure 7.6). The guest particles dispersed homogeneously over the surfaces of paracetamol particles (with no or few agglomerates).

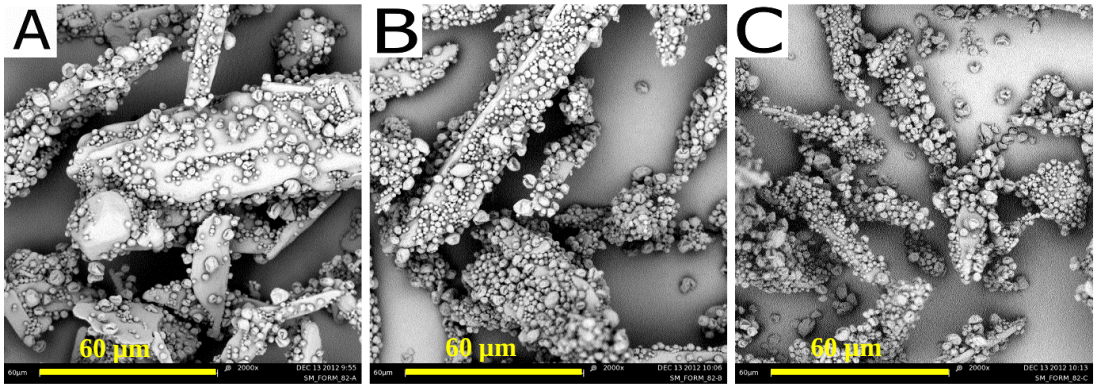

Figure 7.6 – Representative SEM images of interactive mixtures. A-PVP10-Leu/Para; B-PVP40-Leu/Para and C-PV90-Leu/Para.

7.5.8 Tensile strength

7.5.8.1 Guest particles

Guest particle formulations-only (i.e. without paracetamol) were compacted into tablets, and these tablets were tested for tensile strength. Figure 7.7 shows the tensile strength of these guest particle formulation tablets as a function of their Tg and indicated that the tensile strength did not significantly change as a function of the Tg ($p>0.05$) except in case of PVP10-Leu and PVP40-Leu compressed at 154 MPa ($p<0.05$). This implies that Tg has no influence on the inter-particle bonding behaviour of guest particles in absence of a host. The tensile strength of the tablet compressed at 86 MPa could not be measured due to frequent lamination of the tablets.

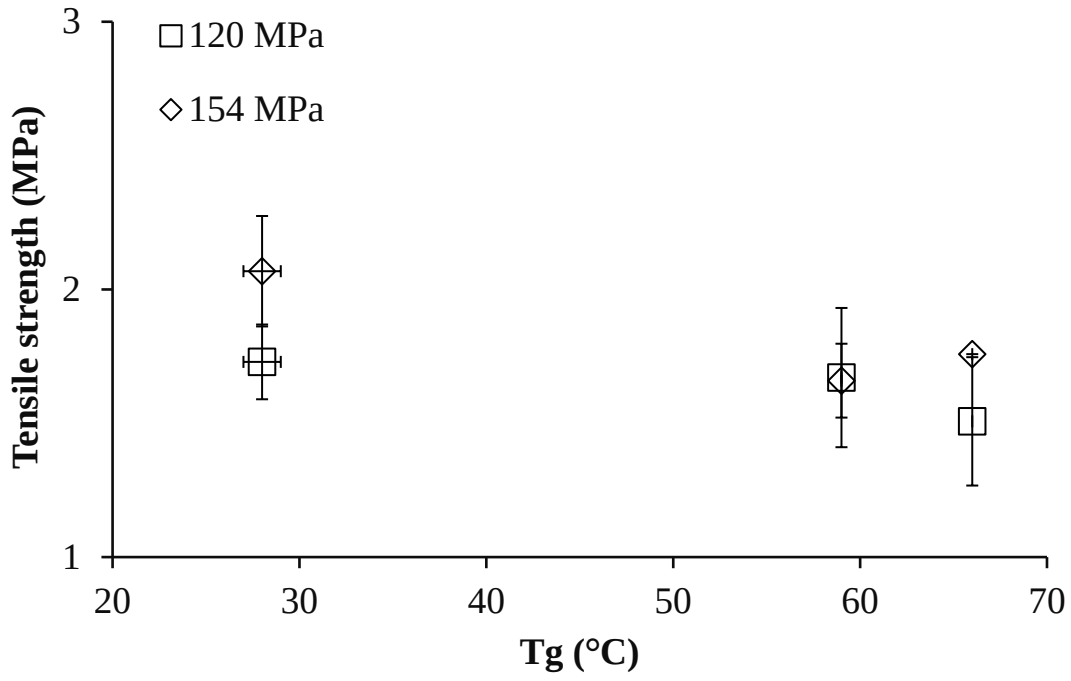

Figure 7.7 – Tensile strength of tablets of guest particle formulations only as a function of their Tg. Data presented as Mean ±SD (n = 3).

7.5.8.2 Interactive mixtures

Figure 7.8 shows the tensile strength of the tablets formed from the interactive mixtures with paracetamol, plotted as a function of the Tg of the guest particles. With a 10% (w/w) guest particle fraction, an increase in the Tg of guest particles showed a marginal reduction in the tensile strength of the tablets of interactive mixtures (Figure 7.8A). This change was more apparent with increasing guest particle fractions (Figure 7.8B and Figure 7.8C). It has been previously proposed that a ”guest particle” surface coverage should exceed a minimum threshold to eliminate host-host contacts, and this typically occurs when the surface coverage by guest particles exceed 40% [13, 43]. Thus, the observed enhanced impact of the Tg on the tensile strength of interactive mixture with higher guest particle fractions may be attributed to greater surface coverage, which allowed such guest-guest interactions to be increasingly influential.

In contrast to guest particles alone, these results show that the Tg of guest particles dictates the tensile strength of the tablets of the interactive mixtures. Of note, the tensile strength of the tablets of interactive mixtures with highest deformability (PVP10-Leu, Tg ~ 28 °C), was higher than the tensile strength of corresponding guest particle only tablets above certain guest particle fractions. This may be attributed to the formation of stronger bonds between guest-host particles than between guest-guest and host-host particles (Appendix 7.3).

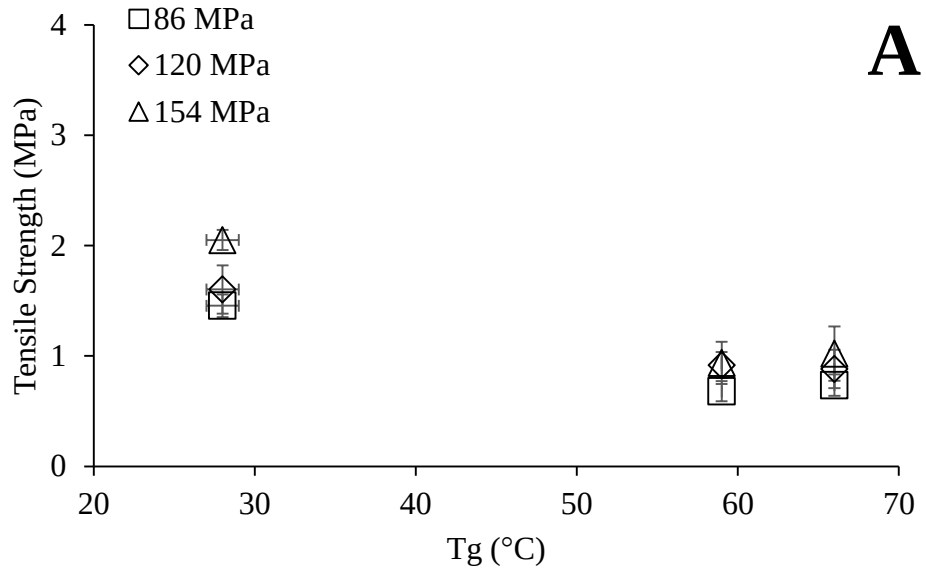
86 MPa
120 MPa
154 MPa
A
Tensile Strength (MPa)
Tg (°C)
0
1
2
3
4
20
30
40
50
60
70

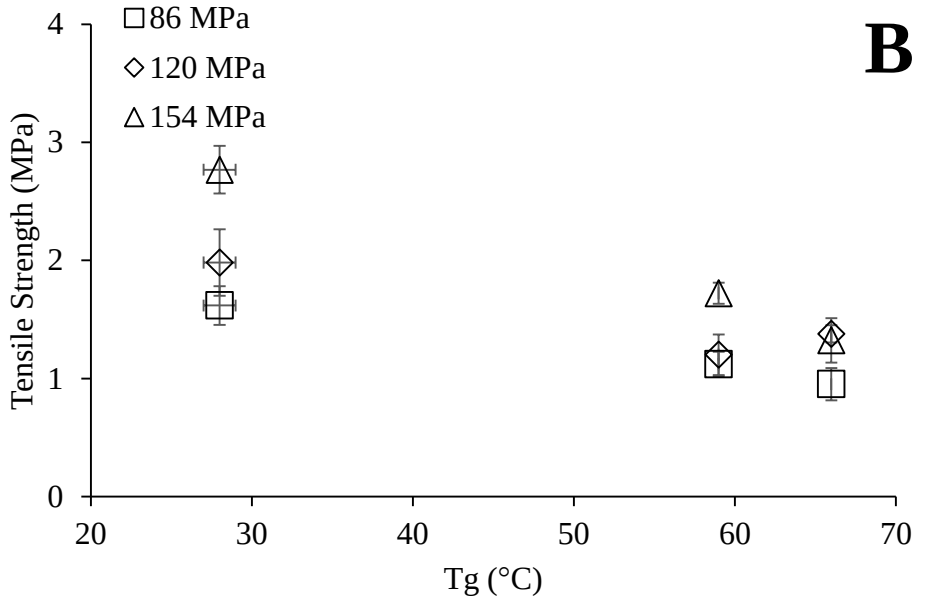
86 MPa
120 MPa
154 MPa
B
Tensile Strength (MPa)
Tg (°C)
0
1
2
3
4
20
30
40
50
60
70

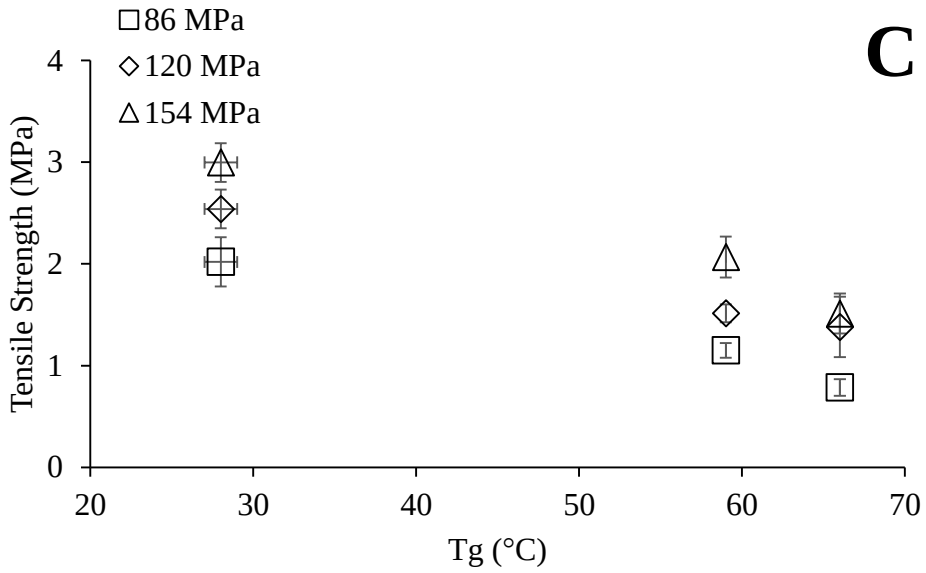
86 MPa
120 MPa
154 MPa
C
Tensile Strength (MPa)
Tg (°C)
0
1
2
3
4
20
30
40
50
60
70

Figure 7.8 – Tensile strength of tablets of interactive mixtures as a function of the Tg of guest particles. A-Host to guest ratio (90% (w/w)/10% (w/w)); B -Host to guest ratio (85% (w/w)/15% (w/w) and C-Host to guest ratio (80% (w/w)/20% (w/w)). Data presented as mean ±SD (n = 5)

7.5.9 Elasticity Factor

The degree of volume reduction that a powder undergoes during compression depends on its mechanical properties. Generally, a plastic material undergoes greater deformation and therefore demonstrated higher volume reduction than an elastic material [44, 45]. The degree of volume reduction of powder during compression can be assessed by measuring tablet height during compaction [38]. We also investigated the effect of Tg of guest particles on the elastic recovery of their tablets as well as the tablets of interactive mixtures.

7.5.9.1 Guest particles

Figure 7.9 shows the elasticity factor of the tablets of guest particles as a function of their Tg, and results indicated that the elasticity factor of the tablets increased with increasing Tg. In general, an increased inter-particle bonding should counteract the elastic expansion of tablets resulting in formation of tablets with higher tensile strength. However, our results indicated that the tensile strength of the tablets of guest particles only did not change as a function of their Tg, indicating no change in inter-particle bonding. Thus, a decline in elasticity factor of the tablets of guest particle only with reducing Tg may be attributed to differences in their mechanical properties, which was desirable for this study. To conclude, this change in deformability had no clear effect on the tensile strength of surface lubricated guest particles indicating a negligible change in inter-particle bonding between guest particles.

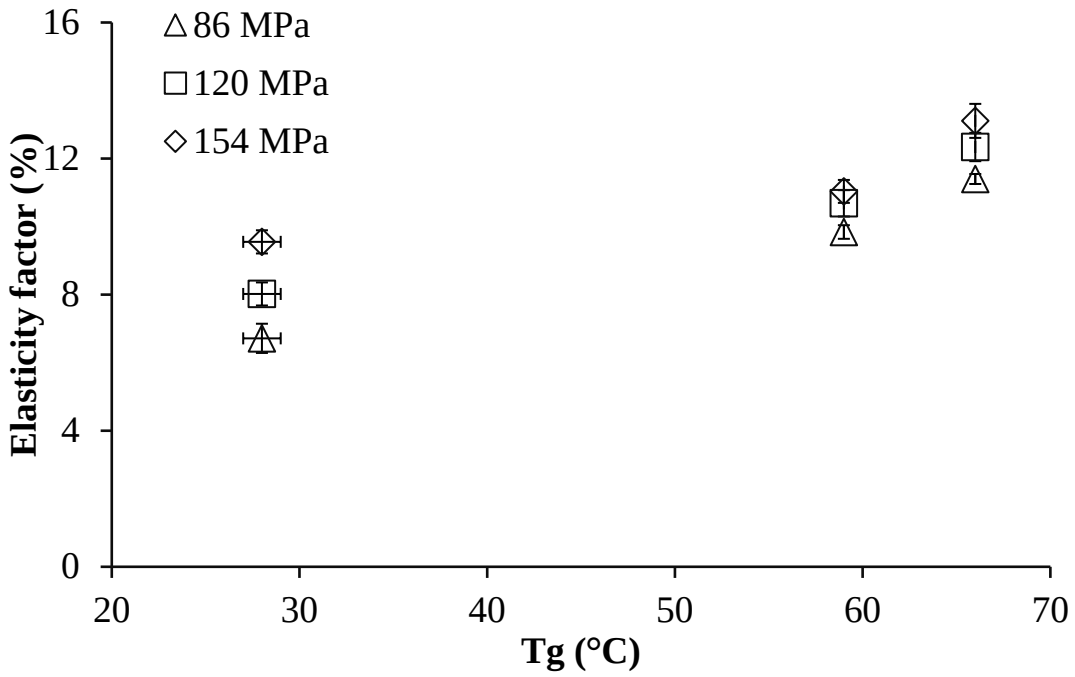

Figure 7.9 – % Elasticity factor of tablets of guest particle formulations only as a function of their Tg. Data presented as mean ±SD (n = 5)

7.5.9.2 Interactive mixtures

We also determined the effect of Tg of guest particles on the elasticity factor of the tablets of the interactive mixtures. A decrease in the elasticity factor of the tablets of the interactive mixture was evident with decreasing Tg of guest particles (Figure 7.10). This suggests that the elastic expansion of the tablets of interactive mixtures depends on the Tg of guest particles. We also compared the elasticity factors of the tablets of the guest particle formulations only and interactive mixtures and a linear relationship was observed (Appendix 7.4). This provides evidence that the volume recovery of the tablets of interactive mixtures depends on the deformability of guest particles.

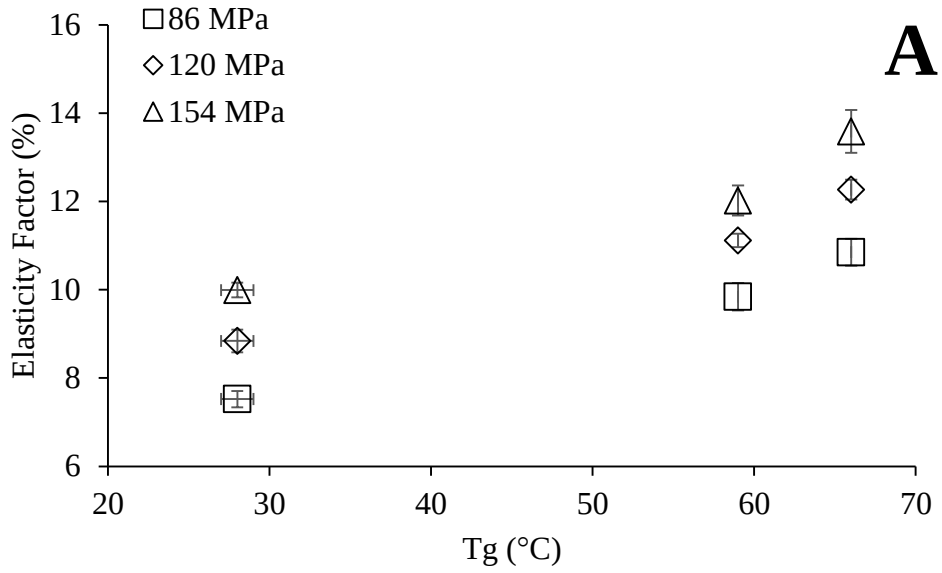
86 MPa
120 MPa
154 MPa
A
Elasticity Factor (%)
16
14
12
10
8
6
20
30
40
50
60
70
Tg (°C)

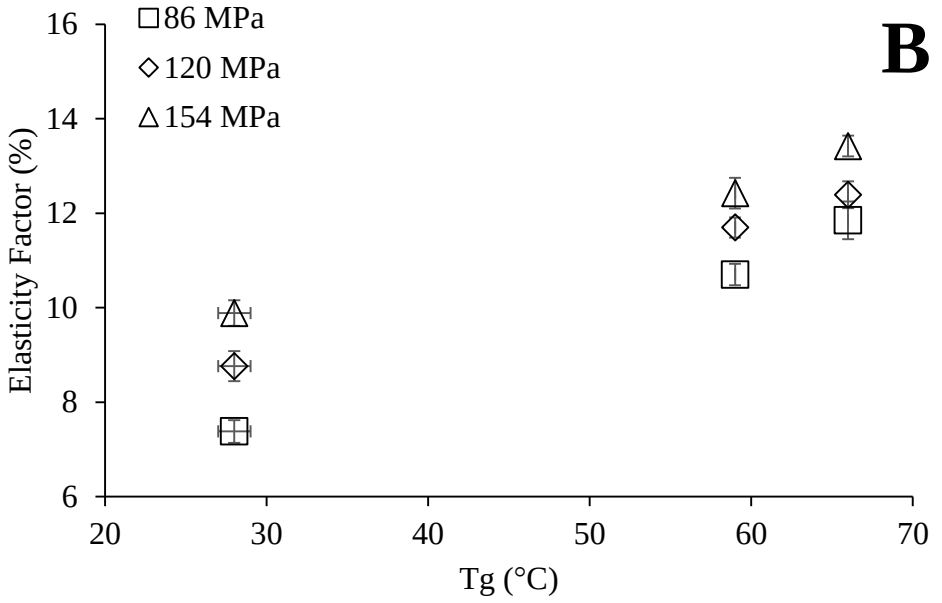
86 MPa
120 MPa
154 MPa
B
Elasticity Factor (%)
16
14
12
10
8
6
20
30
40
50
60
70
Tg (°C)

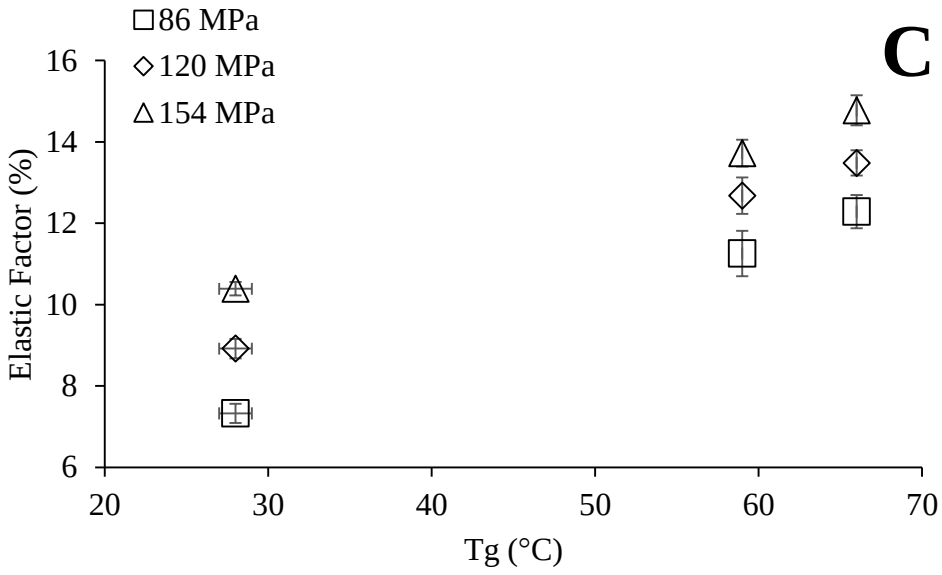
86 MPa
120 MPa
154 MPa
C
Elastic Factor (%)
16
14
12
10
8
6
20
30
40
50
60
70
Tg (°C)

Figure 7.10 – % Elasticity factor of tablets of interactive mixtures as a function of the Tg of guest particles. A-Host to guest ratio (90% (w/w)/10% (w/w)); B -Host to guest ratio (85% (w/w)/15% (w/w) and C-Host to guest ratio (80% (w/w)/20% (w/w)). Data presented as mean ±SD (n = 5)

We also investigated the relationship between the tensile strength and elasticity factor of the tablets of interactive mixtures. In interactive mixtures, an increase in the elasticity factor of the tablets was associated with a decrease in their tensile strength, unlike

the tablets of guest particles only (

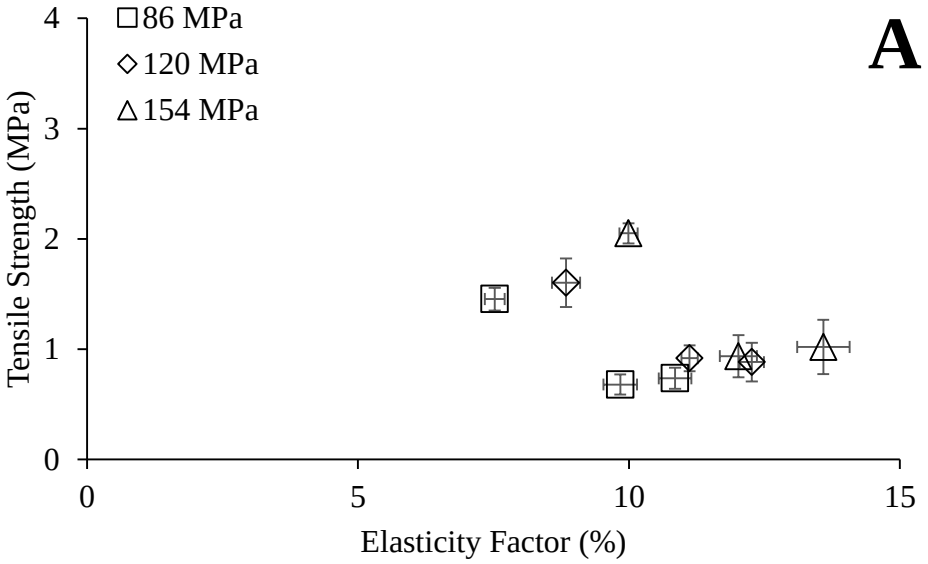

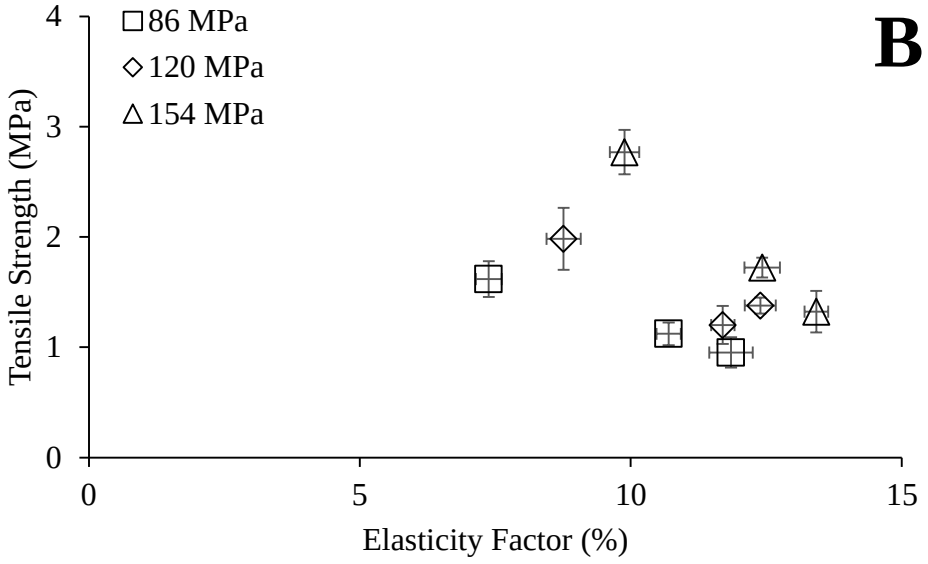

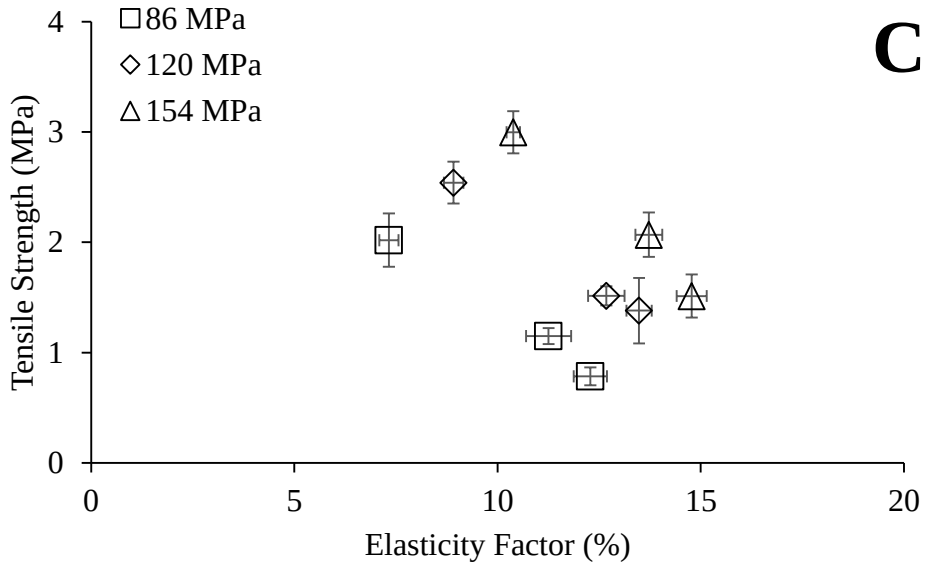

Figure 7.11). This suggests that greater elastic expansion of guest particles resulted in formation of weaker bonds between host particles resulting in lower tensile strength. Therefore, our results provide evidence that the deformability of the guest particles dictates inter-particle bonding in interactive mixtures and consequently their tablet tensile strength.

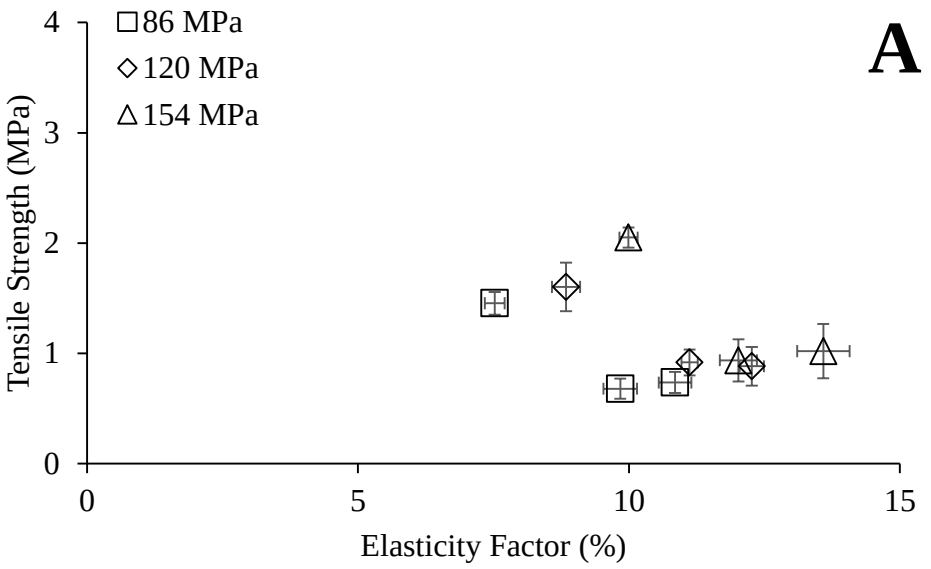
A
86 MPa
120 MPa
154 MPa
Tensile Strength (MPa)
Elasticity Factor (%)
0
1
2
3
4
0
5
10
15

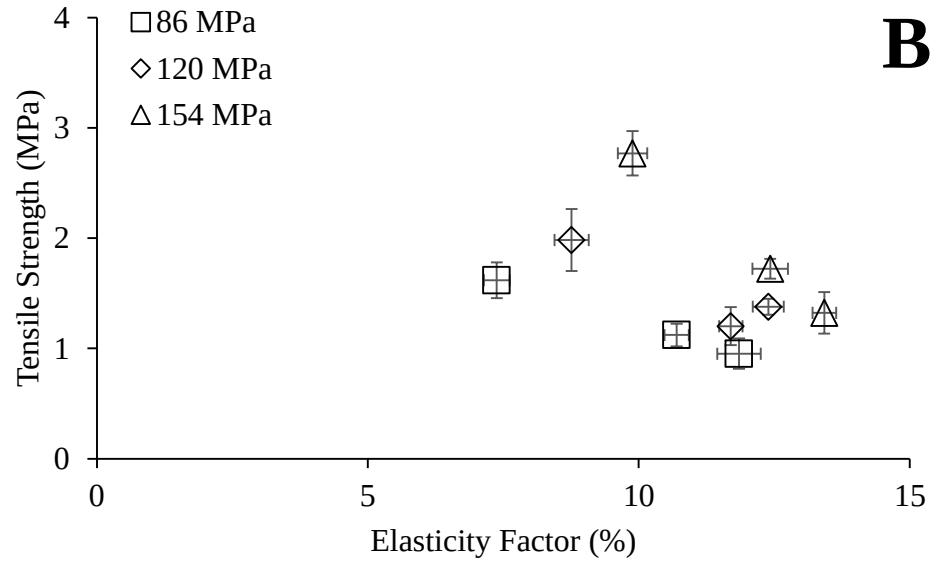
B
86 MPa
120 MPa
154 MPa
Tensile Strength (MPa)
Elasticity Factor (%)
0
1
2
3
4
0
5
10
15

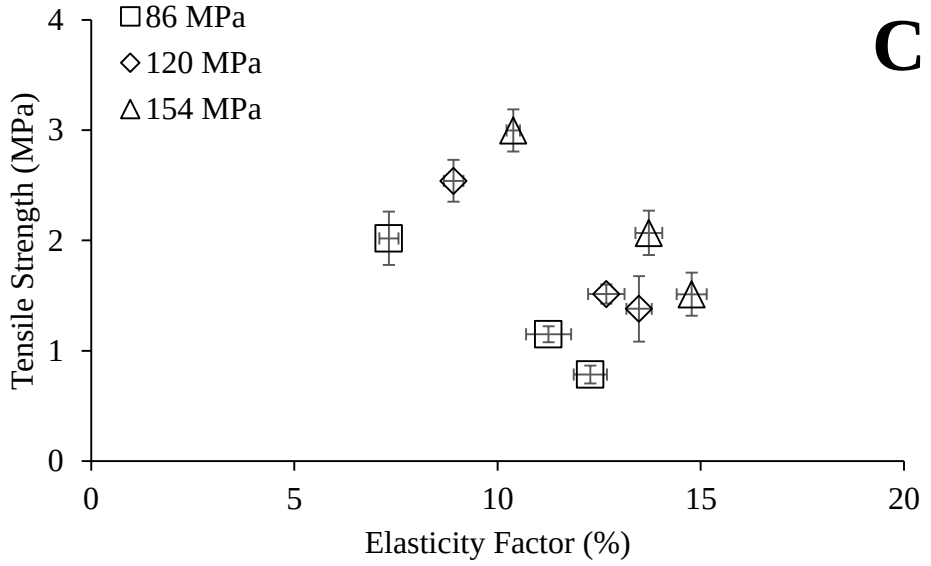
C
86 MPa
120 MPa
154 MPa
Tensile Strength (MPa)
Elasticity Factor (%)
0
1
2
3
4
0
5
10
15
20

Figure 7.11 – Tensile strength as a function of % elasticity factor of tablets of interactive mixtures. A-Host to guest ratio (90% (w/w)/10% (w/w)); B -Host to guest ratio (85% (w/w)/15% (w/w) and C-Host to guest ratio (80% (w/w)/20% (w/w)). Data presented as mean ±SD (n = 5)

7.6 Discussion

Typically, particles sizing <10 µm tend to adhere to relatively large particles leading to formation of interactive mixtures [1]. However, such small particles experience strong inter-particles forces than the gravitational forces and tend to agglomerate [15, 46, 47]. Low shear mixing process is often unable to break these particles agglomerates and blending of small particle with large cohesive particles, results in formation of non-homogeneous interactive mixture [13, 15, 48].

We demonstrated that small PVP particles are also extremely cohesive and does not form homogeneous interactive mixtures upon blending with paracetamol, improves its compactability but had no effect on its flow. Co-spraying with L-leucine efficiently reduces the cohesion of small binder particles, thus allow them to form a homogeneous interactive mixture with host particles. L-leucine coated small binder particles improves the compaction as well as flow of host particles [25]. However, the mechanism through which such L-leucine coated binder particles improves compaction of host particles is not understood. We proposed that under compression binder at the core deforms leading to L-leucine shell ruptures and allowing binder to expose and participate in inter-particle bonding with host particles increasing its compactability. Thus, there is a proportional relationship between deformability of surface L-leucine coated guest particles and compactability of resultant interactive mixture. In this study, the effect of deformability of surface L-leucine coated guest particles on the

compactability interactive mixtures was investigated, by employing Tg as our metric for guest particle mechanical behaviour.

The results indicated that guest particle formulation of different molecular weight PVP exhibited similar particle size and with narrow particle size distribution. Co-sprayed guest particle formulations appeared as discrete particles with a degree of surface asperity. Surfaces of guest particles formulation were L-leucine rich, with negligible PVP. Previous studies have suggested that particle size [49, 50], surface morphology [51], and surface chemical composition [52-54] can affect inter-particle bonding and hence compaction behaviour. Since, these factors did not vary considerably amongst guest particle formulations, they are considered unlikely to strongly affect inter-particle bonding behaviour of these formulations and hence compactability of resultant interactive mixtures. Images of blends showed guest particle formulations adhered to paracetamol particles with no apparent agglomerates of guest particles, indicating formation of homogeneous interactive mixtures.

Our results indicated that the surface L-leucine coated guest particles with the greater deformation showed an enhanced binder activity. This increase in tensile strength of tablets of interactive mixtures with greater guest particle deformability would be a result of either an increase in area and/or strength of bonding [55, 56]. Since, the surface of guest particles are L-leucine enriched, which reduces inter-particle bonding [18, 26-28], it is unlikely that increased availability of L-leucine surfaces (with greater guest particle deformability) will promote inter-particle bonding between host particles. Thus, we propose that with greater guest particle deformability, the availability of PVP surfaces increases, leading to strong inter-particle bonding with host particles and an increase in tablet tensile strength of interactive mixtures. The potential mechanism to explain this is a follows. When an interactive mixture is compressed, guest particles starts to deform/distort at the interfaces of host particles. We propose that due to the lack of deformability/stretchability, L-leucine shell ruptures under

increasing stresses from the core of the particles. Rupturing of L-leucine shell allows L-leucine free PVP sites to come in existence and participate in inter-particle bonding. As the inherent deformability of the core material increases, the amount of stress that, the shell experiences increase resulting in an increased rupturing of L-leucine shell. As the degree to which L-leucine shell ruptures increases, the availability of L-leucine free PVP surfaces increases. Consequently, the strength of inter-particle bonding between guest and host particles also increases, which is evident as an increase in tensile strength of interactive mixtures with reducing Tg of guest particles. This effect is likely enhanced given the host particles are relatively non-plastic (brittle) and so distortion of the more plastic guest particles at the surface of the host may yield more effective puncture of the L-leucine shell.

It was noted that the compactability of PVP/L-leucine co-sprayed formulations remained similar despite an increase in deformability. This suggests that increasing PVP deformasbility does not affect the inter-particle bonding strength and/or area of guest particle formulations to an extent sufficient to cause an observable change tensile strength. This is in sharp contrast to earlier reports indicating that a reduction in Tg of PVP improves the compactability due to increasing deformability [57, 58]. We proposed that due to an excess of L-leucine, the free PVP surfaces created after deformation predominantly interact with L-leucine. Thus the increase in deformability does not show an increase in inter-particle bonding and hence tensile strength of guest particle formulations.

It was also noted that the tensile strength of the tablets of interactive mixtures consisting of guest particles (with least Tg of approximately ~ 28 °C) was higher than corresponding tablets of guest particles only composition. This indicates that the net inter-particle forces between guest-host particles were stronger than guest-guest particles. It may be

speculated that when the pure guest particles are compacted, some L-leucine-free sites are created, but these sites are fewer than when interactive mixtures are compacted,

We have previously shown that small binder particles with L-leucine coated surfaces have the ability to form interactive mixtures that can improve both the flow performance and tabletability of interactive mixtures [25]. This previous study demonstrated that the surface lubrication of small binder particles was necessary to reduce their cohesion, which was critical to achieve a flow additive action. However, this surface lubrication was associated with a reduction in binder activity as well, which highlighted the challenge of creating excipients with optimal flow additive as well as binder activity [25]. The current study, illustrates how material deformability controls the binder activity of surface lubricated binders and it can be manipulated to achieve an improved binder activity, and so optimise the performance of such potential excipients.

These small prototype excipient particles may be effective for addressing problems caused by poor tabletability of APIs and could have potential applications in creating dry blends for tabletting of high-dose API. However, it would be equally important to achieve an optimum balance between functional improvement and cost benefit that can be achieved for the effective implication of such excipients in real-world tablet manufacturing, and further investigation is required.

7.7 Conclusion

In this paper, the influence of mechanical properties of engineered small guest particles on the tableting behaviour of interactive mixtures was investigated. Results showed that the deformability of guest particles dictates the inter-particle bonding between host particles and hence the tensile strength of tablets of resultant interactive mixtures. The knowledge gained

here may be useful in creating a new concept in composite small tablet excipients with multiple functionalities.

7.8 Acknowledgement

Sharad Mangal is thankful to Monash Institute of Graduate Research (MIGR) for providing Monash Graduate Scholarship (MGS) and Monash International Postgraduate Research Scholarship (MIPRS).

7.9 References

[1] Hersey JA. Ordered mixing: a new concept in powder mixing practice. Powder Technol 1975; 11(1): 41-44.

[2] Hersey JA. Powder mixing: theory and practice in pharmacy. Powder Technol 1976; 15(2): 149-153.

[3] Lai F, Hersey JA, Staniforth JN. Segregation and mixing of fine particles in an ordered mixture. Powder Technol 1981; 28(1): 17-23.

[4] Staniforth JN. Ordered mixing or spontaneous granulation? Powder Technol 1985; 45(1): 73-77.

[5] Begat P, Price R, Harris H, Morton DAV, Staniforth JN. The influence of force control agents on the cohesive-adhesive balance in dry powder inhaler formulations. Kona Powder Part J 2005; 23: 109-1231.

[6] Begat P, Morton DAV, Staniforth J, Price R. The cohesive-adhesive balances in dry powder inhaler formulations II: influence on fine particle delivery characteristics. Pharm Res 2004; 21(10): 1826-1833.

[7] Begat P, Morton DV, Staniforth J, Price R. The cohesive-adhesive balances in dry powder inhaler formulations I: direct quantification by atomic force microscopy. Pharm Res 2004; 21(9): 1591-1597.

[8] Orband JLR, Geldart D. Direct measurement of powder cohesion using a torsional device. Powder Technol 1997; 92(1): 25-33.

[9] Zhou Q, Qu L, Gengenbach T, Denman JA, Larson I, Stewart PJ, Morton DAV. Investigation of the extent of surface coating via mechanofusion with varying additive levels and the influences on bulk powder flow properties. Int J Pharm 2011; 413(1–2): 36-43.

[10] Chew NYK, Chan HK. Use of solid corrugated particles to enhance powder aerosol performance. Pharm Res 2001; 18(11): 1570-1577.

[11] Li Q, Rudolph V, Peukert W. London-van der Waals adhesiveness of rough particles. Powder Technol 2006; 161(3): 248-255.

[12] Podczeck F. The influence of particle size distribution and surface roughness of carrier particles on the in vitro properties of dry powder inhalations. Aerosol Sci Tech 1999; 31(4): 301-321.

[13] Han X, Jallo L, To D, Ghoroi C, Dave R. Passivation of high-surface-energy sites of milled ibuprofen crystals via dry coating for reduced cohesion and improved flowability. J Pharm Sci 2013; 102(7): 2282-96.

[14] Zhou Q, Denman JA, Gengenbach T, Das S, Qu L, Zhang H, Larson I, Stewart PJ, Morton DAV. Characterization of the surface properties of a model pharmaceutical fine powder modified with a pharmaceutical lubricant to improve flow via a mechanical dry coating approach. J Pharm Sci 2011; 100(8): 3421-3430.

[15] Yang J, Sliva A, Banerjee A, Dave RN, Pfeffer R. Dry particle coating for improving the flowability of cohesive powders. Powder Technol 2005; 158(1–3): 21-33.

[16] Zhou QT, Armstrong B, Larson I, Stewart PJ, Morton DAV. Understanding the influence of powder flowability, fluidization and de-agglomeration characteristics on the aerosolization of pharmaceutical model powders. Eur J Pharm Sci 2010; 40(5): 412-421.

[17] Chew NY, Shekunov BY, Tong HH, Chow AH, Savage C, Wu J, Chan HK. Effect of amino acids on the dispersion of disodium cromoglycate powders. J Pharm Sci 2005; 94(10): 2289-300.

[18] Staniforth JN, Morton DAV, inventor, assignee Magnesium stearate, a phospholipid, or an amino acid in preparation of pharmaceutical particles for inhalation. 2002.

[19] Sou T, Kaminskas LM, Nguyen T-H, Carlberg R, McIntosh MP, Morton DAV. The effect of amino acid excipients on morphology and solid-state properties of multi-component spray-dried formulations for pulmonary delivery of biomacromolecules. Eur J Pharm Biopharm 2013; 83(2): 234-243.

[20] Feng AL, Boraey MA, Gwin MA, Finlay PR, Kuehl PJ, Vehring R. Mechanistic models facilitate efficient development of leucine containing microparticles for pulmonary drug delivery. Int J Pharm 2011; 409(1–2): 156-163.

[21] Mangal S, Meiser F, Tan G, Gengenbach T, Denman J, Rowles MR, Larson I, Morton DAV. Relationship between surface concentration of l-leucine and bulk powder properties in spray dried formulations. Eur J Pharm Biopharm 2015; 94: 160-169.

[22] Gliński J, Chavepeyer G, Platten J-K. Surface properties of aqueous solutions of L-leucine. Biophysical Chemistry 2000; 84(2): 99-103.

[23] Vehring R, Foss WR, Lechuga-Ballesteros D. Particle formation in spray drying. J. Aerosol Sci. 2007; 38(7): 728-746.

[24] Vehring R. Pharmaceutical particle engineering via spray drying. Pharm Res 2008; 25(5): 999-1022.

[25] Mangal S, Meiser F, Lakio S, Morton D, Larson I. The role of physico-chemical and bulk characteristics of co-spray dried l-leucine and polyvinylpyrrolidone on glidant and binder properties in interactive mixtures. Int J Pharm 2015; 479(2): 338-348.

[26] Ghoroi C, Han X, To D, Jallo L, Gurumurthy L, Davé RN. Dispersion of fine and ultrafine powders through surface modification and rapid expansion. Chem Eng Sci 2013; 85(0): 11-24.

[27] Rotthäuser B, Kraus G, Schmidt PC. Optimization of an effervescent tablet formulation using a central composite design optimization of an effervescent tablet formulation containing spray dried l-leucine and polyethylene glycol 6000 as lubricants using a central composite design. Int J Pharm 1998; 46(1): 85-94.

[28] Röscheisen G, Schmidt PC. Preparation and optimization of l-leucine as lubricant for effervescent tablet formulations. Pharm Acta Helv 1995; 70(2): 133-139.

[29] Cowie JMG. Polymers: Chemistry and Physics of Modern Materials. In, 3 ed. London: Nelson Thornes 2001; pp.

[30] Van der Voort Maarschalk K, Vromans H, Bolhuis GK, Lerk CF. Influence of plasticizers on tableting properties of polymers. Drug Dev Ind Pharm 1998; 24(3): 261-8.

[31] Van der Voort Maarschalk K, Zuurman K, Van Steenbergen MJ, Hennink WE, Vromans H, Bolhuis GK, Lerk CF. Effect of compaction temperature on consolidation of amorphous copolymers with different glass transition temperatures. Pharm Res 1997; 14(4): 415-9.

[32] Picker KM. The relevance of glass transition temperature for the process of tablet formation. J. Therm. Anal. Calorim. 2003; 73(2): 597-605.

[33] Mattsson SF, Nystrom C. Evaluation of critical binder properties affecting the compactibility of binary mixtures. Drug Dev Ind Pharm 2001; 27(3): 181-194.

[34] Buera MDP, Levi G, Karel M. Glass Transition in Poly(vinylpyrrolidone): Effect of Molecular Weight and Diluents. Biotechnol Progr 1992; 8(2): 144-148.

[35] Gharaibeh SF, Aburub A. Use of first derivative of displacement vs. force profiles to determine deformation behavior of compressed powders. AAPS PharmSciTech 2013; 14(1): 398-401.

[36] Gupta A, Hamad M, Tawakkul M, Sayeed V, Khan M. Difference in the lubrication efficiency of bovine and vegetable-derived magnesium stearate during tabletting. AAPS PharmSciTech 2009; 10(2): 500-504.

[37] Fell JT, Newton JM. Determination of tablet strength by the diametral-compression test. J Pharm Sci 1970; 59(5): 688-691.
[38] Armstrong NA, Haines-Nutt RF. Elastic recovery and surface area changes in compacted powder systems. Powder Technol 1974; 9(5–6): 287-290.
[39] Antikainen O, Yliruusi J. Determining the compression behaviour of pharmaceutical powders from the force–distance compression profile. Int J Pharm 2003; 252(1–2): 253-261.
[40] Chew NY, Shekunov BY, Tong HH, Chow AH, Savage C, Wu J, Chan HK. Effect of amino acids on the dispersion of disodium cromoglycate powders. J. Pharm. Sci. 2005; 94(10): 2289-300.
[41] Fox TG, Flory PJ. Second-Order Transition Temperatures and Related Properties of Polystyrene. I. Influence of Molecular Weight. J Appl Phys 1950; 21(6): 581-591.
[42] Li J, Tao L, Dali M, Buckley D, Gao J, Hubert M. The effect of the physical states of binders on high-shear wet granulation and granule properties: A mechanistic approach towards understanding high-shear wet granulation process. part I. physical characterization of binders. J Pharm Sci 2011; 100(1): 164-173.
[43] Chen Y, Quintanilla MA, Yang J, Valverde JM, Dave RN. Pull-off force of coated fine powders under small consolidation. Phys Rev E Stat Nonlin Soft Matter Phys 2009; 79(4 Pt 1): 1-14.
[44] Al-Nasassrah MA, Podczeck F, Newton JM. The effect of an increase in chain length on the mechanical properties of polyethylene glycols. Int J Pharm 1998; 46(1): 31-38.
[45] Olsson H, Mattsson S, Nyström C. Evaluation of the effect of addition of polyethylene glycols of differing molecular weights on the mechanical strength of sodium chloride and sodium bicarbonate tablets. Int J Pharm 1998; 171(1): 31-44.
[46] Kendall K, Stainton C. Adhesion and aggregation of fine particles. Powder Technol 2001; 121(2-3): 223-229.
[47] Chen Y, Yang J, Dave RN, Pfeffer R. Fluidization of coated group C powders. AIChE J 2008; 54(1): 104-121.
[48] Meyer K, Zimmermann I. Effect of glidants in binary powder mixtures. Powder Technol 2004; 139(1): 40-54.
[49] Nyström C, Mazur J, Sjögren J. Studies on direct compression of tablets II. The influence of the particle size of a dry binder on the mechanical strength of tablets. Int J Pharm 1982; 10(3): 209-218.
[50] Alderborn G, Nystrom C. Studies on direct compression of tablets. IV. The effect of particle size on the mechanical strength of tablets. Acta Pharm Suec 1982; 19(5): 381-390.
[51] Alderborn G, Börjesson E, Glazer M, Nyström C. Studies on direct compression of tablets. XIX. The effect of particle size and shape on the mechanical strength of sodium bicarbonate tablets. Acta Pharm Suec 1988; 25(1): 31-40.
[52] Qu L, Zhou Q, Gengenbach T, Denman JA, Stewart PJ, Hapgood KP, Gamlen M, Morton DAV. Investigation of the potential for direct compaction of a fine ibuprofen powder dry-coated with magnesium stearate. Drug Dev Ind Pharm 2014: 1-13.
[53] Zuurman K, Van der Voort Maarschalk K, Bolhuis GK. Effect of magnesium stearate on bonding and porosity expansion of tablets produced from materials with different consolidation properties. Int J Pharm 1999; 179(1): 107-115.
[54] Fichtner F, Mahlin D, Welch K, Gaisford S, Alderborn G. Effect of surface energy on powder compactibility. Pharm Res 2008; 25(12): 2750-2759.
[55] Sun CC. Decoding powder tabletability: Roles of particle adhesion and plasticity. J Adhes Sci Technol 2011; 25(4-5): 483-499.

[56] Nyström C, Alderborn G, Duberg M, Karehill P-G. Bonding surface area and bonding mechanism-two important factors for the understanding of powder comparability. Drug Dev Ind Pharm 1993; 19(17-18): 2143-2196.

[57] Stubberud L, Arwidsson HG, Hjortsberg V, Graffner C. Water-solid interactions. III. Effect of glass transition temperature, T(g), and processing on tensile strength of compacts of lactose and lactose/polyvinyl pyrrolidone. Pharm Dev Technol 1996; 1(2): 195-204.

[58] Stubberud L, Arwidsson HG, Larsson A, Graffner C. Water solid interactions II. Effect of moisture sorption and glass transition temperature on compactibility of microcrystalline cellulose alone or in binary mixtures with polyvinyl pyrrolidone. International Journal of Pharmaceutics 1996; 134(1–2): 79-88.

7.10 Appendix

7.10.1 Appendix 7.1

Typical labelled force-distance curve. Force-distance curve of each tablet was recorded for further analysis. In figure, a represents punch position, where when punch approaches the powder but no force is applied, b represent punch position, where it applies maximum force on powder or in other word maximum punch displacement in the die, c represents the punch position after decompression when punch force is zero again.

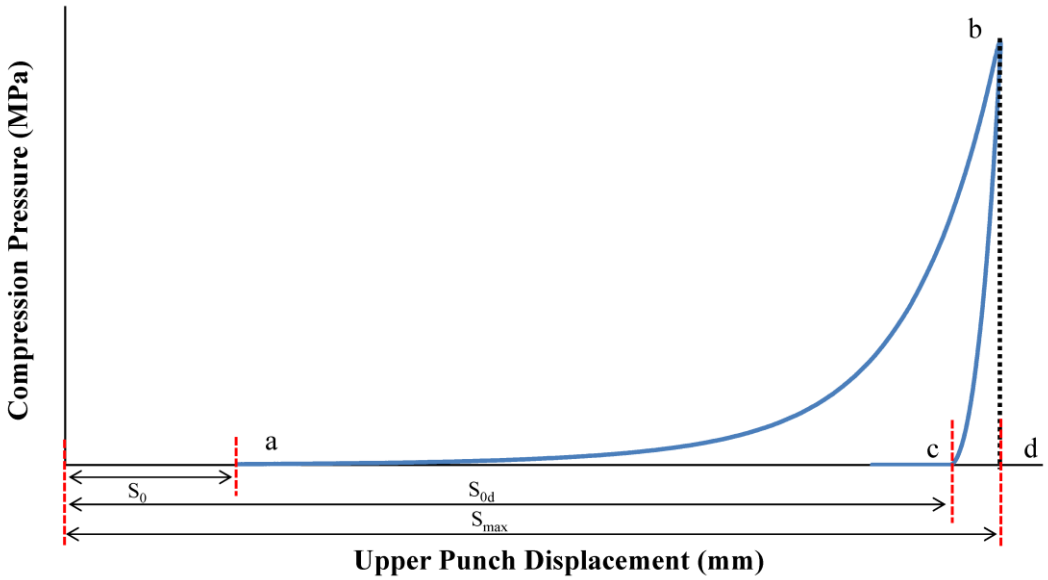

7.10.2 Appendix 7.2

Particle size distribution plots spray dried formulations and paracetamol. Data presented as Mean ±SD (n = 3).

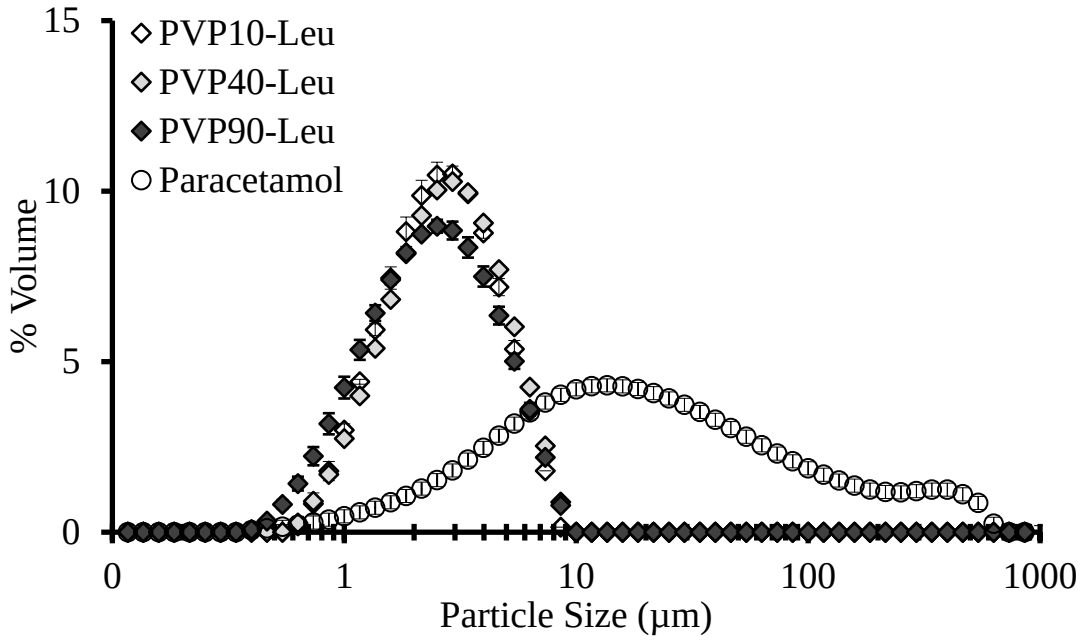

7.10.3 Appendix 7.3

Tensile strength of the tablets of guest particle formulations only (PVP10-Leu, Tg ~ 28 °C) and interactive mixture containing varying proportions of corresponding guest particle formulation. Data presented as Mean ±SD (n = 5).

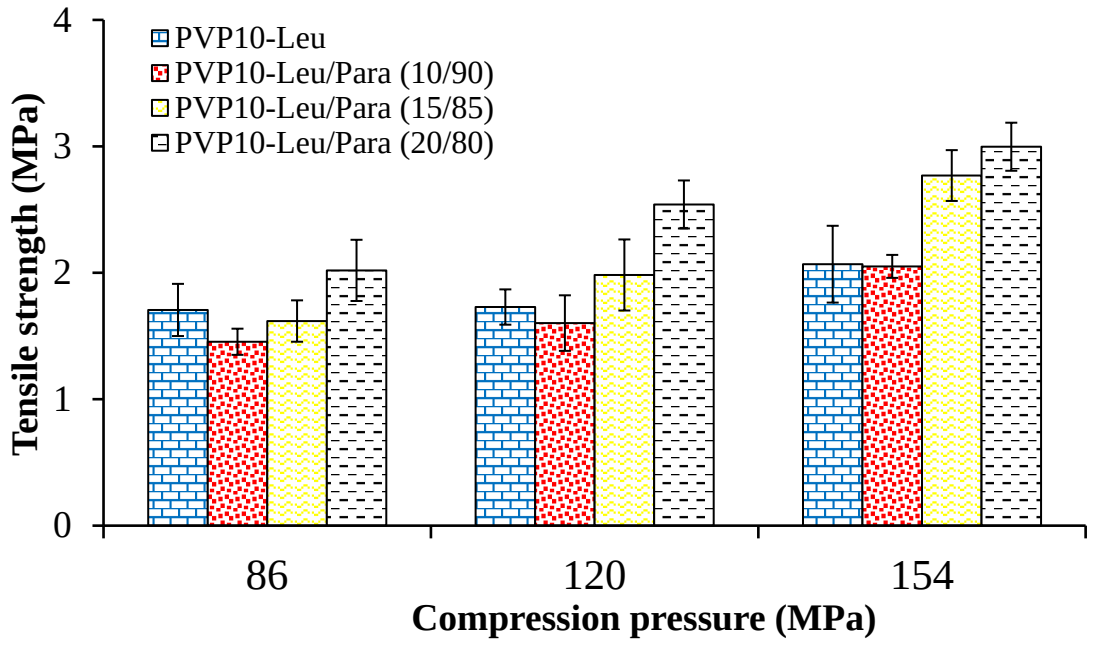

7.10.4 Appendix 7.4

% Elasticity factor of tablets of interactive mixtures as a function of the elasticity factor of the tablets of guest particle formulations only at corresponding compression pressures of 86 MPa, 120 MPa and 154 MPa. A-host to guest ratio (90% (w/w)/10% (w/w)); B -host to guest ratio (85% (w/w)/15% (w/w) and C-host to guest ratio (80% (w/w)/20% (w/w)). Data presented as mean ±SD (n = 5)

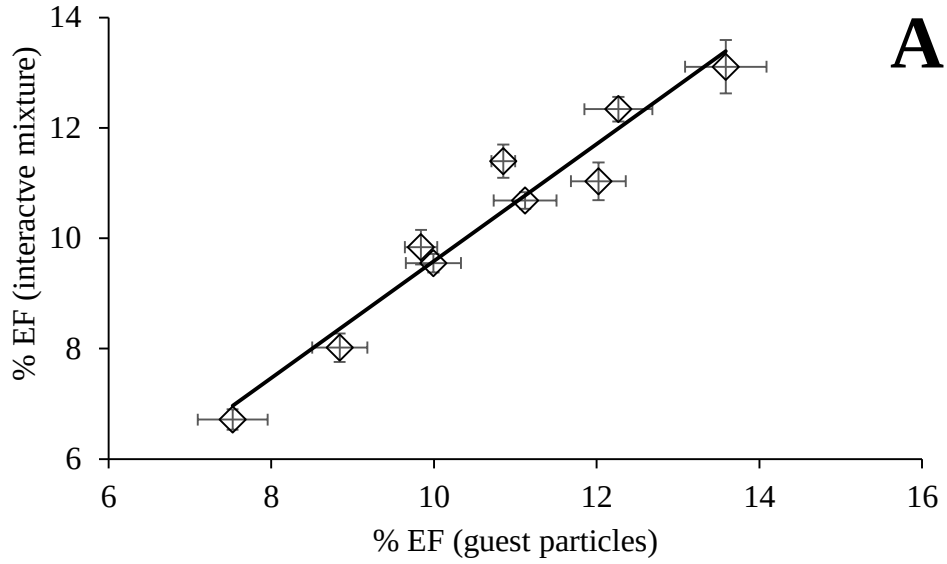
A
% EF (interactve mixture)
% EF (guest particles)
6
8
10
12
14
16

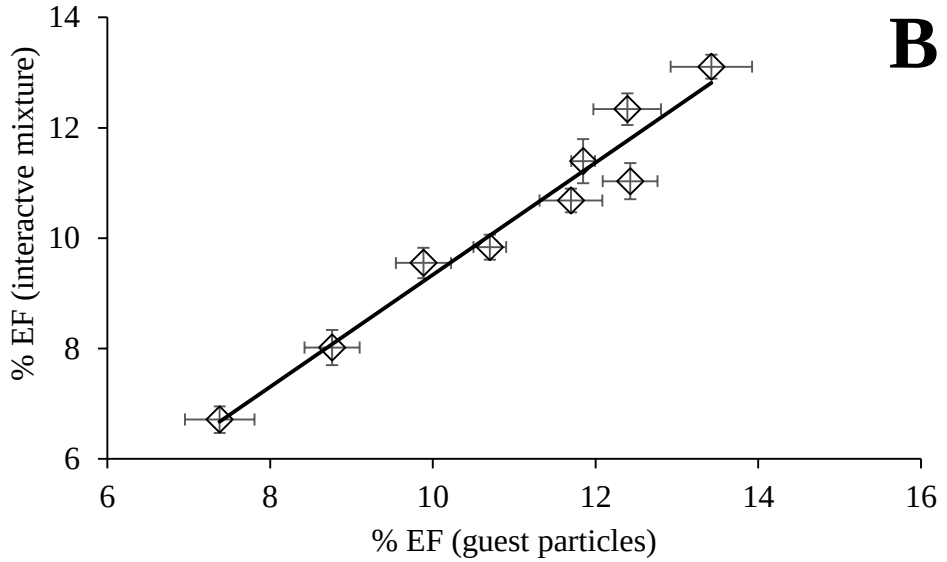
B
% EF (interactve mixture)
% EF (guest particles)
6
8
10
12
14
16

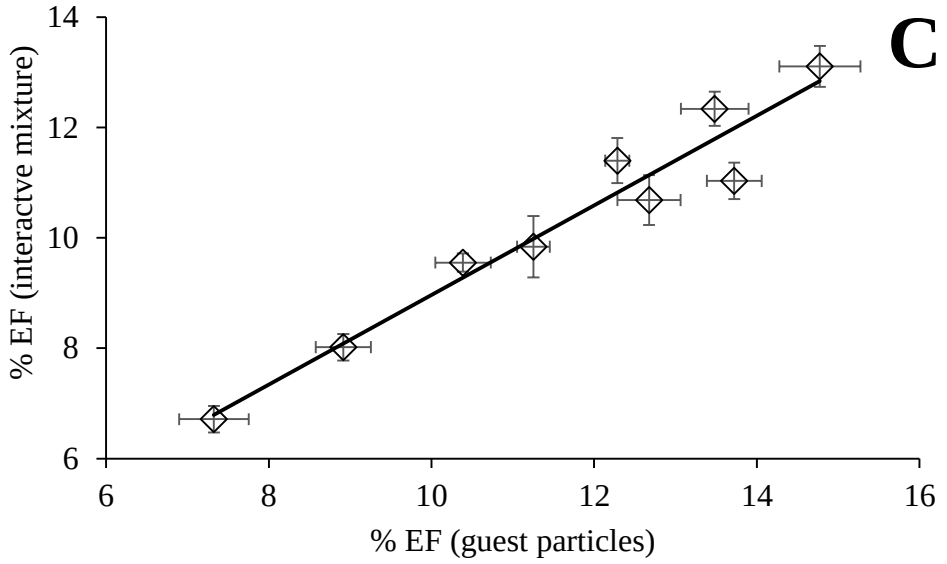
C
% EF (interactve mixture)
% EF (guest particles)
6
8
10
12
14
16

Chapter 8

General conclusions and future directions

8 General conclusions and future directions

8.1 General conclusions

It was hypothesized that small, surface-engineered binder particles with the ability to form interactive mixtures, could exhibit both a flow additive and binder action, which may conventionally be considered exclusive excipient functionalities. Small particles are in general highly cohesive and tend to agglomerate. This limits their ability to de-agglomerate and form homogeneous interactive mixtures. We proposed that the high cohesion of small binder particles would compromise their interactive mixing behaviour, and consequently their functional performance. Therefore, controlling the cohesion and evaluating its effect on the interactive mixing behaviour, and the resulting effects on binder and flow additive action of such small binder particles was a central aspect of this research work.

In this study, a range of low-cohesion small polymer binder particles were produced *via* a particle engineering approach, with L-leucine as the surface-modifying agent, and these performance characteristics of interactive mixing behaviours, flow additive action and binder actions were studied and compared.

We showed that PVP that was co spray-dried with L-leucine created a platform of reduced cohesion small binder particles. The surface L-leucine concentration governed the surface physico-chemical properties such as morphology, surface energy, solid-state nature of L-leucine and consequently the cohesion of resulting small particles. Small particles with surface L-leucine at saturation, were the least cohesive in nature, as determined by shear cell tests. We proposed that this knowledge be employed to design and optimize the bulk performance of such small particles. Our study also provided enhanced insight into how L-leucine first enriches into a droplet's surface and then crystallises upon spray-drying to create core-shell particles.

The reduced cohesion facilitated efficient dispersion and homogenous interactive mixing. Further, surface energy measurements were used to indicate relative magnitudes of the cohesive and adhesive nature of these small binder particles (a cohesive-adhesive balance approach) and could be effectively employed to anticipate the interactive mixing behaviour of the small binder particles with a larger API host particle.

A reduction in cohesion was also shown to accompany a deleterious effect on binder activity of small binder particles. It was proposed to be a result of the competing nature of cohesion and compactability as both depend on the inter-particle interaction between adjacent particles and are therefore related properties. However, despite this reduction, the binder particles did show a notable ability for binder ability. Previous studies have indicated that surface lubrication compromises the compactability of plastic materials. It was also proposed that compactability of such surface-lubricated materials depend on their ability to create lubricant-free sites. We proposed that the binder activity of surface-lubricated (L-leucine coated) small binder particles also depend on their ability to create lubricant-free bonding sites. Thus, a surface lubricated small binder with greater deformability (and a minimum of lubricant) was hypothesized to undergo greater deformation (under compression), create more lubricant-free sites for bonding and express greater binder activity than compared with their lower deformability counterparts. Our results confirmed that small surface lubricated binder particles with greater deformability expressed greater binder activity than high deformability particles, which supported our hypothesis.

We also investigated the effect of cohesion of small binder particles on their flow additive action. The cohesion of small particles was shown to dictate the flow performance of interactive mixtures. This indicated that the cohesion of small particles play determines the

magnitude of inter-particle forces between host particles in interactive mixtures and hence the flow performance of interactive mixtures.

In summary, this study examined the effect of fundamental material properties on the cohesion of small structurally-engineered binder particles as well as the effect of cohesion on the flow additive and binder properties of these particles. The flow additive action of small binder particles was shown to mainly depend on their surface properties. However, both surface as well as mechanical properties of small binder particles were shown to contribute significantly to their binder activity. This suggests that *via* careful selection and optimisation of surface and mechanical material properties, excipients with an optimum flow additive and binder action can be created. Thus, the use of optimal surface-engineered small binder particles may substantially improve the opportunities for the direct compression tablet manufacturing of high-dose API. The findings of our work would also be generally useful for scientists working in the areas of tablet manufacturing, powder flow and interactive mixing.

8.2 Future directions

In this thesis, PVP was used as a model binder to investigate the excipient performance of small binder particles. Further studies are recommended to investigate the excipient performance of a wide range of binder materials. This may include excipients, which tend to compress mainly by brittle fraction and/or a combination of brittle and plastic deformation. Plastic materials exhibit greater susceptibility to lubricant mediated reductions in tensile strength compared to brittle materials. Therefore, small binder particles consisting of brittle materials may exhibit a more limited sensitivity to surface lubrication and hence exhibit better binder activity. However, it should be pointed out that the extent of change in the particle size reduction may also alter mechanical properties of starting materials. For instance, some materials appear to have a critical particle size at which a transition from brittle to ductile behaviour occurs as the particles become smaller.

Additionally, achieving surface L-leucine enrichment is the key to reduced cohesion and hence to achieve homogeneous interactive mixing of the small particles with the API. Thus, to produce low-cohesion binder particles with different materials, it would be necessary to carefully select excipient materials, which allow the mass transport of L-leucine to the surface of the particles during the spray-drying process. Alternatively, other excipients such as magnesium stearate, silicon dioxide may be employed to control the cohesion of small binder particles.

Formation of interactive mixtures depend on the nature of both the small particles and host particles. We have demonstrated that surface engineering can effectively control the surface properties and hence mixing behaviour of small binder particles. Further studies are warranted to investigate the effect of host particles properties such as size, shape and surface energy on interactive mixing behaviour and consequently the flow additive and binder action of excipients. In addition, tablet formulations are typically multi-component systems where

two or more excipients are used. It is would also be very important to understand, how the performance of such excipients change in such multi-component formulation scenarios.

In this study, small excipient particles (1-10 μm) were examined. Further studies are recommended to investigate the effect of particle size of interactive excipients on their performance. In addition, spray-drying is an effective but relatively expensive method of particle engineering. Further studies are recommended to investigate if mechanical milling can be used to effectively produce excipients particles in the size ranges that allows formation of interactive mixtures.